HMGB1 and HMGB2 interactomes in ovarian and prostate tumours

María Cámara Quílez

PhD Thesis

2021

Directors: Dra. Mª Esperanza Cerdán Villanueva and Dra. Mónica Lamas Maceiras

Programa Oficial de Doutoramento en Bioloxía Celular e Molecular

UNIVERSIDADE DA CORUÑA

El presente trabajo, HMGB1 and HMGB2 interactomes in ovarian and prostate tumours, presentado por Doña María Cámara Quílez para aspirar al grado de doctor en Bioquímica, ha sido realizado bajo nuestra dirección en el Departamento de Biología, de la Universidad de A Coruña.

Revisado el texto. Estamos conformes con su presentación para ser juzgado.

A Coruña, 29 de Enero de 2021

VºBº

Dra. Mª Esperanza Cerdán Villanueva

Catedrática de Bioquímica y Biología Molecular

VºBº

Dra. Mónica Lamas Maceiras

Profesora Titular de Bioquímica y Biología Molecular

VºBº

María Cámara Quílez

Alumna predoctoral

Programa de Doctorado de Biología Celular y Molecular

A mis padres

su apoyo incondicional. Sin Marianne no hubiese sobrevivido en Coruña, sin Jaime jamás hubiese acabado Biología y sin Celia no hubiese llegado ni a quinto de primaria.

Por último, nunca agradeceré lo suficiente el apoyo recibido por parte de mi familia durante el doctorado y a lo largo de toda mi vida. Gracias a mis padres, por luchar porque cumpliese mis sueños con todos y cada uno de los medios con los que contaban, por ser mi inspiración y por enseñarme que la carrera científica, como la vida, es un viaje capaz de maravillarte y hacerte fuerte por el camino, pero que siempre merece la pena. Gracias a mis tres hermanos pequeños, por ser los primeros en enseñarme el significado de la palabra compañerismo y por darme una razón para no rendirme jamás y no defraudarles.

Gracias a mis tíos: Ana y Fernando Cámara, por sus valiosos consejos científicos y por todo su cariño; a Carlos Quílez y Rosa Caballero, por ser mis segundos padres y darme cobijo en su casa para realizar el máster en Madrid que me permitió acceder a este doctorado; y a Elisa Quílez y Benito Raggio, por asegurar mi formación en inglés tan necesaria para esta profesión, llevándome con ellos al ILI school en Washington D.C. y dándome un hogar.

Gracias a todas las circunstancias que hicieron que acabase en A Coruña, conociendo a todas las maravillosas personas mencionadas y permitiéndome realizar esta tesis.

Contents

Abbreviations

μg	microgram
μL	microliter
μM	micromolar
μmol	micromole
ºC	Celsius grade
g	gram
ADE	Adenine
AD	Alzheimer Disease
ATCC	American Type Culture Collection
CRPC	Castration Resistant Prostate Cancer
EMBO	European Molecular Biology Organization
EMT	Epithelial-Mesenchymal Transition
EOC	Epithelial Ovarian Cancer
EV	Extracellular Vesicle
FTLA	Finite Track Length Adjustment
GAL4-AD	Activation Domain of transcription factor GAL4
GAL4-BD	Binding Domain of transcription factor GAL4
Gln	Glutamine
Gly	Glycine
GSH	Glutathione reduced
h	hour
HMG	High Mobility Group domain
His	Histidine
HRPC	Hormone Refractory Prostate Cancer
IP	InmunoPrecipitation
Kb	Kilobase

KDa	KiloDalton
L	Litre
LB	Luria Bertani
Leu	Leucine
lncRNA	Long Non Coding Ribinucleic Acid
M	Molar
MALDI-TOF	Matrix Assisted Laser Desorption Ionization-Time Of Flight
MEL	Melobiose
mg	miligram
min	minute
miRNA	Micro Ribonucleic Acid
mL	miliLiter
mM	miliMolar
MMR	MisMatch Repair
mRNA	messenger RiboNucleic Acid
MDR	Multi-Drug Resistance
MVB	Multi-Vesicular Body
NER	Nucleotide Excision Repair
ng	nanogram
NTA	Nano Tracking Assay
OCa	Ovarian Cancer
PBS	Phosphate Buffer Saline
PCa	Prostate Cancer
PCR	Polymerase Chain Reaction
PDB	Protein Data Bank
pH	Hydrogen potential

OCa	Ovarian Cancer
PBS	Phosphate Buffer Saline
PCa	Prostate Cancer
PCR	Polymerase Chain Reaction
PDB	Protein Data Bank
pH	Hydrogen potential
PMSF	PhenylMethylSulfonyl Fluoride
rpm	revolutions per minute
ROS	Reactive Oxygen Species
SASP	Senescence Associated Secretory Phenotype
SDS-PAGE	Sodium Dodecyl Sulphate-PolyAcrylamide Gel Electrophoresis
sec	second
siRNA	Small interfering Ribonucleic Acid
TEM	Transmission Electronic Microscopy
TDE	Tumour-Derived Exosome
Tm	melting Temperature
TMZ	Temozolomide
Trp	Tryptophan
URA	Uracil
WB	Western Blot
Y2H	Yeast Two Hybrid

Short Abstracts

Abstract

The HMGB family of proteins includes nuclear proteins with the ability to bind DNA and participate in transcriptional regulation and DNA repair processes, as well as to respond to cellular oxidative damage. The main objective of this work aims to identify new physical interactions of the HMGB1 and HMGB2 proteins with other proteins in ovarian and prostate tumours. The identification of new physical interactions of these proteins would allow a better understanding of their mechanism of action and their role in cancer-related signaling pathways.

Through experimental approaches based on the double hybrid, proteomic studies have been carried out using cDNA libraries prepared from isolated ovarian and prostate tumours from patients. The functionality of the interactions found has also been validated by bioinformatic meta-analyses of other data collected in databases on their expression levels and association with clinical survival parameters. Two selected interactions have also been validated by co-immunoprecipitation and by cell localization using confocal microscopy from cancer cells in culture.

Some functional characteristics of HMGB1 and HMGB2 proteins, as well as NOP53 and MIEN1, detected in this study as new proteins of physical interaction with HMGB proteins have been analyzed in greater detail. The effects produced by its silencing and the variation in expression levels in reaction to external treatments with compounds used in chemotherapy such as carboplatin, paclitaxel, olaparib and bevacizumab were analyzed. In addition, the HMGB1, HMGB2, NOP53 and MIEN1 proteins, together with the miRNAs miR-155, miR-124 and miR-146a, were detected in extracellular vesicles (EV) derived from prostate cell lines, and variations were observed after treatment with temozolomide (TMZ) or a new hybrid compound based on TMZ and valproic acid (1D).

This study is the basis for the search for new biomarkers or therapeutic targets useful to overcome resistance to anti-tumour drugs currently used in these types of cancer.

Resumen

La familia de proteínas HMGB está formada por proteínas nucleares con capacidad para unirse al ADN y participar en procesos de regulación transcripcional y reparación del ADN, así como para responder a daño oxidativo celular. El desarrollo de este trabajo tiene como objetivo identificar nuevas interacciones físicas de las proteínas HMGB1 y HMGB2 con otras proteínas en tumores de ovario y próstata. La identificación de nuevas interacciones físicas de estas proteínas permitiría comprender mejor su mecanismo de acción y su papel en las vías de señalización relacionadas con cáncer.

Mediante aproximaciones experimentales basadas en el doble híbrido, se han realizado estudios proteómicos utilizando librerías de ADNc preparadas a partir de tumores de ovario y próstata aislados de pacientes. La funcionalidad de las interacciones encontradas también se ha validado mediante meta-análisis bioinformático de una recopilación de datos referentes a sus niveles de expresión y a su asociación con parámetros clínicos de supervivencia. Dos interacciones seleccionadas han sido además validadas por co-Inmunoprecipitación y por localización celular, mediante microscopía confocal a partir de células cancerosas en cultivo.

Algunas características funcionales de las proteínas HMGB1 y HMGB2, así como de NOP53 y MIEN1 - detectadas en este estudio como nuevas proteínas de interacción física con las proteínas HMGB - se han analizado con mayor detalle. Se estudiaron los efectos producidos por su silenciamiento y la variación en los niveles de expresión ante tratamientos externos con compuestos utilizados en quimioterapia como carboplatino, paclitaxel, olaparib y bebacizumab. Además, las proteínas HMGB1, HMGB2, NOP53 y MIEN1, junto con los miRNAs miR-155, miR-124 y miR-146a, se detectaron en vesículas extracelulares (EV) derivadas de líneas celulares de próstata, viéndose alterado su contenido en estas moléculas tras el tratamiento con temozolomida (TMZ) o un nuevo compuesto híbrido basado en la TMZ y el ácido valpróico (1D).

Este estudio es la base para la búsqueda de nuevos biomarcadores o dianas terapéuticas con utilidad para superar la resistencia a fármacos anti-tumorales utilizados actualmente en estos tipos de cáncer.

Resumo

A familia de proteínas HMGB está formada por proteínas nucleares con capacidade de unirse o ADN e participar na regulación transcricional e nos procesos de reparación do ADN, así como para responder aos danos oxidativos celulares. O desenvolvemento deste traballo ten como obxectivo identificar novas interaccións físicas das proteínas HMGB1 e HMGB2 con outras proteínas en tumores de ovario e próstata. A identificación de novas interaccións físicas destas proteínas permitiría unha mellor comprensión do seu mecanismo de acción e do seu papel nas vías de sinalización relacionadas co cancro.

A través de enfoques experimentais baseados no dobre híbrido, leváronse a cabo estudos proteómicos utilizando bibliotecas de ADNc preparadas a partir de tumores de ovario e próstata illados de pacientes. A funcionalidade das interaccións atopadas tamén foi validada por meta-análise bioinformática doutros datos recollidos en bases de datos sobre os seus niveis de expresión e asociación con parámetros de supervivencia clínica. As interaccións seleccionadas tamén foron validadas por co-Inmunoprecipitación e por localización celular mediante microscopía confocal de células cancerosas en cultivo.

Algunhas características funcionais das proteínas HMGB1 e HMGB2, así como de NOP53 e MIEN1 - detectadas neste estudo como novas proteínas de interacción física con proteínas HMGB - analizáronse con maior detalle. Analizáronse os efectos producidos polo seu silenciamento e a variación dos niveis de expresión en resposta a tratamentos externos con compostos usados en quimioterapia como carboplatino, paclitaxel, olaparib e bebacizumab. Ademais, as proteínas HMGB1, HMGB2, NOP53 e MIEN1, xunto cos miRNAs miR-155, miR-124 e miR-146a, detectáronse en vesículas extracelulares (EV) derivadas de liñas celulares de próstata e o seu contido nestas moléculas foi alterado. despois do tratamento con temozolomida (TMZ) ou un novo composto híbrido TMZ-ácido valproico (1D).

Este estudo é a base para a procura de novos biomarcadores ou dianas terapéuticas útiles para superar a resistencia aos fármacos antitumorais que se utilizan na actualidade nestes tipos de cancros.

Introduction

Introduction

High Mobility Group B (HMGB) proteins are described as chromosomal proteins because they play important roles in chromatin modification and DNA binding, but they also participate in other extranuclear functions as well as extracellular alarmins. Four human HMGB proteins have been characterized, with HMGB1 and HMGB2 being the most ubiquitously expressed and abundant[1]. HMGB1, previously called amphoterin, has been extensively studied for over 60 years since the pioneering work on its therapeutic use in meningeal cryptococcosis[2] until nowadays, when this protein is considered a promising drug-target for several pathological conditions[3]. HMGB1 and HMGB2 bend DNA[4], improving DNA flexibility and looping, thus providing a mechanism for transcription factor binding and/or juxtaposition of distant regulatory sequences. Both proteins have nucleosome binding properties and remodeling activities, enhancing SWI/SNF recruitment to the nucleosomes without disturbing its ATPase activity[5]. HMGB proteins also have cytoplasmic functions promoting autophagy and preventing apoptosis[6]. Extracellular functions are related to immune and inflammatory responses[7] that include antimicrobial effects[8]. The extracellular functions of HMGB proteins depend on their redox state, which influences their interaction with different cellular receptors in immune and non-immune cells[9]. The extracellular functions of HMGB1 as cytokine and chemokine are mediated by the receptors for advanced glycation end-products (RAGE), toll-like receptors (TLR)[7] or endocytic HMGB1 uptake[10], which ultimately activate downstream signaling pathways. HMGB proteins are critically important in regulating many estrogen-responsive genes by enhancing the binding of steroid hormone receptors to their cognate response elements[11], as well as transcription[12]. In fact, these proteins regulate many transcriptional events by interacting with transcription factors such as p53[13], HOX[14], OCT[15], RAG1-2[16] or REL factors[17], among others. These interactions activate or repress transcription depending on their partner factors, as a consequence, HMGB proteins have different functions on transcriptional regulation depending on the cell or tissue type. The overexpression of HMGB proteins have been reported in many types of cancer, including those caused by oxidative damage[1]. Indeed, oxidative stress promotes cytosolic HMGB1 localization and extracellular release[9]. HMGB1 enhances proliferation, motility, invasion and survival of cancer cells, while simultaneously attenuates anti-cancer immune responses[18]. Nevertheless, HMGB1 also mediates immunogenic cell death and contributes to immune-mediated eradication of tumours, by the interaction with other factors according to its redox

form[19,20]. HMGB1 is also an important modulator of tumour angiogenesis[21], with all these characteristics contributing to tumour growth and metastasis. HMGB proteins are also involved in stem cell biology and cellular reprogramming[22–24], including the self-renewal of cancer stem cells[25]. Therefore, this family of proteins have multiple functions depending on their partners and they are important in the search for more effective cancer therapies and cell regenerative treatments. Interestingly, HMGB functions are not just limited to cancer, since they have been related to ischemic brain damage[26], neurodegenerative disorders[27], obesity[28], diabetes[29], and autoimmune and inflammatory diseases[30]. It is posited that HMGB proteins function as universal sentinels for nucleic-acid-mediated innate immune responses[31] (Figure 1).
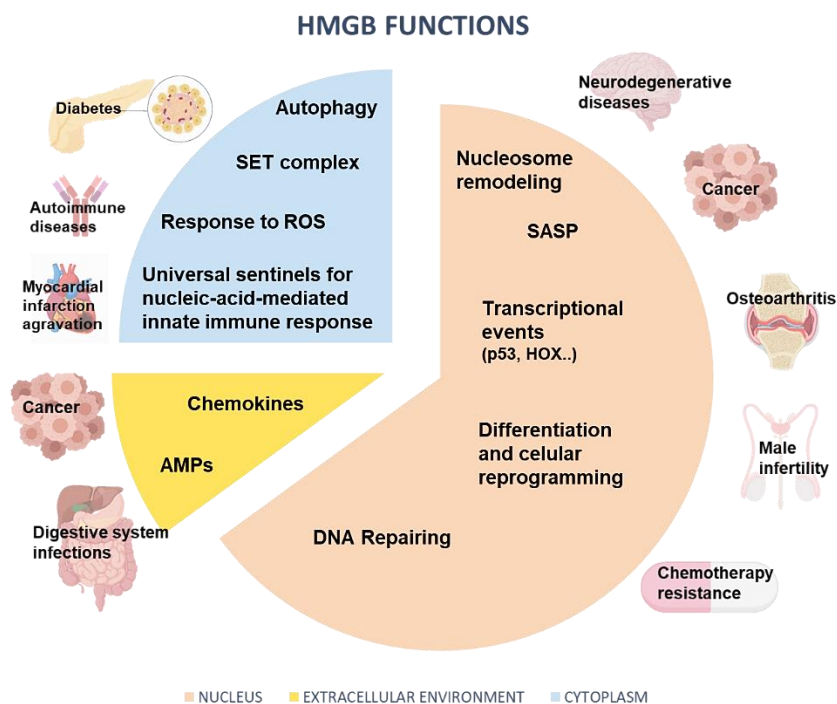
Figure 1. HMGB functions in cellular and extracellular compartments and subsequent effects associated to their dysregulation. SASP: Senescence associated secretory phenotype. AMPs: Antimicrobial proteins. Created with BioRender.com.

HMGB1 and HMGB2 share >80% sequence homology[1] and are well conserved in vertebrates. Studies have reported the presence of either different alleles or a differential splicing mechanism for human HMGB2, resulting in two HMGB2 subtypes: HMGB2a and HMGB2b. The intracellular quantity of each one of these variants depends on the cell type as demonstrated by Boix *et al.* [32].
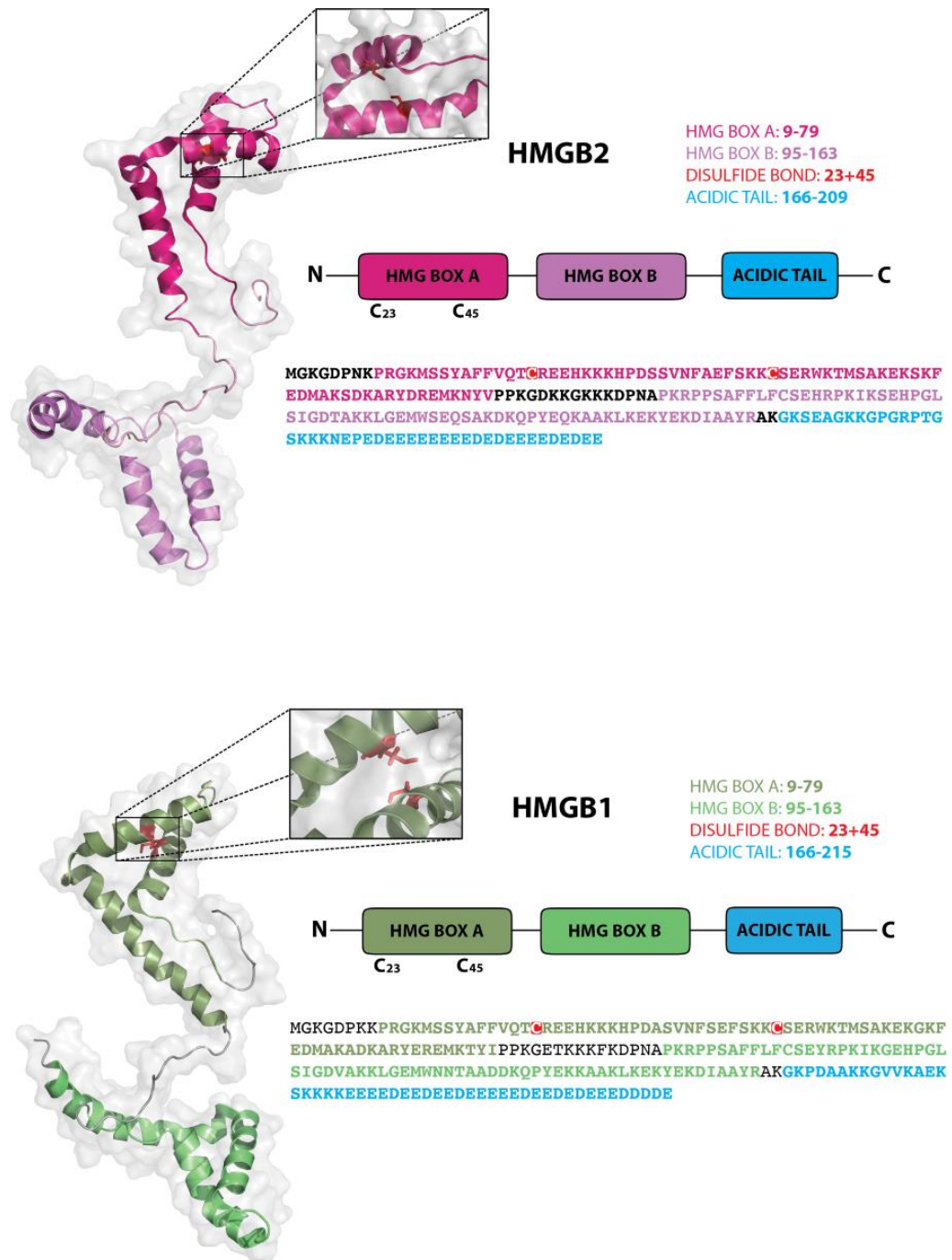
Figure 2. HMGB1 and HMGB2 structures. The cysteines involved in disulfide bond formation are enlarged in the boxes.

HMGB1 and both HMGB2 subtypes have 2 similar HMG-boxes that mediate DNA binding, and a long acidic C-terminal tail containing 30 Glu/Asp residues in HMGB1 and 22 in HMGB2, which modulates DNA binding affinity by intramolecular interactions, and mediate other intermolecular interactions. Despite the high level of

structural homology, the subtle differences in length of their acidic tails affect to their affinity for DNA binding, bringing into light possible functional variations as a consequence of these differences[33,34]. The acidic C-terminal tail modulates the affinity of the tandem HMG-boxes for numerous DNA targets, except for DNA minicircles to which the proteins bind with very high affinity[35]. Furthermore, the HMG-boxes are connected to the acidic C-terminal tail through a basic region of ~20 residues that constitutes the less conserved region between these two proteins[1,34] (Figure 2).

Lastly, both HMGB1 and HMGB2 have to cysteines (23 and 45) taking part of their respective sulfhydryl groups in their HMG-box A, which are vulnerable to suffer oxidation or reduction (Figure 2). Redox changes could cause conformational variations in these proteins affecting their ability to translocate to the different cellular compartments and to interact with other molecules[1,9,36–38]. Although, HMGB2 has been less well studied and characterized than HMGB1, previous studies that point to similarities and differences between HMGB1 and HMGB2 expression, specificity and function will be discussed below.

1. Effects of HMGB1 *and* HMGB2 *silencing in cancer cells*

Relevant information on the similarities and differences between HMGB1 and HMGB2 functions *in vivo* can be retrieved from knock-out and interfering strategies to silence the expression of these genes. The effect of HMGB1 or HMGB2 silencing on decreasing cell proliferation is well documented in several models. In hypoxic hepatocellular carcinoma cells, silencing of HMGB1 reduces mitochondrial biogenesis and cell proliferation[39]. Downregulation of cell proliferation after HMGB1 silencing is also observed on glioma cell lines[40], colorectal cancer cells[41,42], in HEC-1A cells from endometrial carcinoma of the uterus[43], and in LNCaP prostate cancer (PCa) cells[44]. Similarly, HMGB2 silencing in pancreatic cancer cells[45] or in glioblastoma[46] inhibits proliferation. Several mechanisms to explain the effect of HMGB proteins on cell proliferation have been evidenced and some are common to them. HMGB1 silencing[39,44] or HMGB2 silencing[47] have been related to increased apoptosis. The capacity to repair DNA-lesions of lung cancer cell line H1299 (defective p53) increases after silencing HMGB1, whereas in A549 cells (functional p53) silencing of both p53 and HMGB1 is necessary to get this effect[48]. Silencing of HMGB1 in mouse fibroblast cell line NIH-3T3 stimulates DNA-repair[49]. To our knowledge, direct evidence of the effect of HMGB2 silencing on DNA repair has not been reported. Nevertheless, it is known that small interfering RNA (siRNA)-mediated silencing of

HMGB2 increases cell sensitivity to cisplatin and 5- fluorouracil in head and neck squamous cell carcinoma[50].

HMGB1 and HMGB2 proteins are involved in invasion and metastasis. Silencing of HMGB1 using siRNA in the hypopharyngeal carcinoma cell line FaDu, upregulates mRNA expression of the epithelial cell marker, E-cadherin, while downregulating the mesenchymal markers, Vimentin and Snail. This regulatory effect is accompanied by a reduced ability of FaDu cells to invade and metastasize[51]. Similar results were obtained with the RBE cell line from intrahepatic cholangiocarcinoma[52]. HMGB1 silencing inhibits invasion in HEC-1A cells by a mechanism that depends on the p38MAPK signal pathway[43]. The interference of HMGB1's mRNA also inhibits the invasion and migration of gastric cancer cell line, MGC-803, an effect that may be partly mediated by NF-κB and MMP-9 expression[53]. In addition, treatment with HMGB1 siRNA reduces the metastatic ability of non-small cell lung cancer cells, as well as lowers metalloprotease MMP-9 expression[54]. In glioblastoma, HMGB2 siRNA decreases cell invasion *in vitro*, and significantly reduces tumour volume *in vivo*[46]. HMGB2 silencing also significantly decreases the invasion of gastric cancer cells as previously reported[55].

HMGB1 and HMGB2 proteins act through the Hippo pathway[45,56–58]. HMGB1 interaction with GA-binding protein alpha leads to the expression of yes-associated protein (YAP), thus inducing hypoxia-inducible factor 1α (HIF1α)-dependent aerobic glycolysis that contributes to liver tumourogenesis[58,59]. In pancreatic cancer cells, HMGB2 silencing inhibits cell proliferation and viability through decreased protein expression of HIF1α and down-regulation of glycolytic genes GLUT1, HK2, and LDHA[45].

HMGB1 or HMGB2 functions interplay with Metastasis Associated Lung Adenocarcinoma Transcript 1 (MALAT1)[60,61]. Without direct silencing, downregulation of HMGB1 expression also occurs after silencing the long non-coding RNA (lncRNA) MALAT1 in colon cancer cells, which implies a competition of lncRNA MALAT1 and the RNA of HMGB1 for binding to miR-129-5p[61]. In gastric cancer cells, MALAT1 acts as a molecular sponge of miR-1297, antagonizing its ability to suppress HMGB2 expression[60].

An intriguing characteristic of HMGB1 in carcinogenesis is that this molecule, after being released by necrotic cancer cells, and as part of its repertoire of extracellular functions, may act on other cells in the vicinity via RAGE receptors. Downregulation of RAGE expression by siRNA inhibits proliferation of androgen-dependent (LNCaP) and

androgen-independent (DU-145) PCa cells[62]. Similarly, siRNA silencing of RAGE or its ligands reduces the growth and migration of pancreatic ductal adenocarcinoma cells *in vitro*; a similar result was obtained by blocking the interaction of RAGE and its ligands with a competitor peptide[63]. Being HMGB1 a powerful tumour-promoting factor released from cancer cells, the possibility that it elicits immunosuppression pathway(s) has recently been explored[64]. The authors demonstrate that tumour-derived HMGB1 triggers the production of thymic stromal lymphopoietin by tumour cells, both molecules being necessary for the activation of dendritic cells, which in turn activates regulatory T cells (Tregs), a specialized subpopulation of T cells that suppress immune responses, thereby maintaining homeostasis and self-tolerance[64]. Silencing HMGB1 in tumour cells or blocking HMGB1 activity *in vivo* reduces the capacity of tumour cells to activate Tregs, thereby opening up new perspectives for the use of HMGB1 inhibitors into cancer immunotherapy[64].

The above findings on HMGB1 and HMGB2 silencing show that both are important in pathological cell proliferation, invasion and metastasis and that their silencing is a well confirmed and promising therapeutic strategy, if any negative side-effects can be controlled. In spite of their similarities, HMGB2 cannot substitute for the loss of HMGB1 in all its functions. This has been shown in mice, where knock-out of HMGB2 does not affect lifespan, but causes a limited fertility in male mice[65]; whereas HMGB1 knock-out mice do not even reach reproductive age, suggesting that HMGB1 and HMGB2 have different functions in multicellular organisms[66]. A problem in discriminating between specific functions and characteristics of HMGB1 and HMGB2 comes from the fact that only in a few cases have both proteins been studied in the same model and with the same technology. In particular, little data are available about differences in specific nuclear, cytoplasmic or extracellular functions for HMGB1 and HMGB2. Interestingly, HMGB2 is a slightly better substrate for acetylation than HMGB1[67]; since hyperacetylation is required for transport from nucleus to cytoplasm[68], this could have consequences in the differential regulation of their cellular localization and functions. Other difference between these proteins comes from the report that HMGB2, but not HMGB1, is a substrate of granzyme A, a protein secreted by natural killer cells and lymphocytes T, which promotes cell death independently of the caspases route, usually altered in tumour cells[69].

2. Is differential expression of HMGB1 *and* HMGB2 *associated with particular cellular functions?*

During early development of mice embryos, both HMGB1 and HMGB2 proteins are expressed but, apparently, their function is redundant. Muller and collaborators reported that HMGB1 continues to be ubiquitously expressed in adult mice[70], whereas HMGB2 expression is limited to thymus, testes and lymphoid tissues in the same model[65]. We have considered whether this concept can be translated to the human model, and whether there is now experimental data from adult human tissues to support this idea. We compared the expression of HMGB1, 2, 3, and 4 in public databases, obtained either through RNAseq or protein immunostaining, the data is shown in Figure 3.
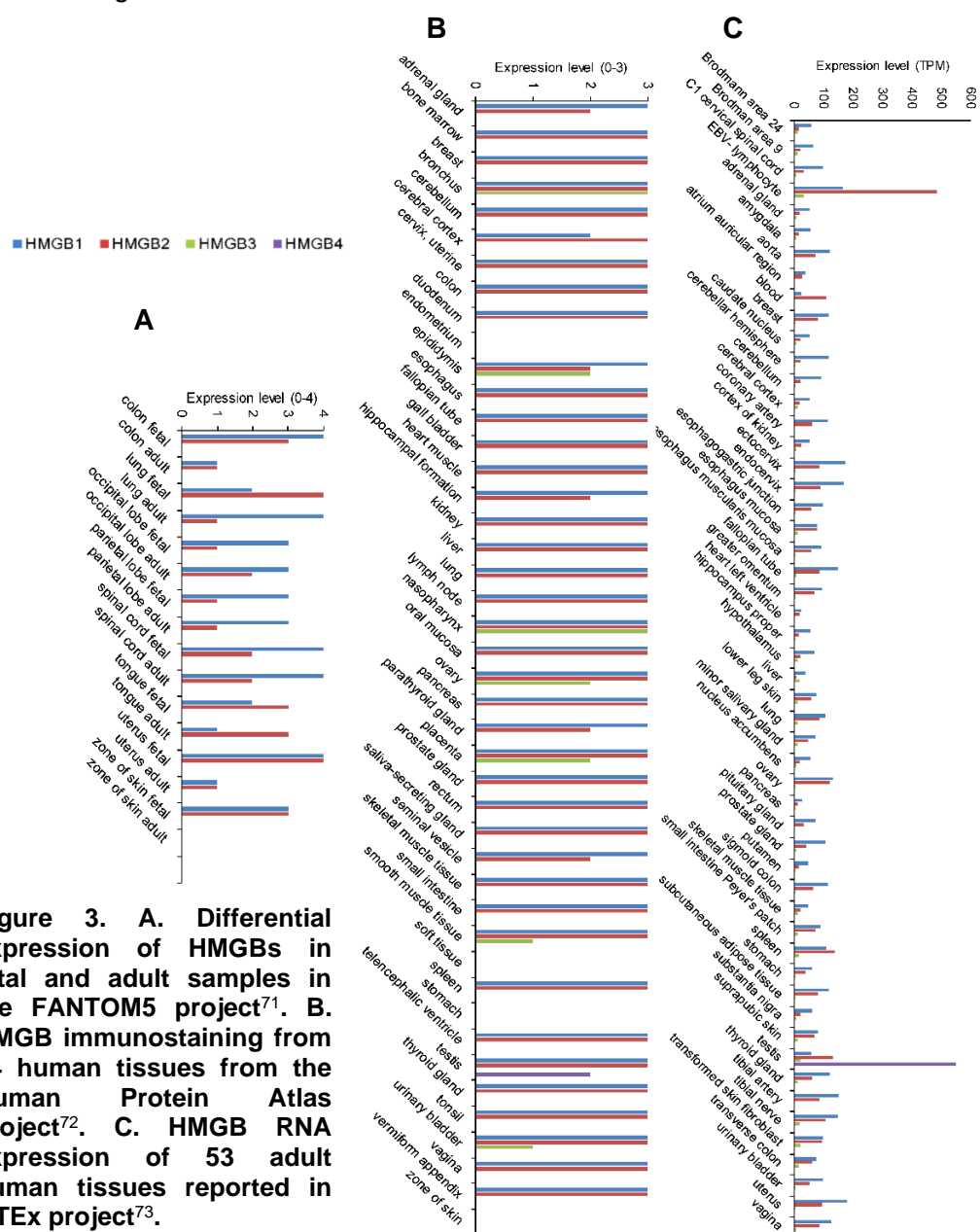
Figure 3. A. Differential expression of HMGBs in fetal and adult samples in the FANTOM5 project[71]. B. HMGB immunostaining from 44 human tissues from the Human Protein Atlas project[72]. C. HMGB RNA expression of 53 adult human tissues reported in GTEx project[73].

Introduction

The FANTOM5 project[71] gives a comparison of data from 8 fetal and adult tissues. HMGB1 expression is diminished relative to fetal expression in 50% of adults, is the same in 37.5%, and increases in 12.5% of them (Figure 3A). HMGB2 expression relative to fetal expression diminishes in 37.5% of adults, is unchanged in 50%, and increases in 12.5% of them (Figure 3A). Therefore, according to these data, the transition from fetal to the adult state seems to be accompanied by maintenance or reduction of HMGB1 and HMGB2 levels, but both are widely expressed in most adult tissues. Immunochemistry data from 44 normal tissues (Figure 3B) from the Human Protein Atlas Project[72] confirm that HMGB1 and HMGB2 genes are expressed at similar levels; much different to HMGB3 that is expressed, but at lower levels, and HMGB4, whose expression is testis-specific. A similar conclusion has been reached from RNA-seq data from 53 adult human tissue samples, from the Genotype-Tissue Expression (GTEx) Project[73] (Figure 3C).

Relative to HMGB1, HMGB2 expression has been correlated more frequently to cell differentiation, cellular senescence, older organisms, and the capacity for differentiation of embryonic and adult stems cells. However, this function is not exclusive to HMGB2 since HMGB1 has also been associated to the pro-osteogenic phenotype change of valvular interstitial cells in calcific aortic valve disease[74]; it might also participate in other cellular differentiation processes that have not yet been fully explored. Several studies have associated HMGB2 function to differentiation programs, such as erythropoiesis[75], chondrogenesis[76], myogenesis[77], neurogenesis[78] and spermatogenesis[65]. Regarding cell differentiation, examples can be found in which HMGB2 expression increases with differentiation and *viceversa*. Contrariwise, in articular cartilage, HMGB2 expression is inversely correlated with chondrocyte differentiation[76]. HMGB2 is also highly expressed in undifferentiated myoblasts and regenerating muscle[77]. Brain cortical development depends on the transition between neurogenesis and gliogenesis, to which HMGB2 has also been related[78]. During perinatal transition in the mouse, HMGB2 controls epigenetic changes, specifically the trimethylation of histone H3 at K27, thereby influencing the shift from neurogenesis to gliogenesis[78]. HMGB2 expression is downregulated during senescence in several models, including extended passaging of cultured IMR90 cells compared with young cells[79]. Immunostaining has shown the specific expression of HMGB2 in the superficial zone of human articular cartilage from young donors, which supports chondrocyte survival. Aging-related loss of HMGB2 expression contributes to the development of osteoarthritis, whereas HMGB1 immunostaining does not diminish with age[80]. In the first phase of cell senescence, proliferation-promoting genes are silenced through chromatin compaction to heterochromatin foci; however other genes

are actively transcribed, such as those encoding for secreted factors, e.g. cytokines and chemokines. Loss of HMGB2 during later senescence leads to the spreading of repressive heterochromatin into these gene loci[79]. Interestingly, HMGB2 is also expressed in all human or mouse immortalized cells that were tested[65], possibly contributing to overcome replicative limits[70].

HMGB2 is a modulator of the pluripotency of mouse embryonic stem cells, acting upstream of OCT4 and SOX2[24]. In this sense, it has been proposed that reducing HMGB2 expression provides a strategy to decrease the pluripotency of tumour initiating cells. Several findings also confirm that HMGB2 expression is directly correlated to adult stem cell populations in several tissues. In articular cartilage, HMGB2 is expressed in regions that contain cells expressing mesenchymal stem cell markers, and HMGB2 expression is inversely correlated with chondrocyte differentiation[80]. The age-related loss of HMGB2 in articular cartilage might be responsible for the decline of stem cell populations in adult cartilage[76]. Expression of HMGB2, but not HMGB1, is restricted to the subset of neural stem cells in the hippocampus and is correlated with transition from the quiescent to the proliferative state of these cells. Therefore, HMGB2 seems to be involved in the regulation of adult neurogenesis supported by these cells[81].

3. Overexpression of HMGB1 *and* HMGB2 *is associated to OCa and PCa*

A meta-analysis of 18 previous studies, including one prostate study and involving 11 different tumour types, has shown that HMGB1 overexpression is associated with a poorer prognosis in cancer patients[46]. HMGB1 overexpression has been also associated to ovarian cancer (OCa)[82,83]. HMGB2 is overexpressed in PCa[84], and in high-grade malignant and invasive tumours of serous epithelial OCa[85]. Moreover, both proteins have been involved in drug resistance. HMGB1 expression has been associated to resistance to conventional chemotherapy (carboplatin + taxol) in serous epithelial OCa[86], whereas HMGB2 expression has been correlated to oxaliplatin-resistance in the ovarian carcinoma cell line, A2780/C10[87]. Data of HMGB RNA expression from Pan-Cancer Analysis of Whole Genomes, PCAWG[88], shows that both HMGB1 and HMGB2 expression differs between normal and cancerous human tissues (Figure 4). In OCa, the fold change of expression between cancerous and normal tissue is 3.4 for HMGB1 and 4.5 for HMGB2. In prostatic cancer, the change fold is minor for both genes: 1.3 for HMGB1 and 1.5 for HMGB2.

Some insight has been gained about the molecular mechanisms that connect HMGB overexpression with carcinogenesis in the ovary or the prostate. In ovarian carcinoma, overexpression of HMGB1 contributes to enhanced metastatic potential via the FAK/PI3K/Akt signalling pathways, which may be connected with transcriptional regulation of the mTOR signalling pathway. The effect of HMGB1 on FAK/mTOR signalling has indeed been confirmed through silencing HMGB1 expression[89].
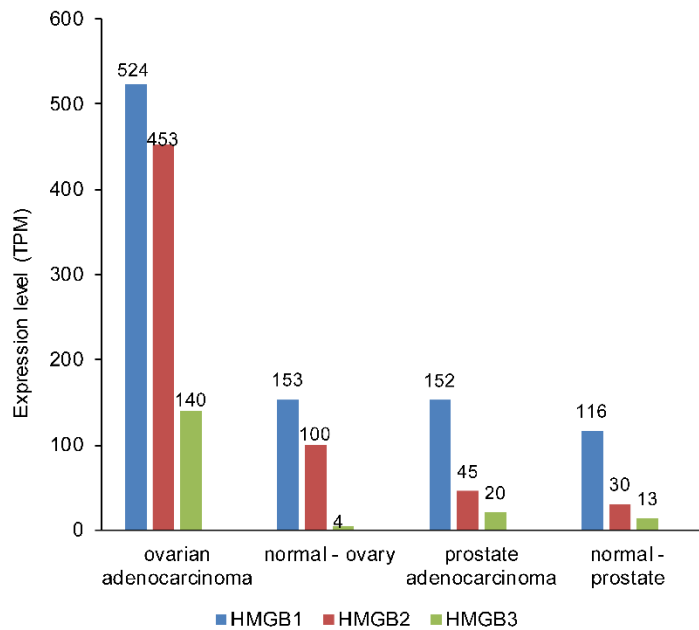
Figure 4. HMGB RNA expression in normal and cancerous human tissues from prostate and ovary

In PCa, recombinant HMGB1 enhances the invasive and metastatic capabilities of the PCa cells PC-3, together with changes in the epithelial to mesenchymal transition marks, and overexpression of matrix metalloproteinases via the RAGE/NF-KB signalling pathway[90]. Besides, the release of HMGB1 after hyperthermic treatment improves prostate tumour immunogenicity[91,92].

4. Post-transcriptional regulations of HMGB1 *and* HMGB2 *expression by miRNAs in OCa and PCa.*

The imbalance in protein expression that leads to tumourigenesis is orchestrated genetically and epigenetically. Small non-coding RNAs, or miRNAs, are single stranded RNA molecules composed by 19-25 nucleotides that avoid the messenger RNAs (mRNA) expression by different mechanisms including the binding to their 3'-untranslated region (3'-UTR) to which they share complementary sequences and interfering with translation[93]. The precursor of these molecules is firstly synthesized by DNA polymerase II in the nucleus and modified by the enzymes Drosha and Pasha. Afterwards, this pre-miRNA is translocated to the cytoplasm, where it undergoes cleavage by Dicer enzyme to reach its functional structure. The miRNA might also act as a silencer with de involvement of RNA-induced silencing complex (RISC) to perform its role silencing mRNAs[94]. miRNAs regulate protein expression in many physiological processes, such as inflammation[95], cancer disease[96–98] or the development and function of the nervous system[99], in response to different stimuli. Usually the deregulation of their expression drives to the development of diseases, including cancer. The miRNAs that silence pro-apoptotic proteins (onco-miRs) are normally overexpressed in cancer cells[100], stopping the translation of this kind of proteins and favoring the development of cancer[101]. For this reason, some of them are being currently used as biomarkers or therapeutic targets in different types of cancer. In OCa and PCa, miRNAs and their interacting proteins have been associated with differentiation and proliferation processes[94,102,103]. In OCa, downregulation of Drosha enzyme correlates with advanced final disease stage[94]. In the literature the post-translational regulation of HMGB1 and HMGB2 by miRNAs in OCa and PCa has not been reported yet. However, several findings show that the interaction of miRNAs, such as miR-124, with well described interacting partners of HMGB1 and HMGB2 could have an indirect repercussion in HMGB1 and HMGB2 expression in these cancers[102,103].

5. HMGB1 *and* HMGB2 *shuttling in tumour derived extracellular vesicles (EVs)*

Cellular cross-talk is indispensable for the maintenance of tissue homeostasis and the performance of effective responses to different stumuli[104]. Cells have different mechanisms to communicate in short distance, but in order to ensure the safe traveling of their information in long distance they transport molecules by packaging them in vesicles[105]. Among the different types of existing EVs, a specific type of EV

known as exosome has been reported to actively select its cargo and to possess different characteristic membrane proteins depending on their cell of origin and their receptor cell[106]. Exosomes have a size of approximately 40-200 nm and their maduration take place in the endosomes, being orchestrated by a range of proteins which control the release of these EVs to the extracellular environment. In tumoral cells, the regulation of the exosomes delivery is usually altered favoring a pro-tumoural extracellular microenvironment[105]. In PCa, isolation of exosomes from urine represents a non-invasive approach in order to detect molecular biomarkers transported in this fluid[107], since these EVs have been described to promote metastasis through the transport of proteins which modulate its biogenesis[108]. Ovarian tumour-derived exosomes have been detected in ascites[109], along with detached cells and immune cells, containing oncogenic miRNAs among other molecules, which perform roles in immunosuppression, angiogenesis, cancer associated fibroblast (CAF) conversion, macrophage polarization and mesothelial cell clearance[109]. Although HMGB proteins have not been identified inside prostate or OCa-derived exosomes yet, HMGB1 presence has been detected in exosomes produced by other types of cancers such as hepatocellular carcinoma, gastric cancer, colorectal cancer[110], cervical cancer[111] or Alzheimer's disease (AD)[112].

6. Drug-therapies involving HMGB1 as a target

Considering that HMGB proteins are dysregulated in diverse human diseases, a wide spectrum of therapeutic approaches has been reported, which target or use HMGB1. The first is associated with inhibition of HMGB1 using anti-HMGB1 antibodies[21,113,114]. The second is based on interference of the HMGB1 binding to its receptors[115]. The third includes drugs that inhibit HMGB1 transport from the nucleus to the cytoplasm and consequently avoid its secretion or release into the extracellular space[116,117]. The fourth, less well explored, tries to restore normal levels of HMGB1 expression[118,119]. All these approaches have been tested in animal models, but none has yet been implemented in clinical practice. Finally, other strategies have included recombinant HMGB1 (rHMGB1) acting as the therapeutic molecule, like in myocardial infarction, where it preserves cardiomyocyte survival[120]. There are different tactics in order to prevent HMGB1 inflammatory extracellular functions used in hepatocellular carcinoma[121], colon carcinomatosis[122], autoimmune encephalomyelitis[113], brain infarction[114,123] and Alzheimer´s disease[124] models. Focusing on extracellular level, anti-HMGB1 antibodies clear this protein from the extracellular medium avoiding its

interaction with RAGE and TLR4 receptors[20]. Another type of compounds operate impeding the HMGB1 binding to these receptors as in the case of Glycyrrhizin that has been tested in cerebral ischemia[125], Parkinson´s[126] and sepsis[127] models. With the same purpose, other compounds antagonize either HMGB1[128] or RAGE receptor, leading to the blocking of HMGB1 signaling, by using HMGA-box peptides or methotrexate, respectively[129]. A different approach involves neutralizing HMGB1 by binding to its acidic tail, like metformin[130], to its HMG-boxes, like inflachromene[131] or salicylic acid and its derivatives[132]. Adding to all previously mentioned, many compounds like chloroquine[116] or ethyl-pyruvate[117], avoid the HMGB1 translocation from the nucleus and the subsequent release to the extracellular medium, having been tested in sepsis and allergic rhinitis[133] models respectively. Concerning to the transcriptional level, the mechanism through which some compounds downregulate HMGB1 expression such as actinomycin D[118] and adriamycin[119], which bind to the promoter of HMGB1 *in vitro*, remain to be elucidated and have not been tested in cancer disease before.

Lastly, there are diverse mechanisms of action of other compounds that target HMGB1 signaling, but they are not generally well known. This is the case of 4,4'-diphenylmethane-bis(methyl) carbamate that reduces RAGE expression[134]; atorvastatin that suppresses TLR4 expression and NF-κB translocation to the nucleus[135]; rhododendroside A[136], stearoyl-lysophosphatidyl-choline[137] and cabozantinib[138], which alleviate pro-inflammatory stimuli.

Although there are many compounds that target HMGB1 and interfere by different mechanisms in its functions, only a limited number has been tested in cancerous models, and the absence of studies in OCa and PCa is remarkable. Only cabozantinib has been successfully used in a model of PCa[138]. Moreover, the effects of this and other compounds on HMGB2 functions have not been tested.

7. Perspectives in HMGB1/2 *cancer research and their putative applications in OCa and PCa*

Upregulation of HMGB1 and HMGB2 is a common feature in cancers of different origins; however, the mechanisms of this regulation at the molecular level are largely unknown. It is assumed that their overexpression is the cause of increased genomic instability and of transport from the nucleus to the cytoplasm. This change of intracellular localization allows the cytoplasmic functions of these proteins in avoiding apoptosis and increasing autophagy, thus aiding the survival and proliferative capacity

of malignant cells. Once released by cancerous cells, the role that HMGB proteins have in cell communication, favoring invasion and metastasis, in addition to promoting evasion of the immune response against a tumour, are still incipient and exciting research areas.

As discussed previously, HMGB2 has several specific functions, related to cell differentiation and senescence, that have not so far been reported for HMGB1. Despite the relevance of HMGB2 in cancer progression, the majority of the experiments conducted so far have been focused only on HMGB1. There are many issues to be addressed in future research to fully understand the differential role of these proteins that are, nevertheless, so similar in structure and have several overlapping functions. A full picture of differentially regulated promoters by these two proteins, a genome-wide description of their localization in chromatin domains, and the completion of interactome-networks of both, will be helpful in the fine dissecting of the specific functions of each. In this PhD Thesis we study diverse aspects of the interactome of HMGB1 and HMGB2 proteins in OCa and PCa, as well as their response to chemotherapy and their perspectives as biomarkers.

References

1. Barreiro-Alonso, A. *et al.* High Mobility Group B Proteins, Their Partners, and Other Redox Sensors in Ovarian and Prostate Cancer. *Oxid. Med. Cell. Longev.* **2016**, 1–17 (2016).

2. Cohen, J., Negroni, R. & Gaggiolo, M. Apropos of a Case of Meningeal Cryptococcosis Cured with Amphoterin B. *Rev. Asoc. Med. Argent.* **78**, 547–552 (1964).

3. Ugrinova, I. & Pasheva, E. HMGB1 Protein: A Therapeutic Target Inside and Outside the Cell. *Adv. Protein Chem. Struct. Biol.* **107**, 37–76 (2017).

4. Paull, T. T., Haykinson, M. J. & Johnson, R. C. The nonspecific DNA-binding and -bending proteins HMG1 and HMG2 promote the assembly of complex nucleoprotein structures. *Genes Dev.* **7**, 1521–1534 (1993).

5. Ugrinova, I., Pashev, I. G. & Pasheva, E. A. Nucleosome binding properties and Co-remodeling activities of native and in vivo acetylated HMGB-1 and HMGB-2 proteins. *Biochemistry* **48**, 6502–6507 (2009).

6. Tang, D. *et al.* Endogenous HMGB1 regulates autophagy. *J. Cell Biol.* **190**, 881–892 (2010).

7. Tang, L. M., Lu, Z. Q. & Yao, Y. M. The extracellular role of high mobility group box-1 protein in regulation of immune response. *Sheng Li Ke Xue Jin Zhan* **42**, 188–194 (2011).

8. Kuchler, R., Schroeder, B. O., Jaeger, S. U., Stange, E. F. & Wehkamp, J. Antimicrobial activity of high-mobility-group box 2: a new function to a well-known protein. *Antimicrob. Agents Chemother.* **57**, 4782–4793 (2013).

9. Tang, D., Kang, R., Zeh 3rd, H. J. & Lotze, M. T. High-mobility group box 1, oxidative stress, and disease. *Antioxid. Redox Signal.* **14**, 1315–1335 (2011).

10. Xu, J. *et al.* Macrophage endocytosis of high-mobility group box 1 triggers pyroptosis. *Cell Death Differ.* **21**, 1229–1239 (2014).

11. Das, D., Peterson, R. C. & Scovell, W. M. High mobility group B proteins facilitate strong estrogen receptor binding to classical and half-site estrogen response elements and relax binding selectivity. *Mol. Endocrinol.* **18**, 2616–2632 (2004).

12. Joshi, S. R., Ghattamaneni, R. B. & Scovell, W. M. Expanding the paradigm for estrogen receptor binding and transcriptional activation. *Mol. Endocrinol.* **25**, 980–994 (2011).

13. Rowell, J. P., Simpson, K. L., Stott, K., Watson, M. & Thomas, J. O. HMGB1-facilitated p53 DNA binding occurs via HMG-Box/p53 transactivation domain interaction, regulated by the acidic tail. *Structure* **20**, 2014–2024 (2012).

14. Zappavigna, V., Falciola, L., Helmer-Citterich, M., Mavilio, F. & Bianchi, M. E. HMG1 interacts with HOX proteins and enhances their DNA binding and transcriptional activation. *EMBO J.* **15**, 4981–4991 (1996).

15. Zwilling, S., Konig, H. & Wirth, T. High mobility group protein 2 functionally interacts with the POU domains of octamer transcription factors. *EMBO J.* **14**, 1198–1208 (1995).

16. Aidinis, V. *et al.* The RAG1 homeodomain recruits HMG1 and HMG2 to facilitate recombination signal sequence binding and to enhance the intrinsic DNA-bending activity of RAG1-RAG2. *Mol. Cell. Biol.* **19**, 6532–6542 (1999).

17. Agresti, A., Lupo, R., Bianchi, M. E. & Muller, S. HMGB1 interacts differentially with members of the Rel family of transcription factors. *Biochem. Biophys. Res. Commun.* **302**, 421–426 (2003).

18. Ohmori, H., Luo, Y. & Kuniyasu, H. Non-histone nuclear factor HMGB1 as a therapeutic target in colorectal cancer. *Expert Opin. Ther. Targets* **15**, 183–193 (2011).

19. Kang, R., Zhang, Q., Zeh 3rd, H. J., Lotze, M. T. & Tang, D. HMGB1 in cancer: good, bad, or both? *Clin. Cancer Res.* **19**, 4046–4057 (2013).

20. He, S. J. *et al.* The dual role and therapeutic potential of high-mobility group box 1 in cancer. *Oncotarget* **8**, 64534–64550 (2017).

21. van Beijnum, J. R. *et al.* Tumor angiogenesis is enforced by autocrine regulation of high-mobility group box 1. *Oncogene* **32**, 363–374 (2013).

22. Abraham, A. B. *et al.* Members of the high mobility group B protein family are dynamically expressed in embryonic neural stem cells. *Proteome Sci.* **11**, 1–18 (2013).

23. Li, M. *et al.* High-mobility group box 1 released from astrocytes promotes the proliferation of cultured neural stem/progenitor cells. *Int. J. Mol. Med.* **34**, 705–

714 (2014).

24. Zhao, Y. *et al.* High-mobility-group protein 2 regulated by microRNA-127 and small heterodimer partner modulates pluripotency of mouse embryonic stem cells and liver tumor initiating cells. *Hepatol. Commun.* **1**, 816–830 (2017).

25. Conti, L. *et al.* The noninflammatory role of high mobility group box 1/Toll-like receptor 2 axis in the self-renewal of mammary cancer stem cells. *FASEB J.* **27**, 4731–4744 (2013).

26. Muhammad, S. *et al.* The HMGB1 receptor RAGE mediates ischemic brain damage. *J. Neurosci.* **28**, 12023–12031 (2008).

27. Venegas, C. & Heneka, M. T. Danger-associated molecular patterns in Alzheimer's disease. *J. Leukoc. Biol.* **101**, 87–98 (2017).

28. Zhang, J. *et al.* HMGB1, an innate alarmin, plays a critical role in chronic inflammation of adipose tissue in obesity. *Mol. Cell. Endocrinol.* **454**, 103–111 (2017).

29. Wang, Y. *et al.* The Role of HMGB1 in the Pathogenesis of Type 2 Diabetes. *J. Diabetes Res.* **2016**, 1–11 (2016).

30. Harris, H. E., Andersson, U. & Pisetsky, D. S. HMGB1: a multifunctional alarmin driving autoimmune and inflammatory disease. *Nat. Rev.* **8**, 195–202 (2012).

31. Yanai, H. & Taniguchi, T. Nucleic acid sensing and beyond: virtues and vices of high-mobility group box 1. *J. Intern. Med.* **276**, 444–453 (2014).

32. Boix, J. Characterization of HMG2 complement changes in chicken tissues. *Exp. Cell Res.* **197**, 333–334 (1991).

33. Catena, R. *et al.* HMGB4, a novel member of the HMGB family, is preferentially expressed in the mouse testis and localizes to the basal pole of elongating spermatids. *Biol. Reprod.* **80**, 358–366 (2009).

34. Lee, K. B. & Thomas, J. O. The effect of the acidic tail on the DNA-binding properties of the HMG1,2 class of proteins: Insights from tail switching and tail removal. *J. Mol. Biol.* **304**, 135–149 (2000).

35. Thomas, J. O. HMG1 and 2: architectural DNA-binding proteins. *Biochem. Soc. Trans.* **29**, 395–401 (2001).

36. Sahu, D., Debnath, P., Takayama, Y. & Iwahara, J. Redox properties of the A-domain of the HMGB1 protein. *FEBS Lett.* **582**, 3973–3978 (2008).

37. Park, S. & Lippard, S. J. Redox State-Dependent Interaction of HMGB1 and Cisplatin- Modified DNA Semi. *Biochemistry* **50**, 2567–2574 (2008).

38. Venereau, E. *et al.* Mutually exclusive redox forms of HMGB1 promote cell recruitment or proinflammatory cytokine release. *J. Exp. Med.* **209**, 1519–1528 (2012).

39. Tohme, S. *et al.* Hypoxia mediates mitochondrial biogenesis in hepatocellular carcinoma to promote tumor growth through HMGB1 and TLR9 interaction. *Hepatology* **66**, 182–197 (2017).

40. Gu, J., Xu, R., Li, Y., Zhang, J. & Wang, S. MicroRNA-218 modulates activities of glioma cells by targeting HMGB1. *Am. J. Transl. Res.* **8**, 3780–3790 (2016).

41. Wang, Z. *et al.* HMGB1 knockdown effectively inhibits the progression of rectal cancer by suppressing HMGB1 expression and promoting apoptosis of rectal cancer cells. *Mol. Med. Rep.* **14**, 1026–1032 (2016).

42. Li, Z. *et al.* Silencing HMGB1 expression by lentivirus-mediated small interfering RNA (siRNA) inhibits the proliferation and invasion of colorectal cancer LoVo cells in vitro and in vivo. *Zhonghua Zhong Liu Za Zhi* **37**, 664–670 (2015).

43. Liu, X. & Wu, J. Mechanism of inhibitory effects of silencing high mobility group box-1 on invasion and migration of endometrial carcinoma of uterus. *Zhong nan da xue xue bao.Yi xue ban [Journal Cent. South Univ. Sci.* **41**, 251–257 (2016).

44. Gnanasekar, M., Thirugnanam, S. & Ramaswamy, K. Short hairpin RNA (shRNA) constructs targeting high mobility group box-1 (HMGB1) expression leads to inhibition of prostate cancer cell survival and apoptosis. *Int. J. Oncol.* **34**, 425–431 (2009).

45. Cai, X. *et al.* Expression of HMGB2 indicates worse survival of patients and is required for the maintenance of Warburg effect in pancreatic cancer. *Acta Biochim. Biophys. Sin. (Shanghai).* **49**, 119–127 (2017).

46. Wu, Z. B. *et al.* High-mobility group box 2 is associated with prognosis of glioblastoma by promoting cell viability, invasion, and chemotherapeutic resistance. *Neuro. Oncol.* **15**, 1264–1275 (2013).

47. Zhang, W. *et al.* Involvement of JNK1/2-NF-kappaBp65 in the regulation of HMGB2 in myocardial ischemia/reperfusion-induced apoptosis in human AC16 cardiomyocytes. *Biomed. Pharmacother.* **106**, 1063–1071 (2018).

48. Yusein-Myashkova, S., Stoykov, I., Gospodinov, A., Ugrinova, I. & Pasheva, E. The repair capacity of lung cancer cell lines A549 and H1299 depends on HMGB1 expression level and the p53 status. *J. Biochem.* **160**, 37–47 (2016).

49. Yusein-Myashkova, S., Ugrinova, I. & Pasheva, E. Non-histone protein HMGB1 inhibits the repair of damaged DNA by cisplatin in NIH-3T3 murine fibroblasts. *BMB Rep.* **49**, 99–104 (2016).

50. Syed, N. *et al.* Silencing of high-mobility group box 2 (HMGB2) modulates cisplatin and 5-fluorouracil sensitivity in head and neck squamous cell carcinoma. *Proteomics* **15**, 383–393 (2015).

51. Li, Y. *et al.* HMGB1 attenuates TGF-beta-induced epithelial-mesenchymal transition of FaDu hypopharyngeal carcinoma cells through regulation of RAGE expression. *Mol. Cell. Biochem.* **431**, 1–10 (2017).

52. Xu, Y. F. *et al.* High-mobility group box 1 expression and lymph node metastasis in intrahepatic cholangiocarcinoma. *World J. Gastroenterol.* **21**, 3256–3265 (2015).

53. Song, B. *et al.* Effect of HMGB1 silencing on cell proliferation, invasion and apoptosis of MGC-803 gastric cancer cells. *Cell Biochem. Funct.* **30**, 11–17 (2012).

54. Liu, P. L. *et al.* High-mobility group box 1-mediated matrix metalloproteinase-9 expression in non-small cell lung cancer contributes to tumor cell invasiveness. *Am. J. Respir. Cell Mol. Biol.* **43**, 530–538 (2010).

55. Cui, G., Cai, F., Ding, Z. & Gao, L. HMGB2 promotes the malignancy of human gastric Cancer and indicates poor survival outcome. *Hum. Pathol.* **84**, 133–141 (2018).

56. Zhang, X. *et al.* Yes-associated protein (YAP) binds to HIF-1α and sustains HIF-1α protein stability to promote hepatocellular carcinoma cell glycolysis under hypoxic stress. *J. Exp. Clin. Cancer Res.* **37**, 1–12 (2018).

57. Pan, Y. *et al.* RASAL2 promotes tumor progression through LATS2/YAP1 axis of hippo signaling pathway in colorectal cancer. *Mol. Cancer* **17**, 102–106

(2018).

58. Chen, R. *et al.* High mobility group protein B1 controls liver cancer initiation through yes-associated protein -dependent aerobic glycolysis. *Hepatology* **67**, 1823–1841 (2018).

59. Sayeon, C. *et al.* Binding and regulation of HIF-1alpha by a subunit of the proteasome complex, PSMA7. *FEBS Lett.* **498**, 62–66 (2001).

60. Li, J., Gao, J., Tian, W., Li, Y. & Zhang, J. Long non-coding RNA MALAT1 drives gastric cancer progression by regulating HMGB2 modulating the miR-1297. *Cancer Cell Int.* **17**, 1–9 (2017).

61. Wu, Q., Meng, W. Y., Jie, Y. & Zhao, H. LncRNA MALAT1 induces colon cancer development by regulating miR-129-5p/HMGB1 axis. *J. Cell. Physiol.* **233**, 6750–6757 (2018).

62. Elangovan, I. *et al.* Targeting receptor for advanced glycation end products (RAGE) expression induces apoptosis and inhibits prostate tumor growth. *Biochem. Biophys. Res. Commun.* **417**, 1133–1138 (2012).

63. Arumugam, T., Ramachandran, V., Gomez, S. B., Schmidt, A. M. & Logsdon, C. D. S100P-derived RAGE antagonistic peptide reduces tumor growth and metastasis. *Clin. Cancer Res.* **18**, 4356–4364 (2012).

64. Zhang, Y. *et al.* Tumor-derived high-mobility group box 1 and thymic stromal lymphopoietin are involved in modulating dendritic cells to activate T regulatory cells in a mouse model. *Cancer Immunol. Immunother.* **67**, 353–366 (2018).

65. Ronfani, L. *et al.* Reduced fertility and spermatogenesis defects in mice lacking chromosomal protein Hmgb2. *Development* **128**, 1265–1273 (2001).

66. Calogero, S. *et al.* The lack of chromosomal protein Hmg1 does not disrupt cell growth but causes lethal hypoglycaemia in newborn mice. *Nat. Genet.* **22**, 276–280 (1999).

67. Pasheva, E. *et al.* In vitro acetylation of HMGB-1 and -2 proteins by CBP: the role of the acidic tail. *Biochemistry* **43**, 2935–2940 (2004).

68. Bonaldi, T. *et al.* Monocytic cells hyperacetylate chromatin protein HMGB1 to redirect it towards secretion. *EMBO J.* **22**, 5551–5560 (2003).

69. Fan, Z., Beresford, P. J., Zhang, D. & Lieberman, J. HMG2 interacts with the nucleosome assembly protein SET and is a target of the cytotoxic T-

lymphocyte protease granzyme A. *Mol. Cell. Biol.* **22**, 2810–2820 (2002).

70.   Muller, S., Ronfani, L. & Bianchi, M. E. Regulated expression and subcellular localization of HMGB1, a chromatin protein with a cytokine function. *J. Intern. Med.* **255**, 332–343 (2004).

71.   Kawaji, H., Kasukawa, T., Forrest, A., Carninci, P. & Hayashizaki, Y. The FANTOM5 collection, a data series underpinning mammalian transcriptome atlases in diverse cell types. *Sci. data* **4**, 1–3 (2017).

72.   Lindskog, C. The Human Protein Atlas - an important resource for basic and clinical research. *Expert Rev. Proteomics* **13**, 627–629 (2016).

73.   Consortium, Gte. The Genotype-Tissue Expression (GTEx) project. *Nat. Genet.* **45**, 580–585 (2013).

74.   Wang, B. *et al.* High-mobility group box-1 protein induces osteogenic phenotype changes in aortic valve interstitial cells. *J. Thorac. Cardiovasc. Surg.* **151**, 255–262 (2016).

75.   Laurent, B. *et al.* High-mobility group protein HMGB2 regulates human erythroid differentiation through trans-activation of GFI1B transcription. *Blood* **115**, 687–695 (2010).

76.   Taniguchi, N. *et al.* Expression patterns and function of chromatin protein HMGB2 during mesenchymal stem cell differentiation. *J. Biol. Chem.* **286**, 41489–41498 (2011).

77.   Zhou, X. *et al.* HMGB2 regulates satellite-cell-mediated skeletal muscle regeneration through IGF2BP2. *J. Cell Sci.* **129**, 4305–4316 (2016).

78.   Bronstein, R., Kyle, J., Abraham, A. B. & Tsirka, S. E. Neurogenic to Gliogenic Fate Transition Perturbed by Loss of HMGB2. *Front. Mol. Neurosci.* **10**, 1–10 (2017).

79.   Aird, K. M. *et al.* HMGB2 orchestrates the chromatin landscape of senescence-associated secretory phenotype gene loci. *J. Cell Biol.* **215**, 325–334 (2016).

80.   Taniguchi, N. *et al.* Chromatin protein HMGB2 regulates articular cartilage surface maintenance via beta-catenin pathway. *Proc. Natl. Acad. Sci. U. S. A.* **106**, 16817–16822 (2009).

81.   Kimura, A., Matsuda, T., Sakai, A., Murao, N. & Nakashima, K. HMGB2 expression is associated with transition from a quiescent to an activated state

of adult neural stem cells. *Dev. Dyn.* **247**, 229–238 (2018).

82. Bukowska, B., Rogalska, A. & Marczak, A. New potential chemotherapy for ovarian cancer - Combined therapy with WP 631 and epothilone B. *Life Sci.* **151**, 86–92 (2016).

83. Paek, J., Lee, M., Nam, E. J., Kim, S. W. & Kim, Y. T. Clinical impact of high mobility group box 1 protein in epithelial ovarian cancer. *Arch. Gynecol. Obstet.* **293**, 645–650 (2016).

84. Rhodes, D. R. *et al.* Large-scale meta-analysis of cancer microarray data identifies common transcriptional profiles of neoplastic transformation and progression. *Proc. Natl. Acad. Sci. U. S. A.* **101**, 9309–9314 (2004).

85. Ouellet, V. *et al.* SET complex in serous epithelial ovarian cancer. *Int. J. Cancer* **119**, 2119–2126 (2006).

86. Bernardini, M. *et al.* High-resolution mapping of genomic imbalance and identification of gene expression profiles associated with differential chemotherapy response in serous epithelial ovarian cancer. *Neoplasia* **7**, 603–613 (2005).

87. Varma, R. R. *et al.* Gene expression profiling of a clonal isolate of oxaliplatin-resistant ovarian carcinoma cell line A2780/C10. *Oncol. Rep.* **14**, 925–932 (2005).

88. Weinstein, J. N. *et al.* The Cancer Genome Atlas Pan-Cancer analysis project. *Nat. Genet.* **45**, 1113–1120 (2013).

89. Ko, Y. B. *et al.* High-mobility group box 1 (HMGB1) protein regulates tumor-associated cell migration through the interaction with BTB domain. *Cell. Signal.* **26**, 777–783 (2014).

90. Zhang, J. *et al.* High mobility group box 1 promotes the epithelial-to-mesenchymal transition in prostate cancer PC3 cells via the RAGE/NF-kappaB signaling pathway. *Int. J. Oncol.* **53**, 659–671 (2018).

91. Brusa, D., Migliore, E., Garetto, S., Simone, M. & Matera, L. Immunogenicity of 56 degrees C and UVC-treated prostate cancer is associated with release of HSP70 and HMGB1 from necrotic cells. *Prostate* **69**, 1343–1352 (2009).

92. De Sanctis, F. *et al.* Hyperthermic treatment at 56 degrees C induces tumour-specific immune protection in a mouse model of prostate cancer in both

prophylactic and therapeutic immunization regimens. *Vaccine* **36**, 3708–3716 (2018).

93. Kopcalic, K., Petrovic, N., Stanojkovic, T. P. & Stankovic, V. Association between miR-21 / 146a / 155 level changes and acute genitourinary radiotoxicity in prostate cancer patients : A pilot study. *Pathol. - Res. Pract.* **215**, 626–631 (2019).

94. Deb, B., Uddin, A. & Chakraborty, S. miRNAs and ovarian cancer: An overview. *J. Cell. Physiol.* **233**, 3846–3854 (2018).

95. Schulte, L. N., Westermann, A. J. & Vogel, J. Differential activation and functional specialization of miR-146 and miR-155 in innate immune sensing. *Nucleic Acids Res.* **41**, 542–553 (2013).

96. Li, J., Feng, Q., Wei, X. & Yu, Y. MicroRNA-490 regulates lung cancer metastasis by targeting poly r(C)-binding protein 1. *Tumour Biol.* **37**, 15221–15228 (2016).

97. Yang, B. *et al.* Expression and mechanism of action of miR-196a in epithelial ovarian cancer. *Asian Pac. J. Trop. Med.* **9**, 1105–1110 (2016).

98. Li, B. *et al.* Morin promotes prostate cancer cells chemosensitivity to paclitaxel through miR-155 / GATA3 axis. *Oncotarget* **8**, 47849–47860 (2017).

99. Blandford, S. N., Galloway, D. A. & Moore, C. S. The roles of extracellular vesicle microRNAs in the central nervous system. *Glia* **66**, 2267–2278 (2018).

100. Cai, Z.-K. *et al.* microRNA-155 promotes the proliferation of prostate cancer cells by targeting annexin 7. *Mol. Med. Rep.* **11**, 533–538 (2015).

101. Fabian, M. R. & Sonenberg, N. The mechanics of miRNA-mediated gene silencing: A look under the hood of miRISC. *Nat. Struct. Mol. Biol.* **19**, 586–593 (2012).

102. Luu, H. N. *et al.* miRNAs associated with prostate cancer risk and progression. *BMC Urol.* **17**, 1–18 (2017).

103. Filella, X. & Foj, L. miRNAs as novel biomarkers in the management of prostate cancer. *Clin. Chem. Lab. Med.* **55**, 715–736 (2017).

104. Gurunathan, S., Kang, M., Jeyaraj, M., Qasim, M. & Kim, J. Review of the Isolation, Characterization, Biological Function, and Multifarious Therapeutic Approaches of Exosomes. *Cells* **8**, 1–36 (2019).

105. Mashouri, L. *et al.* Exosomes: Composition, biogenesis, and mechanisms in cancer metastasis and drug resistance. *Mol. Cancer* **18**, 1–14 (2019).

106. Schorey, J. S. & Bhatnagar, S. Exosome function: From tumor immunology to pathogen biology. *Traffic* **9**, 871–881 (2008).

107. Hoorn, E. J. *et al.* Prospects for urinary proteomics : Exosomes as a source of urinary biomarkers. *NEPHROLOGY* **10**, 283–290 (2005).

108. Saber, S. H. *et al.* Exosomes are the Driving Force in Preparing the Soil for the Metastatic Seeds: Lessons from the Prostate Cancer. *Cells* **9**, 1–26 (2020).

109. Feng, W., Dean, D. C., Hornicek, F. J., Shi, H. & Duan, Z. Exosomes promote pre-metastatic niche formation in ovarian cancer. *Mol. Cancer* **18**, 1–11 (2019).

110. Huang, C. Y. *et al.* HMGB1 promotes ERK-mediated mitochondrial Drp1 phosphorylation for chemoresistance through RAGE in colorectal cancer. *Cell Death Dis.* **9**, 1004–1019 (2018).

111. Jin, Y. *et al.* ALA-PDT promotes HPV-positive cervical cancer cells apoptosis and DCs maturation via miR-34a regulated HMGB1 exosomes secretion. *Photodiagnosis Photodyn. Ther.* **24**, 27–35 (2018).

112. Fernandes, A. *et al.* Secretome from SH-SY5Y APPSwe cells trigger time-dependent CHME3 microglia activation phenotypes, ultimately leading to miR-21 exosome shuttling. *Biochimie* **155**, 67–82 (2018).

113. Uzawa, A. *et al.* Anti-high mobility group box 1 monoclonal antibody ameliorates experimental autoimmune encephalomyelitis. *Clin. Exp. Immunol.* **172**, 37–43 (2013).

114. Liu, K. *et al.* Anti-high mobility group box 1 monoclonal antibody ameliorates brain infarction induced by transient ischemia in rats. *FASEB J.* **21**, 3904–3916 (2007).

115. Gao, T. *et al.* Inhibition of HMGB1 mediates neuroprotection of traumatic brain injury by modulating the microglia/macrophage polarization. *Biochem. Biophys. Res. Commun.* **497**, 430–436 (2018).

116. Yang, M. *et al.* Chloroquine inhibits HMGB1 inflammatory signaling and protects mice from lethal sepsis. *Biochem. Pharmacol.* **86**, 410–418 (2013).

117. Kim, Y. M. *et al.* Ethyl pyruvate inhibits the acetylation and release of HMGB1 via effects on SIRT1/STAT signaling in LPS-activated RAW264.7 cells and

peritoneal macrophages. *Int. Immunopharmacol.* **41**, 98–105 (2016).

118. Lohani, N., Singh, H. N. & Moganty, R. R. Structural aspects of the interaction of anticancer drug Actinomycin-D to the GC rich region of hmgb1 gene. *Int. J. Biol. Macromol.* **87**, 433–442 (2016).

119. Lohani, N., Narayan Singh, H., Agarwal, S., Mehrotra, R. & Rajeswari, M. R. Interaction of adriamycin with a regulatory element of hmgb1: spectroscopic and calorimetric approach. *J. Biomol. Struct. Dyn.* **33**, 1612–1623 (2015).

120. Foglio, E., Puddighinu, G., Germani, A., Russo, M. A. & Limana, F. HMGB1 Inhibits Apoptosis Following MI and Induces Autophagy via mTORC1 Inhibition. *J. Cell. Physiol.* **232**, 1135–1143 (2017).

121. Chen, S. *et al.* Hepatitis B virus X protein stimulates high mobility group box 1 secretion and enhances hepatocellular carcinoma metastasis. *Cancer Lett.* **394**, 22–32 (2017).

122. Cottone, L. *et al.* 5-Fluorouracil causes leukocytes attraction in the peritoneal cavity by activating autophagy and HMGB1 release in colon carcinoma cells. *Int. J. Cancer* **136**, 1381–1389 (2015).

123. Nishibori, M. HMGB1 as a representative DAMP and anti-HMGB1 antibody therapy. *Nihon yakurigaku zasshi.Folia Pharmacol. Jpn.* **151**, 4–8 (2018).

124. Fujita, K. *et al.* HMGB1, a pathogenic molecule that induces neurite degeneration via TLR4-MARCKS, is a potential therapeutic target for Alzheimer's disease. *Sci. Rep.* **6**, 31895 (2016).

125. Xiong, X. *et al.* Glycyrrhizin protects against focal cerebral ischemia via inhibition of T cell activity and HMGB1-mediated mechanisms. *J. Neuroinflammation* **131**, 241–245 (2016).

126. Santoro, M. *et al.* In-vivo evidence that high mobility group box 1 exerts deleterious effects in the 1-methyl-4-phenyl-1,2,3,6-tetrahydropyridine model and Parkinson's disease which can be attenuated by glycyrrhizin. *Neurobiol. Dis.* **91**, 59–68 (2016).

127. Zhao, F. *et al.* Glycyrrhizin Protects Rats from Sepsis by Blocking HMGB1 Signaling. *Biomed Res. Int.* **2017**, 1–10 (2017).

128. Song, J. H. *et al.* Delivery of the high-mobility group box 1 box A peptide using heparin in the acute lung injury animal models. *J. Control. Release* **234**, 33–40

(2016).

129. Kuroiwa, Y. *et al.* Identification and characterization of the direct interaction between methotrexate (MTX) and high-mobility group box 1 (HMGB1) protein. *PLoS One* **8**, 1–12 (2013).

130. Horiuchi, T. *et al.* Metformin directly binds the alarmin HMGB1 and inhibits its proinflammatory activity. *J. Biol. Chem.* **292**, 8436–8446 (2017).

131. Lee, S. *et al.* A small molecule binding HMGB1 and HMGB2 inhibits microglia-mediated neuroinflammation. *Nat. Chem. Biol.* **10**, 1055–1060 (2014).

132. Choi, H. W. *et al.* Aspirin's Active Metabolite Salicylic Acid Targets High Mobility Group Box 1 to Modulate Inflammatory Responses. *Mol. Med.* **21**, 526–535 (2015).

133. Chen, S. *et al.* Ethyl pyruvate attenuates murine allergic rhinitis partly by decreasing high mobility group box 1 release. *Exp. Biol. Med. (Maywood).* **240**, 1490–1499 (2015).

134. Feng, L. *et al.* Amelioration of compound 4,4'-diphenylmethane-bis(methyl)carbamate on high mobility group box1-mediated inflammation and oxidant stress responses in human umbilical vein endothelial cells via RAGE/ERK1/2/NF-kappaB pathway. *Int. Immunopharmacol.* **15**, 206–216 (2013).

135. Yang, J., Huang, C., Yang, J., Jiang, H. & Ding, J. Statins attenuate high mobility group box-1 protein induced vascular endothelial activation : a key role for TLR4/NF-kappaB signaling pathway. *Mol. Cell. Biochem.* **345**, 189–195 (2010).

136. Zhou, W. *et al.* The first cyclomegastigmane rhododendroside A from Rhododendron brachycarpum alleviates HMGB1-induced sepsis. *Biochim. Biophys. Acta* **1840**, 2042–2049 (2014).

137. Kim, J. M. *et al.* Stearoyl lysophosphatidylcholine prevents lipopolysaccharide-induced extracellular release of high mobility group box-1 through AMP-activated protein kinase activation. *Int. Immunopharmacol.* **28**, 540–545 (2015).

138. Patnaik, A. *et al.* Cabozantinib Eradicates Advanced Murine Prostate Cancer by Activating Antitumor Innate Immunity. *Cancer Discov.* **7**, 750–765 (2017).

Objectives

HMGB proteins have been associated to cancerous processes, including prostate and ovarian cancer. The general objective raised in this thesis is to know the interactome of the HMGB1 and HMGB2 proteins in cells isolated from prostate and ovarian tumours in order to identify possible targets for diagnosis or therapy, and analyze their changes in the response to conventional treatments used in chemotherapy. For this we set the following objectives:

1) To analyze the interactome of HMGB1 and HMGB2 from prostate tumour cells obtained from an adenocarcinoma primary tumour.

2) To analyze the interactome of HMGB1 and HMGB2 from ovarian cancer tumour cells obtained from biopsy.

3) To analyze the expression variations of HMGB1, HMGB2 and two selected proteins of the interactome, MIEN1 and NOP53, in response to various chemotherapeutic treatments using tumour cells in culture.

4) To analyze the presence of HMGB1, HMGB2, MIEN1, NOP53 and related miRNAs in exosomes derived from prostate cells in non-tumour and tumour cell lines.

Chapter 1.

Y2H HMGB1 and HMGB2 interactome in Prostate Cancer

Introduction

Human HMGB proteins, HMGB1, 2, and 3 are differentially expressed in many different tissues and cell types, whereas HMGB4 expression is restricted to the testis[1]. HMGB2 has 82.3% sequence similarity with HMGB1, and both proteins have common or redundant functions in inflammation[2], chromosome remodeling activity[3], V(D)J recombination[4], and embryonic development[5]. HMGB1 has been related to the onset and progression of cancer, being involved in events such as replenishing telomeric DNA and maintaining cell immortality[6], autophagic increase[7], evasion of apoptosis[8,9], as well as cell proliferation and invasion[10,11]. HMGB1 is also involved in dedifferentiation during epitelial to mesenchymal transition (EMT)[12] via RAGE and NF-κB signaling pathways[13], and in angiogenesis[14]. The role of HMGB2 in these processes, although less well studied, has also been related to cell viability and invasion[15], EMT[11], and angiogenesis[16]. HMGB2 has been described as a regulator of cell differentiation in different tissues as cartilage[17,18], brain[19], testis[20], or skeletal muscle[21] among others, undergoing a decrease in its expression levels as the differentiation takes place. Furthermore, HMGB2 epigenetically avoids the silencing of the Senecescence Associated Secretory Phenotype (SASP) genes during chromatin compaction to heterochromatin foci, promoting the release of alarmins and cytokines which are enriched in the tumoural environment[22,23]. Besides, several protein complexes, which incorporate HMGB2, translocate to the nucleus in stress conditions to repair or cleavage the DNA, being the SET complex a paradigm[24]. These characteristics seem to confere HMGB2 dysregulation important oncogenic properties. Majority of prostate cancers (PCa) are adenocarcinomas characterized by glandular formation and the expression of androgen receptor (AR) and prostate-specific antigen (PSA). Hormonal inhibition of AR signaling is the therapeutic choice for patients with adenocarcinomas, but unfortunately the disease usually progresses as it becomes independent of exogenous AR induction, leading to castration-resistant prostate cancer (CRPC) with a worse prognosis. In prostatic small cell neuroendocrine carcinoma (SCNC), the tumor cells are negative for AR and PSA expression and do not respond to hormonal therapy[25]. Among the most frequently used PCa cell lines, PC-3 characteristics are considered closer to a SCCN PCa model, and those of DU-145 or LNCaP to adenocarcinoma models[25]. PC-3 and DU-145 are AR-independent and LNCaP is AR-dependent[25,26]. Boonyaratanakornkit and collaborators stablished that HMGB2 enhances the AR ability to bind DNA more than HMGB1, increasing its tanscriptional activity[27]. Proteomic studies in relation to PCa have been reported[28–30], interactome

strategies being outstanding in recent developments[31–33]. The Yeast Two Hybrid (Y2H) approach is a system used to detect physic interactions between a bait protein and proteins of a selected genetic library[34,35]. It allows to discover new protein interactions prior to validate them through other techniques as co-Inmunoprecipitation or co-localization fluorescence. In a previous study, several proteins interacting with HMGB1 and HMGB2 in the cancerous prostate cell line PC-3, as a model of metastatic AR-independent PCa, were found[36].The purpose in this study is to analyze proteins interacting with HMGB1 and HMGB2 by secreening the Y2H approach libraries obtained from PCa adenocarcinoma primary tumor. Analyses of copy number alterations (CNA) and mRNA levels of detected targets in public PCa data bases are discussed showing that dysregulation of some HMGB2 targets is associated to clinical prognosis. Considering that HMGB proteins are known regulators of gene expression, we also tested whether HMGB1 and HMGB2 silencing affects the expression of their Y2H detected partners, finding that this regulatory mechanism is functional in PC-3 cells.

1. Materials and Methods

1.1. Yeast two hybrid (Y2H) methodology

HMGB1 and HMGB2 interacting partners were identified using Matchmaker Gold Yeast 2-Hybrid System (Clontech, Fremont, CA, USA). *Sacchacomyces cerevisiae* strains were Y187 (MATα, *ura*3-52, *his*3-200, *ade*2-101, *trp*1-901, *leu*2-3, 112, *gal*4Δ, *gal*80Δ, *met*-, *URA3*::*GAL*uas-*GAL1*TATA-*LacZ MEL*1) and Y2HGold (MATa, *trp*1-901, *leu*2-3, 112, *ura*3-52, *his*3-200, *gal*4Δ, *gal*80Δ, *LYS2::GAL1*UAS-*GAI1*TATA-*HIS3*, *GAL2*UAS-*GAL2*TATA-*ADE2*, *URA3::MEL1*UAS-*MEL1*TATA-*AUR1-C-MEL1*). Total RNA from PCa adenocarcinoma primary tumour (Biobanco de Andalucía, ES, EU) were used to construct cDNA libraries. RNA was extracted from frozen tissue sections in OCT (Optimal Cutting Temperature) compound, using the Qiacube robot from QIAGEN (QIAGEN N.V., Hilden, DE, EU), based on ion-exchange columns with a silica membrane. RNA was obtained with the miRNeasy mini-kit from QIAGEN (QIAGEN N.V, Hilden, DE, EU) that allows recovery of both total RNA and miRNAs. The samples were finally treated with RNase-free DNAse from QIAGEN (QIAGEN N.V, Hilden, DE, EU). The RNA was quantified at 260 nm and 280 nm by spectrophotometry using Infinite F200 equipment of TECAN with a Nanoquant plate. Finally, the integrity of the samples was evaluated by AGILENT 2200 Tape Station apparatus, the RIN (RNA Integrity Number) parameter being >8. Library construction, bait construction and Yeast 2-Hybrid library screening were done according to the Takara Bio USA Matchmaker® Gold Yeast 2-Hybrid System manual. In brief, the baits were cloned as fusions to the GAL4 activation domain in the plasmid pGBKT7-AD and used to transform the yeast haploid strain, Y187. cDNA libraries were included as fusions to the GAL4 DNA binding domain in the plasmid pGBKT7-BD, and were used to transform the yeast haploid strain, Y2HGold. Efficiency in the constructions of libraries was in the range recommended in the kit (all libraries guaranteed to have >1 x 10^6 independent clones). As a previous control, we confirmed that our baits (HMGB1 and HMGB2) do not autonomously activate the reporter genes in Y2HGold in the absence of a prey protein. Bait and prey fusion proteins are each expressed in different haploid yeast strains that can form diploids. The diploid yeast cells express both proteins, and when fusion proteins interact, the transcriptional activator protein GAL4 is reconstructed and brought into proximity to activate transcription of the reporter genes. For diploid formation, 1 mL of concentrated bait culture was combined with 1 mL of library culture and incubated overnight with slow shaking. A drop of the culture was checked under a phase-contrast microscope (40X objective) to confirm the existence of zygotes before plating on diploid-selective media. Diploids were tested for expression of the reporter genes in

selective media. To reduce the appearance of false positives, a screening based in three different independent markers (*ADE2*, *HIS3*, and *MEL1*) was selected. pGBKT7-BD plasmids carrying the preys were rescued from confirmed positive diploids, and DNA was used to transform *E. coli*. The inserts were sequenced with primer T7 (5´-TAATACGACTCACTATAGGG-3´). Sequences were used for homology searches with BlastN and BlastX at NCBI (https://blast.ncbi.nlm.nih.gov/) and proteins matching the queries annotated as positives. The interactions detected were contrasted with those previously annotated in STRING (https://string-db.org/ Access date 10-22-2020) and BioGRID (https://thebiogrid.org Access date 10-26-2020), and protein function information was extracted from Uniprot database (http://www.uniprot.org/uniprot Access date 10-22-2020).

1.2. Cell culture

PC-3 is an androgen-independent prostate cell line derived from a bone metastasis[37] while DU-145 derives from a brain metastasis of prostate epithelial carcinoma[38]. The human PCa PC-3 and DU-145 cell lines, regularly validated by DNA typing, were obtained from ATTC and grown in RPMI-1640 (Gibco™, Thermo Fisher Scientific Inc., Waltham, MA, USA), supplemented with 10% heat-inactivated fetal bovine serum and 1% penicillin-streptomycin (Thermo Fisher Scientific, Inc., Waltham, MA, USA). Cells were cultured at 37ºC and 5% CO_2 in a humidified incubator. RNA from PCa tissue and adjacent healthy tissue, isolated after radical prostate resection of a 66 years old man diagnosed with adenocarcinoma (Gleason score 6), and not previously treated with radiotherapy or chemotherapy, was obtained from Biobanco de Andalucía (ES, EU). We thank the Biobanco of Andalucía for these facilities.

1.3. Cross-linking and HMGB2 co-immunoprecipitation

Co-immunoprecipitation (co-IP) was used in validation of Y2H results. After reaching 70-80% confluence of DU-145 culture, medium was removed and substituted by medium without fetal bovine serum and supplemented with 1% formaldehyde used as cross-linker. The cells were incubated with formaldehyde during 10 min at room temperature. To stop the cross-linking reaction, the medium with formaldehyde was changed by a solution containing 0.125 M glycine in PBS (Phosphate Buffered saline) pH 7.4 (NZYTech Lda., Lisbon, PT, EU) and incubated during 5 min at room temperature. Cells were washed three times with PBS and harvested by scrapping.

After subsequent collection by centrifugation at 1200 rpm for 10 min at 4ºC, cells were re-suspended in lysis buffer (50 mM Tris-HCl pH 8, 150 mM NaCl, 0.1% NP-40, 1 mM EDTA, 2 mM MgCl2) containing a cocktail of EDTA-free protease inhibitors (Roche Diagnostics, Hoffmann-La Roche, Basel, CH, EU). Cell lysates were clarified for 15 min at 14000 rpm to pellet cell debris. Supernatants were collected and protein quantified using the Bradford reagent (Bio-Rad Laboratories, Hercules, CA, USA). 16 mg of total protein extracts from cells were immunoprecipitated (IPs) using 10 µg HMGB2 rabbit polyclonal antibody (ab67282, Abcam, Cambridge, UK, EU) bound to 50 µL dynabeads-protein A (Thermo Fisher Scientific Inc., Waltham, MA, USA) following manufacturer´s instructions. The presence of MIEN1 and NOP53 in the immunoprecipitations (IPs) was confirmed by Western blot using the antibodies against MIEN1 (1:200, XTP4, 40-400, Invitrogen, Thermo Fisher Scientific Inc., Waltham, MA, Waltham, USA) and NOP53 (1:500, sc-517088, Santa Cruz Biotechnology, Dallas, TX, USA). After second incubation with 1:5000 G-protein HRP-linked (18-161, Millipore-Merck-KGaA, Darmstadt, DE, EU), 5% (w/v) non-fat milk diluted in PBST, PBS containing 0.1% Tween 20 (P1379, Sigma-Aldrich Inc., St. Louis, MO, USA), was used as blocking solution. Western blots were developed using Luminata™ Crescendo Western HRP Substrate (Millipore Corporation, Burlington, MA, USA), and visualized in a ChemiDoc™ imager (Bio-Rad Laboratories, Hercules, CA, USA).

1.4. Expression analysis by quantitative polymerase chain reaction (RT-qPCR)

Individual analyses of gene expression were carried out as follows. RNA samples were retro-transcribed into cDNA and labeled with the KAPA SYBR FAST universal one-step RT-qPCR kit (Kappa Biosystems Inc., Woburn, MA, USA). The primers for qPCR are shown in Table 1. Reaction conditions for thermal cycling were: retrotranscriptase activation at 42ºC for 5 min, denaturation of double-stranded cDNA and polymerase activation at 95ºC for 5 min, followed by 40 amplification cycles including denaturation of double-stranded cDNA at 95ºC for 3 s, and annealing of primers and amplification at 60ºC for 30 s. The melting curve was 95ºC for 15 s previous to 60ºC for 1 min. ECO Real-Time PCR System was used for the experiments (Illumina, Inc., San Diego, CA, USA), and calculations made by the $2^{-\Delta\Delta Ct}$ method[39]. Student's test was used to check the statistical significance of differences between samples (p<0.05). The relative mRNA levels of the experimentally selected genes (target-genes) were calculated by referring to the mRNA levels of the housekeeping gene, *GADPH*, which had been verified as being expressed constitutively under the assay conditions. For valid quantification using

the 2 $^{-\Delta\Delta Ct}$ method, it is crucial that target and housekeeping PCR amplification efficiencies are approximately equal: we therefore verified that the efficiencies of the 2 PCR reactions differed by <10%. At least 2 independent biological replicas and 3 technical replicas of each of them were made for all the experiments.

Table 1. qPCR oligonucleotides.

Gene Name	Sequence	TM (°C) *	Hybridization Site **	Amplicon Size (bp)
AGER (RAGE)	F: 5′-TGTGTGGCCACCCATTCC-3′ R: 5′-CTGATCCTCCCACAGAGCC-3′	60.47 59.75	901–918 991–1009	109
DLAT	F: 5′-AACAGCGTGACTACAGGGTATG-3′ R: 5′-CCCAAAAGCTGCAGCAGTAAG-3′	60.68 60.64	795–816 875–895	101
FLNA	F: 5′-ACAGTGTCAATCGGAGGTCAC-3′ R: 5′-TGCACGTCACTTTGCCTTTG-3′	60.58 60.47	4942–4961 5040–5059	118
CFOS	F: 5′-GGGATAGCCTCTCTTACTACCAC-3′ R: 5′-GTGACCGTGGGAATGAAGTTG-3′	59.77 60.04	71–93 174–194	124
GAPDH	F: 5′-CCTCCTGCACCACCAACTG-3′ R: 5′-TGGCAGTGATGGCATGGA-3′	61.18 59.50	449–467 533–550	102
HMGB1	F: 5′-TCAAAGGAGAACATCCTGGCC-3′ R: 5′- GCTTGTCATCTGCAGCAGTGTT-3′	60.59 62.54	338–358 403–424	87
HMGB2	F: 5′-GAGCAGTCAGCCAAAGATAAACAA-3′R: 5′-TCCTGCTTCACTTTTGCCCTT-3′	60.37 61.01	403–426 493–513	111
HOXA10	F: 5′-CTCCCACACTCGCCATCTC-3′ R: 5′-CAAACCCAGCCCAGTCAGG-3′	60.43 61.19	1341–1359 1509–1527	187
KLK3 (PSA)	F: 5′-ACCCTGGCAGGTGCTTG-3′ R: 5′-GCAAGATCACGCTTTTGTTCCT-3′	60.08 60.61	108–124 202–223	116
KRT7	F: 5′-TGAATGATGAGATCAACTTCCTCAG-3′ R: 5′-TGTCGGAGATCTGGGACTGC-3	59.25 61.91	653–677 708–727	75
MAP1B	F: 5′-ACATCTTGGAACCTCCCACATC-3′ R: 5′-TGCAAACAAGGCAGAATCGC-3′	60.62 60.61	731–752 809–828	98
MIEN1	F: 5′-TTGGGGGCAGGAGAGAGAC-3′ R: 5′-TTACCGAGGCGAAGAGTGG-3′	61.21 59.68	519–537 607–625	107
MNAT1	F: 5′-TGTGCGGACACACTCTCTGTGAAA-3′ R: 5′-TCAACCTCCTTGTCAACAGTGGGA-3′	65.09 64.37	74–97 195–218	145
MT2A	F: 5′-AAAGGGGCGTCGGACAAG-3′ R: 5′- GGTCACGGTCAGGGTTGTAC-3′	60.54 60.90	223–240 321–340	118
NOP53	F: 5′-ACCAGTTCCTGGAAGACGTG-3′ R: 5′-CCTTTTTCCTTGGAGCCAG-3′	60.19 56.66	182–201 272–290	109
PMEPA1	F: 5′-AAGAGGAGTGAGAGGAAGGC-3′ R: 5′-GCTTGTGCATTCAGACCAGA-3′	59.02 59.05	929–948 1019–1038	110
SNAPIN	F: 5′-TGACAACCTAGCCACAGAACTG-3′ R: 5′-TCGCCGGGCATTAAGTAGC-3′	60.81 60.80	174–195 252–270	97
UBE2E3	F: 5′-AAGGTTACTTTCCGCACCAG-3′ R: 5′-AATAGTCAAAGCGGGACTCCA-3′	58.69 59.69	376–395 457–477	102
UHRF2	F: 5′-GGACCTTCCAATCAGCCATC-3′ R: 5′-GACATCTCTGGCATCCACCA-3′	58.90 60.04	316–335 395–414	99
YY1	F: 5′-AGCGGCAAGAAGAGTTACCTC-3′ R: 5′-TCTTGATCTGCACCTGCTTCTG-3′	60.65 61.20	538–558 619–640	103
ZNF428	F: 5′-CCCGAGCATTCCTCTGATTC-3′ R: 5′-TCGTCAGTGGTCTCCTCTTC-3′	58.70 59.04	79–98 154–173	95

* Tms were calculated using MFEprimer3.0 (http://mfeprimer.igenetech.com/) ** Hybridization sites are referenced to the starting codon (cDNA) for each gene (Ensembl database)

1.5. Western blot analysis

After performing protein cuantification through Bradford method (Bio-Rad Laboratories, Hercules, CA, USA), equal amounts of protein were subject to electrophoresis in a 10% SDS-PAGE at 80 V for 20 min followed by 200 V for 45-60 min. Proteins were transferred onto a PVDF membrane at 0.2 A for 1 h. The membrane was afterwards blocked with 5% (w/v) non-fat milk diluted in PBST 0.1% (PBS containing 0.1% Tween 20, Sigma-Aldrich, St. Louis, MO, USA) for 1 h at room temperature, followed by incubation with primary antibodies of HMGB2 (1:1000, ab67282, Abcam, Cambridge, UK, EU), PICT-1 (1:500, sc-517088, Santa Cruz Biotechnology, Dallas, TX, USA), or MIEN1 (1:200, XTP4,40-400, Invitrogen, Thermo Fisher Scientific Inc., MA, Waltham, USA) diluted in 5% (w/v) non-fat milk solution overnight at 4°C. Subsequent to overnight incubation, membrane was three times washed during 10 min with PBST 0.1% prior to incubation with G-protein HRP-linked (1:5000, 18-161 Millipore, Merck KGaA, Darmstadt, DE, EU) diluted in blocking solution for 1 h at room temperature. Lastly, three membrane washings of 10 min with PBST 0.1% were run before chemiluminescence-detection using Pierce ECL Western Blotting Substrate (A00042, Sigma-Aldrich, St. Louis, MO, USA). Bands were visualized in the ChemiDoc XRS System (Bio-Rad Laboratories, Hercules, CA, USA). The relative intensities of protein bands were analysed using the ImageLab analysis software (Bio-Rad Laboratories, Hercules, CA, USA).

1.6. HMGB1 and HMGB2 silencing by siRNA

The PC-3 cell line was transfected with small interfering (si)RNA oligonucleotides using Lipofectamine® 2000 (Life-Technologies-Invitrogen, Thermo Fisher Scientific Inc., MA, Waltham, USA). siRNA and Lipofectamine 2000 were each diluted separately with Opti-MEM (Gibco™, Thermo Fisher Scientific Inc., Waltham, MA, USA), mixed together and incubated for 5 min at RT. The mixture was added to cells plated in 3 mL RPMI 1610 medium (Gibco™, Thermo Fisher Scientific Inc., MA, Waltham, USA) (final concentration of siRNA, 50 nM). Cells were collected at 48h post transfection for further analysis. The following siRNAs from Ambion Inc. (Thermo Fisher Scientific Inc., Waltham, MA, USA) were used for the silencing of each gene: s20254 Silencer Select for HMGB1, s6650 for HMGB2 and AS02A5Z3 for the siRNA negative control. Total RNA was extracted from different conditions (siHMGB1, siHMGB2, siCtrl2) of the PC-3 cell line using GeneJET RNA Purification Kit (K0731, Thermo Fisher Scientific Inc., Waltham, MA, USA). The remaining DNA was removed by incubating with DNase I,

RNase-free (EN0521, Thermo Fisher Scientific Inc., Waltham, MA, USA). DNA-free RNA was finally purified using GeneJET RNA Cleanup and Concentration Micro Kit (K0842, Thermo Fisher Scientific Inc., Waltham, MA, USA). qPCR reactions were run in triplicate in an Eco™ Real-Time PCR System (Illumina Inc., San Diego, CA, USA) using 1ng per reaction. PC-3 lysates of each condition were extracted with lysis buffer (50 mM Tris-HCl pH 8, 150 mM NaCl, 0.1 % NP40, 1 mM EDTA, 2 mM MgCl2), and protein concentration was quantified using Bradford Reagent (Bio-Rad Laboratories, Hercules, CA, USA). Protein samples of 25-40 µg were loaded for Western blotting. PVDF membranes were incubated overnight at 4°C with primary antibodies against HMGB1 (1:1000, ab18256, Abcam, Cambridge, UK, EU), HMGB2 (1:1000, ab67282, Abcam, Cambridge, UK, EU), or α-tubulin (1:1000, sc-53646, Santa Cruz Biotechnology, Dallas, TX, USA).

1.7. Heat maps

Heat maps from change-fold ratios (Figures 5 and 6) were drawn with Heatmapper (http://heatmapper.ca/expression/), using complete linkage as clustering method and Euclidean distance as the measurement method[40].

1.8. Statistical analysis

Analyses were carried out using GraphPad Prism 6. Continuous variables were expressed as mean ± SE. Relative gene expression assays were tested using independent t-tests. A 2-tailed p-value test was used with $p < 0.05$ considered significant.

2. Results

2.1. HMGB1 and HMGB2 Y2H interactomes in adenocarcinoma primary tumour Human PCa

cDNA libraries were constructed using total RNA from PCa adenocarcinoma primary tumour. Y2H assays were carried out as described in Materials and Methods, using HMGB1 and HMGB2 as baits and triple screening by 3 independent selection markers. The panel of proteins interacting with HMGB proteins in these libraries is summarized in Table 2.

Table 2. Proteins identified in the HMGB1 and HMGB2 Y2H interactome in primary tumour adenocarcinoma. N: redundancy in clone isolation; Aa: sequenced region in clones relative to ATG.

HMGB1 interactants					
Genes (Aliases)	**Uniprot Code**	**N**	**Aa**	**Biological Function**	**Previous references to prostate cancer (PCa)**
c-FOS (G0S7)	P01100	2	27-184	Transcriptional regulation and control of cell growth and apoptosis[41].	Expression is elevated in the prostate upon castration-mediated androgen withdrawal[41].
GOLM1 (C9orf155, G OLPH2)	Q8NBJ4	1	236-376	PI3-AKT-mTOR signaling[42].	Up-regulated in PCa has oncogenic functions[42].
HNRNPU (C1orf199, HNRPU, SAFA)	Q00839	1	91-296	DNA and RNA binding[43].	Not previously reported.
MAP1B	P46821	2	2187-2409	Vesicle formation. It can interact with p53[44].	Not previously reported.
MAPKAPK5	Q8IW41	1	1-95	Involved in mTOR signaling[45]. MAPKAPK5 has diverse roles in cell growth, programmed cell death, senescence and motility[46].	Not previously reported.
MIEN1 (C35, C17orf37, RDX12, XTP4)	Q9BRT3	3	24-204	Regulator of cell migration and invasion[47].	MIEN1 increases invasive potential of PCa cells by NF-κB mediated downstream target genes[47].
MT2A (CES1, MT2)	P02795	1	8-61	Binding to heavy metals[48].	MT2A is up-regulated under hypoxia in PCa cell lines, PCa tissue and residual cancer cells after androgen ablation therapy[49].

Table 2 Continued

HMGB1 interactants					
Genes (Aliases)	**Uniprot Code**	**N**	**Aa**	**Biological Function**	**Previous references to prostate cancer (PCa)**
PSMA7 (HSPC)	O14818	1	173-248	Enhances AR transactivation in a dose-dependent manner[50] and inhibits the transactivation function[51].	Proposed biomarker in PSA[52].
PTPN2 (PTPT)	P17706	3	1-221	Tyrosine-specific phosphatase (TCPTP) negatively regulates STAT3 that is involved in proliferation, differentiation migration, and apoptosis[53].	Not previously reported.
RASAL2 (NGAP)	Q9UJF2	1	97-334	Tumour suppressor via Ras[54].	Not previously reported.
RSF1 (HBXAP, XAP8)	Q96T23	1	572-795	Chromatin remodeling factor necessary for p53-dependent gene expresión in response to DNA damage[55].	RSF1 is overexpressed in PCa and contributes to prostate cancer cell growth and invasion[56].
SRSF3 (SFRS3, SRP20)	P84103	2	1-164	Oncogenic splicing factor[57].	SRSF3 expression is induced by hypoxia in prostate cancerous cells[58].
TAF3	Q5VWG9	5	2-222	Transcriptional regulation.Interacts with and inhibits p53[59].	Not previously reported.
TGM3	Q08188	1	480-693	Catalyze the irreversible cross-linking of peptide-bound glutamine residues to lysines or primary amines. Involved in apoptosis[60].	Not previously reported.
UBC	P0CG48	1	28-181	Unanchored-polyubiquitin has several roles in activation of protein kinases and signaling[61].	Not previously reported.
WNK4 (PRKWNK4)	Q96J92	4	9-208	Regulates STE2- related protein kinases that function upstream of MAPK pathways[62].	Not previuosly reported.
YY1 (INO80S)	P25490	1	27-223	Transcriptional regulation[63].	Involved in PCa[63–65].
ZNF428 (C19orf37)	Q96B54	2	89-188	Unknown.	Not previously reported.

Table 2 Continued

Genes (Aliases)	Uniprot Code	N	Aa	Biological Function	Previous references to prostate cancer (PCa)
C1QBP (GC1QBP, HABP1, SF2P32)	Q07021	10	57-282	Control of mitochondrial energetic metabolism. Promotes cell proliferation, migration and resistance to cell death[66].	Highly expressed in PCa and associated with shorter prostate-specific antigen relapse time after radical prostatectomy[67].
FLNA (FLN, FLN1)	P21333	5	106-366	A C-terminal fragmento of FLNA co-localizes with the androgen receptor AR to the nucleus, and downregulates AR function[68].	FLNA has been clinically validated for better diagnosis of PCa[69]. Regulated by miRNA205[70].
MIEN1 (C35, C17orf37, RDX12, XTP4)	Q9BRT3	4	1-116	Regulates cell migration and apoptosis[47].	Overexpressed in PCa cells. MIEN1 overexpression functionally enhances invasion of tumour cells via modulating the activity of AKT[47].
MYL6	P60660	2	1-150	Regulatory light chain of myosin II. Myosin II, expressed in non-muscle tissues, plays a central role in cell adhesión, migration and division[71].	Not previously reported.
NOP53 (GLTSCR2, PICT-1, GLT)	Q9NZM5	35	163-428	Nucleolar NOP53 stabilizes p53 in response to ribosomal stresses[72–74]. NOP53 is involved in DNA damge response[75,76].	Nuclear NOP53 is downregulated in prostatic adenocarcinomas compared to non-cancerous prostatic tissues and aberrantly ex-pressed in the cytoplasm of prostatic cancer cells[77].
RPS28	P62857	1	8-52	Ribosome component. Its decrease blocks pre-18S ribosomal RNA processing, resulting in a reduction in the assembly of 40S ribosomal subunits[78].	Not previously reported.
COMMD1 (C2orf5, MURR1)	Q8N668	1	1-180	Regulates oxidative stress, NF-κB activity in prostate cancer cells[79].	Degradation of COMMD1 and I-kappaB induced by clusterin enhances NF-κB activity in prostate cancer cells[80].

The interactions of identified proteins with HMGB1 or HMGB2 have not previously been reported on BioGRID, STRING or other public databases, although we have previously reported that Vigilin (encoded by HDLBP gene) and ZNF428 interact with HMGB2 in non-cancerous epithelial cells[81]. Interestingly, several identified proteins have previously been related to PCa, supporting the functional significance of our Y2H interactome data in PCa research. Indeed, the oncogenic capacities of several identified proteins in our Y2H interactome had been already reported in PCa or other cancerous models by a wide range of functional approaches. Figure 1 presents a summary of the functional characteristics of proteins identified in the adenocarcinoma PCa screening and previous screenings performed in our laboratory on the PC-3 cell line[36]. The detected proteins are remarkably associated to cancer hallmarks (Figure 1A), and the number of available references of each protein functionally related to cancer progression in diverse models is also shown (Figure 1B).
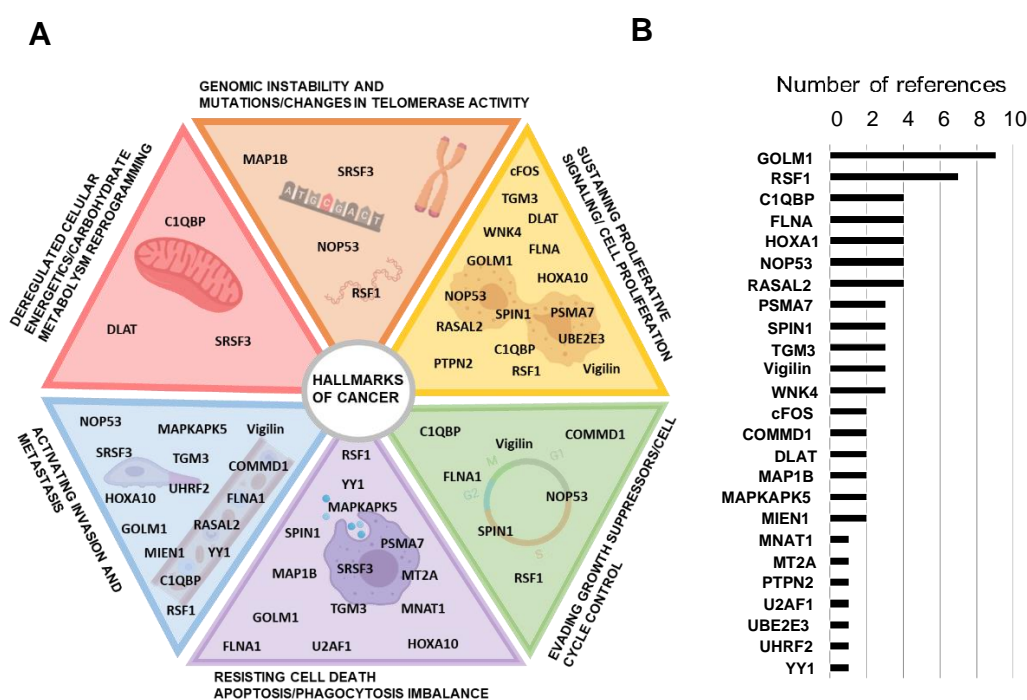
Figure 1. Relatioship between identified proteins and cancer hallmarks. (a) Distribution of HMGB1 and HMGB2 interactome targets according to cancer hallmarks: MAP1B[82,83], NOP53[72,84–86], RSF1[56,87–89], SRSF3[90–94], C1QBP[67,95–97], cFOS[98,99], DLAT[100], FLNA[68,101], GOLM1[42,102–105], HOXA10[106,107], PSMA7[108,109], PTPN2[110], RASAL2[111–113], SPIN1[114], TGM3[115], UBE2E3[116], Vigilin[117], WNK4[62], COMMD1[118,119], MAPKAPK5[46,120], MNAT1[121], MT2A[122], YY1[123–125], MIEN1[126,127]. (**b**) Number of references that associate these proteins with cancer hallmarks according tu PUBMED (7-31-2019). Created with BioRender.com.

In order to confirm HMGB2 interactions with MIEN1 and NOP53 identified in the adenocarcinoma PCa Y2H approach, a co-immunoprecipitation assay was performed using the DU-145 tumoural prostate cell line (Figure 2). This line was selected because PC-3 overexpresses miR-940, which targets MIEN1 mRNA[127] decreasing significantly its protein concentration and making more difficult its detection through Western blot.
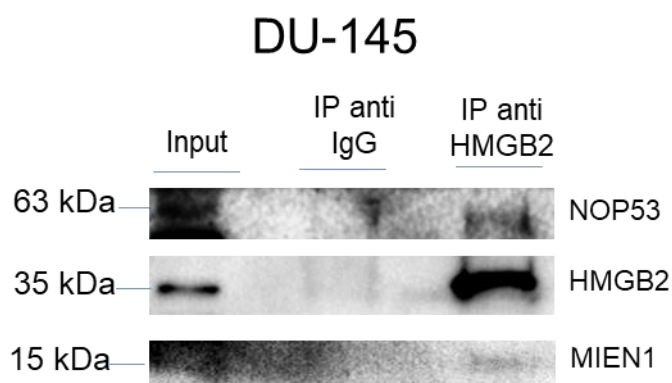
Figure 2. Co-immunoprecipitation of HMGB2, NOP53 and MIEN1 in DU-145 cells.

2.2. Mutations and copy number alterations in HMGB1 *and* HMGB2 *interactome-targets in PCa*

The frequency of mutations and copy number alterations (CNA) in genes encoding HMGB1 and HMGB2 proteins were analyzed, as well as in those genes encoding proteins detected in the Y2H search carried out in this study; previous data obtained screening PC-3 libraries were also included to have a more general analysis. We have used the open platform for exploring cancer genomics data, c-Bioportal[128,129]. We included 14 PCa studies available at cBioPortal (https://www.cbioportal.org/)[130,131,140–145,132–139]. From these, 10 were adenocarcinoma studies[131,132,134–137,140–145], with 3218 samples; the other 3 studies correspond to metastatic PCa[130,138,146], including 655 samples; and finally one study corresponds to neuroendocrine PCa, which was carried with 114 samples[139].
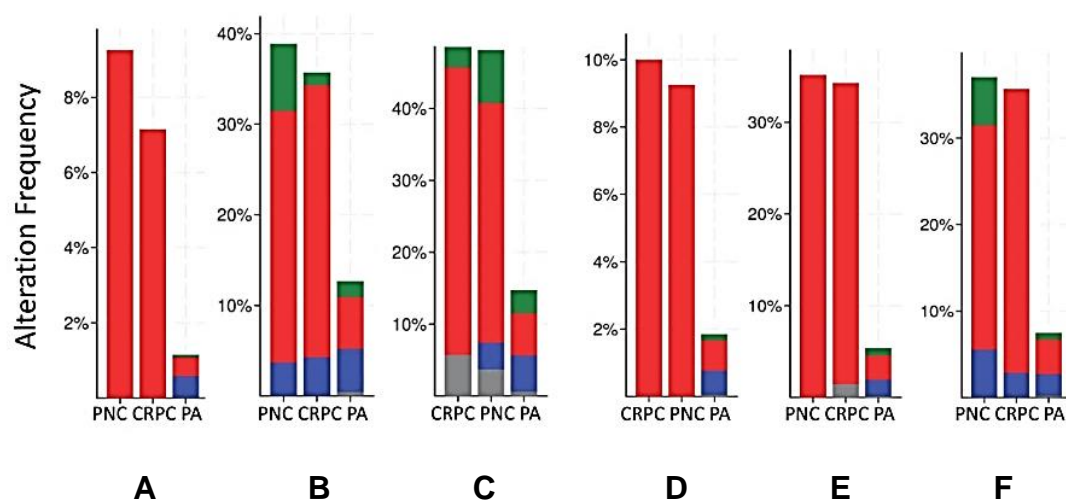
Figure 3. **Copy Number Alteration frecuency of HMGB1 and HMGB2 and its targets in Prostate Cancer.** (**A**) HMGB1, (**B**) HMGB1 interactome targets from PC-3 library[36], (**C**) HMGB1 interactome targets from prostate adenocarcinoma tissue library, (**D**) HMGB2, (**E**) HMGB2 interactome targets from PC-3 library[36], (**F**) HMGB2 interactome targets from prostate adenocarcinoma tissue library. PNC, Prostate Neuroendocrine Carcinoma; CRPC, Castration Resistant Prostate Cancer; PA, prostate adenocarcinoma; Data source: combined study from data available through c-Bioportal. Color legend: Deep deletion (Blue), Multiple alteration (Grey), Mutation (Green), Amplification (Red).

The data show that mutations and CNA affecting HMGB1, HMGB2 and the proteins identified in the corresponding Y2H interactome are more frequently present in neuroendocrine PCa and castration-resistant PCa than in adenocarcinoma (Figure 3).

Since neuroendocrine PCa is an aggressive PCa[25], we tested whether CNA of these genes was also related to the poor prognosis in patients diagnosed with adenocarcinoma. Being amplification the most frequent detected CNA in Figure 3, we compared Disease/Progression-free Kaplan-Meier Estimate rates calculated from the study of Taylor *et al.*[145] among the group of samples having gains or amplifications of these genes and the group integrated by the rest of samples. Figure 4 shows that gain or amplification of HMGB2 interactome targets results in a notorious decrease of the median of months disease-free, with high significant p-values in the Logrank test.
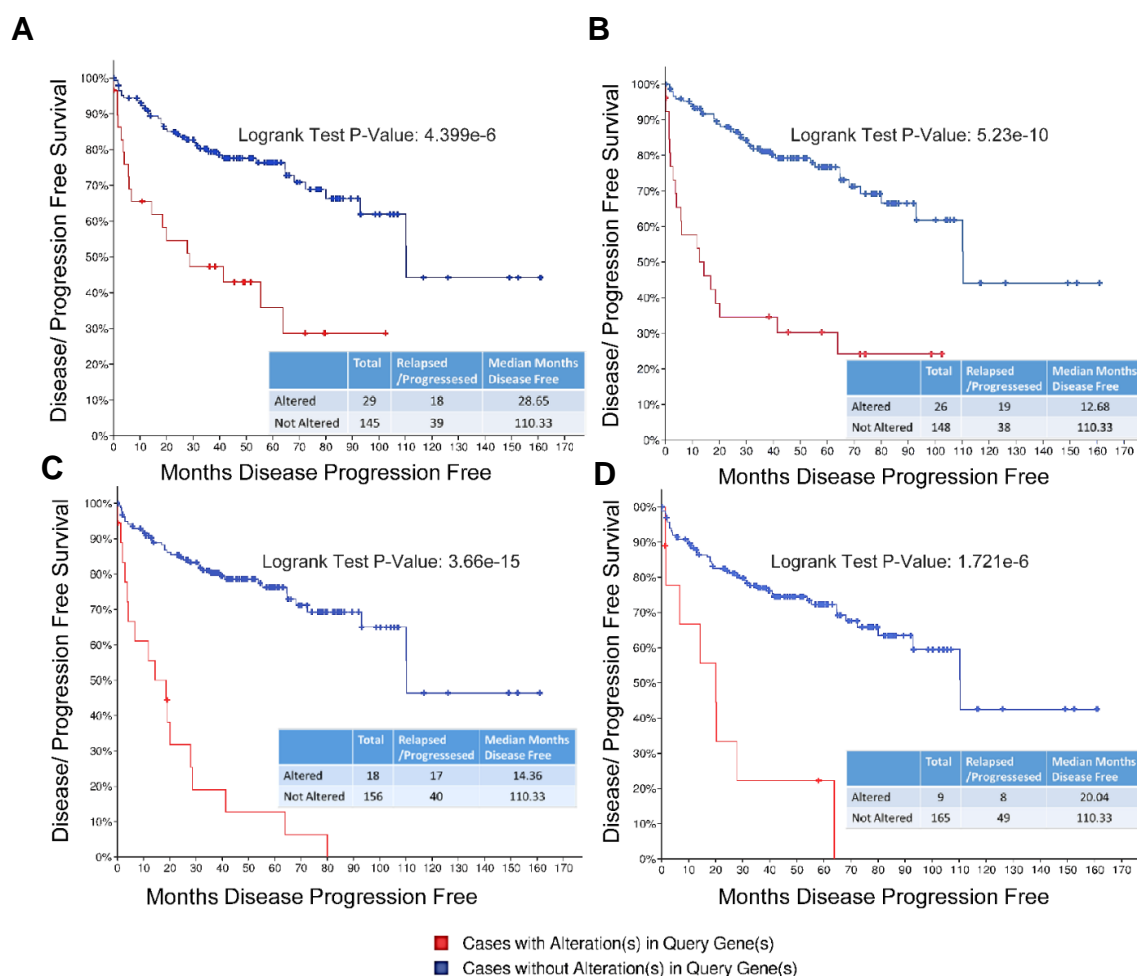
Figure 4. Disease/Progression-free Kaplan-Meier Estimate. A. Cases altered in HMGB1 interactome targets from PC-3 library[36]. **B.** Cases altered in HMGB1 interactome targets from Prostate Adenocarcinoma tissue library. **C.** Cases altered in HMGB2 interactome targets from PC-3 library[36]. **D.** Cases altered in HMGB2 interactome targets from Prostate Adenocarcinoma tissue library. Data source Prostate adenocarcinoma study[145], including 194 patients/samples.

2.3. Expression of HMGB1 and HMGB2 interactome-targets in PCa

According to published data, while HMGB1 has been related with the epithelial to mesenchymal transition (EMT) in prostate tumoural cells and its overexpression has been associated with poor prognosis in this type of cancer[13,147], there are also studies which stablish that HMGB2 expression increases in PCa cell lines and tissues from PCa, especially in metastasis[148]. With published data of RNA levels in PCa samples[145]

retrieved from Gene Expression Omnibus (GEO Accession: GSE21032), the change fold expression of HMGB1 and HMGB2 interactome-targets were evaluated. Data obtained in this study and previous works in our laboratory[36] in the PCa PC-3 cell line[36] were compared *versus* non-cancerous cells, from which a heat-map was constructed (Figure 5A). Using the same source, data was retrieved from 181 adenocarcinoma primary tumours, which were distributed in 3 groups clinically classified by Gleason scores, and a 4th group integrated by 37 metastatic tumours. The change fold expression of HMGB1 and HMGB2 interactome-targets in each group *versus* non-cancerous cells from healthy tissues were calculated, from which the heat-map shown in Figure 5B was constructed.

The classification of each gene in the main clusters of the heat-maps proved to be unrelated with the experimental library origin of the clone (PC-3 cell line or PCa adenocarcinoma primary tumour). The results reveal that genes encoding 11 proteins interacting with HMGB1 (Figure 5A top panel) are also upregulated in the 2 PCa cell lines (PC-3, DU-145 or LNCaP), and 8 more are upregulated in one or two PCa cell lines. Among the detected HMGB2 partners, 2 are upregulated in the 3 PCa cell lines, 1 in 2 and 3 in at least one (Figure 5A lower panel). In HMGB1 and HMGB2 interactomes, the targets upregulated in metastatic tissue (Figure 5B) are a subset of those upregulated in one or more of the PCa cell lines. Analyzing the genes expression in reference to Gleason score, 2 genes (TMG3 and GOLM1) are upregulated in all the groups, whereas the others are only upregulated in groups classified with a Gleason score of less than or equal to 7 (PTPN2, HDLBP, SRF3, FOS, WNK4). Regarding a pattern associated to the existence of metastasis, 3 genes that are not upregulated in samples from primary tumours are upregulated in metastasis: PSMA7, UBE2E3 and MIEN1 (Figure 5B). The classification of each gene in the main clusters of the heat-maps proved to be unrelated with the experimental library origin of the clone (PC-3 cell line or PCa adenocarcinoma primary tumour). The results reveal that genes encoding 11 proteins interacting with HMGB1 (Figure 5A top panel) are also upregulated in the 2 PCa cell lines (PC-3, DU-145 or LNCaP), and 8 more are upregulated in one or two PCa cell lines. Among the detected HMGB2 partners, 2 are upregulated in the 3 PCa cell lines, 1 in 2 and 3 in at least one (Figure 5A lower panel).
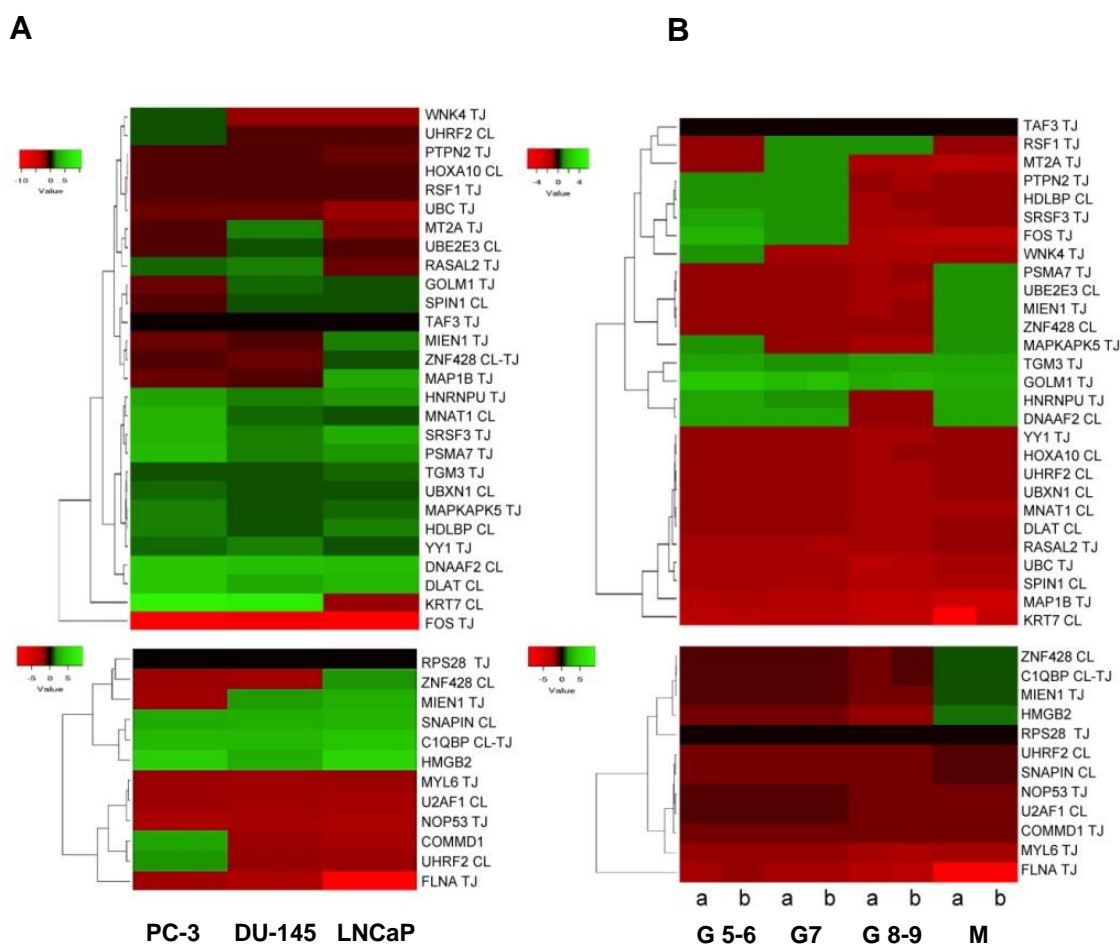
Figure 5. **Heat map expression in prostate cancer.** (a) Expression of HMGB1 (upper panel) and HMGB2 interactome targets (lower panel) in 3 prostate cancer cell lines. (b) Expression of HMGB1 interactome partners (upper panel) and HMGB2 interactome targets in prostate adenocarcinoma cases classified by Gleason (G) score groups or metastatic (M) tumours. CL, targets detected in the PC-3 library[36]. TJ, target detected in the prostate adenocarcinoma library. Data extracted from GEO Accession: GSE21032.

In HMGB1 and HMGB2 interactomes, the targets upregulated in metastatic tissue (Figure 5B) are a subset of those upregulated in one or more of the PCa cell lines. Analyzing the genes expression in reference to Gleason score, 2 genes (TMG3 and GOLM1) are upregulated in all the groups, whereas the others are only upregulated in groups classified with a Gleason score of less than or equal to 7 (PTPN2, HDLBP, SRF3, FOS, WNK4). Regarding a pattern associated to the existence of metastasis, 3 genes that are not upregulated in samples from primary tumours are upregulated in metastasis: PSMA7, UBE2E3 and MIEN1 (Figure 5B).

2.4. Silencing of HMGB1 *and* HMGB2 *reveals regulation of the expression of genes encoding their interactome-targets*

To test whether changes in HMGB1/2 protein levels in PCa cells could also be influencing the expression of their interactome-targets, HMGB1 and HMGB2 in PC-3 cells were silenced by siRNA (Figure 6A) with the colaboration of Martín Salamini Montemurri[149].
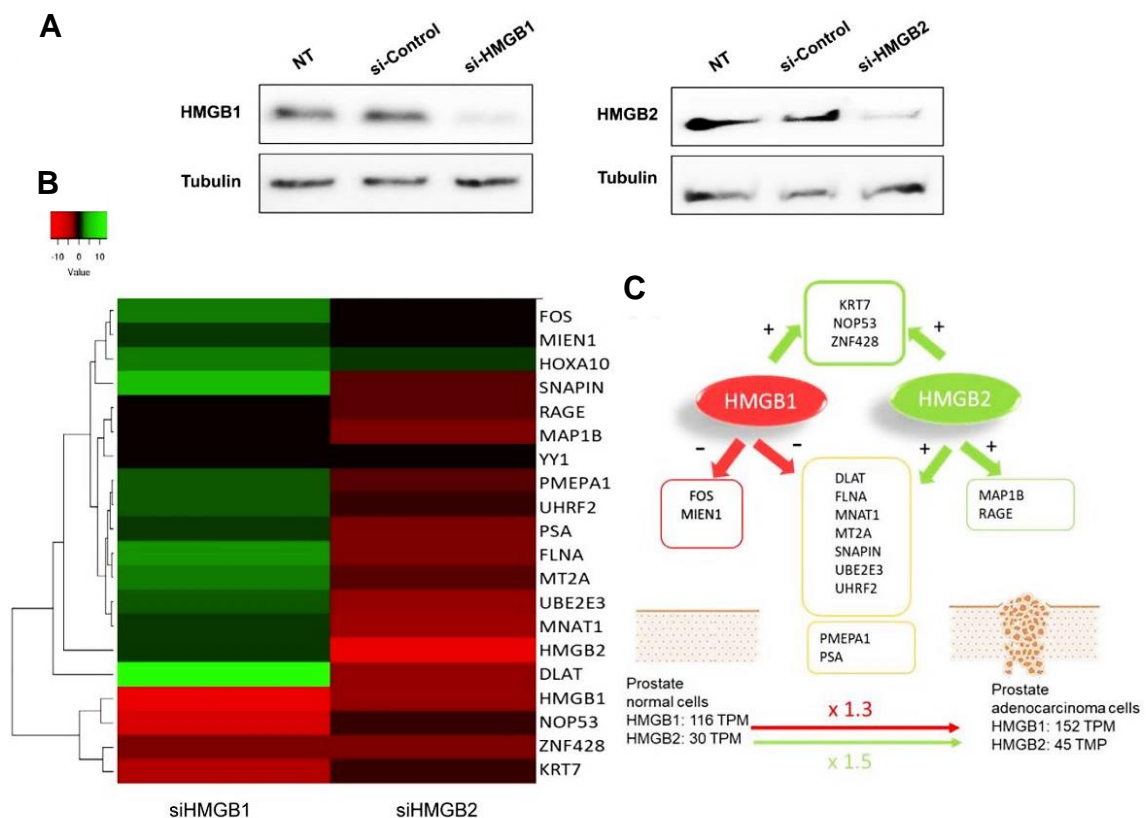
Figure 6. HMGB1 and HMGB2 silencing. **A.** Western Blot showing HMGB1 and HMGB2 silencing. **B.** Heat map comparing the pattern of expression (siHMGB1/HMGB1 and siHMGB2/HMGB2). **C.** Summary of regulatory effects of HMGB1 and HMGB2 on the selected genes.

Levels of mRNA from 14 partners analyzed by RT-qPCR and changes (siHMGB/HMGB) are summarized in the Figure 6B. This analysis also included HMGB1, HMGB2, and the well-known PCa biomarker, PSA (encoded by KLK3); PMEPA1, which is involved in downregulation of the androgen receptor, promoting androgen receptor-negative prostate cell proliferation[150], and RAGE, one of the membrane receptors in the extracellular signaling function of HMGB1[151].

Silencing of HMGB1 causes overexpression of the larger cluster of the Y2H interactome, whereas siHMGB2 has the opposite effect (Figure 6B). HMGB1 downregulates the expression of the majority targets analyzed, and conversely HMGB2 upregulates them. Therefore, the expression level of each regulated target would depend on the relative imbalance of HMGB1 and HMGB2, and the differential effect of both HMGB proteins on the expression of each partner. PMEPA1 and PSA, well-known PCa biomarkers, are also oppositely regulated by HMGB1 and HMGB2 (Figure 6C).

3. Discussion

High mobility group box B (HMGB) proteins are pivotal in the development of cancer[6,9,11], and HMGB1 overexpression has been related to principal cancer hallmarks[8]. Interactome targets of HMGB1 and HMGB2 that have been identified in our Y2H study were previously found to be related to cancer hallmarks (Figure 1), and are also dysregulated in PCa, as confirmed by detection of changes in mRNA or protein levels. DNAAF2[61], U2AF1[152], C1QBP[67], Snapin[153] or Vigilin[153] are upregulated in prostate tumours or PCa cell lines[36]. Other proteins detected in Y2H approaches increase their expression after androgen-deprivation therapy, such as KRT7 or NOP53[154]. Functional studies interfering the expression of several of the proteins revealed by our study also directly associated them to PCa. In this sense, selective knockdown of C1QBP through siRNA decreased cyclin D1, increased p21 expression and led to G1/S arrest in PCa cells, and had no effect on a non-cancerous cell line[67]. NOP53 acts as a tumour suppressor, and knockdown of the gene in the PCa LNCaP cell line increased the invasiveness of these cells as measured in a xenograft animal model[77]. Two already known regulatory factors have been found among the HMGB1 interactome targets, Ying Yang 1 (YY1) and Homeobox A10 (HOXA10), and both are associated with PCa. YY1 is upregulated in human PCa cell lines and tissues[64]. Inhibition of YY1 reduces expression of genes related to the Krebs cycle and electron transport chain in PCa cell lines[155], and YY1 depletion correlates with delayed progression of PCa[123]. Overexpression of YY1 can promote epithelial-mesenchymal transition by reducing hnRNPM expression[156]. YY1 can also silence tumour suppressor genes, such as XAF1 in PCa[65]. In summary, YY1 is a recognized PCa driver[64], and different complexes in which YY1 takes part can induce activation or repression of gene expression, including also AR-YY1-mediated PSA transcription[157], which we found is also regulated by HMGB1 and HMGB2 silencing. HOXA10 is upregulated in PCa[158], and inverse correlations between HOXA10 expression and Gleason pattern, Gleason score, and pathological stage are known[159], although downregulation of HOXA10 gene

expression may enhance lipogenesis to promote PCa cell growth and tumour progression to the castration-resistant stage[160]. Silencing of HOXA10 expression in PC-3 cells by iRNA decreased proliferation rates, whereas HOXA10 overexpression had the opposite effect[158].

Concerning HMGB2, among novel proteins detected through this Y2H approach two are outstanding: NOP53 and MIEN1. NOP53 is a nucleolar protein involved in ribogenic and cell cycle regulation processes[161]. Although this protein generally localizes in the nucleoli[156,157], it eventually associates with other proteins and complexes in the nuclei and cytoplasm. It is also involved in key pathways associated to p53 regulation and cancer though mechanisms in which the RPL11 protein and the 5 RNP complex take part[73,75,162,163]. There is controversy concerning to NOP53's role in cancer. Different studies have characterize it as both oncogenic or tumour supressor protein, being its role in Phosphatase and Tensin homolog (PTEN) stabilization, caused by promotion of kinase mediated phosphorilation[164] of PTEN, an example of the last one (Figure 7). PTEN mutations are in the origin of many cancers and its subtained phosphatase enzymatic activity caused by NOP53 promotes the inactivation of oncogenic downstream signaling pathways such as those associated to protein kinase B also known as Akt, which isoforms are overexpressed in a variety of human tumours[86,163,165].
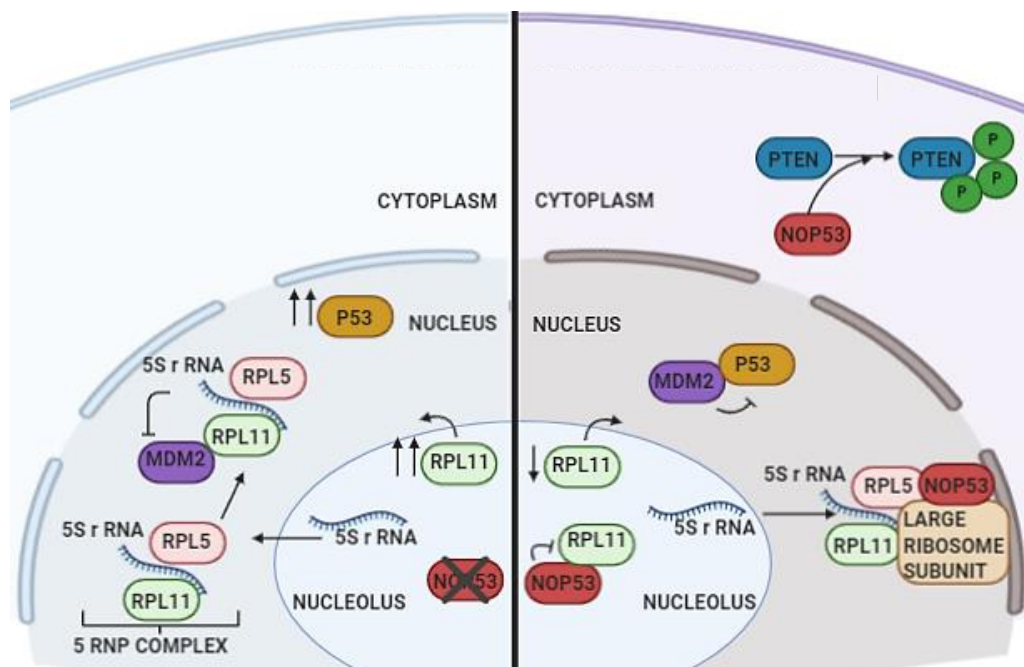
Figure 7. NOP53 protein interactions related with tumourogenesis. (⟶):activation. (⊣): inhibition. (↑↑): upregulation. (↓): downregulation. (↱): translocation. Both, presence and absence of NOP53 protein lead to ambiguous effects conditioning proliferation as well as apoptosis pathways. Created with BioRender.com.

On the other hand, MIEN1 is anchored to the inner celular membrane and has a role in the regulation of cytoskeleton, modulating proteins such as actin[166], cofilin[126,167], annexin A2[168], and PTK2 protein tyrosine kinase 2 (PTK2), also known as focal adhesion kinase (FAK)[118]. The modulation of actin polymerization and its depolymerization through cofilin allows the extension of the leading cell edge when cells migrate[169]. Its association with the cytoskeleton and Akt pathway[47], described in Figure 8, conferes MIEN1 oncogenic properties and involves it in invasion and metastatic processes[47]. The HMGB2 translocation to different compartments of the cell from the nuclei has been already described[170], which would allow to explain the interaction between HMGB2 and MIEN1.
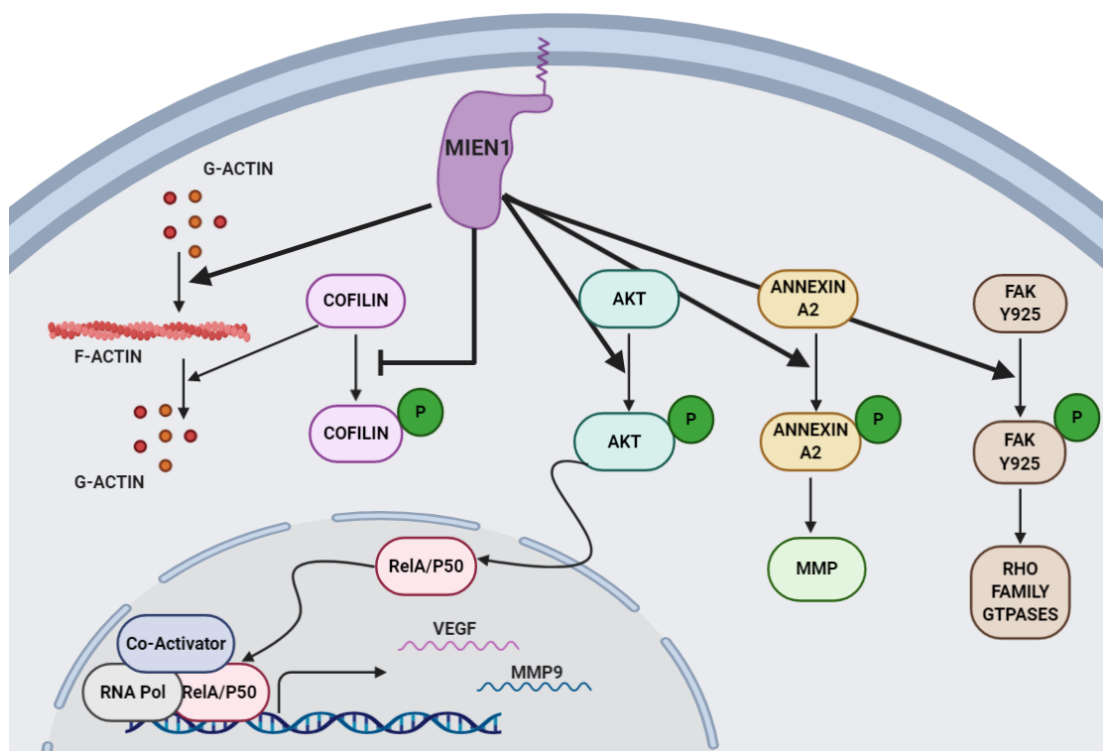
Figure 8. MIEN1 protein interactions related with tumourogenesis. (⟶ **): activation. (** ⊣ **): inhibition. (** ⇄ **): translocation.** MIEN1 interacts with key proteins involved in cell motility and in the promotion of transcription oncogenes such as vascular endothelial growth factor (VEGF), a potent and specific angiogenic factor, or matrix metalloproteinase (MMP) 9 an important component of the metastatic niche early in tumourigenesis, which promotes circulating tumour cells to colonize other tissues. RELA and p50 is the mostly commonly found heterodimer complex among NF-κB homodimers and heterodimers, and is the functional component participating in nuclear translocation and activation of NF-κB. FAK-Y925 represents FAK phosphorilated in Y925. Created with BioRender.com.

Physical interaction between these PCa associated proteins and HMGB proteins has not previously been described, and our results therefore show that there is a connection between HMGB1 and HMGB2 functions and those of their binding partners in PCa. Considering that HMGB2 and a subset of their interactome partners, including HMGB1, are upregulated in PCa, we silenced HMGB1 and HMGB2 and analyzed the mRNA levels of a group of randomly selected partners in PC-3 cells (Figure 6). The data show that HMGB1 and HMGB2 control the expression of them, which might contribute to the orchestrated action of all these proteins in PCa. HMGB2 activates many of the tested targets, but unexpectedly HMGB1 has the opposite effect.

One can propose several reasons to explain upregulation of targets in these circumstances. Data from GTEx Project[171] indicates that, although both HMGB1 and HMGB2 are upregulated in PCa versus non-cancerous cells, the relative increase is higher for HMGB2 (1.5 fold) than HMGB1 (1.3 fold); this could explain the increased expression of several of their targets, assuming that positive regulation caused by HMGB2 predominates over negative regulation caused by HMGB1 during the onset of PCa. Alternatively, differential interaction of HMGB1 or HMGB2 with their different nuclear partners, the transcript factors detected in our Y2H analysis being among them, might condition their positive or negative regulatory role on the expression of specific genes.

Clinically, a high frequency of CNA of the genes encoding the identified proteins is associated to the most aggressive forms of PCa, small cell neuroendocrine carcinoma (SCNC) or castration-resistant PCa (Figure 3). Their gain or amplification in the genome of the cancerous cells are positively correlated to a lesser disease-free period for PCa patients (Figure 4). The mRNA levels of a subset of these proteins are also higher in metastases than primary tumours (Figure 5). In conclusion, the set of proteins detected through our HMGB1-HMGB2 Y2H analysis are associated to the most aggressive cases of PCa. Although the PSA-based test is routinely employed for screening of PCa, it has resulted in over diagnosis and over treatment of non-aggressive cancers, thus reducing the quality of life of patients. Consequently, an improvement is necessary in the initial stages to discriminate between high-risk from low risk cancers. Our data on HMGB1 and HMGB2 interactome targets, considering their correlation to high aggressiveness and bad prognosis, is a good starting point to develop new serum protein panels for improvement of PCa diagnosis. Indeed, FLNA has already been proposed in a clinical validated PCa biomarker panel in serum[69]. Considering the relative expression levels of our HMGB1 and HMGB2 interactome targets in non-cancerous cells or in blood of health subjects differ quite notably (Figure 9), one might

anticipate that more sensitive analyses could be carried out using as biomarkers those proteins that are usually lowly expressed in non-cancerous cells; thus their levels are also low in the blood of healthy individuals. For instance, FLNA reported as a possible biomarker[69] is one of the 50 proteins most strongly expressed in normal prostate, and high levels are also detected in the blood of healthy individuals, whereas other detected HMGB1 or HMGB2 interactome targets in our study,e.g. DNAAF2, GOLM1 or TGM3, are in the lowest rank of detection in non-cancerous samples and their increase should
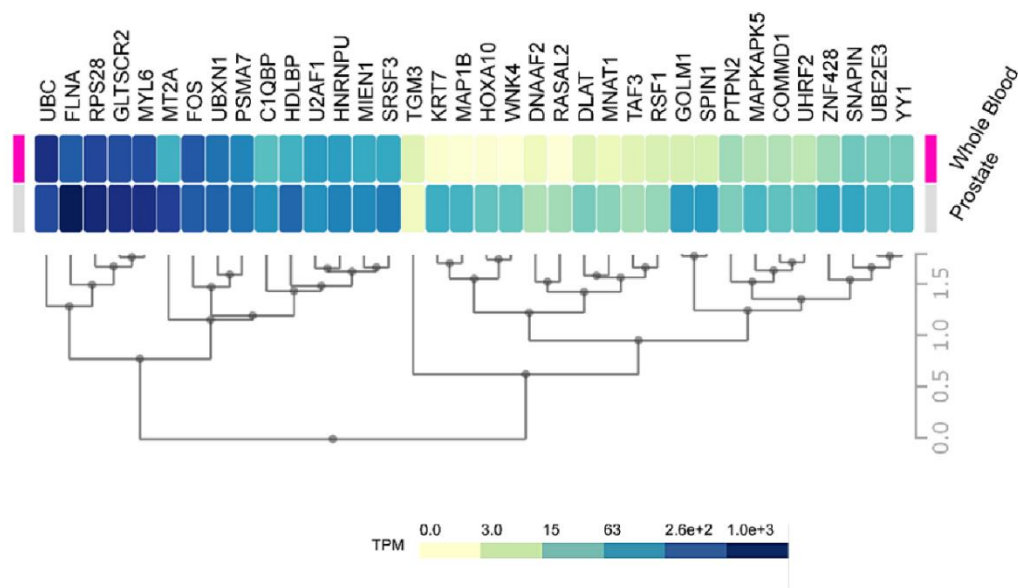
Figure 9. Prostate and blood levels of HMGB1 and HMGB2 interactome partners in healthy men. Expression of HMGB1 and HMGB1 interactome targets in prostate tissue and whole blood in healthy men. Data were directly obtained and processed from the GTEx Project through Expression Atlas, an integrated database of gene and protein expression in humans, animals and plants[172] accessed through https://www.ebi.ac.uk/gxa/experiments/E-MTAB-5214/Results.

In conclusion, we have carried out the first HMGB1/HMGB2 interactome approach in PCa using adenocarcinoma tissue. Gene or protein expression of the majority targets are dysregulated in PCa, and functional relationships between these proteins and PCa had also previously been confirmed by different laboratories using different models and technical approaches. We have shown by interference analysis that several HMGB1 and HMGB2 partners are regulated by HMGB1 and HMGB2, which might contribute to the coordination of their cellular action in PCa. Copy number alterations in the detected HMGB1 and HMGB2 partners are associated to aggressive forms of PCa and a poor prognosis. These characteristics can potentially be used as discriminatory biomarkers between high and low risk patients.

References

1. Catena, R. *et al.* HMGB4, a novel member of the HMGB family, is preferentially expressed in the mouse testis and localizes to the basal pole of elongating spermatids. *Biol. Reprod.* **80**, 358–366 (2009).

2. Pusterla, T., de Marchis, F., Palumbo, R. & Bianchi, M. E. High mobility group B2 is secreted by myeloid cells and has mitogenic and chemoattractant activities similar to high mobility group B1. *Autoimmunity* **42**, 308–310 (2009).

3. Ugrinova, I., Pashev, I. G. & Pasheva, E. A. Nucleosome binding properties and Co-remodeling activities of native and in vivo acetylated HMGB-1 and HMGB-2 proteins. *Biochemistry* **48**, 6502–6507 (2009).

4. Swanson, P. C. Fine structure and activity of discrete RAG-HMG complexes on V(D)J recombination signals. *Mol. Cell. Biol.* **22**, 1340–1351 (2002).

5. Bagherpoor, A. J. *et al.* Properties of Human Embryonic Stem Cells and Their Differentiated Derivatives Depend on Nonhistone DNA-Binding HMGB1 and HMGB2 Proteins. *Stem Cells Dev.* **26**, 328–340 (2017).

6. Ke, S. *et al.* Downregulation of high mobility group box 1 modulates telomere homeostasis and increases the radiosensitivity of human breast cancer cells. *Int. J. Oncol.* **46**, 1051–1058 (2015).

7. Yin, H. *et al.* HMGB1-mediated autophagy attenuates gemcitabine-induced apoptosis in bladder cancer cells involving JNK and ERK activation. *Oncotarget* **8**, 71642–71656 (2017).

8. Tang, D., Kang, R., Zeh 3rd, H. J. & Lotze, M. T. High-mobility group box 1 and cancer. *Biochim. Biophys. Acta* **1799**, 131–140 (2010).

9. Liu, K. *et al.* MIR34A regulates autophagy and apoptosis by targeting HMGB1 in the retinoblastoma cell. *Autophagy* **10**, 442–452 (2014).

10. Chandrasekaran, K. S., Sathyanarayanan, A. & Karunagaran, D. Downregulation of HMGB1 by miR-34a is sufficient to suppress proliferation, migration and invasion of human cervical and colorectal cancer cells. *Tumour Biol.* **37**, 13155–13166 (2016).

11. Tang, C. *et al.* Downregulation of miR-130a promotes cell growth and epithelial to mesenchymal transition by activating HMGB2 in glioma. *Int. J. Biochem. Cell*

Biol. **93**, 25–31 (2017).

12. Liu, P. L. *et al.* microRNA-200c inhibits epithelial-mesenchymal transition, invasion, and migration of lung cancer by targeting HMGB1. *PLoS One* **12**, 1–19 (2017).

13. Zhang, J. *et al.* High mobility group box 1 promotes the epithelial-to-mesenchymal transition in prostate cancer PC3 cells via the RAGE/NF-kappaB signaling pathway. *Int. J. Oncol.* **53**, 659–671 (2018).

14. van Beijnum, J. R. *et al.* Tumor angiogenesis is enforced by autocrine regulation of high-mobility group box 1. *Oncogene* **32**, 363–374 (2013).

15. Wu, Z. B. *et al.* High-mobility group box 2 is associated with prognosis of glioblastoma by promoting cell viability, invasion, and chemotherapeutic resistance. *Neuro. Oncol.* **15**, 1264–1275 (2013).

16. Wang, W. *et al.* Overexpression of high mobility group box 1 and 2 is associated with the progression and angiogenesis of human bladder carcinoma. *Oncol. Lett.* **5**, 884–888 (2013).

17. Taniguchi, N. *et al.* Expression patterns and function of chromatin protein HMGB2 during mesenchymal stem cell differentiation. *J. Biol. Chem.* **286**, 41489–41498 (2011).

18. Taniguchi, N. *et al.* Chromatin protein HMGB2 regulates articular cartilage surface maintenance via beta-catenin pathway. *Proc. Natl. Acad. Sci. U. S. A.* **106**, 16817–16822 (2009).

19. Balani, P. *et al.* High mobility group box2 promoter-controlled suicide gene expression enables targeted glioblastoma treatment. *Mol. Ther.* **17**, 1003–1011 (2009).

20. Ronfani, L. *et al.* Reduced fertility and spermatogenesis defects in mice lacking chromosomal protein Hmgb2. *Development* **128**, 1265–1273 (2001).

21. Zhou, X. *et al.* HMGB2 regulates satellite-cell-mediated skeletal muscle regeneration through IGF2BP2. *J. Cell Sci.* **129**, 4305–4316 (2016).

22. Aird, K. M. *et al.* HMGB2 orchestrates the chromatin landscape of senescence-associated secretory phenotype gene loci. *J. Cell Biol.* **215**, 325–334 (2016).

23. Guerrero, A. & Gil, J. HMGB2 holds the key to the senescence-associated secretory phenotype. *J. Cell Biol.* **215**, 297–299 (2016).

24. Fan, Z., Beresford, P. J., Zhang, D. & Lieberman, J. HMG2 interacts with the nucleosome assembly protein SET and is a target of the cytotoxic T-lymphocyte protease granzyme A. *Mol. Cell. Biol.* **22**, 2810–2820 (2002).

25. Tai, S. *et al.* PC3 is a cell line characteristic of prostatic small cell carcinoma. *Prostate* **71**, 1668–1679 (2011).

26. Elangovan, I. *et al.* Targeting receptor for advanced glycation end products (RAGE) expression induces apoptosis and inhibits prostate tumor growth. *Biochem. Biophys. Res. Commun.* **417**, 1133–1138 (2012).

27. Boonyaratanakornkit, V. *et al.* High-mobility group chromatin proteins 1 and 2 functionally interact with steroid hormone receptors to enhance their DNA binding in vitro and transcriptional activity in mammalian cells. *Mol. Cell. Biol.* **18**, 4471–4487 (1998).

28. Flores-Morales, A. & Iglesias-Gato, D. Quantitative Mass Spectrometry-Based Proteomic Profiling for Precision Medicine in Prostate Cancer. *Front. Oncol.* **7**, 267 (2017).

29. Muller, A. K. *et al.* Proteomic Characterization of Prostate Cancer to Distinguish Nonmetastasizing and Metastasizing Primary Tumors and Lymph Node Metastases. *Neoplasia* **20**, 140–151 (2018).

30. Zhang, Y. *et al.* Quantitative Proteomics of TRAMP Mice Combined with Bioinformatics Analysis Reveals That PDGF-B Regulatory Network Plays a Key Role in Prostate Cancer Progression. *J. Proteome Res.* **17**, 2401–2411 (2018).

31. Stelloo, S. *et al.* Endogenous androgen receptor proteomic profiling reveals genomic subcomplex involved in prostate tumorigenesis. *Oncogene* **37**, 313–322 (2018).

32. Berger, A. *et al.* N-Myc-mediated epigenetic reprogramming drives lineage plasticity in advanced prostate cancer. *J. Clin. Invest.* **129**, 3924–3940 (2019).

33. Zhang, Z. *et al.* An AR-ERG transcriptional signature defined by long-range chromatin interactomes in prostate cancer cells. *Genome Res.* **29**, 223–235 (2019).

34. Takara Bio Inc. Yeast two-hybrid system. https://www.takarabio.com/products/protein-research/two-hybrid-and-one-hybrid-systems/yeast-two-hybrid-system (2018).

35.	Lin, J. & Lai, E. Protein–Protein Interactions: Yeast Two-Hybrid System. In: Journet L., Cascales E. (eds) Bacterial Protein Secretion Systems. *Methods Mol. Biol.* **1615**, 177–187 (2017).

36.	Barreiro-Alonso, A. Interactome of Ixr1, HMGB1 and HMGB2 proteins in relation to their cellular function. *PhD Thesis* (2018).

37.	Kaighn, M. E., Narayan, K. S., Ohnuki, Y., Lechner, J. F. & Jones, L. W. Establishment and characterization of a human prostatic carcinoma cell line (PC-3). *Invest. Urol.* **17**, 16–23 (1979).

38.	Stone, K. R., Mickey, D. D., Wunderli, H., Mickey, G. H. & Paulson, D. F. Isolation of a human prostate carcinoma cell line (DU 145). *Int. J. Cancer* **21**, 274–281 (1978).

39.	Livak, K. J. & Schmittgen, T. D. Analysis of relative gene expression data using real-time quantitative PCR and the 2(-Delta Delta C(T)) Method. *Methods* **25**, 402–408 (2001).

40.	Babicki, S. *et al.* Heatmapper: web-enabled heat mapping for all. *Nucleic Acids Res.* **44**, W147-53 (2016).

41.	Shankar, E. *et al.* A Signaling Network Controlling Androgenic Repression of c-Fos Protein in Prostate Adenocarcinoma Cells. *J. Biol. Chem.* **291**, 5512–5526 (2016).

42.	Yan, G. *et al.* GOLM1 promotes prostate cancer progression through activating PI3K-AKT-mTOR signaling. *Prostate* **78**, 166–177 (2018).

43.	Zhang, L., Song, D., Zhu, B. & Wang, X. The role of nuclear matrix protein HNRNPU in maintaining the architecture of 3D genome. *Semin. Cell Dev. Biol.* **90**, 161–167 (2018).

44.	Lee, S. Y. *et al.* Microtubule-associated protein 1B light chain (MAP1B-LC1) negatively regulates the activity of tumor suppressor p53 in neuroblastoma cells. *FEBS Lett.* **582**, 2826–2832 (2008).

45.	Zheng, M. *et al.* Inactivation of Rheb by PRAK-mediated phosphorylation is essential for energy-depletion-induced suppression of mTORC1. *Nat. Cell Biol.* **13**, 263–272 (2011).

46.	Dwyer, S. F. & Gelman, I. H. Cross-Phosphorylation and Interaction between Src/FAK and MAPKAP5/PRAK in Early Focal Adhesions Controls Cell Motility.

J. cancer Biol. Res. **2**, (2014).

47. Dasgupta, S. *et al.* Novel gene C17orf37 in 17q12 amplicon promotes migration and invasion of prostate cancer cells. *Oncogene* **28**, 2860–2872 (2009).

48. Chen, S. H., Chen, L. & Russell, D. H. Metal-induced conformational changes of human metallothionein-2A: a combined theoretical and experimental study of metal-free and partially metalated intermediates. *J. Am. Chem. Soc.* **136**, 9499–9508 (2014).

49. Yamasaki, M., Nomura, T., Sato, F. & Mimata, H. Metallothionein is up-regulated under hypoxia and promotes the survival of human prostate cancer cells. *Oncol. Rep.* **18**, 1145–1153 (2007).

50. Lin, H. K. *et al.* Proteasome activity is required for androgen receptor transcriptional activity via regulation of androgen receptor nuclear translocation and interaction with coregulators in prostate cancer cells. *J. Biol. Chem.* **277**, 36570–36576 (2002).

51. Sayeon, C. *et al.* Binding and regulation of HIF-1alpha by a subunit of the proteasome complex, PSMA7. *FEBS Lett.* **498**, 62–66 (2001).

52. Romanuik, T. L. *et al.* Novel biomarkers for prostate cancer including noncoding transcripts. *Am. J. Pathol.* **175**, 2264–2276 (2009).

53. Kim, M., Morales, L. D., Jang, I. S., Cho, Y. Y. & Kim, D. J. Protein Tyrosine Phosphatases as Potential Regulators of STAT3 Signaling. *Int. J. Mol. Sci.* **19**, 2708–2727 (2018).

54. Hui, K. *et al.* RASAL2, a RAS GTPase-activating protein, inhibits stemness and epithelial-mesenchymal transition via MAPK/SOX2 pathway in bladder cancer. *Cell Death Dis.* **8**, e2600 (2017).

55. Min, S., Kim, K., Kim, S. G., Cho, H. & Lee, Y. Chromatin-remodeling factor, RSF1, controls p53-mediated transcription in apoptosis upon DNA strand breaks. *Cell Death Dis.* **9**, 1072–1079 (2018).

56. Li, H. *et al.* Rsf-1 overexpression in human prostate cancer, implication as a prognostic marker. *Tumour Biol.* **35**, 5771–5776 (2014).

57. Jia, R., Ajiro, M., Yu, L., McCoy Jr, P. & Zheng, Z. M. Oncogenic splicing factor SRSF3 regulates ILF3 alternative splicing to promote cancer cell proliferation and transformation. *RNA* **25**, 630–644 (2019).

58. Bowler, E. *et al.* Hypoxia leads to significant changes in alternative splicing and elevated expression of CLK splice factor kinases in PC3 prostate cancer cells. *BMC Cancer* **18**, 355–357 (2018).

59. Bereczki, O. *et al.* TATA binding protein associated factor 3 (TAF3) interacts with p53 and inhibits its function. *BMC Mol. Biol.* **9**, 57 (2008).

60. Fesus, L., Thomazy, V. & Falus, A. Induction and activation of tissue transglutaminase during programmed cell death. *FEBS Lett.* **224**, 104–108 (1987).

61. Bull, J. H. *et al.* Identification of potential diagnostic markers of prostate cancer and prostatic intraepithelial neoplasia using cDNA microarray. *Br. J. Cancer* **84**, 1512–1519 (2001).

62. Moniz, S. & Jordan, P. Emerging roles for WNK kinases in cancer. *Cell. Mol. Life Sci.* **67**, 1265–1276 (2010).

63. Seligson, D. *et al.* Expression of transcription factor Yin Yang 1 in prostate cancer. *Int. J. Oncol.* **27**, 131–141 (2005).

64. Kashyap, V. & Bonavida, B. Role of YY1 in the pathogenesis of prostate cancer and correlation with bioinformatic data sets of gene expression. *Genes Cancer* **5**, 71–83 (2014).

65. Camacho-Moctezuma, B., Quevedo-Castillo, M., Melendez-Zajgla, J., Aquino-Jarquin, G. & Martinez-Ruiz, G. U. YY1 negatively regulates the XAF1 gene expression in prostate cancer. *Biochem. Biophys. Res. Commun.* **508**, 973–979 (2019).

66. McGee, A. M., Douglas, D. L., Liang, Y., Hyder, S. M. & Baines, C. P. The mitochondrial protein C1qbp promotes cell proliferation, migration and resistance to cell death. *Cell Cycle* **10**, 4119–4127 (2011).

67. Amamoto, R. *et al.* Mitochondrial p32/C1QBP is highly expressed in prostate cancer and is associated with shorter prostate-specific antigen relapse time after radical prostatectomy. *Cancer Sci.* **102**, 639–647 (2011).

68. Salimi, R. *et al.* Blocking the Cleavage of Filamin A by Calpain Inhibitor Decreases Tumor Cell Growth. *Anticancer Res.* **38**, 2079–2085 (2018).

69. Ravipaty, S. *et al.* Clinical Validation of a Serum Protein Panel (FLNA, FLNB and KRT19) for Diagnosis of Prostate Cancer. *J. Mol. Biomark. Diagn.* **8**, 1–16

(2017).

70. Luu, H. N. *et al.* miRNAs associated with prostate cancer risk and progression. *BMC Urol.* **17**, 1–18 (2017).

71. Park, I. *et al.* Myosin regulatory light chains are required to maintain the stability of myosin II and cellular integrity. *Biochem. J.* **434**, 171–180 (2011).

72. Lee, S. *et al.* Nucleolar protein GLTSCR2 stabilizes p53 in response to ribosomal stresses. *Cell Death Differ.* **19**, 1613–1622 (2012).

73. Uchi, R. *et al.* PICT1 regulates TP53 via RPL11 and is involved in gastric cancer progression. *Br. J. Cancer* **109**, 2199–2206 (2013).

74. Sasaki, M. *et al.* Regulation of the MDM2-P53 pathway and tumor growth by PICT1 via nucleolar RPL11. *Nat. Med.* **17**, 944–951 (2011).

75. Chen, H. *et al.* PICT-1 is a key nucleolar sensor in DNA damage response signaling that regulates apoptosis through the RPL11-MDM2-p53 pathway. *Oncotarget* **7**, 83241–83257 (2016).

76. Kim, J. Y. *et al.* Involvement of GLTSCR2 in the DNA Damage Response. *Am. J. Pathol.* **179**, 1257–1264 (2011).

77. Kim, J. Y. *et al.* Down-regulation and aberrant cytoplasmic expression of GLTSCR2 in prostatic adenocarcinomas. *Cancer Lett.* **340**, 134–140 (2013).

78. Kim, H. K. *et al.* A transfer-RNA-derived small RNA regulates ribosome biogenesis. *Nature* **552**, 57–62 (2017).

79. Riera-Romo, M. COMMD1: A Multifunctional Regulatory Protein. *J. Cell. Biochem.* **119**, 34–51 (2018).

80. Zoubeidi, A. *et al.* Clusterin facilitates COMMD1 and I-kappaB degradation to enhance NF-kappaB activity in prostate cancer cells. *Mol. Cancer Res.* **8**, 119–130 (2010).

81. Barreiro-Alonso, A., Lamas-Maceiras, M., Cerdan, E. M. & Vizoso-Vazquez, A. The HMGB protein Ixr1 interacts with Ssn8 and Tdh3 involved in transcriptional regulation. *FEMS Yeast Res.* **18**, 1–10 (2018).

82. Gylfe, A. E. *et al.* Identification of candidate oncogenes in human colorectal cancers with microsatellite instability. *Gastroenterology* **145**, 540–3.e22 (2013).

83. Harrison, B. *et al.* DAPK-1 binding to a linear peptide motif in MAP1B stimulates

autophagy and membrane blebbing. *J. Biol. Chem.* **283**, 9999–10014 (2008).

84. Kim, J. Y., An, Y. M. & Park, J. H. Role of GLTSCR2 in the regulation of telomerase activity and chromosome stability. *Mol. Med. Rep.* **14**, 1697–1703 (2016).

85. Moon, A. *et al.* Downregulation of GLTSCR2 expression is correlated with breast cancer progression. *Pathol. Res. Pract.* **209**, 700–704 (2013).

86. Yoshimoto, M., Tokuda, A., Nishiwaki, K., Sengoku, K. & Yaginuma, Y. Abnormal Expression of PICT-1 and Its Codon 389 Polymorphism Is a Risk Factor for Human Endometrial Cancer. *Oncology* **95**, 43–51 (2018).

87. Sheu, J. J. *et al.* Rsf-1, a chromatin remodeling protein, induces DNA damage and promotes genomic instability. *J. Biol. Chem.* **285**, 38260–38269 (2010).

88. Liu, Y., Li, G., Liu, C., Tang, Y. & Zhang, S. RSF1 regulates the proliferation and paclitaxel resistance via modulating NF-kappaB signaling pathway in nasopharyngeal carcinoma. *J. Cancer* **8**, 354–362 (2017).

89. Zhang, X. *et al.* Overexpression of Rsf-1 correlates with poor survival and promotes invasion in non-small cell lung cancer. *Virchows Arch.* **470**, 553–560 (2017).

90. He, X. & Zhang, P. Serine/arginine-rich splicing factor 3 (SRSF3) regulates homologous recombination-mediated DNA repair. *Mol. Cancer* **14**, 151–158 (2015).

91. Zhou, L., Guo, J. & Jia, R. Oncogene SRSF3 suppresses autophagy via inhibiting BECN1 expression. *Biochem. Biophys. Res. Commun.* **509**, 966–972 (2019).

92. Kim, J. *et al.* Splicing factor SRSF3 represses the translation of programmed cell death 4 mRNA by associating with the 5'-UTR region. *Cell Death Differ.* **21**, 481–490 (2014).

93. Kim, H. R. *et al.* SRSF3-regulated miR-132/212 controls cell migration and invasion by targeting YAP1. *Exp. Cell Res.* **358**, 161–170 (2017).

94. He, X. *et al.* Knockdown of splicing factor SRp20 causes apoptosis in ovarian cancer cells and its expression is associated with malignancy of epithelial ovarian cancer. *Oncogene* **30**, 356–365 (2011).

95. Scully, O. J. *et al.* Complement component 1, q subcomponent binding protein is a marker for proliferation in breast cancer. *Exp. Biol. Med. (Maywood).* **240**,

846–853 (2015).

96.   Zhang, X. *et al.* Interactome analysis reveals that C1QBP (complement component 1, q subcomponent binding protein) is associated with cancer cell chemotaxis and metastasis. *Mol. Cell. Proteomics* **12**, 3199–3209 (2013).

97.   Chen, R. *et al.* Identification of a novel mitochondrial interacting protein of C1QBP using subcellular fractionation coupled with CoIP-MS. *Anal. Bioanal. Chem.* **408**, 1557–1564 (2016).

98.   Long, Y. *et al.* MicroRNA-101 inhibits the proliferation and invasion of bladder cancer cells via targeting c-FOS. *Mol. Med. Rep.* **14**, 2651–2656 (2016).

99.   Lu, C. *et al.* cFos is critical for MCF-7 breast cancer cell growth. *Oncogene* **24**, 6516–6524 (2005).

100.   Goh, W. Q., Ow, G. S., Kuznetsov, V. A., Chong, S. & Lim, Y. P. DLAT subunit of the pyruvate dehydrogenase complex is upregulated in gastric cancer-implications in cancer therapy. *Am. J. Transl. Res.* **7**, 1140–1151 (2015).

101.   Vitali, E. *et al.* FLNA is implicated in pulmonary neuroendocrine tumors aggressiveness and progression. *Oncotarget* **8**, 77330–77340 (2017).

102.   Gai, X. *et al.* mTOR/miR-145-regulated exosomal GOLM1 promotes hepatocellular carcinoma through augmented GSK-3beta/MMPs. *J. Genet. Genomics* **46**, 235–245 (2019).

103.   Zhang, R. *et al.* Golgi Membrane Protein 1 (GOLM1) Promotes Growth and Metastasis of Breast Cancer Cells via Regulating Matrix Metalloproteinase-13 (MMP13). *Med. Sci. Monit.* **25**, 847–855 (2019).

104.   Yang, L., Luo, P., Song, Q. & Fei, X. DNMT1/miR-200a/GOLM1 signaling pathway regulates lung adenocarcinoma cells proliferation. *Biomed. Pharmacother.* **99**, 839–847 (2018).

105.   Zhou, M., Chen, X., Wu, J., He, X. & Ren, R. microRNA-143 regulates cell migration and invasion by targeting GOLM1 in cervical cancer. *Oncol. Lett.* **16**, 6393–6400 (2018).

106.   Li, B. *et al.* HOXA10 is overexpressed in human ovarian clear cell adenocarcinoma and correlates with poor survival. *Int. J. Gynecol. Cancer* **19**, 1347–1352 (2009).

107.   Tang, W. *et al.* miR-135a functions as a tumor suppressor in epithelial ovarian

cancer and regulates HOXA10 expression. *Cell. Signal.* **26**, 1420–1426 (2014).

108. Ren, C. C. *et al.* Effects of shRNA-mediated silencing of PSMA7 on cell proliferation and vascular endothelial growth factor expression via the ubiquitin-proteasome pathway in cervical cancer. *J. Cell. Physiol.* **234**, 5851–5862 (2019).

109. Yang, L. *et al.* PSMA7 directly interacts with NOD1 and regulates its function. *Cell. Physiol. Biochem.* **31**, 952–959 (2013).

110. Morales, L. D. *et al.* The role of T-cell protein tyrosine phosphatase in epithelial carcinogenesis. *Mol. Carcinog.* **58**, 1640–1647 (2019).

111. Fang, J. F., Zhao, H. P., Wang, Z. F. & Zheng, S. S. Upregulation of RASAL2 promotes proliferation and metastasis, and is targeted by miR-203 in hepatocellular carcinoma. *Mol. Med. Rep.* **15**, 2720–2726 (2017).

112. Pan, Y. *et al.* RASAL2 promotes tumor progression through LATS2/YAP1 axis of hippo signaling pathway in colorectal cancer. *Mol. Cancer* **17**, 102–106 (2018).

113. Li, N. & Li, S. RASAL2 promotes lung cancer metastasis through epithelial-mesenchymal transition. *Biochem. Biophys. Res. Commun.* **455**, 358–362 (2014).

114. Li, Y., Ma, X., Wang, Y. & Li, G. miR-489 inhibits proliferation, cell cycle progression and induces apoptosis of glioma cells via targeting SPIN1-mediated PI3K/AKT pathway. *Biomed. Pharmacother.* **93**, 435–443 (2017).

115. Li, W., Zhang, Z., Zhao, W. & Han, N. Transglutaminase 3 protein modulates human esophageal cancer cell growth by targeting the NF-kappaB signaling pathway. *Oncol. Rep.* **36**, 1723–1730 (2016).

116. Plafker, K. S., Farjo, K. M., Wiechmann, A. F. & Plafker, S. M. The human ubiquitin conjugating enzyme, UBE2E3, is required for proliferation of retinal pigment epithelial cells. *Invest. Ophthalmol. Vis. Sci.* **49**, 5611–5618 (2008).

117. Yang, W. L. *et al.* Vigilin is overexpressed in hepatocellular carcinoma and is required for HCC cell proliferation and tumor growth. *Oncol. Rep.* **31**, 2328–2334 (2014).

118. Mu, P., Akashi, T., Lu, F., Kishida, S. & Kadomatsu, K. A novel nuclear complex of DRR1, F-actin and COMMD1 involved in NF-kappaB degradation and cell growth suppression in neuroblastoma. *Oncogene* **36**, 5745–5756 (2017).

119. van de Sluis, B. *et al.* COMMD1 disrupts HIF-1alpha/beta dimerization and

inhibits human tumor cell invasion. *J. Clin. Invest.* **120**, 2119–2130 (2010).

120. Zhou, J. *et al.* MK5 is degraded in response to doxorubicin and negatively regulates doxorubicin-induced apoptosis in hepatocellular carcinoma cells. *Biochem. Biophys. Res. Commun.* **427**, 581–586 (2012).

121. Zhou, S. *et al.* MNAT1 is overexpressed in colorectal cancer and mediates p53 ubiquitin-degradation to promote colorectal cancer malignance. *J. Exp. Clin. Cancer Res.* **37**, 283–284 (2018).

122. Marikar, F. M., Jin, G., Sheng, W., Ma, D. & Hua, Z. Metallothionein 2A an interactive protein linking phosphorylated FADD to NF-kappaB pathway leads to colorectal cancer formation. *Chinese Clin. Oncol.* **5**, 76 (2016).

123. Huang, Y. *et al.* Upregulation of miR-146a by YY1 depletion correlates with delayed progression of prostate cancer. *Int. J. Oncol.* **50**, 421–431 (2017).

124. Bonavida, B. Linking Autophagy and the Dysregulated NFkappaB/ SNAIL/YY1/RKIP/PTEN Loop in Cancer: Therapeutic Implications. *Crit. Rev. Oncog.* **23**, 307–320 (2018).

125. Galloway, N. R., Ball, K. F., Stiff, T. & Wall, N. R. Yin Yang 1 (YY1): Regulation of Survivin and Its Role In Invasion and Metastasis. *Crit. Rev. Oncog.* **22**, 23–36 (2017).

126. Kpetemey, M., Chaudhary, P., Van Treuren, T. & Vishwanatha, J. K. MIEN1 drives breast tumor cell migration by regulating cytoskeletal-focal adhesion dynamics. *Oncotarget* **7**, 54913–54924 (2016).

127. Rajendiran, S. *et al.* microRNA-940 suppresses prostate cancer migration and invasion by regulating MIEN1. *Mol. Cancer* **13**, 1–15 (2014).

128. Cerami, E. *et al.* The cBio cancer genomics portal: an open platform for exploring multidimensional cancer genomics data. *Cancer Discov.* **2**, 401–404 (2012).

129. Gao, J. *et al.* Integrative analysis of complex cancer genomics and clinical profiles using the cBioPortal. *Sci. Signal.* **6**, pl1 (2013).

130. Abida, W. *et al.* Genomic correlates of clinical outcome in advanced prostate cancer. *Proc. Natl. Acad. Sci. U. S. A.* **116**, 11428–11436 (2019).

131. Armenia, J. *et al.* The long tail of oncogenic drivers in prostate cancer. *Nat. Genet.* **50**, 645–651 (2018).

132. Armenia, J. *et al.* Publisher Correction: The long tail of oncogenic drivers in prostate cancer. *Nat. Genet.* **51**, 1187–1194 (2019).

133. Network, C. G. A. R. The Molecular Taxonomy of Primary Prostate Cancer. *Cell* **163**, 1011–1025 (2015).

134. Rosario, S. R. *et al.* Pan-cancer analysis of transcriptional metabolic dysregulation using The Cancer Genome Atlas. *Nat. Commun.* **9**, 5330–5338 (2018).

135. Hieronymus, H. *et al.* Copy number alteration burden predicts prostate cancer relapse. *Proc. Natl. Acad. Sci. U. S. A.* **111**, 11139–11144 (2014).

136. Gao, D. *et al.* Organoid cultures derived from patients with advanced prostate cancer. *Cell* **159**, 176–187 (2014).

137. Abida, W. *et al.* Prospective Genomic Profiling of Prostate Cancer Across Disease States Reveals Germline and Somatic Alterations That May Affect Clinical Decision Making. *JCO Precis. Oncol.* **1**, 1–17 (2017).

138. Robinson, D. *et al.* Integrative clinical genomics of advanced prostate cancer. *Cell* **161**, 1215–1228 (2015).

139. Beltran, H. *et al.* Divergent clonal evolution of castration-resistant neuroendocrine prostate cancer. *Nat. Med.* **22**, 298–305 (2016).

140. Baca, S. C. *et al.* Punctuated evolution of prostate cancer genomes. *Cell* **153**, 666–677 (2013).

141. Barbieri, C. E. *et al.* Exome sequencing identifies recurrent SPOP, FOXA1 and MED12 mutations in prostate cancer. *Nat. Genet.* **44**, 685–689 (2012).

142. Fraser, M. *et al.* Genomic hallmarks of localized, non-indolent prostate cancer. *Nature* **541**, 359–364 (2017).

143. Leyh-Bannurah, S. R. *et al.* Local Therapy Improves Survival in Metastatic Prostate Cancer. *Eur. Urol.* **72**, 118–124 (2017).

144. Kumar, A. *et al.* Substantial interindividual and limited intraindividual genomic diversity among tumors from men with metastatic prostate cancer. *Nat. Med.* **22**, 369–378 (2016).

145. Taylor, B. S. *et al.* Integrative genomic profiling of human prostate cancer. *Cancer Cell* **18**, 11–22 (2010).

146. Grasso, C. S. *et al.* The mutational landscape of lethal castration-resistant prostate cancer. *Nature* **487**, 239–243 (2012).

147. Li, T. *et al.* Overexpression of high mobility group box 1 with poor prognosis in patients after radical prostatectomy. *BJU Int.* **110**, 1–6 (2012).

148. Suzuki, S. *et al.* Early detection of prostate carcinogens by immunohistochemistry of HMGB2. *J. Toxicol. Sci.* **43**, 359–367 (2018).

149. Barreiro-Alonso, A. *et al.* Characterization of HMGB1/2 Interactome in Prostate Cancer by Yeast Two Hybrid Approach: Potential Pathobiological Implications. *Cancers (Basel).* **11**, 1–21 (2019).

150. Liu, R., Zhou, Z., Huang, J. & Chen, C. PMEPA1 promotes androgen receptor-negative prostate cell proliferation through suppressing the Smad3/4-c-Myc-p21 Cip1 signaling pathway. *J. Pathol.* **223**, 683–694 (2011).

151. Zhao, C. B. *et al.* Co-expression of RAGE and HMGB1 is associated with cancer progression and poor patient outcome of prostate cancer. *Am. J. Cancer Res.* **4**, 369–377 (2014).

152. Daures, M. *et al.* A new metabolic gene signature in prostate cancer regulated by JMJD3 and EZH2. *Oncotarget* **9**, 23413–23425 (2018).

153. Iglesias-Gato, D. *et al.* The Proteome of Primary Prostate Cancer. *Eur. Urol.* **69**, 942–952 (2016).

154. Rajan, P. *et al.* Next-generation sequencing of advanced prostate cancer treated with androgen-deprivation therapy. *Eur. Urol.* **66**, 32–39 (2014).

155. Park, A. *et al.* Identification of Transcription Factor YY1 as a Regulator of a Prostate Cancer-Specific Pathway Using Proteomic Analysis. *J. Cancer* **8**, 2303–2311 (2017).

156. Yang, T. *et al.* hnRNPM, a potential mediator of YY1 in promoting the epithelial-mesenchymal transition of prostate cancer cells. *Prostate* **79**, 1199–1210 (2019).

157. Deng, Z., Cao, P., Wan, M. M. & Sui, G. Yin Yang 1: a multifaceted protein beyond a transcription factor. *Transcription* **1**, 81–84 (2010).

158. Li, B. *et al.* HoxA10 induces proliferation in human prostate carcinoma PC-3 cell line. *Cell Biochem. Biophys.* **70**, 1363–1368 (2014).

159. Hatanaka, Y. *et al.* HOXA10 expression profiling in prostate cancer. *Prostate* **79**,

554–563 (2019).

160. Long, Z. *et al.* Roles of the HOXA10 gene during castrate-resistant prostate cancer progression. *Endocr. Relat. Cancer* **26**, 279–292 (2019).

161. Chen, H. *et al.* PICT-1 triggers a pro-death autophagy through inhibiting rRNA transcription and AKT/mTOR/p70S6K signaling pathway. *Oncotarget* **7**, 78747–78763 (2016).

162. Sloan, K. E., Bohnsack, M. T. & Watkins, N. J. The 5S RNP couples p53 homeostasis to ribosome biogenesis and nucleolar stress. *Cell Rep.* **5**, 237–247 (2013).

163. Okahara, F. *et al.* Critical role of PICT-1, a tumor suppressor candidate, in phosphatidylinositol 3,4,5-trisphosphate signals and tumorigenic transformation. *Mol. Biol. Cell* **17**, 4888–4895 (2006).

164. Okumura, K., Zhao, M., DePinho, R. A., Furnari, F. B. & Cavenee, W. K. PTEN: A novel anti-oncogenic function independent of phosphatase activity. *Cell Cycle* **4**, 540–542 (2005).

165. Kim, J. Y., Park, J. H. & Lee, S. GLTSCR2 contributes to the death resistance and invasiveness of hypoxia-selected cancer cells. *FEBS Lett.* **586**, 3435–3440 (2012).

166. Kpetemey, M. *et al.* MIEN1 drives breast tumor cell migration by regulating cytoskeletal-focal adhesion dynamics. *Oncotarget* **7**, 54913–54924 (2016).

167. Kushwaha, P. P., Gupta, S., Singh, A. K. & Kumar, S. Emerging Role of Migration and Invasion Enhancer 1 (MIEN1) in Cancer Progression and Metastasis. *Front. Oncol.* **9**, 1–13 (2019).

168. Kpetemey, M. *et al.* MIEN1, a novel interactor of Annexin A2 , promotes tumor cell migration by enhancing AnxA2 cell surface expression. *Mol. Cancer* **14**, 1–13 (2015).

169. Gardel, M. L., Schneider, I. C., Aratyn-schaus, Y. & Waterman, C. M. Mechanical Integration of Actin and Adhesion Dynamics in Cell Migration. *Annu Rev Cell Dev Bio* **26**, 315–333 (2010).

170. Han, Q. *et al.* Long noncoding RNA CRCMSL suppresses tumor invasive and metastasis in colorectal carcinoma through nucleocytoplasmic shuttling of HMGB2. *Oncogene* **38**, 3019–3032 (2019).

171. Consortium, Gte. The Genotype-Tissue Expression (GTEx) project. *Nat. Genet.* **45**, 580–585 (2013).

172. Petryszak, R. *et al.* Expression Atlas update--an integrated database of gene and protein expression in humans, animals and plants. *Nucleic Acids Res.* **44**, D746–D752 (2016).

Chapter 2.

HMGB1 and HMGB2 interactomes in Epithelial Ovary Cancer

Introduction

Ovarian cancer is nowadays the 7th most common cancer in women with a median 5-year relative survival rate between 30%-40%. Earlier diagnosis is a clear advantage, since the detection when the tumour is still localized in ovary increases the 5-year relative survival rate up to 92%[1]. More than 90% of malignant ovarian tumours are epithelial in origin (EOC) and the rest derive from stromal cells and germ cells. The histology of malignant EOCs, or carcinomas, is heterogeneous and they have been classified in five main histotypes: high-grade serous (HGSOC with an incidence of 70% among total EOC), low-grade serous (LGSOC; incidence <5%); endometrioid (ENOC; incidence of 10%), clear cell (CCOC; incidence of 10%), and mucinous (MOC; incidence 3%). This classification takes into account the resemblance to normal gynecological cell line; serous: resembling epithelium lining the Fallopian tubes; mucinous: resembling epithelium lining endocervix, and containing intracytoplasmic mucin; endometrioid: resembling epithelium of uterine corpus; clear cell: comprising clear cells and hobnail cells[1]. Each histotype has been associated to a particular set of somatic mutations. HGSOC to BRCA1/2 and TP53 mutations; LGSOC to BRAF and, KRAS mutations; MOC to KRAS; ENOC to PTEN, CTNNB1, ARID1A and PIK3CA mutations; and finally CCOC to ARID1A and PIK3CA mutations[1]. High mobility group box proteins (HMGB), enriched in chromatin as non-histone components, exert global regulatory functions in the establishment of active or inactive chromatin domains. They are able to promote cancer development and metastasis when released from cells into the extracellular environment, and their overexpression is associated to diverse types of cancer including ovarian cancer[2]. Among the HMGB family, HMGB1 has been the more studied being proposed as a diagnosis and prognosis biomarker for human ovarian cancer[3–5]. Meanwhile, recent research relate HMGB2 with poor prognosis in ovarian cancer and suggest it as potential therapeutic target against this disease[6–8]. Oppositely to HMGB1, HMGB2 is a substrate for the tryptase Granzyme-A secreted by Cytotoxic T lymphocytes (CTL) and Natural Killer (NK) cells in order to trigger a caspase alternative apoptosis pathway in tumour cells[9]. In serous epithelial ovarian cancer, HMGB2 and SET protein are highly overexpressed, conforming along with APE1 a protein complex named "SET complex" that inhibits the tumour suppressor protein NM23-H1. Granzyme-A targets SET complex allowing NM23-H1 to perform its DNAse activity[10,11]. Moreover, Li et al. evidenced in their work the correlation between HMGB2 and centromere protein U (CENPU) overexpression in ovarian cancer cells, such as SKOV-3, and their critical role in tumour development and metastasis[7]. Furthermore,

ovarian serous borderline and invasive tumours (TOVs) resistant to chemotherapy were found to highly express HMGB2, bringing out its involvement in resistance to DNA conformation-altering chemotherapeutic drugs[10,12]. Altogether, HMGB2 and its interactant partner HMGB1 have been both related to drug resistance during cancer treatment[8,13].

Interactomes associated to a particular disease are valuable tools to understand their molecular mechanisms and to re-define diagnostic panels of specific biomarkers[14]. The low rates of survival after first diagnose, clearly show that clinical management of ovarian cancer patients needs of earlier diagnose and more specific prognosis and therapies[15,16]. Considering the relevance of HMGB proteins in EOC, the determination of the HMGB1-2 interactome in ovarian cancerous cells is an attractive line of research to reach this objective. We have followed a Y2H approach to obtain the HMGB1-2 interactomes. We have used libraries derived from cancerous tissue from a patient diagnosed of primary transitional cell carcinoma (TCC) of the ovary, a relatively rare subtype of serous epithelial ovarian cancer, which represents approximately 2% of all ovarian tumours[17]. Results have been compared to those previously obtained using libraries derived from SKOV-3 cells[18]. Common targets in both libraries could discover important interactions, which are independent of the histological subtypes and their specific mutations. Functional significance of the discovered targets in relation to cancer progression is discussed, with special focus on MIEN1 and NOP53.

1. Materials and Methods

1.1. Yeast two hybrid methodology

HMGB1 and HMGB2 interacting partners were identified using "Matchmaker Gold Yeast Two-Hybrid System" (Clontech, Fremont, CA, USA) as described previously in chapter 1. RNAs from human samples used to prepare the Y2H libraries were provided by Biobanco de Andalucía (ES, EU). Tumour and paired non-tumour tissue were obtained from a 63-year-old woman diagnosed with grade III ovarian transitional cell carcinoma without previous chemotherapy treatment. Homology searches were done with BlastN and BlastX at NCBI (https://blast.ncbi.nlm.nih.gov/ accessed on 02-02-2020) and the proteins matching the queries annotated as positives. Positive interactions were compared with those previously described in public databases as STRING (https://string-db.org/ Access date 10-22-2020) and BioGRID (https://thebiogrid.org Access date 10-26-2020), and Uniprot database (http://www.uniprot.org/uniprot Access date 10-22-2020) was used as reference platform for the description of the proteins function.

1.2. Cell Lines

The SKOV-3 and PEO-1 cell lines (originally derived from human EOC) were obtained from the American Type Culture Collection (ATCC), and regularly tested for mycoplasma by Eurofins Scientific (Eurofins Scientific Inc., Luxembourg, FR, EU). SKOV-3 was grown in McCoy's-5A medium (Gibco™, Thermo Fisher Scientific Inc., Waltham, MA, USA) and PEO-1 in RPMI-1640 medium (Gibco™, Thermo Fisher Scientific Inc., Waltham, MA, USA), both supplemented with 10% heat-inactivated fetal bovine serum and 1% penicillin-streptomycin (Thermo Fisher Scientific Inc., Waltham, MA, USA). Cells were cultured in a humidified incubator at 37 ºC and 5% CO_2. The non-cancerous human ovarian primary culture HOSEpiC RNA was purchased (Innoprot, Biscay, ES, EU). Cell viability-cytotoxicity assays were done using the Cell Counting Kit-8, CCK-8 (Tebu-Bio., Le-Perray-en-Yvelines, FR, EU).

1.3. Cross-linking and HMGB2 co-immunoprecipitation

After reaching 70-80% confluence of SKOV-3 and PEO-1 cultures, cross-linking and HMGB2 co-immunoprecipitation were done as previously described in chapter 1. The presence of MIEN1 and NOP53 in the Immunoprecipitations (IPs) was confirmed by Western blot using the antibodies against MIEN1 (1:200, XTP4, 40-400, Invitrogen,

Thermo Fisher Scientific Inc. Waltham, MA, USA) and NOP53 (sc-517088, Santa Cruz, Dallas, TX, USA). After second incubation with 1:5000 G-protein HRP-linked (18-161. Millipore-Merck-KGaA, Darmstadt, DE, EU), 5% (w/v) non-fat milk diluted in PBST, PBS (NZYTech Lda., Lisbon, PT, EU) containing 0.1% Tween 20 (P1379, Sigma-Aldrich Inc., St., Louis, MO, USA), was used as blocking solution. Western blots were developed using Luminata™ Crescendo Western HRP Substrate (Millipore Corporation, Burlington, MA, USA), and visualized in a ChemiDoc™ imager (Bio-Rad Laboratories, Hercules, CA, USA).

1.4. Protein identification by LC-MS/MS

1.4.1. Mass Spectrometric analysis

Total protein from SKOV-3 cells was extracted in lysis buffer (50 mM Tris-HCl pH 8.0, 150 mM NaCl, 0.1% NP-40, 1 mM EDTA, 2 mM $MgCl_2$ and Complete™ Mini, EDTA-free Protease Inhibitor Cocktail (Hoffmann-La Roche , Basel, CH, EU) and incubated for 30 min at 4° C with Benzonase® Nuclease (Sigma-Aldrich Inc. St. Louis, MO, USA) to eliminate nucleic acids from the lysates. Total protein was quantified using the Bradford reagent (Bio-Rad Laboratories, Hercules, CA, USA). Prior to the immunoprecipitation, Protein G-Dynabeads (Invitrogen, Thermo Fisher Scientific Inc., Waltham, MA, USA) were cross-linked to 40 µg of HMGB2 antibody (ab67282, Abcam, Cambridge, UK, EU) or anti-rabbit IgG antibody (Millipore, Darmstadt, DE, EU) as previously described in chapter 1. For each Immunoprecipitation 2.5-3 mg of protein were incubated for 4 h at 4 °C with the corresponding HMGB1 or control rabbit antibody-linked beads. Nonspecific binding proteins were removed by four washes with IPP150 buffer (10 mM Tris-HCl pH 8.0, 150 mM NaCl and 0.1% NP-40) and four washes with 50 mM ammonium bicarbonate. On-bead digestion was carried out overnight at 37 °C with trypsin (Trypsin Sequencing Grade, Hoffmann-La Roche, Basel, CH, EU). Peptides were then collected, acidified with formic acid, filtered through Millipore Multiscreen HTS plates and dried in a Speed Vac (Thermo Fisher Scientific Inc., Waltham, MA, USA). Peptides were then resuspended in 20 mM TCEP and formic acid was added to a final concentration of 0.5%.

Peptides were processed and identified by the Proteomics Platform of "Instituto de Investigación de Santiago de Compostela" (IDIS) (Santiago de Compostela, ES, EU). 44 µg of digested peptides of each sample were separated using Reverse Phase Chromatography. Gradient was developed using a micro liquid chromatography system (Eksigent Technologies nanoLC 400, SCIEX, Foster City, CA, USA) coupled to high speed Triple TOF 6600 mass spectrometer (SCIEX, Foster City, CA, USA) with a micro

flow source. The analytical column used was a Chrom XP C18 150 × 0.30 mm, 3 mm particle size and 120 Å pore size (Eksigent, SCIEX, Foster City, CA, USA). The trap column was a YMC-TRIART C18 (YMC Technologies, Teknokroma Analítica S.A., Barcelona, ES, EU) with a 3 mm particle size and 120 Å pore size, switched on-line with the analytical column. The loading pump delivered a solution of 0.1% formic acid in water at 10 µl/min. The micro-pump provided a flow-rate of 5 µl/min and was operated under gradient elution conditions, using 0.1% formic acid in water as mobile phase A, and 0.1% formic acid in acetonitrile as mobile phase B. Peptides were separated using a 90 minutes gradient ranging from 2% to 90% mobile phase B (mobile phase A: 2% acetonitrile, 0.1% formic acid; mobile phase B: 100% acetonitrile, 0.1% formic acid). Injection volume was 4 µl (4 µg of sample).

Data acquisition was carried out in a TripleTOF 6600 System (SCIEX, Foster City, CA, USA) using a Data dependent workflow. Source and interface conditions were as follows: ion spray voltage floating (ISVF) 5500 V, curtain gas (CUR) 25, collision energy (CE) 10 and ion source gas 1 (GS1) 25. Instrument was operated with Analyst TF 1.7.1 software (SCIEX, Foster City, CA, USA). Switching criteria was set to ions greater than mass to charge ratio (m/z) 350 and smaller than m/z 1400 with charge state of 2–5, mass tolerance 250 ppm and an abundance threshold of more than 200 counts (cps). Former target ions were excluded for 15 s. Instrument was automatically calibrated every 4 hours using tryptic peptides from pepcalMix as external calibrant.

1.4.2. Data Analysis

After MS/MS collection, data files were processed using ProteinPilot™ 5.0.1 software from Sciex which uses the algorithm Paragon™ for database search and Progroup™ for data grouping. Data were searched using Human expecific Uniprot database (http://www.uniprot.org/uniprot). False discovery rate was performed using a nonlineal fitting method, and displaying only those results that reported a 1% Global false discovery rate (FRR) or better[19,20].

Relative quantification of peptides identified in HMGB2 and IgG IPs was performed using a Spectral count method. MS/MS were normalized between samples using Scaffold 3 method by the sum of the unweighted spectral counts for each sample in order to determine a sample specific scaling factor, and then this was applied to all proteins in all the samples[19,20].

1.5. Plasmid Construction

1.5.1. Bacterial Strain and Plasmids

XL1-Blue, a strain derivative of *Escherichia coli* K12, was cultured in LB supplemented with kanamycin. The plasmids used were pGBKT7 (630443, Clontech, Fremont, CA, USA), pGAD (K1612-1, Clontech, Fremont, CA, USA), pDsRed-C1 (632466, Clontech, Fremont, CA, USA) and pAcGFP-C1 (6084-1, Clontech, Fremont, CA, USA).

1.5.2. In Vivo Assembly (IVA) Cloning

The cloning of NOP53 and MIEN1 in pDsRed-Monomer-C1 and HMGB2 in pAcGFP-C1 plasmids respectively were performed by IVA cloning. A technique consisting of a single PCR reaction with end-tagged primers, which amplifies both vector and fragment, followed by DpnI digestion and bacteria transformation, where the two amplified DNA fragments are joined *in vivo* by recombination. Plasmid homologous regions (15-18 bp) are included in 5′-end of gene primers and plasmid primers must be divergent[21] 25 µL PCR reactions were performed using Phusion High-Fidelity DNA Polymerase (Thermo Fisher Scientific Inc., Waltham, MA, USA) with 0.1 µM primers and 1 ng for each DNA template, according to the following protocol: 2 min at 95 °C, 18 cycles of 10 sec at 95 °C, 30 sec at 52 °C, 5 min at 72 °C, and a final 5 min extension at 72 °C The oligonucleotide sequences were as follows:
HMGB2: TCCGGACTCAGATCTCGAATGGGTAAAGGAGACCCCAACAAG and CG CCCTACCGTCGACTGCTTATTCTTCATCTTCATCCTCTTCCTCC3. NOP53: TCGA ATTCTGCAGTCGACATGGCGGCAGGAGGCAG and TCCGGTGGATCCCGGGCC CTACAACTGGATCTCACGGAACG. MIEN1: TCGATTTC TGCAGTCGACATG AGCGGGGAGCCGGG and TCCGGTGGATCCCGGGCCTCACAGGATGACGCA GGGAGG; pDsRed-Monomer-C1: ACCGTCGACTGCAGAATTCGA and GGCC CGGGATCCACCGGA; pAcGFP-C1: GCAGTCGACGGTACCG and AGCTCGAG ATCTGAGTCCGGACTT.

1.6. Plasmid Transfection

PEO-1 cells were transfected with the plasmids using Lipofectamine®2000 (Invitrogen, Thermo Fisher Scientific Inc., Waltham, MA, USA) and Opti-MEM medium (Gibco™, Thermo Fisher Scientific Inc., Waltham, MA, USA) following manufacturer's protocol. In brief, PEO-1 cells were cultured in 6-well plates at a confluence of 300000 cells/well. 10 µL lipofectamine and 2 µg plasmid were separately diluted in 250 µL of Opti-MEM for each well, incubated for 5 min, mixed together and incubated for other 20 min. On

the other hand, cells were washed, Opti-MEM media was added to a volume of 1,5 mL per well, transfection reaction was mixed to the cell culture and incubated for 6 hours. The mixture was replaced by RPMI medium (Gibco™, Thermo Fisher Scientific Inc., Waltham, MA, USA) supplemented with 600 µg/mL neomycin (NZYTech Lda., Lisbon, PT, EU) and incubated for 48h. Neomycin was used as selection marker and transfection was confirmed by fluorescence microscopy using an inverted microscope Eclipse Ts2 (Nikon, Tokyo, JP). Empty vector transfection was made as a control.

1.7. *Confocal microscopy*

Transfected cells were passed to another 6-well plate containing sterile 13 mm glass coverslips. When cells reached 80% of confluence in the coverslips, fixation was performed using 100% methanol for 10 minutes at -20°C. The cells were washed 3 times (5 min/wash) in DPBS depleted from calcium and magnesium (Gibco™, Thermo Fisher Scientific Inc., Waltham, MA, USA). The coverslips were mounted on a clean slide using ProLong™ Gold Antifade reagent (P36941, Invitrogen, Thermo Fisher Scientific Inc., Waltham, MA, USA) and they were incubated for 1-5 min, protected from light. Confocal fluorescence images were obtained with Confocal Microscope A1R (Nikon, Tokyo, JP) coupled with an inverted microscope Eclipse Ti-E (Nikon, Tokyo, JP) in SAI center of the University of A Coruña.

1.8. Western blot analysis

Equal amounts of protein were subjected to 10% SDS-PAGE and transferred to a PVDF membrane. After blocking the PVDF membrane with 5% (w/v) non-fat milk diluted in PBST, PBS (NZYTech Lda., Lisbon, PT, EU) containing 0.1% Tween 20 (P1379, Sigma-Aldrich Inc., St. Louis, MO, USA), membranes were incubated with primary antibodies against HMGB2 (1:1000, ab67282, Abcam. Cambridge, UK, EU), MIEN1 (1:200, XTP4,40-400, Invitrogen, Thermo Fisher Scientific Inc., MA, Waltham), or NOP53, (1:500, sc-517088, Santa Cruz, Dallas, TX, USA) diluted in blocking solution overnight at 4°C, followed by G-protein HRP-linked (18-161, Millipore, Merck KGaA, Darmstadt, DE, EU) diluted 1:5000 in blocking solution. Chemiluminescence-detection was performed by using Luminata™ Crescendo Western HRP Substrate (Millipore Corporation. Burlington, MA, USA) and bands were visualized in a ChemiDoc™ imager (Bio-Rad Laboratories. Hercules, CA, USA). The relative intensities of protein bands were analysed using the ImageLab analysis software (Bio-Rad Laboratories. Hercules, CA, USA).

1.9. Gene expression analysis by quantitative polymerase chain reaction (RT-qPCR)

RNA samples from cell cultures were obtained as previously described in chapter 1. RNA samples from SKOV-3, PEO-1 and human ovarian surface epithelial cells (HOSEpiC) were retro-transcribed into cDNA and labeled with the KAPA SYBR FAST universal one-step qRT-PCR kit (Kappa Biosystems Inc., Woburn, MA, USA).

1.10. siRNA silencing

Transfection of PEO-1 or SKOV-3 cells with siRNAs was done with siRNA directed against HMGB1, HMGB2, NOP53 and MIEN1, previously described in chapter 1 and following the same procedures.

1.11. Survival Analysis

The Overall Survival Kaplan-Meier Estimate analysis was performed through cBioPortal (http://www.cbioportal.org/) using the databases Ovarian Serous Cystadenocarcinoma (TCGA, Provisional), composed of 606 samples. Results obtained for the genes giving Logrank Test $p < 0.05$ were selected for discussion.

2. Results

2.1. HMGB1 *and* HMGB2 *Y2H-interactomes in ovarian tumour tissue*

Protein interactions were detected using the yeast two-hybrid (Y2H) approach already explained in chapter 1. A cDNA library was constructed using total RNA extracted from tissue obtained from primary transitional cell carcinoma (TCC) of the ovary, and Y2H assays were carried out as described in Materials and Methods, using HMGB1 and HMGB2 as baits. Although the Y2H strategy usually reports a lesser number of targets than other interactome techniques (i.e. MS-based strategies) it has the advantage that those detected actually represent physical and direct interactions. In the library prepared from ovarian tumour tissue (Table 1), 5 genes encoding proteins were identified using the HMGB1 bait (C1QA, DAG1, RPL29, RSF1, TGM2) and 6 genes encoding proteins (COMMD1, MIEN1, PCBP1, TBC1D25, ZFR, ZNF428) were identified with the HMGB2 bait.

Table 1. Clones from the cancerous ovarian tissue libraries, which interact with HMGB1 or HMGB2 in the Y2H assays

Interacting Partner	Bait	Aa	Uniprot Code	Brief functional description according to Uniprot
C1QA	HMGB1	47-177	P02745	Complement C1q subcomponent subunit A
DAG1	HMGB1	311-516	Q14118	Dystroglycan. The dystroglycan complex is involved in a number of processes including laminin and basement membrane assembly, sarcolemmal stability, cell survival, peripheral nerve myelination, nodal structure, cell migration, and epithelial polarization
RPL29	HMGB1	36-143	P47914	60S ribosomal protein L29
RSF1	HMGB1	616-799	Q96T23	Remodeling and spacing factor 1 required for assembly of regular nucleosome arrays by the RSF chromatin-remodeling complex
TGM2	HMGB1	377-480	P21980	Transmembrane gamma-carboxyglutamic acid protein 2
COMMD1	HMGB2	4-189	Q8N668	COMM domain-containing protein 1. Proposed scaffold protein that is implicated in diverse physiological processes and whose function may be in part linked to its ability to regulate ubiquitination of specific cellular proteins.
MIEN1 (alias C35)	HMGB2	1-116	Q9BRT3	Migration and invasion enhancer 1 that increases cell migration by inducing filopodia formation at the leading edge of migrating cells. Plays a role in regulation of apoptosis, possibly through control of CASP3.
PCBP1	HMGB2	26-202	Q15365	Poly(rC)-binding protein 1. Single-stranded nucleic acid binding protein that binds preferentially to oligo dC.
TBC1D25	HMGB2	309-366	Q3MII6	TBC1 domain family member 25. Acts as a GTPase-activating protein specific for RAB33B. Involved in the regulation of autophagosome maturation.
ZFR	HMGB2	294-722	Q96KR1	Zinc finger RNA-binding protein. Involved in post-implantation and gastrulation stages of development. Involved in the nucleocytoplasmic shuttling of STAU2.
ZNF428	HMGB2	153-188	Q96B54	Zinc finger protein 428.

In previous experiments[18] using libraries derived from SKOV-3 cells (Table 2), a clone showing homology to lncRNA *MALAT1* and 5 genes encoding proteins (AKIP1, KRT7, ATF71P, UHRF2, WDR60) were identified using the HMGB1 bait, and 7 genes encoding proteins were identified with the HMGB2 bait (BCCIP, COMMD1, NOP53, MIEN1, ROCK1, U2AF1, ZNF668)[18]. Table 2 summarizes results previously obtained using libraries derived from SKOV-3 cell cultures[18] in order to compare results obtained with libraries derived from EOC tissue in this study.

Table 2. Previously defined HMGB1 and HMGB2 interactions using SKOV-3 libraries[18].

Interacting Partner	Bait	Aa	Uniprot Code	Brief functional description according to Uniprot
AKIP1	HMGB1	29-210	Q9NQ31	A-kinase-interacting protein 1 that regulates the effect of the cAMP-dependent protein kinase signaling pathway on the NF-kappa-B activation cascade.
KRT7	HMGB1	102-289	P08729	Keratin, type II cytoskeletal 7 that blocks interferon-dependent interphase and stimulates DNA synthesis.
MALAT1	HMGB1	lncRNA		
ATF7IP	HMGB1	8-250	Q6VMQ6	Recruiter that couples transcriptional factors to general transcription apparatus and thereby modulates transcription regulation and chromatin formation. Facilitates telomerase TERT and TERC gene expression by SP1 in cancer cells
UHRF2	HMGB1	157-277	Q96PU4	E3 ubiquitin-protein ligase UHRF2 that is an intermolecular hub protein in the cell cycle network. Through cooperative DNA and histone binding, may contribute to a tighter epigenetic control of gene expression in differentiated cells.
WDR60	HMGB1	170-336	Q8WVS4	WD repeat-containing protein 60.
BCCIP	HMGB2	8-257	Q9P287	BRCA2 and CDKN1A-interacting protein that is required for microtubule organizing activities during interphase.
COMMD1	HMGB2	2-189	Q8N668	COMM domain-containing protein 1. Proposed scaffold protein that is implicated in diverse physiological processes and whose function may be in part linked to its ability to regulate ubiquitination of specific cellular proteins.
NOP53 (alias GLTSCR2 or PICT1)	HMGB2	186-453	Q9NZM5	Ribosome biogenesis protein NOP53. Originally identified as a tumour suppressor, it may also play a role in cell proliferation and apoptosis by positively regulating the stability of PTEN, thereby antagonizing the PI3K-AKT/PKB signaling pathway.
MIEN1 (alias C35)	HMGB2	1-116	Q9BRT3	Migration and invasion enhancer 1 that increases cell migration by inducing filopodia formation at the leading edge of migrating cells. Plays a role in regulation of apoptosis, possibly through control of CASP3.
ROCK1	HMGB2	141-197	Q13464	Rho-associated protein kinase 1 that is a key regulator of actin cytoskeleton and cell polarity.
U2AF1	HMGB2	35-202	Q01081	Splicing factor U2AF 35 kDa subunit, that plays a critical role in both constitutive and enhancer-dependent splicing by mediating protein-protein, and protein-RNA interactions required for accurate 3'-splice site selection.
ZNF668	HMGB2	16-239	Q96K58	Zinc finger protein 668

Two proteins that interact with HMGB2, COMMD1 and MIEN1, were identified in both libraries (Table 1 and 2), which cross-validate these results. In both tables, the coding region of the protein which is recognized in each detected interaction with HMGB1 or HMGB2 is indicated, as well as a brief functional description according to Uniprot. The interactions of HMGB1 with RLP29 and the interaction of HMGB2 with ZNF428 were previously described in non-cancerous ovarian HOSEpiC cells from epithelial origin[22]. We have reviewed in the literature the experimentally proved functions of the proteins that interact with HMGB1 and HMGB2 in both Y2H-interactome studies (from SKOV-3 cells and from TCC of the ovary cancer tissue), and results clearly show the association of these proteins with several current cancer hallmarks: sustained proliferation, metastasis, angiogenesis, resisting cell death, altered cellular energetics, and immune evasion. Data are shown in Figure 1.
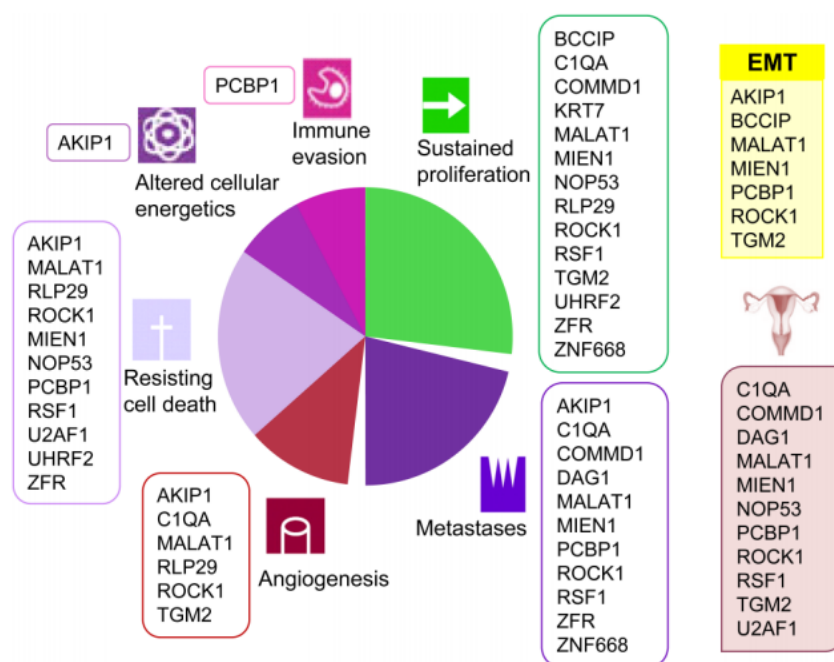
Figure 1. Associations of proteins detected in the Y2H EOC-HMGB-interactome and cancer hallmarks or epithelial to mesenchymal transition (EMT). Those previously related to cancer from ovarian origin are also shown under the ovary pictogram. References supporting the scheme are indicated for each protein as follows. AKIP1[23–27], KRT7[28], MALAT1[29–31], UHRF2[32,33], BCCIP[34,35], COMMD1[36–40], NOP53[41–43], MIEN1[44–46], ROCK1[47–61], U2AF1[62], ZNF668[63,64], C1QA[65], DAG1[66], RLP29[67], RSF1[68–71], TGM2[72,73], PCBP1[74–76], ZFR[77–79].

Remarkably, 60% of the proteins found in this EOC-HMGB-interactome study have been previously associated to ovarian cancer and/or to the Epithelial to Mesenchymal Transition (EMT), typical of epithelial cells in malignant differentiation processes, although they were not previously related to interactions with HMGB proteins. Such is the case of COMMD1[38], NOP53[80], MIEN1[81], ROCK1[49,53,60], PCBP1[82], TGM2[83], U2AF1[84], C1QA[85], DAG1[86] and RSF1[70,71,87,88]. Furthermore, BCCIP[89], ROCK1[50], PCBP1[90], AKIP1[26], TGM2[91], and MIEN1[45] proteins have been cited in relation to the EMT, typical of epithelial cells in malignant differentiation processes. MALAT1, a lncRNA, has also been related to ovarian cancer[29,92–95], and EMT[96].

2.2. Analysis of expression of detected preys according to public cancer data bases and influence on survival to ovarian cancer

Taking advantage of public available data accessible through Expression Atlas[97] at European Bioinformatics Institute (https://www.ebi.ac.uk), we have compared gene expression levels of *HMGB1*, *HMGB2* and genes encoding their detected protein interacting partners, from ovarian tumour tissue compiled with those previously identified in our laboratory from SKOV-3 cells[18], in ovary tissue from healthy individuals (39 samples from GTEx Project[98]), and public data extracted from Pan-Cancer Analysis of Whole Genomes (PCAWG) corresponding to 110 tumours of ovarian adenocarcinomas (Table 3). Results indicate that HMGB1 and HMGB2, as well as most of their detected interacting partners (91%) are expressed at higher levels in ovarian adenocarcinoma than in normal ovarian tissue (Table 3), following a pattern of co-regulation with *HMGB1* and *HMGB2* that is frequent among genes encoding interacting proteins[99]. The highest ratios of RNA changes between cancerous and healthy ovarian samples correspond to *KRT7* (ratio >1700), *C1QA* (ratio 12.5) and *MIEN1* (ratio 6.3). Only two genes, NOP53 and MALAT1 are less expressed in cancerous than in healthy ovarian cells in this comparison.

Table 3. Differential expression of HMGB1, HMGB2 and their interacting partners in healthy individuals and ovary cancer patients. mRNA levels obtaining by RNAseq are expressed in TPM (Transcripts per million).

Gene Name	Ovarian Adenocarcinoma	Normal Ovary (GTEx)	Ratio cancerous/healthy
AKIP1	45	28	1.6
ATF7IP	46	14	3.3
BCCIP	131	33	4.0
C1QA	613	49	12.5
COMMD1	65	17	3.8
DAG1	264	51	5.2
HMGB1	524	153	3.4
HMGB2	453	100	4.5
KRT7	1258	0.7	1797
MALAT1	244	886	0.3
MIEN1	144	23	6.3
NOP53	427	576	0.7
PCBP1	1554	386	4.0
ROCK1	42	21	2.0
RPL9	2526	1540	1.6
RSF1	37	13	2.8
TBC1D25	40	20	2.0
TGM2	118	50	2.4
U2AF1	81	42	1.9
UHRF2	35	28	1.3
WDR60	34	21	1.6
ZFR	149	57	2.6
ZNF428	197	64	3.1
ZNF668	25	5	5.0

The structure of MIEN1 and their function in relation to ovary cancer has been recently reviewed[100]. Selecting three of the baits interacting with HMGB1 and HMGB2, MIEN1, NOP53 and KRT7, we have also directly observed in experiments carried in our laboratory that HMGB1, HMGB2, MIEN1 and KRT7 are expressed at higher levels in SKOV-3 cancerous cells than in HOSEPic normal ovary cells (Figure 2). Also, in accordance with patient data (Table 3), NOP53 is expressed at lower levels in the cancerous cell line than in the healthy ovary cell line (Figure 2).
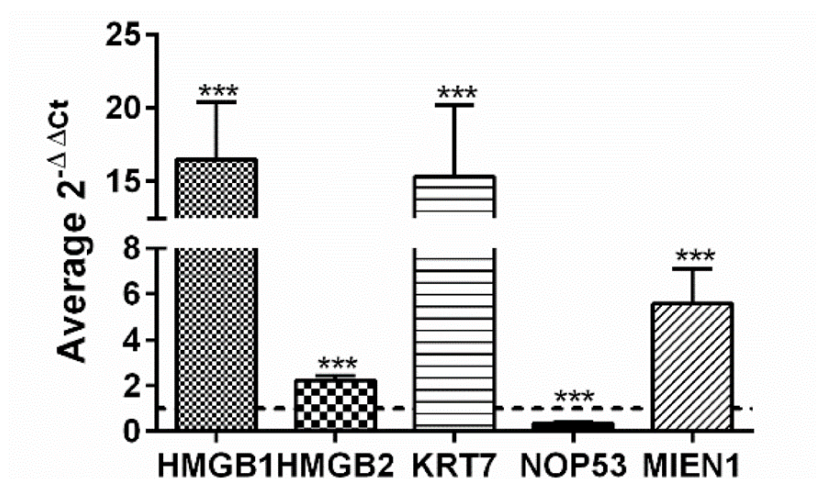
Figure 2. **Relative expression of HMGB1, HMGB2, KRT7, MIEN1 and NOP53 genes in SKOV-3 cells _versus_ non-cancerous human ovarian HOSEPic cells**. The dotted line indicates no variation, boxes upper the line show genes over-expressed in SKOV-3 cells, and those under the line are genes under-expressed in SKOV-3 cells. *** ($p < 0.001$). ** ($p < 0.01$). * ($p < 0.05$).

We also analyzed our set of identified HMGB1 and HMGB2 preys (listed in Table 1 and 2) with the tools available in cBioportal (http://www.cbioportal.org/)[101,102]. We analyzed samples from the study "Ovarian Serous Cystadenocarcinoma (TCGA)" with information of 606 samples from 594 patients (access through https://www.cbioportal.org/study/summary?id=ov_tcga Date 03-03-2020). Patients who have higher expression of some of the genes identified in our study have lower survival expectation than the rest (Figure 3). Analysis of expression data based on microarray technology reveled that up-regulation of mRNA levels of MIEN1 (Figure 3A) or TGM2 (Figure 3B), negatively correlated to survival.
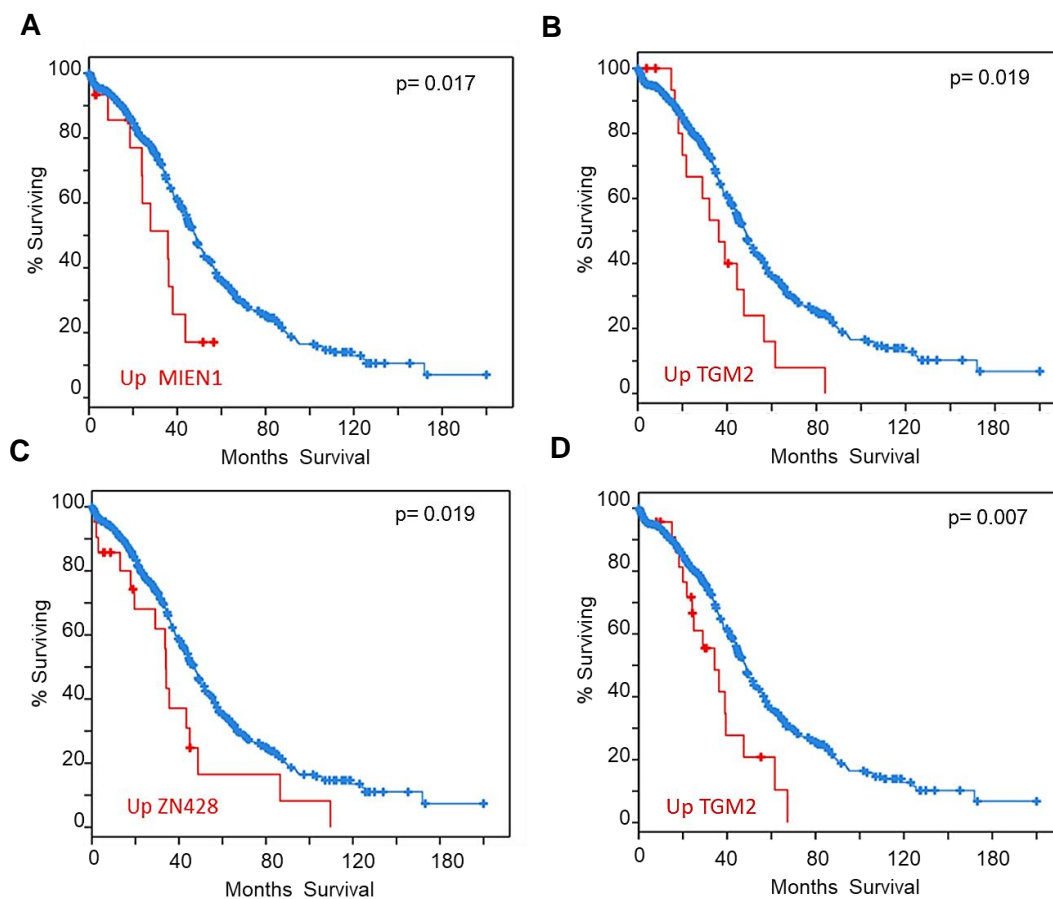
Figure 3. **Survival analysis.** Analysis of expression data based on microarray technology reveled that up-regulation of mRNA levels of MIEN1 (Figure 3A) or TGM2 (Figure 3B), negatively correlated to survival. Analysis of expression data based on RNAseq technology showed that up-regulation of ZN428 (Figure 3C) or TGM2 (Figure 3D) worsens survival outcomes.

Analysis of expression data based on RNAseq technology showed that up-regulation of ZN428 (Figure 3C) or TGM2 (Figure 3D) worsens survival outcomes. It has also been reported that patients with RSF1 amplification or overexpression had a significantly shorter overall survival than those without[103].

2.3. Effect of HMGB1 *and* HMGB2 *silencing on the expression of genes encoding proteins detected in the ovary-HMGB-interactome*

HMGB1 and HMGB2 genes were silenced as explained in materials and methods. Levels of mRNA from several detected interacting partners of HMGB1 and HMGB2 in ovary cancer were analyzed by qPCR and changes (siHMGB/HMGB) are shown in Figure 4.
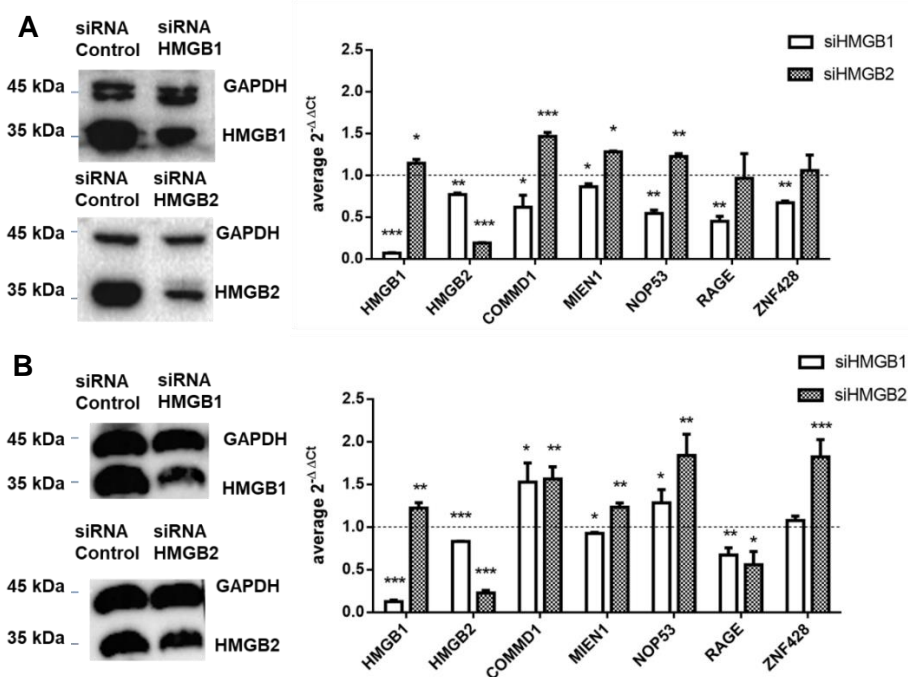
Figure 4. Control of EOC-HMGB interactome. Changes in gene expression after HMGB1 and HMGB2 silencing in SKOV-3 cells (A) and PEO-1 cells (B). The dotted line indicates no variation, boxes upper the line show genes over-expressed in SKOV-3 cells, and those under the line are genes under-expressed in SKOV-3 cells. *** (p< 0.001). ** (p<0.01). * (p<0.05).

This analysis also included HMGB1, HMGB2, and RAGE, one of the membrane receptors in the extracellular signaling function of HMGB1[104], which is also present in the surface of cancerous cells[105]. HMGB2 silencing causes mainly overexpression, whereas HMGB1 silencing has the opposite effect.

2.4. Co-immunoprecipitation of HMGB2 *with* NOP53 *and* MIEN1 *in PEO-1 and SKOV-3 cells*

Since the Y2H interactome from tissue was extracted from primary transitional cell carcinoma (TCC) of the ovary, which is a relatively unfrequently diagnosed serous EOC, we decided to validate HMGB2 interactions with MIEN1 and NOP53 by co-Immunoprecipitation, an orthogonal method to the Y2H approach, and using SKOV-3 cells and PEO-1 cells; since these last are considered as derived from the most common form of ovary cancer, high-grade serous adenocarcinome. Data are shown in Figure 5.

A

B
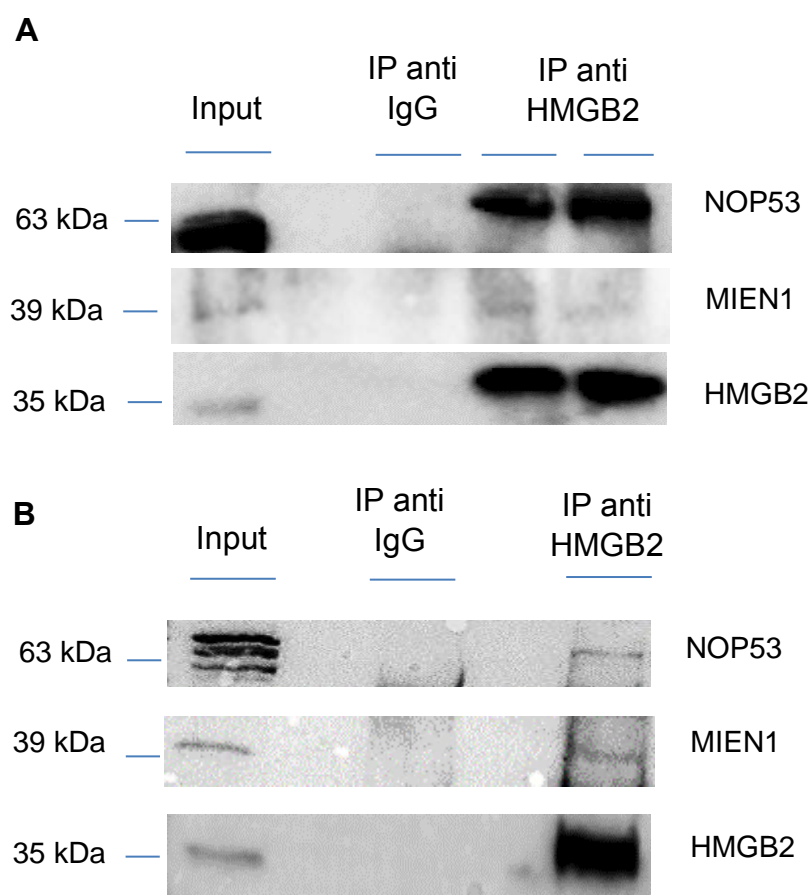
Figure 5. **Validation of HMGB2 interactions with MIEN1 and NOP53 in SKOV-3 (A) and PEO-1 (B) cells by co-immunoprecipitation.**

2.5. Confocal co-localization of HMGB2 *with* NOP53 *and* MIEN1 *in PEO-1*

A co-localization assay was performed in order to confirm the physical interactions identified through Y2H of both NOP53 and MIEN1 with HMGB2, as well as to determine the specific cellular compartment in which these interactions take place. The transfection of PEO-1 cells with plasmid constructions containing our genes of interest fused to a fluorescent protein allowed us to evaluate their intracellular distribution. Using this alternative approach, the physical interaction between HMGB2 and MIEN1 (Figure 6) was detected in the perinuclear region. Despite of co-localized regions show a characteristic yellow color, a co-localization pixel map was generated using the Fiji's program "Colocalization" tool in order to verify this co-localization (Figure 6A). Furthermore, the analysis of the co-localization rate in the images was analyzed using Fiji's program "JaCoP" to discard possible random co-localization. Pearson's coefficient produced by JaCoP for HMGB2 and MIEN1 co-localization was p=0.2-0.3 (being 1 total co-localization, 0 random co-localization and -1 opposite distribution). Although the fluorescence analysis result suggests that there is no random co-localization, the p value is not high enough to determine a reliable and well stablished co-localization.

On the other hand, NOP53 and HMGB2 physical interaction (Figure 7) was detected mostly in nucleoli, but also in nucleoplasm and cytoplasm. The high colocalization rate denoted by the yellow staining was confirmed by the co-localization pixel map (Figure 7A) as well as by the Pearson's coefficient with a p=0.7-0.8. This result validates that there is a physical interaction and colocalization between HMGB2 and NOP53 that was observed overexpressing both genes under the CMV promoter present in pDsRED-C1 or pAcGFP-C1 vectors.

A

B
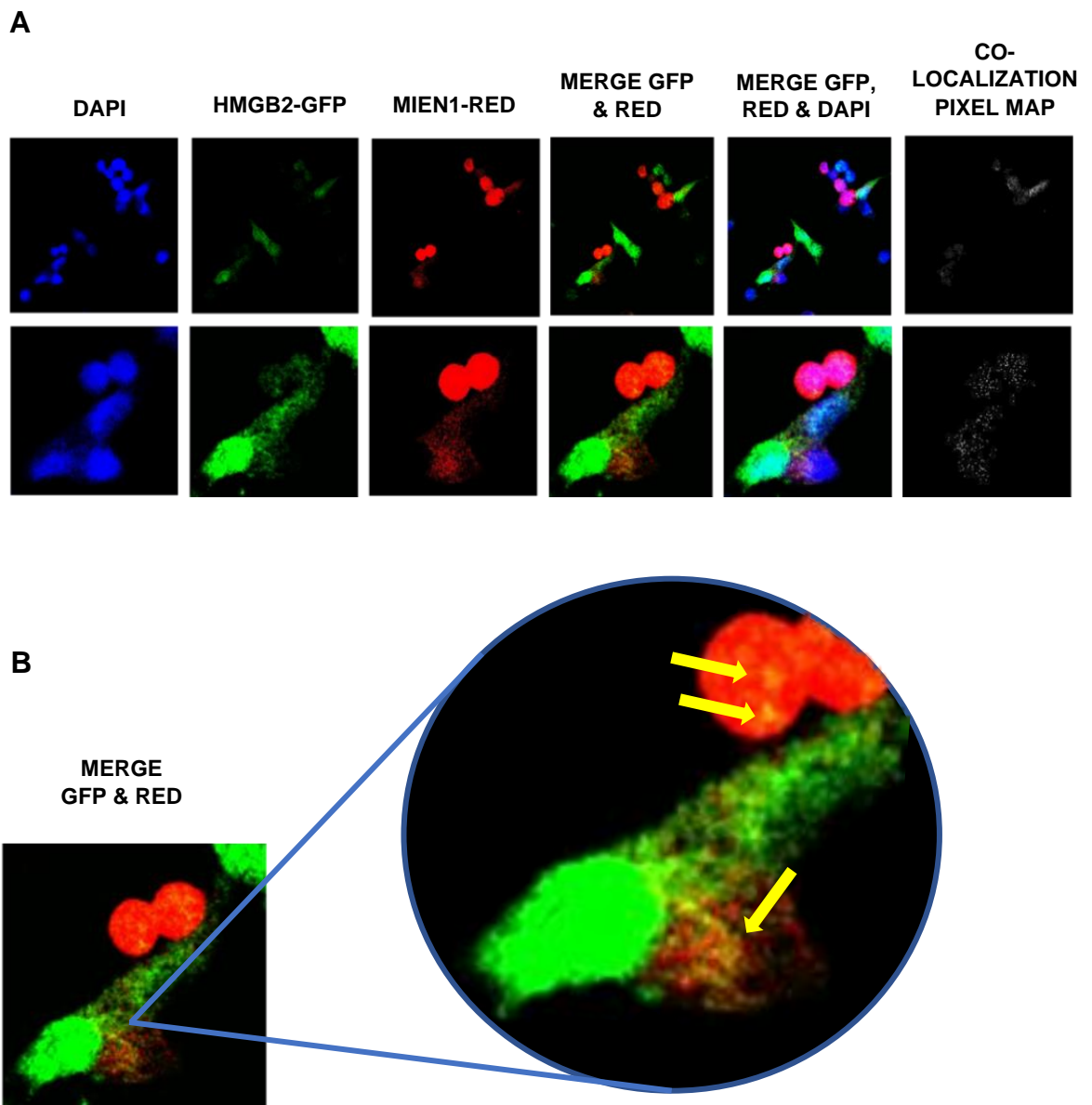
Figure 6. **Co-localization of HMGB2 with MIEN1 in PEO-1 cells**. **(A)** Nuclear staining with DAPI shows in blue, HMGB2 fused to GFP fluorescent tag is seen in green and MIEN1 fused to RED fluorescent tag in red. Co-localization appears in yellow staining and co-localization pixel map. **(B)** Augmented image of merge denoting important HMGB2 and MIEN1 co-localization in cytoplasm.

A

B
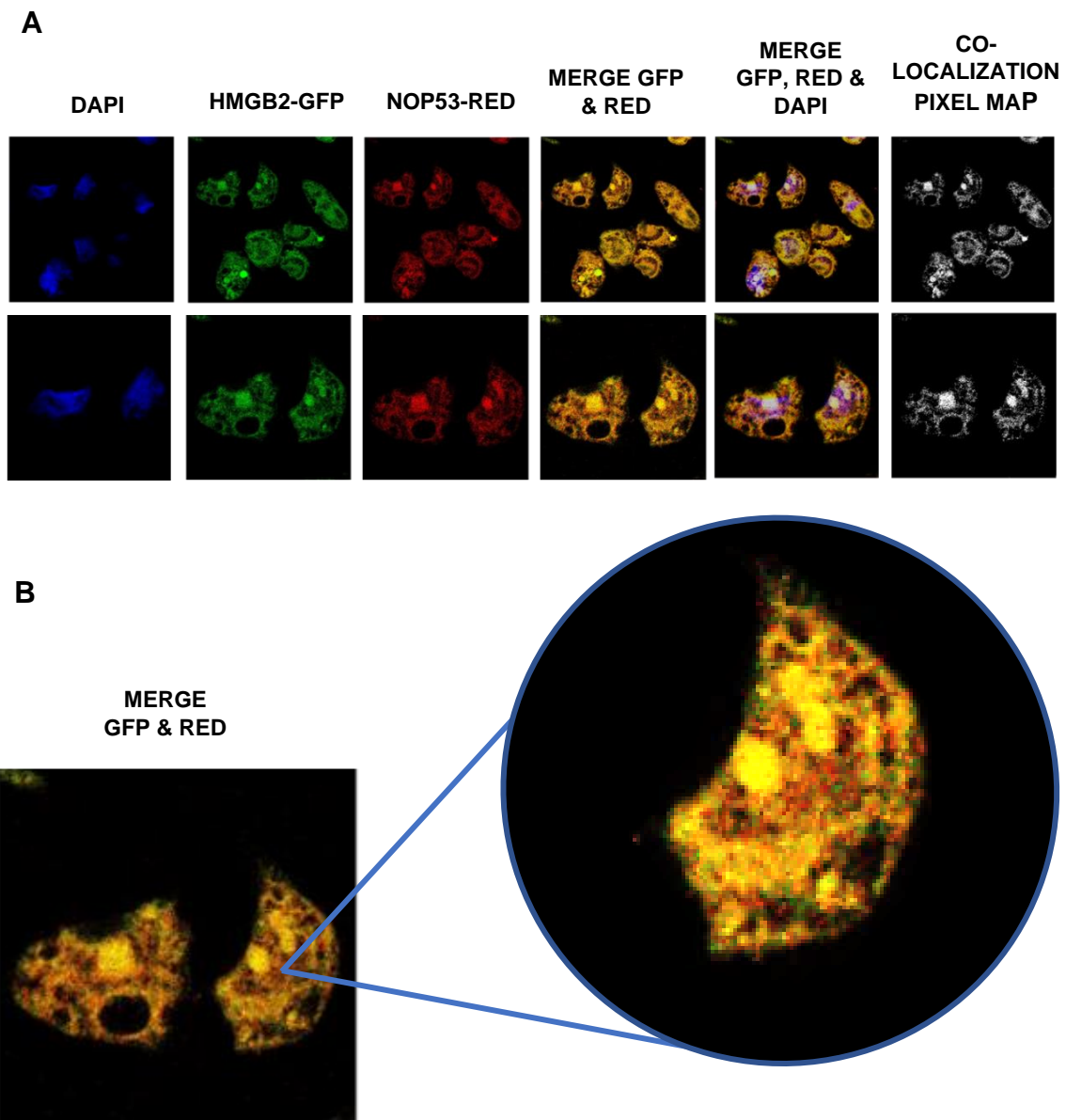
Figure 7. **Co-localization of HMGB2 with NOP53 in PEO-1 cells**. **(A)** Nuclear staining with DAPI shows in blue, HMGB2 fused to GFP fluorescent tag is seen in green and NOP53 fused to RED fluorescent tag in red. Co-localization appears in yellow staining and co-localization pixel map. **(B)** Augmented image of merge denoting important HMGB2 and NOP53 co-localization regions in the nucleoli.

2.6. HMGB2 *interactome by co-immunoprecipitation and Mass Spectrometry*

There are different proteomic approaches to determine protein interactions and BioGRID collets 310 interactors for HMGB1 but only 90 for HMGB2. Taking into account that after the approach used initially in this thesis, Y2H, we had characterized a limited number of interactions with HMGB2 in the cancerous cells from a primary transitional cell carcinoma (TCC) of the ovary tumour, we decided to complement this study with a IP-MS approach. This approach is based on immunoprecipitation (IP) with an antibody directed against HMGB2 and identification, by mass spectrometry (MS), of other proteins pulled down with HMGB2 by co-IP. Three biological replicates of HMGB2 IP coupled with MS-based proteomics was performed with the aim of characterize HMGB2 interactome of the ovarian tumour cell line SKOV-3. In order to discard possible non-specific interactions, parallel IgG IPs were carried out along with HMGB2 IPs. Details of the method have been explained in the Materials and Methods section. After analysis of data with Protein Pilot results from the three biological replica identified 256, 99 and 136 proteins respectively that co-immunoprecipitated with HMGB2.

We first analyzed the presence of HMGB2 in the three biological replica. The results are quantified in table 4 and they clearly show that replica 3 (R3) was not comparable to the previous ones, therefore we decided to further analyze only data from replica 1 and 2 (R1 and R2) (Table 5).

Table 4. Quality of HMGB2 recovery in the immunoprecipitations.

Biological replica	Coverage	Identified HMGB2 peptides	HMGB2's position (scored by spectral frequency)	Total of proteins identified as co-IPs
R1 (18059)	58.13%	44	7	256
R2 (18068)	38.76%	22	2	99
R3 (20029)	19.23%	2	92	136

After identifying the interacting proteins using MS/MS the samples R1 and R2 were analyzed through the Significance Analysis of INTeractome (SAINT)[106] score SAINTexpress107 and only interactions with a minimum SP of 0.7 were accounted. A sum of 23 proteins were detected matching this requisite (Table 5; Figure 8).

Table 5. HMGB2 interacting proteins in SKOV-3 cells identified through two independent immunoprecipitation experiments coupled to Mass Spetrometry with a SP>0.7. C: coverage (%). P: peptides. S: spectra.

| | First Experiment (18059) | | | | | | Second Experiment (18068) | | | | | | |
| | IP HMGB2 | | | IP IgG | | | IP HMGB2 | | | IP IgG | | | |
Proteins	C	P	S	C	P	S	C	P	S	C	P	S	SP
RPL7A	44.3	15	30	0	0	0	10.9	2	4	0	0	0	1
NCL	43.2	45	88	0	0	0	5	2	4	0	0	0	1
CCAR2	64.9	77	169	0	0	0	37.9	33	57	0	0	0	1
HNRNPM	45.6	48	58	0	0	0	12.6	7	16	0	0	0	1
CMAS	19.1	5	8	0	0	0	6.4	2	4	0	0	0	1
GIPC1	25.2	7	9	0	0	0	17.7	5	8	0	0	0	1
RPL7	46.3	16	27	0	0	0	10.0	2	3	0	0	0	1
HMGB2	57.4	37	95	0	0	0	38.7	22	57	0	0	0	1
RPS8	40.8	12	26	0	0	0	13.4	2	4	7.2	1	0	1
H1.4	33.3	20	5	0	0	0	27.4	13	2	0	0	0	0.99
HNRNPK	16.2	6	7	0	0	0	9.5	3	4	3.6	1	1	0.99
RPL18A	12.5	5	12	0	0	0	14.2	2	2	0	0	0	0.99
INPP5E	3.57	2	2	0	0	0	10.4	4	7	0	0	0	0.99
H2AC4	57.6	37	7	26.9	3	0	35.3	5	2	0	0	0	0.99
SPTY2D1	21.7	9	14	0	0	0	9.3	2	2	0	0	0	0.99
RPL32	38.5	7	9	0	0	1	11.1	1	2	0	0	0	0.88
RPL6	52.7	28	59	0	0	0	12.8	2	2	5.2	1	1	0.88
MYL6	54.3	10	16	0	0	0	20.5	2	2	19.2	2	1	0.88
RPS2	39.2	12	22	0	0	1	5.8	1	2	2.9	1	0	0.88
MATR3	17.1	9	11	0	0	0	5.4	2	3	0	0	1	0.88
RPL34	22.2	4	6	0	0	0	6.8	1	3	6.8	1	2	0.83
RPL38	18.5	1	2	18.5	1	1	18.5	1	2	17.1	1	0	0.76
H2A2C	58.1	44	114	0	0	2	35.6	8	13	0	0	3	0.72

Comparing with HMGB2 described partners in BioGRID database, no match with the identified proteins by IP-MS was found, implying the physical interaction between HMGB2 and these 23 proteins has not been described before. However, some of them have been reported to interact with HMGB1 in BioGRID: RPL6, RPL7, RPL7A, RPL18A, RPL32, RPS2, RPS8, HMGB2 and NCL.

The 23 proteins selected include proteins described for perform their function in the nucleoli, nucleus or cytoplasm, denoting HMGB2 ability to translocate among these compartments. Considering the different biological functions displayed by these proteins (Table 6), they carry out some important roles associated with cancer development such as apoptosis regulation, ribosomal biogenesis modulation or stress response. Among the functions illustrated in Table 6, the regulation of gene expression is an interesting function that would explain the results obtained through HMGB2 siRNA silencing (Figure 4).

Table 6. Biological functions of HMGB2 selected interacting proteins with an SP value higher than 0.7.

Protein	Aa	Uniprot Code	Brief functional description according to Uniprot
RPL7A (Ribosomal protein L7a)	266	P62424	RPL7A is a structural constituent of ribosome that is involved in maturation of LSU-rRNA, nuclear-transcribed mRNA catabolic process, nonsense-mediated decay, SRP-dependent co-translational protein targeting to membrane, viral transcription and translation.
NCL (Nucleolin)	710	P19338	Nucleolin is the major nucleolar protein of growing eukaryotic cells. It is found associated with intranucleolar chromatin and pre-ribosomal particles. It induces chromatin decondensation by binding to histone H1. It is thought to play a role in pre-rRNA transcription and ribosome assembly. May play a role in the process of transcriptional elongation. Binds RNA oligonucleotides with 5'-UUAGGG-3' repeats more tightly than the telomeric single-stranded DNA 5'-TTAGGG-3' repeats.
CCAR2 (Cell cycle and apoptosis regulator protein 2)	923	Q8N163	Core component of the DBIRD complex, a multiprotein complex that acts at the interface between core mRNP particles and RNA polymerase II (RNAPII) and integrates transcript elongation with the regulation of alternative splicing: the DBIRD complex affects local transcript elongation rates and alternative splicing of a large set of exons embedded in (A + T)-rich DNA regions .Inhibits SIRT1 deacetylase activity leading to increasing levels of p53/TP53 acetylation and p53-mediated apoptosis. Plays an important role in tumour suppression through p53/TP53 regulation; stabilizes p53/TP53 by affecting its interaction with ubiquitin ligase MDM2. Represses the transcriptional activator activity of BRCA1.

Table 6 Continued

Protein	Aa	Uniprot Code	Brief functional description according to Uniprot
HNRNPM (Heterogeneous nuclear ribonucleo-protein M)	730	P52272	Pre-mRNA binding protein in vivo, binds avidly to poly(G) and poly(U) RNA homopolymers in vitro. Involved in splicing. Acts as a receptor for carcinoembryonic antigen in Kupffer cells, may initiate a series of signaling events leading to tyrosine phosphorylation of proteins and induction of IL-1 alpha, IL-6, IL-10 and tumour necrosis factor alpha cytokines.
CMAS (CMP-N-acetylneuraminic acid synthase)	434	Q8NFW8	Catalyzes the activation of N-acetylneuraminic acid (NeuNAc) to cytidine 5'-monophosphate N-acetylneuraminic acid (CMP-NeuNAc), a substrate required for the addition of sialic acid. Has some activity toward NeuNAc, N-glycolylneuraminic acid (Neu5Gc) or 2-keto-3-deoxy-D-glycero-D-galacto-nononic acid (KDN).
GIPC1 (GAIP C-terminus-interacting protein 1)	333	O14908	GIPC1 is involve in cellular response to interleukin-7, endothelial cell migration, G protein-coupled receptor signaling pathway, negative regulation of proteasomal ubiquitin-dependent protein catabolic process, or positive regulation of cytokinesis.
RPL7 (60S ribosomal protein L7)	248	P18124	Component of the large ribosomal subunit. Binds to G-rich structures in 28S rRNA and in mRNAs. Plays a regulatory role in the translation apparatus; inhibits cell-free translation of mRNAs. Binds to DNA, mRNA and identic proteins and is involved in maturation of LSU-rRNA, nuclear-transcribed mRNA catabolic process, nonsense-mediated decay, SRP-dependent co-translational protein targeting to membrane, viral transcription and translation.
HMGB2 (High mobility group protein B2)	209	P26583	Multifunctional protein with various roles in different cellular compartments. May act in a redox sensitive manner. In the nucleus is an abundant chromatin-associated non-histone protein involved in transcription, chromatin remodeling and V(D)J recombination and probably other processes. Binds DNA with a preference to non-canonical DNA structures such as single-stranded DNA. Can bent DNA and enhance DNA flexibility by looping thus providing a mechanism to promote activities on various gene promoters by enhancing transcription factor binding.
RPS8 (Ribosomal protein S8)	208	P62241	Belongs to the eukaryotic ribosomal protein eS8 family. RPS8 is a structural constituent of ribosome involved in maturation of SSU-rRNA from tricistronic rRNA transcript (SSU-rRNA, 5.8S rRNA, LSU-rRNA), along with cytoplasmic translation, nuclear-transcribed mRNA catabolic process, nonsense-mediated decay, SRP-dependent co-translational protein targeting to membrane, RNA binding, viral transcription and translation.

Table 6 Continued

Protein	Aa	Uniprot Code	Brief functional description according to Uniprot
H1.4 (Histone H1.4)	21	P10412	Histone H1.4; Histone H1 protein binds to linker DNA between nucleosomes forming the macromolecular structure known as the chromatin fiber. Histones H1 are necessary for the condensation of nucleosome chains into higher-order structured fibers. Acts also as a regulator of individual gene transcription through chromatin remodeling, nucleosome spacing and DNA methylation.
HNRNPK (Heterogeneous nuclear ribonucleoprotein K)	463	P61978	One of the major pre-mRNA-binding proteins. Binds tenaciously to poly(C) sequences..Can also bind poly(C) single-stranded DNA. Plays an important role in p53/TP53 response to DNA damage, acting at the level of both transcription activation and repression. When sumoylated, acts as a transcriptional coactivator of p53/TP53, playing a role in p21/CDKN1A and 14-3-3 sigma/SFN induction. As far as transcription repression is concerned, acts by interacting with long intergenic RNA p21 (lincRNA-p21), a non-coding RNA induced by p53/TP53.
RPL18A (60S ribosomal protein L18a)	176	Q02543	RPL18A is an structural component of ribosomes and plays a role in cytoplasmic translation, nuclear-transcribed mRNA catabolic process, nonsense-mediated decay or SRP-dependent cotranslational protein targeting to membrane
INPP5E (Phosphatidylinositol polyphosphate 5-phosphatase type IV)	644	Q9NRR6	Phosphatidylinositol (PtdIns) phosphatase that specifically hydrolyzes the 5-phosphate of phosphatidylinositol-3,4,5-trisphosphate (PtdIns(3,4,5) P3), phosphatidylinositol 4,5-bisphosphate (PtdIns(4,5)P2) and phosphatidylinositol 3,5-bisphosphate (PtdIns(3,5)P2). Specific for lipid substrates, inactive towards water soluble inositol phosphates. Plays an essential role in the primary cilium by controlling ciliary growth and phosphoinositide 3-kinase (PI3K) signaling and stability.
H2AC4 (Histone H2A type 1B/E)	130	P04908	Core component of nucleosome. Nucleosomes wrap and compact DNA into chromatin, limiting DNA accessibility to the cellular machineries which require DNA as a template. Histones thereby play a central role in transcription regulation, DNA repair, DNA replication and chromosomal stability. DNA accessibility is regulated via a complex set of post-translational modifications of histones, also called histone code, and nucleosome remodeling
SPTY2D1 (SPT2 domain-containing protein 1)	685	Q68D10	Histone chaperone that stabilizes pre-existing histone tetramers and regulates replication-independent histone exchange on chromatin. Required for normal chromatin refolding in the coding region of transcribed genes, and for the suppression of spurious transcription. Binds DNA and histones and promotes nucleosome assembly (in vitro). Facilitates formation of tetrameric histone complexes containing histone H3 and H4. Modulates RNA polymerase 1-mediated transcription (By similarity). Binds DNA, with a preference for branched DNA species.

Table 6 Continued

Protein	Aa	Uniprot Code	Brief functional description according to Uniprot
RPL32 (Ribosomal protein L32)	135	P62910	Belongs to the eukaryotic ribosomal protein eL32 family. RPL32 is a structural constituent of ribosome with the ablity of RNA binding and cytoplasmic translation, in addition to displaying roles in nuclear-transcribed mRNA catabolic process, nonsense-mediated decay, SRP-dependent co-translational protein targeting to membrane, viral transcription and translation.
RPL6 (60S ribosomal protein L6)	288	Q02878	Component of the large ribosomal subunit. RPL6 bind to nucleic acids and cadherin, having a role in the regulation of transcription, DNA-templated, ribosomal large subunit assembly, nuclear-transcribed mRNA catabolic process, nonsense-mediated decay, SRP-dependent co-translational protein targeting to membrane, viral transcription and translation.
RPS2 (40S ribosomal protein s2)	293	P1588	RPS2 is a structural component of ribosomes that binds tp RNA, cadherin, enzymes and fibroblast growth factor binding. It is described to perform a role in cytoplasmic translation, nuclear-transcribed mRNA catabolic process, nonsense-mediated decay, SRP-dependent co-translational protein targeting to membrane, viral transcription and translation.
MATR3 (Matrin-3)	847	P43243	May play a role in transcription or may interact with other nuclear matrix proteins to form the internal fibrogranular network. In association with the SFPQ-NONO heteromer may play a role in nuclear retention of defective RNAs. Plays a role in the regulation of DNA virus-mediated innate immune response by assembling into the HDP-RNP complex, a complex that serves as a platform for IRF3 phosphorylation and subsequent innate immune response activation through the cGAS-STING pathway. May bind to specific miRNA hairpins.
RPL34 (60S ribosomal protein L34)	117	P49207	Component of the large ribosomal subunit. RPL34 bind to nucleic acids and cadherin, having a role in the regulation of transcription, DNA-templated, ribosomal large subunit assembly, nuclear-transcribed mRNA catabolic process, nonsense-mediated decay, SRP-dependent co-translational protein targeting to membrane, viral transcription and translation.
RPL38 (60S ribosomal protein L38)	70	P63173	RPL38 is a structural component of the large ribosomal subunit. Its described cellular functions involve 90S preribosome assembly, regulation of cytoplasmic translation, nuclear-transcribed mRNA catabolic process, nonsense-mediated decay, ribonucleoprotein complex assembly and SRP-dependent cotranslational protein targeting to membrane translational initiation. It has also been associated with important biological processes such a axial mesoderm development, middle ear morphogenesis, ossification, sensory perception of sound, or skeletal system development.

Table 6 Continued

Protein	Aa	Uniprot Code	Brief functional description according to Uniprot
H2A2C (Histone H2A type 2-C)	12	Q16777	Core component of nucleosome. Nucleosomes wrap and compact DNA into chromatin, limiting DNA accessibility to the cellular machineries which require DNA as a template. Histones thereby play a central role in transcription regulation, DNA repair, DNA replication and chromosomal stability. DNA accessibility is regulated via a complex set of post-translational modifications of histones, also called histone code, and nucleosome remodeling.

Despite none of these 23 proteins have been described to physically interact with HMGB2 until now, we searched for reported functional protein associations networks in this set of novel physical interactors using STRING. The functional network was filtered by a threshold of 0.7 of confidence score and 1% of FDR stringency.
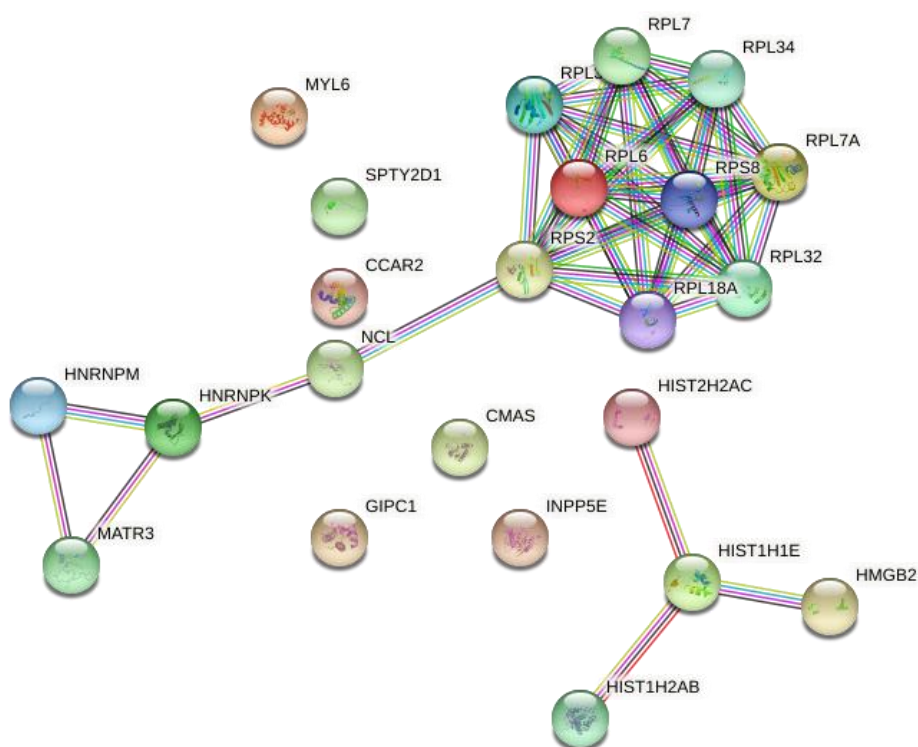
Figure 8. Clustering of proteins that interact with HMGB2 in SKOV-3 cells generated by STRING.

In the clustering produced by STRING under these conditions (Figure 8), a principal cluster can be differentiated including ribosomal proteins (RP) involved in cytoplasmic translation or SRP-dependent co-translational protein targeting to membrane, among other functions, that evidence HMGB2 cytoplasmic location. This principal cluster is related through NCL to a subgroup three proteins (HNRNPK, HNRNPM and MATR3) related with immune-response triggered by DNA binding (DNA-mediated innate immune response and DNA damage response) and RNA binding. Lastly, a third independent group of four proteins, composed by Histones and HMGB2, are associated with regulation of DNA expression through chromatin remodeling.

3. Discussion

Considering the relevance of HMGB proteins in Epithelial Ovary Cancer (EOC), we have determined, for the first time using cancerous tissue, the interactome of HMGB1 and HMGB2 related to this gynecological cancer. To this purpose, we have screened Y2H libraries, prepared from tumour tissue diagnosed as primary transitional cell carcinoma (TCC) of the ovary, with HMGB1 and HMGB2 baits. Supporting the functional significance of proteins detected in this Y2H EOC-HMGB-interactome and comparing with prior screenings performed in our laboratory from SKOV-3 cells[18], we have found in the literature that all of them are experimentally associated to cancer hallmarks, and in a high proportion (54 %) they had been directly related to ovary cancer (Figure 1). Furthermore, ROCK1[50], PCBP1[90], AKIP1[26], TGM2[91], BCCIP[89], and MIEN1[45] proteins have been cited in relation to the epithelial to mesenchymal transition (EMT). Since EMT is an initial step in carcinogenesis, the importance of these proteins in early EOC diagnosis should be considered. Although these proteins as well as HMGB1 and HMGB2 had been previously and independently related to EOC, the implication of a direct interaction between them, as part of their mechanism of action in cancer progression, had not been previously envisaged. Remarkably, the function of HMGB1 in EOC has been previously associated to NF-KB[107,108] through HMGB1/TLR/PI3K/AKT/mTOR/NF-κB or HMGB1/RAGE/ROS/MAPK/NF-κB signaling cascades[109–114] (Figure 9) . Inhibitors for these cascades are being tested as new cancer chemotherapy[114].
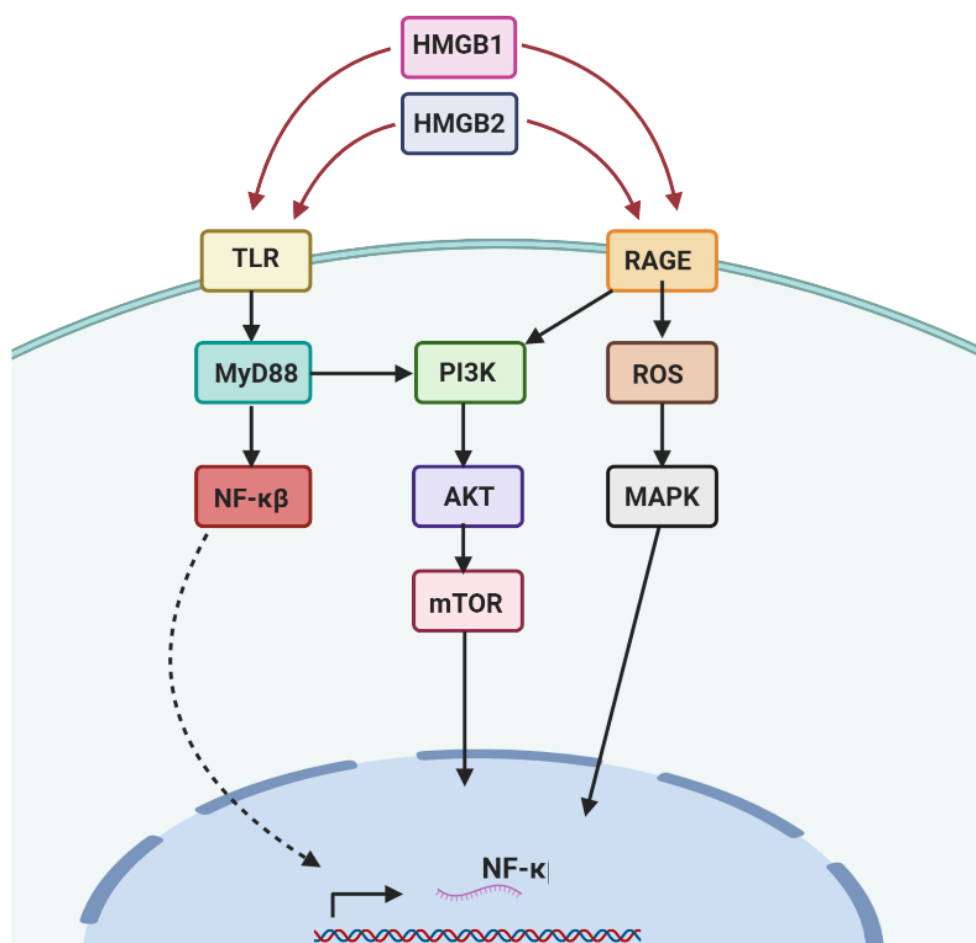
Figure 9. Scheme of described association of HMGB1 and HMGB2 in AKT/PI3K/mTOR pathway. (➡): indirect interaction. (➡): physical interaction. (⋯➤): translocation. Created with BioRender.com.

HMGB2 also interacts with TLR and RAGE receptors[115,116] (Figure 9) in myeloid cells and it is associated to nucleic-acid-mediated innate immune response in mouse embryonic fibroblasts (MEFs), as well as in the AKT/mTOR pathway in pancreatic cancer cells[6].

In this sense, it is interesting to remark that many of the proteins that interact with HMGB1 or HMGB2 in the Y2H EOC interactomes characterized so far (from SKOV-3 or from TCC of the ovary tissue) are related to NF-κB function. AKIP1 is a binding partner of NF-κB p65 subunit, which enhances the NF-κB-mediated gene expression[23]. MALAT1 and NF-κB signaling cross-talk during cancer and other diseases has been reported[117]. BCCIP binds to the protein LYRIC/AEG-1, which promotes tumour cell migration and invasion through activation of NF-κB[118]. COMMD1 inhibits NF-κB by

promoting the ubiquitination and subsequent proteasomal degradation of RELA, component of NF-кB dimer, RELA/p50, bound to chromatin[37]. MIEN1 (C35) functionally enhances migration and invasion via NF-кB/AKT activity[119]. Rho-kinase isoform ROCK1 and its downstream target p38 MAPK regulate nuclear translocation of NF-кB RelA/p65 and subsequent DNA binding activity[58]. Over expression of C1QA up-regulates NF-кB reporters[120]. RSF1-overexpressing paclitaxel-resistant ovarian cancer cell lines were found to express elevated levels of genes regulated by NF-кB[87]. MALAT1, a lncRNA, related to ovarian cancer[92–95], and EMT[96], has also been detected in our results of HMGB1 interactome in EOC (Table 1). We have verified by sequencing that the micropeptide MTEVEMKLLHGVKNVFKRKLRERTTEPRINTNRRAMLLD, derived from lncRNA MALAT1, is in frame and fused to GAL4 in the recovered Y2H clone. Therefore, we suggest that the interaction of this micro-peptide with HMGB1 might be responsible of the positive result obtained in the Y2H screening. The translation of this micro-peptide from the lncRNA MALAT1 has been previously reported in several experiments of ribosome-profiling using colon carcinoma HCT116 cells[121] and embryonic kidney HEK293 cells[122].

Also reinforcing the significance of the interactions detected in our study in relation to clinics, data of gene expression according to Pan-Cancer Analysis of Whole Genomes (PCAWG), and corresponding to 110 tumours of ovarian adenocarcinomas, show that HMGB1, HMGB2 and 91% of their preys detected in this EOC-HMGB-interactome are up-regulated in the comparison between tumour tissue and adjacent non-tumoural tissue (Table 3). Besides, according to the "Ovarian Serous Cystadenocarcinoma (TCGA)" study and using the tools from cBioportal, up-regulation of MIEN1, TGM2 or ZN428 and down-regulation of ZFR or DAG1 in samples from these patients is correlated to poorer survival outcomes (Figure 3). Previous studies reported that NOP53 expression was inversely correlated with the aggressiveness of ovarian serous tumours[43,123]. This indicates that using HMGB proteins, as baits in the search for interacting proteins in a particular type of cancerous cells is a good strategy to find targets with putative use in specific diagnosis, prognosis or therapy in this cancer type. It is interesting to remark that none of the proteins found in our study would be discovered by gene expression analysis. Indeed, none of these genes, including also the baits HMGB1 and HMGB2, are among the top-100 more dysregulated genes in the four Epithelial Ovarian Cancer (EOC) subtype groups previously defined based on expression changes[124]. Taking into consideration that the biological sample for our Y2H interactome came from the uncommon primary transitional cell carcinoma (TCC) of the ovary, the confirmation of the detected interactions in a most representative type of

ovarian cancer was carried out. With the aim of validating the detected interactions, ovarian tumour cell lines with different intracellular background were cultured: SKOV-3, a cell line derived from ovarian serous cystadenocarcinoma, and PEO-1, obtained from a patient with the most common form of ovary cancer, high-grade serous adenocarcinoma, that already underwent chemotherapy treatment. Four different approaches were displayed in one or two of the two mentioned cell lines: siRNA silencing, co-immunoprecipitation, co-localization and mass spectrometry. After detecting the dysregulation of HMGB1, HMGB2, NOP53 and MIEN1 in SKOV-3 (Figure 2), we confirmed that silencing of HMGB1 and HMGB2 by siRNAs in SKOV-3 and PEO-1 cells caused alterations in the expression of NOP53 and MIEN1 among other interacting proteins detected through Y2H (Figure 4). Specifically, HMGB1 seems to have an activator effect, since its silencing led to the downregulation of its interacting proteins, while HMGB2 appears to have the opposite effect causing the upregulation of the same interacting proteins. This antagonistic roles of HMGB1 and HMGB2 were previously described in prostate cancer cells[125].

Previous experiments have repeatedly reported differences in HMGB2/HMGB1 expression, suggesting a diversification of their functions, such as the specific role of HMGB2 in SET complex conformation[9,10] or in cellular differentiation[126–132]. The co-immunoprecipitation of NOP53 and MIEN1 with HMGB2 in both cell lines corroborates the physical interaction *in vivo* and confers higher significance to the studied physical interaction. The differences between the signal intensities observed in Western blots of NOP53 and MIEN1 co-immunoprecipitated with HMGB2 in the two cell lines (Figure 5) could be caused by heterogeneity of epigenetic alterations and mutations in them[133].

According to the co-localization assay, confocal images show that MIEN1 in PEO-1 cells localizes majorly in the perinuclear region (Figure 6) as previously reported in oral cancer cell lines[134,135]. However, the Pearson coefficient of HMGB2 and MIEN1 intracellular co-localization is not significant enough (p=0.3-0.2) to report a stable strong physical interaction, and a better explanation for this result would be a transient weak interaction. Interestingly, in Figure 6B, the confocal picture captured a cell division in which MIEN1 seems to overexpress and localize in the cellular cortex. MIEN1 is known to undergo translational modifications by isoprenylation that allows its translocation to plasma membrane[100]. Furthermore, MIEN1 has been described to indirectly regulate F-actin through the interaction with cytoskeletal focal adhesions[136]. The characteristic spherical shape of mitotic cells is due to the formation and specific distribution of the spindle, promoted by the F-actin structure known as the actomyosin cortex displayed in the cell periphery[137]. Although no co-localization has been found so far between

MIEN1 and F-actin by co-staining, a specific location of MIEN1 underneath the actin rich structures of the membrane was evidenced[138].

Conversely, the interaction between HMGB2 and NOP53 seems to be strong enough to reveal their stable co-localization (Figure 7) with a p=0.8-07. Our data indicate that HMGB2 co-localizes with NOP53 in the nucleoli, nucleoplasm and cytoplasm, where both are visualized in common structures. NOP53 is a bona-fide nucleolar protein[139,140] with capacity to translocate to the nucleoplasm[141] and cytoplasm[142]. However, the presence of HMGB2 in the nucleoli has been reported only in rainbow trout[143]. In mammals HMGB2 is considered a nuclear protein that migrates to cytoplasm[9,144] and the extracellular medium[116,144] in cancerous cells. Interestingly, NOP53 has been reported to sequester proteins with which it interacts in the nucleoli, such as RPL11, under nucleolar stress conditions[123]. In our experiments the overexpression of the HMGB2 and NOP53 genes under the control of the human cytomegalovirus (CMV) immediate early promoter, present in pDsRed-C1 or pAcGFP-C1, could lead to ribosomal stress conditions favoring NOP53 sequestering functions and cell dead. NOP53 overexpression has been described to trigger pro-death autophagy processes through rDNA inhibitory binding and AKT/mTOR/p7Ss6K signaling in glioblastoma and breast cancer cells[145]. This pro-death autophagy occurs without nucleoli disruption or p53 activation, implying that the major cause of cellular death is ribosomal biogenesis-impairing and nucleolar protein translocation[145] .

In the results of HMGB2 interactome obtained by immunoprecipitation coupled with mass spectrometry (IP-MS) (Table 5; Figure 8) using SKOV-3 cells, among the proteins reaching the selected threshold (SP>0.7), Nucleolin (NCL), with a SP=1, is an abundant and typical nucleolar protein, and therefore their interaction supports the localization of HMGB2 in the nucleoli, also detected in the confocal images of PEO-1 cells as commented above (Figure 7). NCL has been also described in the literature for being an interacting protein of Nucleophosmin (NPM) which interestingly is regulated by NOP53[145], other confirmed interacting partner of HMGB2 according to our results. Both of them, NCL and NPM, have a role in DNA repair[146], a possible connection with HMGB2 function in DNA repair[147], which would explain HMGB2 co-localization in the nucleoli.

Despite of the lack of extended coincidence between Y2H and IP-MS results for HMGB2 interactomes, some resemblance in the function of the proteins detected in each approach can be noticed. Data obtained from IP-MS show proteins related with RNA binding (HNENPM, HNRNPK and MATR3) (Table 5) and the Y2H approach also reveals proteins such as ZFR or U2AF1 (Table 1 and 2), which directly bind RNA and

mediate protein-RNA interactions respectively. Moreover, both experiments bring out proteins that emphasize HMGB2 cytoplasmic functions. Through the Y2H assay, cytoskeleton related proteins like MIEN1 and ROCK1, or BCCIP (Table 1 and 2), an autophagosome modulating protein, were detected, while the IP-MS approach showed ribosomal proteins associated with cytoplasmic translocation of proteins (Table 5).

References

1.   Reid, B. M., Permuth, J. B. & Sellers, T. A. Epidemiology of ovarian cancer: a review. *Cancer Biol. Med.* **14**, 9–32 (2017).

2.   Cámara-Quílez, M. *et al.* Differential Characteristics of HMGB2 Versus HMGB1 and their Perspectives in Ovary and Prostate Cancer. *Curr. Med. Chem.* **27**, 3271–3289 (2019).

3.   Paek, J., Lee, M., Nam, E. J., Kim, S. W. & Kim, Y. T. Clinical impact of high mobility group box 1 protein in epithelial ovarian cancer. *Arch. Gynecol. Obstet.* **293**, 645–650 (2016).

4.   Li, Y. *et al.* Serum high mobility group box protein 1 as aclinical marker for ovarian cancer. *Neoplasma* **61**, 579–584 (2014).

5.   Wang, H. *et al.* Relationship between high-mobility group box 1 overexpression in ovarian cancer tissue and serum: a meta-analysis. *Onco. Targets. Ther.* **8**, 3523–3531 (2015).

6.   Cai, X. *et al.* Expression of HMGB2 indicates worse survival of patients and is required for the maintenance of Warburg effect in pancreatic cancer. *Acta Biochim. Biophys. Sin. (Shanghai).* **49**, 119–127 (2017).

7.   Li, H., Zhang, H. & Wang, Y. Centromere protein U facilitates metastasis of ovarian cancer cells by targeting high mobility group box 2 expression. **8**, 835–851 (2018).

8.   Bernardini, M. *et al.* High-resolution mapping of genomic imbalance and identification of gene expression profiles associated with differential chemotherapy response in serous epithelial ovarian cancer. *Neoplasia* **7**, 603–613 (2005).

9.   Fan, Z., Beresford, P. J., Zhang, D. & Lieberman, J. HMG2 interacts with the nucleosome assembly protein SET and is a target of the cytotoxic T-lymphocyte protease granzyme A. *Mol. Cell. Biol.* **22**, 2810–2820 (2002).

10.   Ouellet, V. *et al.* SET complex in serous epithelial ovarian cancer. *Int. J. Cancer* **119**, 2119–2126 (2006).

11.   Fan, Z., Beresford, P. J., Oh, D. Y., Zhang, D. & Lieberman, J. Tumor suppressor NM23-H1 is a granzyme A-activated DNase during CTL-mediated apoptosis, and the nucleosome assembly protein set is its inhibitor. *Cell* **112**, 659–672 (2003).

12.   Presneau, N., Shen, Z., Provencher, D., Mes-Masson, A. M. & Tonin, P. N. Identification of novel variant, 1484delG in the 3'UTR of H3F3B, a member of the histone 3B replacement family, in ovarian tumors. *Int. J. Oncol.* **26**, 1621–1627 (2005).

13.   Varma, R. R. *et al.* Gene expression profiling of a clonal isolate of oxaliplatin-resistant ovarian carcinoma cell line A2780/C10. *Oncol. Rep.* **14**, 925–932 (2005).

14.   Poornima, P., Kumar, J. D., Zhao, Q., Blunder, M. & Efferth, T. Network pharmacology of cancer: From understanding of complex interactomes to the design of multi-target specific therapeutics from nature. *Pharmacol. Res.* **111**, 290–302 (2016).

15. Eisenhauer, E. A. Real-world evidence in the treatment of ovarian cancer. *Ann. Oncol. Off. J. Eur. Soc. Med. Oncol.* **28**, viii61–viii65 (2017).

16. Henderson, J. T., Webber, E. M. & Sawaya, G. F. Screening for Ovarian Cancer: Updated Evidence Report and Systematic Review for the US Preventive Services Task Force. *Jama* **319**, 595–606 (2018).

17. Ichigo, S. *et al.* Transitional cell carcinoma of the ovary (Review). *Oncol. Lett.* **3**, 3–6 (2012).

18. Barreiro-Alonso, A. Interactome of lxr1, HMGB1 and HMGB2 proteins in relation to their cellular function. *PhD Thesis* (2018).

19. Shilov, I. V. *et al.* The paragon algorithm, a next generation search engine that uses sequence temperature values sequence temperature values and feature probabilities to identify peptides from tandem mass spectra. *Mol. Cell. Proteomics* **6**, 1638–1655 (2007).

20. Tang, W. H., Shilov, I. V. & Seymour, S. L. Nonlinear fitting method for determining local false discovery rates from decoy database searches. *J. Proteome Res.* **7**, 3661–3667 (2008).

21. García-nafría, J., Watson, J. F. & Greger, I. H. IVA cloning : A single-tube universal cloning system exploiting bacterial In Vivo Assembly. *Sci. Rep.* **6**, 1–12 (2016).

22. Barreiro-Alonso, A. *et al.* Delineating the HMGB1 and HMGB2 interactome in prostate and ovary epithelial cells and its relationship with cancer. *Oncotarget* **9**, 19050–19064 (2018).

23. Gao, N., Asamitsu, K., Hibi, Y., Ueno, T. & Okamoto, T. AKIP1 enhances NF-kappaB-dependent gene expression by promoting the nuclear retention and phosphorylation of p65. *J. Biol. Chem.* **283**, 7834–7843 (2008).

24. Yu, H. *et al.* AKIP1 expression modulates mitochondrial function in rat neonatal cardiomyocytes. *PLoS One* **8**, 1–11 (2013).

25. Zhang, W. *et al.* AKIP1 promotes angiogenesis and tumor growth by upregulating CXC-chemokines in cervical cancer cells. *Mol. Cell. Biochem.* **448**, 311–320 (2018).

26. Guo, X. *et al.* AKIP1 promoted epithelial-mesenchymal transition of non-small-cell lung cancer via transactivating ZEB1. *Am. J. Cancer Res.* **7**, 2234–2244 (2017).

27. Lin, C. *et al.* Overexpression of AKIP1 promotes angiogenesis and lymphangiogenesis in human esophageal squamous cell carcinoma. *Oncogene* **34**, 384–393 (2015).

28. Pohl, M. *et al.* Keratin 34betaE12/keratin7 expression is a prognostic factor of cancer-specific and overall survival in patients with early stage non-small cell lung cancer. *Acta Oncol.* **55**, 167–177 (2016).

29. Jin, Y., Feng, S. J., Qiu, S., Shao, N. & Zheng, J. H. LncRNA MALAT1 promotes proliferation and metastasis in epithelial ovarian cancer via the PI3K-AKT pathway. *Eur. Rev. Med. Pharmacol. Sci.* **21**, 3176–3184 (2017).

30. Tee, A. E. *et al.* The long noncoding RNA MALAT1 promotes tumor-driven angiogenesis by up-regulating pro-angiogenic gene expression. *Oncotarget* **7**, 8663–8675 (2016).

31. Ji, D. G. *et al.* Inhibition of MALAT1 sensitizes liver cancer cells to 5-flurouracil by regulating apoptosis through IKKalpha/NF-kappaB pathway. *Biochem. Biophys. Res. Commun.* **501**, 33–40 (2018).

32. Lu, H. & Hallstrom, T. C. The nuclear protein UHRF2 is a direct target of the transcription factor E2F1 in the induction of apoptosis. *J. Biol. Chem.* **288**, 23833–23843 (2013).

33. Lu, X., Wang, J., Shan, X. & Li, Y. Selecting key genes associated with ovarian cancer based on differential expression network. *J. B.U.ON. Off. J. Balk. Union Oncol.* **22**, 48–57 (2017).

34. Huang, Y. Y. *et al.* BCCIP suppresses tumor initiation but is required for tumor progression. *Cancer Res.* **73**, 7122–7133 (2013).

35. Lin, Z. *et al.* Expression pattern of BCCIP in hepatocellular carcinoma is correlated with poor prognosis and enhanced cell proliferation. *Tumour Biol.* **37**, 16305–16315 (2016).

36. van de Sluis, B. *et al.* COMMD1 disrupts HIF-1alpha/beta dimerization and inhibits human tumor cell invasion. *J. Clin. Invest.* **120**, 2119–2130 (2010).

37. Maine, G. N., Mao, X., Komarck, C. M. & Burstein, E. COMMD1 promotes the ubiquitination of NF-kappaB subunits through a cullin-containing ubiquitin ligase. *EMBO J.* **26**, 436–447 (2007).

38. Fedoseienko, A. *et al.* Nuclear COMMD1 Is Associated with Cisplatin Sensitivity in Ovarian Cancer. *PLoS One* **11**, 1–21 (2016).

39. Mu, P., Akashi, T., Lu, F., Kishida, S. & Kadomatsu, K. A novel nuclear complex of DRR1, F-actin and COMMD1 involved in NF-kappaB degradation and cell growth suppression in neuroblastoma. *Oncogene* **36**, 5745–5756 (2017).

40. Zoubeidi, A. *et al.* Clusterin facilitates COMMD1 and I-kappaB degradation to enhance NF-kappaB activity in prostate cancer cells. *Mol. Cancer Res.* **8**, 119–130 (2010).

41. Sasaki, M. *et al.* Regulation of the MDM2-P53 pathway and tumor growth by PICT1 via nucleolar RPL11. *Nat. Med.* **17**, 944–951 (2011).

42. Okahara, F. *et al.* Critical role of PICT-1, a tumor suppressor candidate, in phosphatidylinositol 3,4,5-trisphosphate signals and tumorigenic transformation. *Mol. Biol. Cell* **17**, 4888–4895 (2006).

43. Chen, H. *et al.* PICT-1 is a key nucleolar sensor in DNA damage response signaling that regulates apoptosis through the RPL11-MDM2-p53 pathway. *Oncotarget* **7**, 83241–83257 (2016).

44. Kwon, M. J. *et al.* Genes co-amplified with ERBB2 or MET as novel potential cancer-promoting genes in gastric cancer. *Oncotarget* **8**, 92209–92226 (2017).

45. Ren, H., Qi, Y., Yin, X. & Gao, J. miR-136 targets MIEN1 and involves the metastasis of colon cancer by suppressing epithelial-to-mesenchymal transition. *Onco. Targets. Ther.* **11**, 67–74 (2017).

46. Liu, Q. Q. *et al.* Inhibition of C35 gene expression by small interfering RNA induces apoptosis of breast cancer cells. *Biosci. Trends* **4**, 254–259 (2010).

47. Julian, L. & Olson, M. F. Rho-associated coiled-coil containing kinases (ROCK): structure, regulation, and functions. *Small GTPases* **5**, e29846-1-e29846-12 (2014).

48. Li, G. *et al.* RhoA/ROCK/PTEN signaling is involved in AT-101-mediated apoptosis in human leukemia cells in vitro and in vivo. *Cell Death Dis.* **5**, 1–12 (2014).

49. Liu, Y., Wang, Y., Fu, X. & Lu, Z. Long non-coding RNA NEAT1 promoted ovarian cancer cells' metastasis via regulating of miR-382-3p/ROCK1 axial. *Cancer Sci.* **109**, 2188–2198 (2018).

50. Luo, H. & Liang, C. MicroRNA-148b inhibits proliferation and the epithelial-mesenchymal transition and increases radiosensitivity in non-small cell lung carcinomas by regulating ROCK1. *Exp. Ther. Med.* **15**, 3609–3616 (2018).

51. Xu, B. *et al.* Hsa-miR-146a-5p modulates androgen-independent prostate cancer cells apoptosis by targeting ROCK1. *Prostate* **75**, 1896–1903 (2015).

52. Zhang, R. *et al.* Hirsutine induces mPTP-dependent apoptosis through ROCK1/PTEN/PI3K/GSK3beta pathway in human lung cancer cells. *Cell Death Dis.* **9**, 597–598 (2018).

53. Park, G. B. & Kim, D. PI3K Catalytic Isoform Alteration Promotes the LIMK1-related Metastasis Through the PAK1 or ROCK1/2 Activation in Cigarette Smoke-exposed Ovarian Cancer Cells. *Anticancer Res.* **37**, 1805–1818 (2017).

54. Wang, Y., Wang, Y. & Zhang, Z. Adipokine RBP4 drives ovarian cancer cell migration. *J. Ovarian Res.* **11**, 1–10 (2018).

55. Bryan, B. A. *et al.* RhoA/ROCK signaling is essential for multiple aspects of VEGF-mediated angiogenesis. *FASEB J.* **24**, 3186–3195 (2010).

56. Tocci, P. *et al.* Endothelin-1/endothelin A receptor axis activates RhoA GTPase in epithelial ovarian cancer. *Life Sci.* **159**, 49–54 (2016).

57. Zhang, C. *et al.* ROCK has a crucial role in regulating prostate tumor growth through interaction with c-Myc. *Oncogene* **33**, 5582–5591 (2014).

58. Matoba, K. *et al.* Rho-kinase regulation of TNF-alpha-induced nuclear translocation of NF-kappaB RelA/p65 and M-CSF expression via p38 MAPK in mesangial cells. *Am. J. Physiol. Physiol.* **307**, F571–F580 (2014).

59. Wei, L., Surma, M., Shi, S., Lambert-Cheatham, N. & Shi, J. Novel Insights into the Roles of Rho Kinase in Cancer. *Arch. Immunol. Ther. Exp. (Warsz).* **64**, 259–278 (2016).

60. Ohta, T. *et al.* Inhibition of the Rho/ROCK pathway enhances the efficacy of cisplatin through the blockage of hypoxia-inducible factor-1alpha in human ovarian cancer cells. *Cancer Biol. Ther.* **13**, 25–33 (2012).

61. Montalvo, J. *et al.* ROCK1 & 2 perform overlapping and unique roles in angiogenesis and angiosarcoma tumor progression. *Curr. Mol. Med.* **13**, 205–219 (2013).

62. Fei, D. L. *et al.* Wild-Type U2AF1 Antagonizes the Splicing Program Characteristic of U2AF1-Mutant Tumors and Is Required for Cell Survival. *PLoS Genet.* **12**, 1–26 (2016).

63. Hu, R. *et al.* ZNF668 functions as a tumor suppressor by regulating p53 stability and function in breast cancer. *Cancer Res.* **71**, 6524–6534 (2011).

64. Zhang, Y. *et al.* NAC1 modulates sensitivity of ovarian cancer cells to cisplatin by altering the HMGB1-mediated autophagic response. *Oncogene* **31**, 1055–1064 (2012).

65. Bulla, R. *et al.* C1q acts in the tumour microenvironment as a cancer-promoting factor independently of complement activation. *Nat. Commun.* **7**, 1–11 (2016).

66. Brennan, P. A., Jing, J., Ethunandan, M. & Gorecki, D. Dystroglycan complex in cancer. *Eur. J. Surg. Oncol.* **30**, 589–592 (2004).

67. Li, C., Ge, M., Yin, Y., Luo, M. & Chen, D. Silencing expression of ribosomal protein L26 and L29 by RNA interfering inhibits proliferation of human pancreatic cancer PANC-1 cells. *Mol. Cell. Biochem.* **370**, 127–139 (2012).

68. Liu, Y., Li, G., Liu, C., Tang, Y. & Zhang, S. RSF1 regulates the proliferation and paclitaxel resistance via modulating NF-kappaB signaling pathway in nasopharyngeal carcinoma. *J. Cancer* **8**, 354–362 (2017).

69. Li, Q., Dong, Q. & Wang, E. Rsf-1 is overexpressed in non-small cell lung cancers and regulates cyclinD1 expression and ERK activity. *Biochem. Biophys. Res. Commun.* **420**, 6–10 (2012).

70. Maeda, D. *et al.* Rsf-1 (HBXAP) expression is associated with advanced stage and lymph node metastasis in ovarian clear cell carcinoma. *Int. J. Gynecol. Pathol.* **30**, 30–35 (2011).

71. Sheu, J. J. *et al.* Rsf-1, a chromatin remodelling protein, interacts with cyclin E1 and promotes tumour development. *J. Pathol.* **229**, 559–568 (2013).

72. Lei, Z. *et al.* Novel peptide GX1 inhibits angiogenesis by specifically binding to transglutaminase-2 in the tumorous endothelial cells of gastric cancer. *Cell Death Dis.* **9**, 1–16 (2018).

73. Hidaka, H. *et al.* Tumor suppressive microRNA-1285 regulates novel molecular targets: aberrant expression and functional significance in renal cell carcinoma. *Oncotarget* **3**, 44–57 (2012).

74. Li, J., Feng, Q., Wei, X. & Yu, Y. MicroRNA-490 regulates lung cancer metastasis by targeting poly r(C)-binding protein 1. *Tumour Biol.* **37**, 15221–15228 (2016).

75. Schiarea, S. *et al.* Secretome analysis of multiple pancreatic cancer cell lines reveals perturbations of key functional networks. *J. Proteome Res.* **9**, 4376–4392 (2010).

76. Zhang, W. *et al.* Poly C binding protein 1 represses autophagy through downregulation of LC3B to promote tumor cell apoptosis in starvation. *Int. J. Biochem. Cell Biol.* **73**, 127–136 (2016).

77. Zhang, H., Zhang, C. F. & Chen, R. Zinc finger RNA-binding protein promotes non-small-cell carcinoma growth and tumor metastasis by targeting the Notch signaling pathway. *Am. J. Cancer Res.* **7**, 1804–1819 (2017).

78. Zwang, Y. *et al.* Synergistic interactions with PI3K inhibition that induce apoptosis. *Elife* **6**, 1–18 (2017).

79. Zhao, X., Chen, M. & Tan, J. Knockdown of ZFR suppresses cell proliferation and invasion of human pancreatic cancer. *Biol. Res.* **49**, 23–26 (2016).

80. Merritt, M. A. *et al.* Expression profiling identifies genes involved in neoplastic transformation of serous ovarian cancer. *BMC Cancer* **9**, 1–13 (2009).

81. Leung, T. H. Y. *et al.* The interaction between C35 and Δnp73 promotes chemo-resistance in ovarian cancer cells. *Br. J. Cancer* **109**, 965–975 (2013).

82. Wegdam, W. *et al.* Label-free LC-MSe in tissue and serum reveals protein

networks underlying differences between benign and malignant serous ovarian tumors. *PLoS One* **9**, 1–12 (2014).

83. Sodek, K. L., Ringuette, M. J. & Brown, T. J. Compact spheroid formation by ovarian cancer cells is associated with contractile behavior and an invasive phenotype. *Int. J. cancer* **124**, 2060–2070 (2009).

84. Je, E. M., Yoo, N. J., Kim, Y. J., Kim, M. S. & Lee, S. H. Mutational analysis of splicing machinery genes SF3B1, U2AF1 and SRSF2 in myelodysplasia and other common tumors. *Int. J. cancer* **133**, 260–265 (2013).

85. Kim, S., Hagemann, A. & DeMichele, A. Immuno-modulatory gene polymorphisms and outcome in breast and ovarian cancer. *Immunol. Invest.* **38**, 324–340 (2009).

86. Pathak, H. B. *et al.* A Synthetic Lethality Screen Using a Focused siRNA Library to Identify Sensitizers to Dasatinib Therapy for the Treatment of Epithelial Ovarian Cancer. *PLoS One* **10**, 1–19 (2015).

87. Yang, Y. I., Ahn, J. H., Lee, K. T., Shih, I. & Choi, J. H. RSF1 is a positive regulator of NF-kappaB-induced gene expression required for ovarian cancer chemoresistance. *Cancer Res.* **74**, 2258–2269 (2014).

88. Choi, J. H. *et al.* Functional analysis of 11q13.5 amplicon identifies Rsf-1 (HBXAP) as a gene involved in paclitaxel resistance in ovarian cancer. *Cancer Res.* **69**, 1407–1415 (2009).

89. Liu, X. *et al.* Differential BCCIP gene expression in primary human ovarian cancer, renal cell carcinoma and colorectal cancer tissues. *Int. J. Oncol.* **43**, 1925–1934 (2013).

90. Zhang, H. Y. & Dou, K. F. PCBP1 is an important mediator of TGF-beta-induced epithelial to mesenchymal transition in gall bladder cancer cell line GBC-SD. *Mol. Biol. Rep.* **41**, 5519–5524 (2014).

91. He, W., Sun, Z. & Liu, Z. Silencing of TGM2 reverses epithelial to mesenchymal transition and modulates the chemosensitivity of breast cancer to docetaxel. *Exp. Ther. Med.* **10**, 1413–1418 (2015).

92. Lin, Q. *et al.* MALAT1 affects ovarian cancer cell behavior and patient survival. *Oncol. Rep.* **39**, 2644–2652 (2018).

93. Wu, L., Wang, X. & Guo, Y. Long non-coding RNA MALAT1 is upregulated and involved in cell proliferation, migration and apoptosis in ovarian cancer. *Exp. Ther. Med.* **13**, 3055–3060 (2017).

94. Chen, Q. *et al.* Plasma long non-coding RNA MALAT1 is associated with distant metastasis in patients with epithelial ovarian cancer. *Oncol. Lett.* **12**, 1361–1366 (2016).

95. Liu, S. *et al.* Inhibition of the long non-coding RNA MALAT1 suppresses tumorigenicity and induces apoptosis in the human ovarian cancer SKOV3 cell line. *Oncol. Lett.* **11**, 3686–3692 (2016).

96. Shi, B., Wang, Y. & Yin, F. MALAT1/miR-124/Capn4 axis regulates proliferation, invasion and EMT in nasopharyngeal carcinoma cells. *Cancer Biol. Ther.* **18**, 792–800 (2017).

97. Papatheodorou, I. *et al.* Expression Atlas: gene and protein expression across multiple studies and organisms. *Nucleic Acids Res.* **46**, D246–D251 (2018).

98. Consortium, Gte. The Genotype-Tissue Expression (GTEx) project. *Nat. Genet.* **45**, 580–585 (2013).

99. Wang, J., Peng, X., Peng, W. & Wu, F. X. Dynamic protein interaction network construction and applications. *Proteomics* **14**, 338–352 (2014).

100. Kushwaha, P. P., Gupta, S., Singh, A. K. & Kumar, S. Emerging Role of Migration and Invasion Enhancer 1 (MIEN1) in Cancer Progression and Metastasis. *Front. Oncol.* **9**, 1–13 (2019).

101. Cerami, E. *et al.* The cBio cancer genomics portal: an open platform for exploring multidimensional cancer genomics data. *Cancer Discov.* **2**, 401–404 (2012).

102. Gao, J. *et al.* Integrative analysis of complex cancer genomics and clinical profiles using the cBioPortal. *Sci. Signal.* **6**, pl1 (2013).

103. Shih, I. *et al.* Amplification of a chromatin remodeling gene, Rsf-1/HBXAP, in ovarian carcinoma. *Proc. Natl. Acad. Sci. U. S. A.* **102**, 14004–14009 (2005).

104. Kuroiwa, Y. *et al.* Identification and characterization of the direct interaction between methotrexate (MTX) and high-mobility group box 1 (HMGB1) protein. *PLoS One* **8**, 1–12 (2013).

105. Nasser, M. W. *et al.* RAGE mediates S100A7-induced breast cancer growth and metastasis by modulating the tumor microenvironment. *Cancer Res.* **75**, 974–985 (2016).

106. Guoci, T. *et al.* SAINTexpress: improvements and additional features in Significance Analysis of Interactome software. *J. Proteomics* **100**, 37–43 (2015).

107. Jiang, C. *et al.* Association between the HMGB1/TLR4 signaling pathway and the clinicopathological features of ovarian cancer. *Mol. Med. Rep.* **18**, 3093–3098 (2018).

108. Li, Z. *et al.* Silencing HMGB1 expression by lentivirus-mediated small interfering RNA (siRNA) inhibits the proliferation and invasion of colorectal cancer LoVo cells in vitro and in vivo. *Zhonghua Zhong Liu Za Zhi* **37**, 664–670 (2015).

109. Li, X. *et al.* Short-Term Hesperidin Pretreatment Attenuates Rat Myocardial Ischemia / Reperfusion Injury by Inhibiting High Mobility Group Box 1 Protein Expression via the PI3K / Akt Pathway. *Cell. Physiol. Biochem.* **39**, 1850–1862 (2016).

110. Meng, L. *et al.* The protective effect of dexmedetomidine on LPS-induced acute lung injury through the HMGB1-mediated TLR4 / NF- κ B and PI3K / Akt / mTOR pathways. *Mol. Immunol.* **94**, 7–17 (2018).

111. Li, R., Ren, T. & Zeng, J. Mitochondrial Coenzyme Q Protects Sepsis-Induced Acute Lung Injury by Activating PI3K/Akt/GSK-3 β /mTOR Pathway in Rats. *Biomed Res. Int.* **2019**, 1–9 (2019).

112. Qu, L. *et al.* Glycyrrhizic acid ameliorates LPS-induced acute lung injury by regulating autophagy through the PI3K/AKT/mTOR pathway. *Am. J. Transl. Res.* **11**, 2042–2055 (2019).

113. Zhao, F. *et al.* Glycyrrhizin Protects Rats from Sepsis by Blocking HMGB1 Signaling. *Biomed Res. Int.* **2017**, 1–10 (2017).

114. Mabuchi, S., Kuroda, H., Takahashi, R. & Sasano, T. The PI3K / AKT / mTOR pathway as a therapeutic target in ovarian cancer. *Gynecol. Oncol.* **137**, 173–179 (2015).

115. Yanai, H. *et al.* HMGB proteins function as universal sentinels for nucleic-acid-mediated innate immune responses. *Nature* **462**, 99–103 (2009).

116. Pusterla, T., de Marchis, F., Palumbo, R. & Bianchi, M. E. High mobility group B2 is secreted by myeloid cells and has mitogenic and chemoattractant activities similar to high mobility group B1. *Autoimmunity* **42**, 308–310 (2009).

117. Gupta, S. C. *et al.* Long non-coding RNAs and nuclear factor-kappaB crosstalk in cancer and other human diseases. *Biochim. Biophys. acta.Reviews cancer* **1873**, 1–35 (2020).

118. Ash, S. C., Yang, D. Q. & Britt, D. E. LYRIC/AEG-1 overexpression modulates BCCIPalpha protein levels in prostate tumor cells. *Biochem. Biophys. Res. Commun.* **371**, 333–338 (2008).

119. Chang, K. S. *et al.* Migration and Invasion Enhancer 1 Is an NF-kB-Inducing Gene Enhancing the Cell Proliferation and Invasion Ability of Human Prostate Carcinoma Cells In Vitro and In Vivo. *Cancers (Basel).* **11**, 1–17 (2019).

120. Wang, Y., Tong, X., Zhang, J. & Ye, X. The complement C1qA enhances retinoic acid-inducible gene-I-mediated immune signalling. *Immunology* **136**, 78–85 (2012).

121. Crappe, J. *et al.* PROTEOFORMER: deep proteome coverage through ribosome profiling and MS integration. *Nucleic Acids Res.* **43**, 1–10 (2015).

122. Lee, S. *et al.* Global mapping of translation initiation sites in mammalian cells at single-nucleotide resolution. *Proc. Natl. Acad. Sci. U. S. A.* **109**, E2424–E2432 (2012).

123. Suzuki, A. *et al.* A new PICTure of nucleolar stress. *Cancer Sci.* **103**, 632–637 (2012).

124. Chang, C. M. *et al.* Gene Set-Based Integrative Analysis Revealing Two Distinct Functional Regulation Patterns in Four Common Subtypes of Epithelial Ovarian Cancer. *Int. J. Mol. Sci.* **17**, 1–20 (2016).

125. Barreiro-Alonso, A. *et al.* Characterization of HMGB1/2 Interactome in Prostate Cancer by Yeast Two Hybrid Approach: Potential Pathobiological Implications. *Cancers (Basel).* **11**, 1–21 (2019).

126. Laurent, B. *et al.* High-mobility group protein HMGB2 regulates human erythroid differentiation through trans-activation of GFI1B transcription. *Blood* **115**, 687–695 (2010).

127. Taniguchi, N. *et al.* Chromatin protein HMGB2 regulates articular cartilage surface maintenance via beta-catenin pathway. *Proc. Natl. Acad. Sci. U. S. A.* **106**, 16817–16822 (2009).

128. Taniguchi, N. *et al.* Expression patterns and function of chromatin protein HMGB2 during mesenchymal stem cell differentiation. *J. Biol. Chem.* **286**, 41489–41498 (2011).

129. Dowthwaite, G. P. *et al.* The surface of articular cartilage contains a progenitor cell population. *J. Cell Sci.* **117**, 889–897 (2004).

130. Balani, P. *et al.* High mobility group box2 promoter-controlled suicide gene expression enables targeted glioblastoma treatment. *Mol. Ther.* **17**, 1003–1011 (2009).

131. Zhou, X. *et al.* HMGB2 regulates satellite-cell-mediated skeletal muscle

regeneration through IGF2BP2. *J. Cell Sci.* **129**, 4305–4316 (2016).

132. Ronfani, L. *et al.* Reduced fertility and spermatogenesis defects in mice lacking chromosomal protein Hmgb2. *Development* **128**, 1265–1273 (2001).

133. Hu, X. & Zhang, Z. Understanding the Genetic Mechanisms of Cancer Drug Resistance Using Genomic Approaches. *Trends Genet.* **32**, 127–137 (2015).

134. Rajendiran, S. *et al.* MIEN1 promotes oral cancer progression and implicates poor overall survival. *Cancer Biol. Ther.* **16**, 876–885 (2015).

135. Kpetemey, M. *et al.* MIEN1, a novel interactor of Annexin A2 , promotes tumor cell migration by enhancing AnxA2 cell surface expression. *Mol. Cancer* **14**, 1–13 (2015).

136. Kpetemey, M., Chaudhary, P., Van Treuren, T. & Vishwanatha, J. K. MIEN1 drives breast tumor cell migration by regulating cytoskeletal-focal adhesion dynamics. *Oncotarget* **7**, 54913–54924 (2016).

137. Duarte, S. *et al.* Vimentin filaments interact with the actin cortex in mitosis allowing normal cell division. *Nat. Commun.* **10**, 1–19 (2019).

138. Kpetemey, M. *et al.* MIEN1 drives breast tumor cell migration by regulating cytoskeletal-focal adhesion dynamics. *Oncotarget* **7**, 54913–54924 (2016).

139. Chen, H. *et al.* PICT-1 is a key nucleolar sensor in DNA damage response signaling that regulates apoptosis through the RPL11-MDM2-p53 pathway. *Oncotarget* **7**, 83241–83257 (2016).

140. Kalt, I., Levy, A., Borodianskiy-shteinberg, T. & Sarid, R. Nucleolar Localization of GLTSCR2 / PICT-1 Is Mediated by Multiple Unique Nucleolar Localization Sequences. **7**, 4–6 (2012).

141. Kim, J. Y., Park, J. H. & Lee, S. GLTSCR2 contributes to the death resistance and invasiveness of hypoxia-selected cancer cells. *FEBS Lett.* **586**, 3435–3440 (2012).

142. Defense, H. *et al.* Cytoplasmic Translocation of Nucleolar Protein NOP53 Promotes Viral Replication by Suppressing. *Viruses* **10**, 1–16 (2018).

143. Bhullar, B. S., Hewitt, J. & Candido, E. P. The large high mobility group proteins of rainbow trout are localized predominantly in the nucleus and nucleoli of a cultured trout cell line. *J. Biol. Chem.* **256**, 8801–8806 (1981).

144. Kuchler, R., Schroeder, B. O., Jaeger, S. U., Stange, E. F. & Wehkamp, J. Antimicrobial activity of high-mobility-group box 2: a new function to a well-known protein. *Antimicrob. Agents Chemother.* **57**, 4782–4793 (2013).

145. Chen, H. *et al.* PICT-1 triggers a pro-death autophagy through inhibiting rRNA transcription and AKT/mTOR/p70S6K signaling pathway. *Oncotarget* **7**, 78747–78763 (2016).

146. Scott, D. D. & Oeffinger, M. Nucleolin and Nucleophosmin: nucleolar proteins with multiple functions in DNA repair. *Biochem. Cell Biol.* **94**, 419–432 (2014).

147. Kim, H. K. *et al.* Transcriptional repression of high-mobility group box 2 by p21 in radiation-induced senescence. *Mol. Cells* **41**, 362–372 (2018).

Chapter 3.

RNA-Expression changes of MIEN1 and NOP53 in reference to treatment with chemotherapy drugs in PC-3 *versus* PNT-2 and SKOV-3 *versus* IOSE-80 cells.

Introduction

Multi-Drug resistance (MDR) is one of the major problems in prostate and ovarian cancer treatment. Despite of all the efforts and scientific progress MDR keeps interfering with the cure of these diseases which nowadays still have a high mortality rate. In the case of PCa, once the hormonal therapy has failed, chemotherapy is the last defense to stop the progression of the disease. The emerging resistances to chemotherapeutic treatments drive to the searching of new chemotherapy targets and biomarkers enabling an early diagnose. Proteins HMGB1 and HMGB2 have been both associated with chemoresistance processes. HMGB1 has been described to improve the survival of tumoural cells that overexpress it when treated with paclitaxel. The primary cell necrosis induced by this compound leads to a passive secretion of HMGB1 to the extracellular medium. When the released HMGB1 binds to the surrounding tumoural cells RAGE receptors, it counteracts the apoptotic effect of the chemotherapy[1]. Furthermore, at the intracellular level, HMGB1 can avoid apoptosis recognizing DNA adducts caused by chemotherapy agents[2] or promoting auto-phagocytosis by competing with Bcl-2 in Beclin-1 binding[3]. Despite of being less studied than HMGB1, HMGB2 has been also related with chemoresistance in liver, melanoma, glioma or gastric cancers among others[4,5]. Although the mechanisms through which HMGB2 seems to promote chemoresistance are similar to HMGB1's in terms of autophagy regulation[4] and DNA binding[6], the fact that HMGB2 is not ubiquitous, being present only in specific tissues, and overexpresses mostly in less differentiated cells, makes it a suitable target for a more specific chemotherapy[7].

According to the HMGB2´s potential interacting partner MIEN1, recent studies have correlated it with malignancy processes in prostate and ovarian cancer[3,8,9] what redefines it as an emerging target to restore the chemosensitivity of resistant cells[10].

NOP53, also known as GLTSCR2 or PICT-1, is the other novel HMGB2´s interacting protein discussed in this thesis. It is a nucleolar protein that has been described as both oncogenic and anti-tumoural in different tissues. It performs mostly as tumour suppressor protein in prostate[11] and as an oncogenic protein in ovary[12]. It was first identified in brain tissue, and it is involved in the p53 regulation pathway through RPL11, and MDM2[13]. Furthermore, this protein has been as well related with decreased mortality of cancer cells[14], autophagy and AKT/mTOR/p7086k pathway, which could imply a role in chemoresistance processes[15].

Several studies have already proven the transcriptional dysregulation of HMGB1 and HMGB2 genes in response to chemotherapeutic agents in different types of tumoural

processes including prostate and ovarian cancer[16]. In this chapter, a series of different compounds was selected in order to study their effect on HMGB1, HMGB2, MIEN1 and NOP53 expression: paclitaxel, olaparib and bevacizumab in prostate cells and paclitaxel, olaparib, bevacizumab and carboplatin in ovarian cells.

Paclitaxel, olaparib, bevacizumab and carboplatin are being currently used in the ovarian cancer treatment[17]. The therapeutic dose of these compounds depend on patient parameters such as body surface area (BSA), body weight (BW)[18] or the Area Under the Curve (AUC, Area under the plasma drug concentration-time curve)[19] but, in general terms, the dose for an adult consists on: carboplatin 400-200 mg/m^2 intravenously[20], paclitaxel 150-175 mg/m^2 intravenously[21], bevacizumab 15 mg/kg intravenously[22,23] and olaparib 300 mg orally twice a day[24]. Concerning prostate cancer treatment, olaparib and bevacizumab are still under clinical studies[25,26], while paclitaxel constitutes a first line treatment to confront this disease[27,28].

Paclitaxel is a taxane that promotes the depolymerization of microtubules avoiding the formation of the achromatic spindle during metaphase that lately leads to apoptosis. In addition, paclitaxel also activates multiple signaling pathways to exert pro-apoptotic activity by increasing reactive oxygen species (ROS) and hydroperoxide production as a result of the induction of NADPH-oxidase activity[29]. The known capacity of HMGB proteins to respond to oxidative stress might interfere with the mitochondrial damage produced by paclitaxel, counteracting its activity. Besides, since HMGB proteins are also regulators of gene expression, they also might influence the expression of microtubule proteins affecting cell cycle and the cellular response to paclitaxel. On the other hand, MIEN1 directly interacts with cytoskeletal proteins such as actin, which could also be modified by microtubuli alteration caused by paclitaxel[30,31]. NOP53 involvement in the cell cycle[32], through its interaction with p53 and Akt pathway, could drive to a dysregulation on its expression responding to this treatment.

Olaparib is a PARP-1 inhibitor, which promotes apoptosis in cells that already have a mutation in alternative DNA repairing systems such as BRCA1/2. As a matter of fact, this is usually the case of some ovarian cancer cells[33,34] and metastatic castration-resistant prostate cancer cells[35]. The correlation between PARP-1 and HMGB1 proteins, as well as the effects of PARP-1 inhibition in HMGB1's function, has been already reported[36] which suggest also a putative effect on its structural homolog HMGB2 and its interacting proteins. In the same line, NOP53 is a nucleolar protein that detects DNA damage and is also associated with DNA repair through DNA Damage Respone (DDR). Under stressful conditions, the nucleoli disrupts, thus releasing

nucleolar proteins to the nucleoplasm. NOP53 has been associated with proteins involved in DNA repair, and specifically to Ataxia telanagiectasia protein kinase (ATM-PK) and the DNA-dependent protein kinase (DNA-PK), both playing an important role during the repair of double strand breaks. DNA damage activate ATM-PK and DNA-PK, which phosphorylate PARP-1 and other DDR involved proteins in order to recruit them for DNA repairing. PARP-1 can only interact with ATM-PK when it is ADP-rybosilated (parylated), and PARP-1 inhibitors such as olaparib interfere with this process. At the same time, ATM-PK and DNA-PK phosphorylate NOP53 promoting its degradation through a proteasome-dependent pathway, allowing its clearance and avoiding its inhibitory function over p53. Therefore, NOP53 is downstream in the PARP-1/ATM-PK pathway, and might be affected by the inhibition of PARP-1, preventing apoptosis[37–40]. Bevacizumab is an antibody directed against vascular endothelial growth factor (VEGF), a protein which promotes angiogenesis and metastasis. This compound is usually administrated to the patients along with other chemotherapeutic drugs in order to improve their effectivity. Bevacizumab clears the extracellular medium of VEGF avoiding its interaction with the VEGF cell receptors (VEGFR)[41,42]. Previous studies proved that MIEN1 gene expression directly correlates with VEGF expression[8,43]. Besides, MIEN1 and NOP53 are involved in the protein kinase B (AKT) pathway, which connects with the NF-KB/ MMP-9/VEGF pathway[44].

Carboplatin constitutes the first-line therapy for the treatment of some types of cancer such as ovarian cancer. Opposite to its highly related analog cisplatin, carboplatin has been proved to cause less side-effects. It is a platinum compound that binds to DNA forming inter-catenary covalent cross-links between purine bases, which interfere with DNA repair and promote cell death. As we mentioned before, HMGB2 binds to DNA and might contribute to the recruitment of transcription factors or DNA repair machinery, suggesting a putative role of this protein in cell sensitivity to this compound[45–47]. Furthermore, HMGB2 has been associated in the response to oxidative stress[48,49]. When carboplatin is inside the cell, it undergoes hydrolysis and its derived products react with sulfhydryl groups present in proteins, with reduced glutathione (GSH), and with the nitrogen atoms present in nucleic acids. This could decrease the availability of GSH to counteract oxidative stress, increasing the importance of other proteins involved in the response to oxidative stress such as HMGB2[16,48-50].

Previous studies have provided evidence about the correlation between the expression of specific genes and the sensitivity to different chemotherapeutic compounds[51,52]. The aim of this chapter is to test if HMGB1, HMGB2, MIEN1 and NOP53 mRNA levels

change when ovarian and prostatic cells are treated with different drugs used in cancer treatments.

1. Materials and Methods

1.1. Cell culture, treatments and cell viability assays

The SKOV-3 (human ovarian cancerous) cell line and the PC-3 (human prostate cancerous) derives from a bone metastasis[53], were obtained from ATCC. IOSE-80 (CVCL_5546, Normal ovary epithelium cells immortalized with SV40) was kindly provided by Professor David Hunstman (OvCaRe Cell Bank, Vancouver, CA). PC-3, PNT-2 and IOSE-80 cell lines were regularly validated by DNA typing and grown in RPMI-1640 medium (Gibco™, Thermo Fisher Scientific Inc., Waltham, MA, USA) supplemented with 10% heat-inactivated fetal bovine serum and 1% penicillin-streptomycin (Thermo Fisher Scientific Inc., Waltham, MA, USA).

Cells at 80% confluence were exposed to different treatments with drug concentrations and conditions selected according to previous studies. Paclitaxel (taxol) was used at 25 µM[54]; carboplatin at 25 µg/mL[55]; olaparib (lynparza) to 2 µM[56]; and bevacizumab (avastin) at 100 µg/mL[57]. Paclitaxel was purchased to Sigma Aldrich (Sigma-Aldrich, St. Louis, MO, USA) and bevacizumab, olaparib and carboplatin were provided by the Pharmacy Service of the Teresa Herrera hospital (INIBIC, A Coruña, ES, EU). In parallel, cells were grown with the same amount of vehicle-buffer used to prepare drug solutions, or with an unspecific IgG not directed to vascular endothelial growth factor as control of bevacizumab treatment.

Cell viability-cytotoxicity assays were done using the Cell Counting Kit-8 (CCK-8, Tebu-Bio, Le-Perray-en-Yvelines, FR, EU).

1.2. Gene expression analysis by quantitative polymerase chain reaction (RT-qPCR)

RNA samples from SKOV-3, IOSE-80, PC-3, and PNT-2 , and the non-cancerous human ovarian, HOSEpiC, and prostate, HEpiC, primary culture were retro-transcribed into cDNA and labeled with the KAPA SYBR FAST universal one-step RT-qPCR kit (Kappa Biosystems Inc., Woburn, MA, USA). The primers and conditions for RT-qPCR were already described in previous chapters. At least 3 independent biological replicas and two technical replica of each of them, were made.

1.3. siRNA silencing

The siRNAs directed against each mRNA and unspecific controls were purchased. siRNA-HMGB1 (s20254 Silencer Select) and siRNA-HMGB2 (s6650) from Life technologies (Thermo Fisher Scientific Inc., Waltham, MA, USA); siRNA-MIEN1

(S228354), siRNA-NOP53, (S26871) and siRNAControl2 (4390846) from Ambion Inc. (Thermo Fisher Scientific Inc., Waltham, MA, USA). Transfection of cells with siRNAs was done using Lipofectamine ®2000 (Life Technologies, Invitrogen, Thermo Fisher Scientific Inc., Waltham, MA, USA) and following the protocol recommended by the vendor. Silencing was verified by qRT-PCR, with the methods described in the previous section, and Western blot using the antibodies against HMGB1 and HMGB2, NOP53 and MIEN1 already described and anti-GAPDH (60004-I-Ig, Proteintech. Manchester, UK, EU) used for loading control. After second incubation with 1:5000 G-protein HRP-linked (18-161, Millipore-Merck-KGaA, Darmstadt, DE, EU), Western blot was developed as above described.

1.4. Survival Analysis

The Overall Survival Kaplan-Meier Estimate analysis was performed through cBioPortal (http://www.cbioportal.org/) using the databases Ovarian Serous Cystadenocarcinoma (TCGA, Provisional), composed of 606 samples. Results obtained for the genes giving Logrank Test $p < 0.05$ were selected for discussion.

2. Results

2.1. Several detected proteins in the EOC-HMGB2-interactome and PCa-HMGB2-interactome are related to resistance against drugs used in cancer chemotherapy

Considering that HMGB1 and HMGB2 proteins have been associated to drug resistance during cancer treatment[58,59] we also reviewed available literature to see whether the proteins detected in our interactome study could also be related to this unfavorable event in ovary and prostate cancer. Comparing gene expression in SKOV-3 cells and a paclitaxel resistant derived cell line (available in the GEO accession GSE54772), only a gene encoding a protein detected in our EOC-HMGB2-interactome, U2AF1, is expressed at higher levels in sensitive than in resistant cells**.** On the other side, a previous study identified an overexpressed protein, BAG3, in a paclitaxel resistant prostate cell line (PC-3-TXR) by analyzing its expression profile against the one of its naive parental cell line PC-3[60]. The interaction of BAG3 with various proteins identified through the performed Y2H assay have been reported on BioGRID: PSMA7, SPIN1, ZNF428, HNRNPU and PTPN2. In the mentioned study, the overexpression in the PC-3-TXR cell line of the long noncoding RNA H19 was also detected, stabilizing HMGB1 and activating the HMGB1/TLR4/NF-KB pathway[61].

The MIEN1 gene is located in the 17q12[9] amplicon along with HER/ERBB2 and GRB7, which are overexpressed in various human cancers[10]. The structure of MIEN1 (alias C35, XTP4 or C17orf37) and their emerging functions in relation to cancer have been recently reviewed[62]. Although the role of MIEN1 in pathophysiology of both types of cancer has not been explored in depth, it was reported that high levels of MIEN1 are involved in cisplatin drug resistance in ovary[9] and prostate[63], through its interaction with ΔNp73 and AKT, respectively[8,64–66]. Furthermore, MIEN1 has been also related with paclitaxel resistance in ovary by the MIEN1/Focal Adhesion Kinase (FAK)/Y-Box binding protein 1 (YB-1) pathway[10,67,68], doxorubicin and etoposide resistance in pediatric neuroblastoma through MIEN1/Annexin-A2/NF-κβ pathway[10,62,69,70] and adriamycin resistance in prostate cancer by MIEN1/COFILIN-1/P-Glycoprotein (P-gp) signaling cascade[10,62,71] (Figure 1).
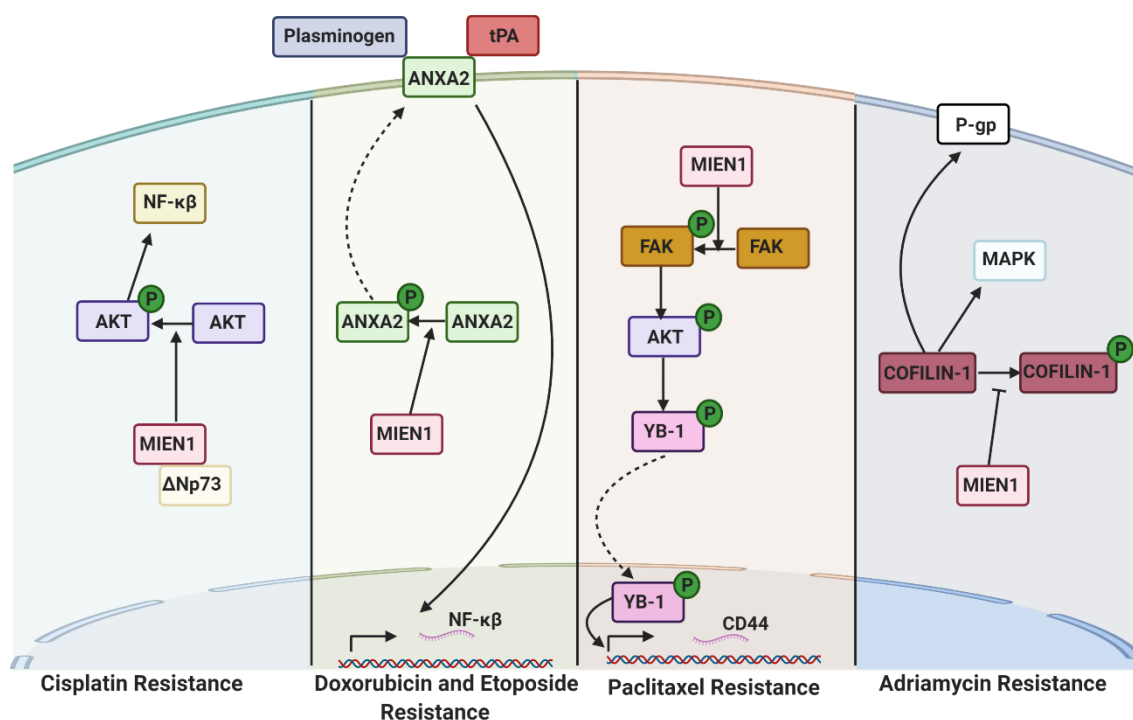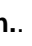
Figure 1. Scheme of different described MIEN1 mechanisms associated with chemoresistance processes against cisplatin[9], doxorubicin and etoposide[62,69,70], paclitaxel[67,68,72], and adriamycin[10,62,71]. (⟶): activation. (⊢): inhibition. (⋰): translocation.. The interaction between MIEN1 and the transactivation-deficient isoform of the tumour suppressor protein p73, ΔNp73[9,73], mediates AKT phosphorylation leading to NF-κβ activation and the subsequent promotion of cisplatin resistance[9]. Doxorubicin and etoposide resistance is prompted by NF-κβ overexpression as a result of Annexin-A2 (ANXA2) interaction with Plasminogen and Tissue plasminogen activator (tPA) in the plasmatic membrane, after prior MIEN1 modulated ANXA2 translocation from cytoplasm[62,69,70]. The role of MIEN1 in focal adhesion kinase (FAK) phosphorylation[68] triggers the phosphorylation cascade of AKT and Y-box binding protein 1 (YB-1) that results in the enhancing of CD44 transcription and Paclitaxel resistance[67,68,72]. Adriamycin resistance is promoted by MIEN1 activity through the inhibition of COFILIN-1 inactivation by phosphorylation, enabling COFILIN-1 interaction with the Multi-drug Resistance (MDR) protein, P-Glycoprotein (P-gp), and enhancing its transmembrane transport activity that cleanse adryamicin from the intracellular medium[10,62,71]. Created with BioRender.com.

NOP53 regulates the activation of the tumour suppressor p53 when ribosome biogenesis is perturbed or DNA damage is produced[32,74,75]. Analyses on the role of NOP53 in ovarian and prostate cancer are scarce, but down-regulation was observed in invasive serous ovarian tumours and prostatic adenocarcinomas when compared with normal tissues[12,76]. In fact, NOP53 was originally identified as a tumour suppressor, which is downregulated in brain tumour cells[77,78]. However, in other cancers

(esophagus or colon) NOP53 behaves as an oncogene that increments its expression in malignant cells[79]. The inhibition of murine doble minute 2 protein (MDM2), a downstream protein in NOP53 pathway (NOP53/RPL11/MDM2/P53), has been reported to revert chemoresistance in cell lines representing different cancers[80–82] (Figure 2), but the role of NOP53 in this field remains to be elucidated.
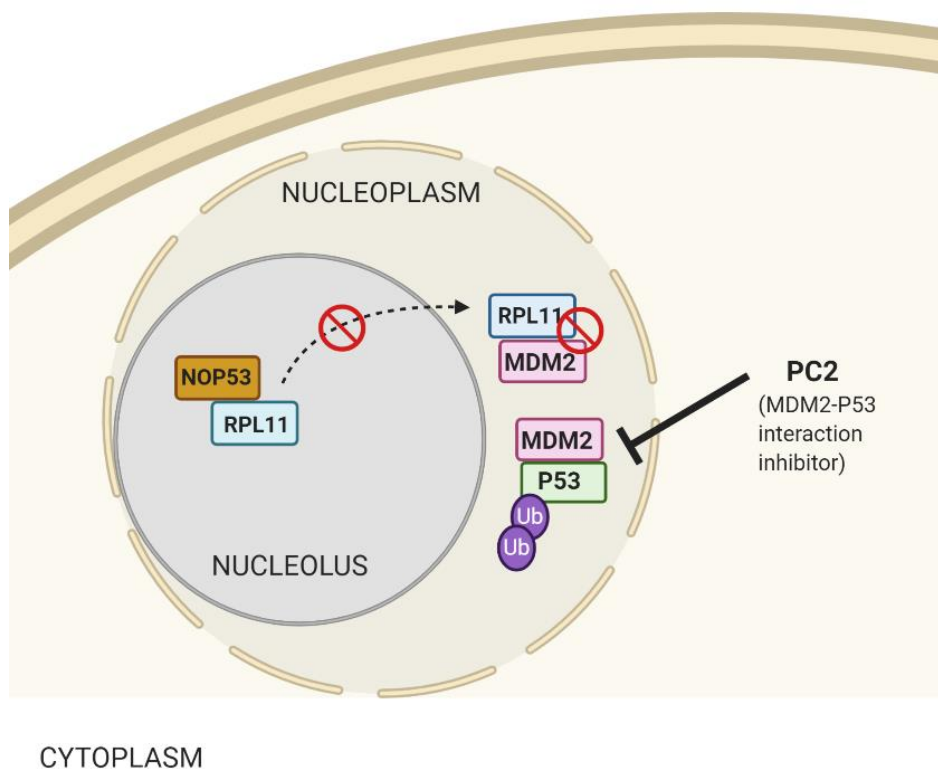
Figure 2. Scheme of NOP53 role in p53 degradation upstream of MDM2-p53, interaction disrupted by Prenylated Chalcone 2 (PC2)[81]. (🚫): events inhibited by NOP53 binding to RPL11. (⊣): inhibition. (⋯➤): translocation.. Created with BioRender.com

Although the role of HMGB proteins in cisplatin resistance is widely accepted[83], there is scarce information about the role of HMGB proteins in the resistance towards its derivatives like carboplatin, or other drugs used in prostate and ovarian cancer treatment. Indeed, no data are available about the role of HMGB1 or HMGB2 in the resistance to olaparib or bevacizumab in the treatment of this types of cancers. With these precedents we decided to investigate the role of HMGB1, HMGB2, MIEN1 and NOP53 in cell viability as well as in response and sensibility to drugs currently used in prostate and ovarian cancer therapy.

2.2. Effect of anti-cancer drugs on HMGB1*,* HMGB2*,* MIEN1 *and* NOP53 *gene expression in EOC*

We tested the effect of four compounds, used in ovary and prostate cancer therapy, over the expression of the genes HMGB1, HMGB2, MIEN1 and NOP53 in cultured SKOV-3 and IOSE-80 (Table 1).

Table 1. Comparative effect of treatments on gene expression in cancerous (SKOV-3) versus non-cancerous (IOSE-80) ovarian cells at 48h.

		SKOV-3					IOSE-80				
T	**GENE**	$2^{-\Delta\Delta Ct}$	**SD**	**Effect**	**CF**	**p value**	$2^{-\Delta\Delta Ct}$	**SD**	**Effect**	**CF**	**p value**
P	HMGB1	0.23	0.05	Down	4.44	7.50E-08	0.03	0.01	Down	30.76	4.92E-04
P	HMGB2	0.36	0.11	Down	2.80	6.11E-09	0.77	0.10	Ns	-	9.47E-02
P	MIEN1	0.23	0.07	Down	4.40	1.14E-10	0.005	0.003	Down	215.5	1.18E-03
P	NOP53	8.29	3.03	Up	8.29	2.62E−09	3.01	0.29	Up	3.01	6.60E-04
C	HMGB1	0.17	0.08	Down	5.90	2.31E-03	1.74	0.76	Ns	-	3.48E-01
C	HMGB2	0.24	0.02	Down	4.12	3.07E-05	1.26	0.22	Ns	-	2.31E-01
C	MIEN1	0.11	0.03	Down	9.49	6.78E-05	0.74	0.15	Ns	-	3.04E-01
C	NOP53	0.49	0.08	Down	2.06	4.09E-03	1.11	0.34	Ns	-	6.94E-01
O	HMGB1	0.66	0.16	Ns	-	1.24E-02	0.83	0.12	Ns	-	1.65E-01
O	HMGB2	1.12	0.35	Ns	-	4.90E-01	0.72	0.09	Ns	-	2.82E-02
O	MIEN1	1.72	0.33	Ns	-	9.61E-01	0.66	0.20	Ns	-	9.92E-02
O	NOP53	12.27	2.97	Up	12.27	2.41E-06	0.68	0.08	Ns	-	7.38E-02
B	HMGB1	0.68	0.11	Ns	-	4.19E-02	0.17	0.11	Ns	-	2.72E-02
B	HMGB2	0.56	0.09	Down	1.78	3.15E-04	0.49	0.14	Down	2.05	8.52E-03
B	MIEN1	0.89	0.13	Ns	-	2.37E-01	0.06	0.05	Ns	-	1.62E-02
B	NOP53	0.31	0.07	Down	3.22	6.75E-08	0.98	0.49	Ns	-	7.41E-01
P+C	HMGB1	0.05	0.02	Down	19.05	4.55E-04	Nt	Nt	Nt	Nt	Nt
P+C	HMGB2	0.10	0.05	Down	10.37	1.02E-03	Nt	Nt	Nt	Nt	Nt
P+C	MIEN1	0.04	0.01	Down	25.66	8.60E-05	Nt	Nt	Nt	Nt	Nt
P+C	NOP53	1.63	0.50	Ns	-	3.76E-01	Nt	Nt	Nt	Nt	Nt

T: Treatment. P: Paclitaxel. O: Olaparib. B: Bevacizumab. C: Carboplatin. Up/Down: the treatment causes increased/diminished mRNA expression. Ns: the effect is not significant having a p value >0.01. Nt: non tested.

Each selected compound has a different mechanism of action. As already explained, carboplatin is derivative of cisplatin that generates lesions in DNA, thereby inhibiting replication and transcription and leading to cell death[84,85]. Olaparib (AZD-2281, lynparza[24]) inhibits PARP, an enzyme necessary in DNA repair, leading to apoptosis of cancer cells[86]. Bevacizumab (avastin), a humanized anti-vascular endothelial growth factor (VEGF) monoclonal antibody for cancer therapy is used as anti-angiogenic[87]; and paclitaxel (anzatax, taxol, praxel), a cyclodecane first isolated from *Taxus brevifolia*, stabilizes microtubules in their polymerized form, leading to cell death[88]. SKOV-3, IOSE-80, PC-3 and PNT-2 cells were exposed to drug concentrations selected according to previous studies[54–57]. Paclitaxel was used at 25 µM[54]; carboplatin at 25 µg/mL[55]; olaparib to 2 µM[56]; and bevacizumab at 100 µg/mL[57] for 48 hours. A comparative analysis between the effects caused by these drugs on SKOV-3 and non-cancerous ovarian IOSE-80 cells is shown in Table 1.

Relative RNA expression after these treatments was measured by RT-qPCR in reference to cells cultured in absence of the drugs but treated with the corresponding vehicle-buffer used in the preparation of drug-solutions. In general, significant effects were more frequently observed in cancerous than in non-cancerous cells. For carboplatin or paclitaxel treatments, which are generally used in first line therapy of EOC, results indicate that they cause down regulation of the genes that are over-expressed in EOC cells (HMGB1, HMGB2 and MIEN1). Combined treatment with paclitaxel and carboplatin potentiates downregulation of these genes in comparison to individual treatments, as deduced from the fold-changes observed. NOP53, which is expressed at lower levels in EOC than in non-cancerous cells, was upregulated after 48h treatment with paclitaxel. Among the genes assayed, the treatment with olaparib in cancerous cells only affected NOP53, increasing its expression (Table 1). Bevacizumab had also minor effects on HMGB2 and NOP53 expression, in this case diminishing their expression.

2.3. Effect of HMGB1*,* HMGB2*,* MIEN1 *and* NOP53 *silencing on SKOV-3 drug sensitivity*

The genes HMGB1, HMGB2, MIEN1 and NOP53 were silenced by siRNA as described in Materials and Methods and the effect on cell viability after treatments with paclitaxel, carboplatin, olaparib and bevacizumab were compared in cells transfected with the corresponding specific siRNAs and siC (unrelated Control). Results are shown in Figure 3. Silencing of HMGB1 or HMGB2 diminished SKOV-3 cell viability after treatment with carboplatin. However, silencing of HMGB1 increased cell viability after treatment with paclitaxel. Cell viability after treatment with olaparib diminished with HMGB2 silencing. Finally, silencing of NOP53 increased cell viability after treatment with bevacizumab**.**
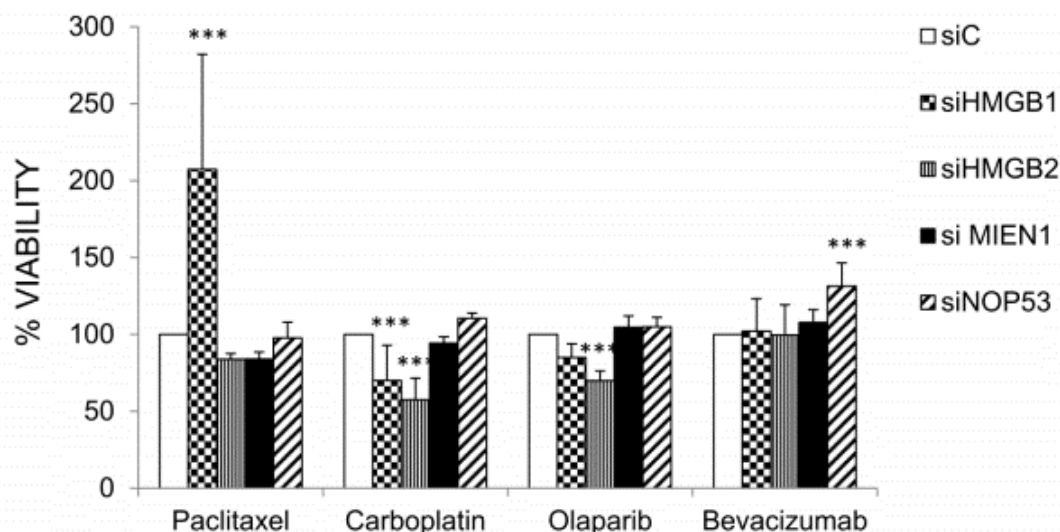
Figure 3. **Changes in cell viability of drug-treated versus untreated SKOV-3 cells after HMGB1, HMGB2, NOP53 and MIEN1 silencing**. Data about silencing of HMGB1 and HMGB2 are shown in chapter 2. *** (p< 0.001). ** (p<0.01). * (p<0.05).

2.4. Effect of anti-cancer drugs on HMGB1, HMGB2, MIEN1 *and* NOP53 *gene expression in PCa*

We tested the effect of paclitaxel, olaparib, bevacizumab, and combinations of the two first with the antiangiogenic bevacizumab in cancerous (PC-3) and non-cancerous (PNT-2) prostate cell lines. Results are shown in Table 2.

Table 2. Comparative effect of treatments on gene expression in cancerous (PC-3) versus non-cancerous (PNT-2) prostate cells at 48h.

T	GENE	PC-3					PNT-2				
		$2^{-\Delta\Delta Ct}$	SD	Effect	CF	p value	$2^{-\Delta\Delta Ct}$	SD	Effect	CF	p value
P	HMGB1	0.84	0.14	Ns	-	-	2.91	0.6	Up	2.9	1.3E-03
P	HMGB2	0.59	0.23	Ns	-	-	1.12	0.19	Ns	-	-
P	MIEN1	1.09	0.38	Ns	-	-	1.07	0.18	Ns	-	-
P	NOP53	0.86	0.33	Ns	-	-	1.65	0.08	Up	1.6	7.32E-03
O	HMGB1	0.45	0.08	Ns	-	-	1.68	0.45	Ns	-	-
O	HMGB2	0.55	0.05	Ns	-	-	3.24	0.29	Up	3.8	7.01E-03
O	MIEN1	0.056	0.009	Down	17.9	3.53E-05	1.75	0.14	Ns	-	-
O	NOP53	0.065	0.02	Down	15.2	7.5E-04	0.37	0.1	Down	2.63	9.30E-03
B	HMGB1	2.81	0.6	Ns	-	-	1.57	0.04	Up	1.57	2.16E-03
B	HMGB2	0.34	0.07	Down	2.9	2.5E-03	1.94	0.38	Up	1.7	9.69E-03
B	MIEN1	0.14	0.02	Down	7.1	2.5E-04	0.95	0.15	Ns	-	-
B	NOP53	0.18	0.03	Down	5.4	2.41E-03	0.48	0.11	Down	2.07	8.57E-03
O+B	HMGB1	1.05	0.12	Ns	-	-	0.52	0.12	Ns	-	-
O+B	HMGB2	0.81	0.17	Ns	-	-	2.8	0.8	Up	2.8	8.03E-03
O+B	MIEN1	1.47	0.34	Ns	-	-	1.6	0.18	Ns	-	-
O+B	NOP53	4.07	0.9	Up	4.07	3.5E-03	0.67	0.09	Ns	-	-
P+B	HMGB1	0.58	0.12	Ns	-	-	2.06	0.15	Up	2.06	2.09E-03
P+B	HMGB2	0.18	0.05	Down	5.4	1.3E-03	1.8	0.28	Ns	-	-
P+B	MIEN1	1.47	0.34	Ns	-	-	1.55	0.2	Ns	-	-
P+B	NOP53	1.92	0.2	Up	1.9	4.3E-03	2.17	0.3	Ns	-	-

T: Treatment. P: Paclitaxel. O: Olaparib. B: Bevacizumab. Up/Down: the treatment causes increased/diminished mRNA expression. Ns: the effect is not significant having a p value >0.01. Nt: non tested.

Oppositely to which had been observed in EOC cells, in PC-3 the treatment with paclitaxel does not significantly change the expression of the analyzed genes. The treatment with olaparib differentially down-regulates de expression of HMGB1 and MIEN1 in PC-3 cells, which is not observed in PNT-2; and although NOP53 is also downregulated in PC-3, this effect is not exclusive of prostate cancerous cells since it is also observed in non-cancerous prostate PNT-2 cells. Bevacizumab downregulates the expression of HMGB2 and MIEN1, which is not observed in PNT-2; and again, although NOP53 is also downregulated in PC-3, this effect is also observed in PNT-2 cells. Surprisingly, the combination of taxol and bevacizumab or olaparib and bevacizumab, completely changed the regulatory patterns observed in single treatments.

3. Discussion

Taking into consideration the importance of HMGB proteins in Epithelial Ovary Cancer (EOC) and Prostate Cancer (PCa), as well as in chemoresistance processes, we have analyzed the response to compounds used in chemotherapy on the expression of HMGB1, HMGB2 and two proteins previously identified in our laboratory as novel physical interacting partners of them: NOP53 and MIEN1. Although the role of HMGB proteins in cisplatin resistance is widely accepted[83], there is scarce information about the role of HMGB proteins in the resistance towards its derivatives like carboplatin[55], or drugs nowadays used in cancer treatment. Bevacizumab, olaparib, paclitaxel, carboplatin, or a combination of them are generally used in first line therapy of EOC, whereas in the treatment of PCa, paclitaxel is a first-line chemotherapy agent against this disease, and combination of taxanes with olaparib, bevacicumab or other drugs are still under clinical trials[27,28,89].

Implications of HMGB1*,* HMGB2 *and their interactants in drug resistance during EOC chemotherapy*

Concerning to ovarian cancer cell lines, we have shown in our study that HMGB1, HMGB2 and their EOC-HMGB-interactome partners MIEN1 and NOP53 are involved in the response to these drugs in ovarian cancer cells. Expression levels of the pro-oncogenic genes HMGB1, HMGB2, and MIEN1 are downregulated after treatment with paclitaxel, carboplatin or a combination of both (Table 1). We further discuss the association of our results with the previously proposed mechanisms for these compounds.

Paclitaxel

Paclitaxel is a chemotherapeutic agent with several mechanisms of action. These involve i) microtubular stabilization that avoids the achromatic spindle formation[90,91], ii) the impairing of the mitochondrial respiratory chain[92], and iii) activation of apoptosis and autophagic cell death due to cytoplasmic Ca^{2+} overload[90–94]. It has been previously reported that the treatment with elevated paclitaxel dosage triggers the release of Ca^{+2} stored in the Endoplasmic Reticulum (ER) and also activates the Capacitative Calcium Entry (CCE), which promotes the Ca^{+2} influx from the extracellular medium to the cytosol in order to finally restore the Ca^{+2} ER store[93]. The substantial incoming of Ca^{+2} provoked by the treatment with paclitaxel prompts autophagic cell death[93]. Since autophagic cell death is also mediated by HMGB1 and HMGB2 among other proteins[4,95], the downregulation of HMGB1 and HMGB2 in paclitaxel treated SKOV-3 cells observed in our study could play a role in paclitaxel resistance by avoiding autophagic cell death. Accordingly, HMGB1 silencing should increase cell viability of SKOV-3 cells exposed to paclitaxel, as verified in our experiments (Figure 3).

Carboplatin

It is described that carboplatin causes platin dimer formation with DNA strands, which lately promotes apoptosis when these abnormal structures are recognized by the DNA repairing machinery[20]. In this process, HMGB1 and HMGB2 recruit DNA repairing proteins and function as DNA adaptors favoring their restoring activity. NOP53 is involved in DDR[32], other mechanism for DNA repair. Therefore, the observed downregulation of these genes in response to carboplatin treatment could provide survival advantages, evading the identification of carboplatin DNA damages and allowing tumour cell growth. Accordingly, HMGB1 or HMGB2 silencing decrease cell-viability of SKOV-3 cells exposed to carboplatin (Figure 3). Our data support the role of HMGB1 in resistance to carboplatin that was previously reported[55].

The concurrence of different molecular mechanisms contributing to paclitaxel or carboplatin resistance are also supported by our data, since these chemotherapeutic agents have a synergic effect over the expression of our selected genes in SKOV-3 cells, causing a more accused downregulation than the respective treatments independently.

Olaparib

A previous study indicated the participation of HMGB1 in the resistance of cancerous cells to PARP-1 inhibitors such as olaparib in leukemia[96,97]. HMGB1 is a target for polyADP-ribosilation (PARylation) catalyzed by PolyADP-ribose Polymerase 1 (PARP-1), which subsequently promotes HMGB1 acetylation. HMGB1 acetylation interferes with HMGB1 DNA binding abilities, thus promoting HMGB1 translocation from the nucleus to both cytosol and extracellular medium[96,98]. PARP-1 interacts with SIRT1 and both proteins interplay for modulating DNA repair and redox response among other processes. Interestinlgy, PARP-1 promotes HMGB1 acetylation and SIRT1 deacetylates it. The inhibition of PARP-1 causes the imbalance of these equilibrium and the subsequent excess in HMGB1 deacetylation that avoids its translocation to the cytoplasm and extracellular medium[96,99–101]. The inhibition of PARP-1 also increases the transactivation of peroxisome proliferation-activated receptor gamma (PPARɣ)[102], which suppresses HMGB1 expression[103,104]. In our study with EOC cells we have not detected significant changes in HMGB1 or HMGB2 expression induced by olaparib (Table1) and, although we have found that HMGB2 silencing affects SKOV-3 viability, further analyses will be necessary to clarify the implied mechanism that in our model does not affect HMGB1 or HMGB2 expression.

Bevacizumab

Cancerous and not cancerous ovarian cell lines were incubated with bevacizumab, and a significant downregulation in HMGB2 and NOP53 expression levels in SKOV-3 cells was observed (Table 1). According to previous data it is possible to delineate a hypothetical signal regulatory pathway between bevacizumab induced cellular signaling and the downregulation of NOP53. Human telomerase reverse transcriptase (hTERT) is commonly overexpressed in cancer cells in order to maintain chromosomal stability through massive cellular multiplication. It was demonstrated that bevacizumab promotes VEGF clearance and therefore a decrease in the VEGF-VEGFR interaction would disrupt signaling pathways that control the expression of hTERT which in turn controls VEGF expression[105]. The decrease in VEGF expression is related to the disruption of the Akt mediated signal pathway[106] to which NOP53 expression is related[78], and this could explain the observed down regulation of NOP53 when SKOV-3 cell are treated with bevacizumab. The experimental confirmation of the Akt signaling pathway modulation as part of NOP53's response to bevacizumab treatment in EOC is however pending. Since, in the assayed conditions, we have not detected effects of silencing HMGB1, HMGB2, MIEN1 or NOP53 in ovarian cancerous cells viability after

bevacizumab treatment, the functional significance of this regulatory effect upon NOP53 expression is probably limited. By other hand, we have observed in our study that bevacizumab downregulates HMGB2 expression. Considering that the interaction between HMGB2 and hTERT decreases hTERT activity[107], the expected decrease of hTERT expression by the direct effect of bevacizumab could be balanced by bevacizumab indirect effect over HMGB2, downregulating its expression and resulting in an increase of hTERT activity.

Implications of HMGB1*,* HMGB2 *and their interactants in drug resistance during PCa chemotherapy*

We have not found a common pattern of response to paclitaxel in the EOC or PCa cell lines analyzed. Downregulation of HMGB1, HMGB2, MIEN1 and NOP53, observed in SKOV-3 cells after paclitaxel treatment, was not observed in PC-3 cells. Therefore, according to our results these genes are not potential markers of prognosis during this treatment of PCa.

In PC-3 cells the treatment with olaparib diminishes MIEN1 and NOP53 expression with a high fold change value (17.9 and 15.2 respectively). Interestingly the expression of MIEN1 is not affected in the non-tumoural prostate cell line PNT-2, and although NOP53 is also regulated in PNT-2, the change fold observed has a lower value (2.6) (Table 2). Olaparib is an inhibitor of PARP-1 and therefore interferes with the AKT signaling pathway, which is actively involved in the regulation of NF-KB, and NF-κB activity is essential for oncogenic transformation. Prior studies in PC-3 indicated that the depletion of PARP-1 caused the suppression of cell growth and migration by interfering with Akt pathway and consequently impairing the NF-κB activity[108]. The downregulation of MIEN1 and NOP53 is probably implied in the therapeutic mechanism of action of olaparib in PCa, since both genes have been related to the Akt/ NF-κB pathway[9,15,78]. Besides, other relationships between PARP-1 inhibition and NOP53 protein downregulation are found in the literature. It has been reported that the expression and enzymatic activity of the ATM protein is inversely correlated with olaparib efficacy in gastric and prostate cancers[109–111]. Moreover, prostate adenocarcinoma cells, such as PC-3, have been reported to overexpress miR106-a, which upregulates ATM[112]. ATM migrates to DNA damage sites and undergoes and increase in its kinase activity deriving into the phosphorylation of various target proteins including NOP53[37,40]. This ATM-NOP53 interaction leads to NOP53 translocation from the nucleolus to the nucleoplasm where it interacts with a range of proteins and is vulnerable to undergo proteasomal degradation[37,40,113].

Bevacizumab caused a similar downregulation of HMGB2 and NOP53 in the EOC or PCa cell lines analyzed. Therefore, these genes could be tested in the future as prognosis markers of response to bevacizumab in clinical trials. HMGB1 and HMGB2 are proteins with oncogene/tumour suppressor duality, and therefore final contribution to oncogenesis or apoptosis depends on the cellular context[104,114,115]. HMGB2 negatively regulates hTERT which has been described to promote VEGF transcription[105,107].
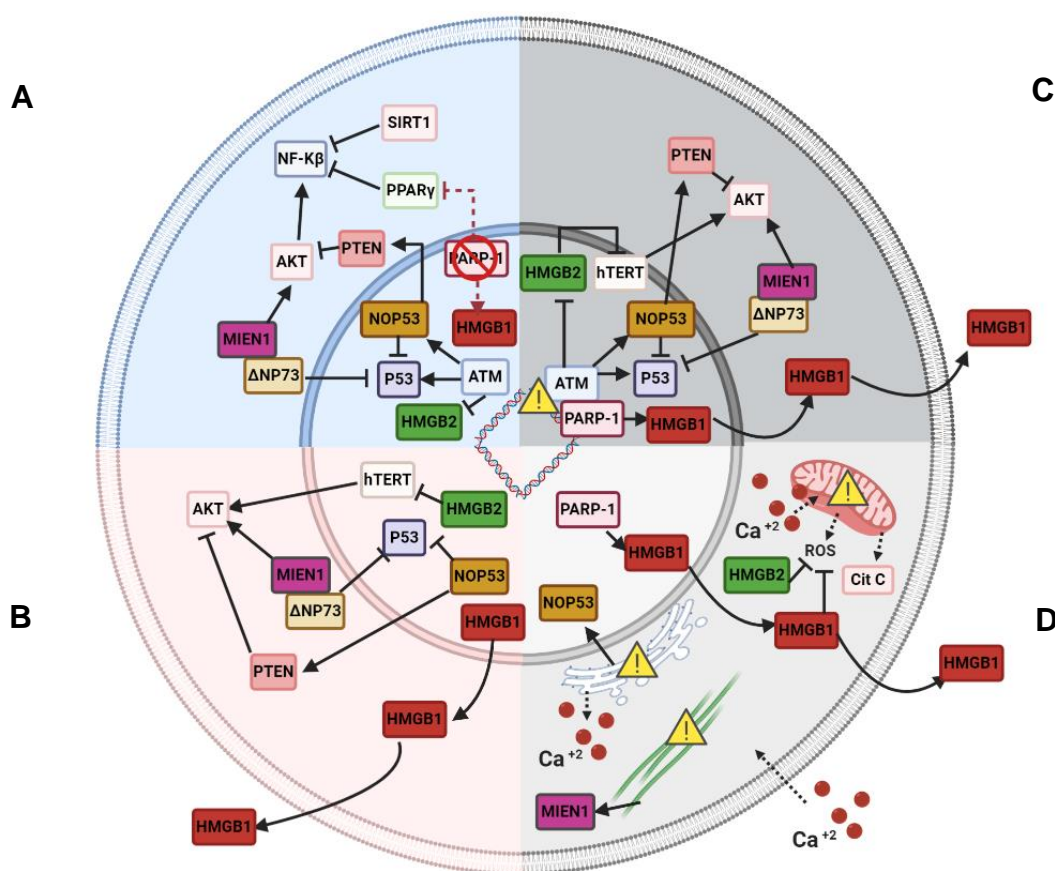
Figure 4. Scheme of described altered pathways in response to respectives chemotherapy treatments: A. Olaparib[9,15,78,108]**, B. Bevacizumab**[8,9,15,63,77–79,105,107,116] **C. Carboplatin**[20,32,55] **and D. Paclitaxel**[4,90–95]**. (** ⟶ **): activation. (** ⊣ **): inhibition. (** ▪▪▶ **)(**▪▪▪▪ı**): inhibited interactions. (**┄┄▶ **)(** ⚡ **): translocation. (** ⚠ **) : damage.** Created with BioRender.com.

Due to MIEN1 and NOP53 association with Akt[8,9,15,63,77–79,116], the clearance of VEGF through bevacizumab activity could affect the transcriptional regulation of these genes due to a decrease in Akt activation. Additionally, HMGB1 and HMGB2 have been

described to interact with RAGE[117,118] receptors through which they enhance VEGF expression[105,119]. Taking into consideration previous studies that confirm a cellular response to bevacizumab that consist in the increase of VEGF intracellular levels[105], it would be also interesting to further investigate if the downregulation of HMGB2 observed in our result is involved in this enhancing of VEGF transcription. Finally, it is remarkable that the effect observed upon NOP53 expression is maintained even when bevacizumab is combined with other treatments like olaparib or paclitaxel, which is an advantage in the clinical practice in which combinatory therapy is used to treat PCa.

References

1.   Amornsupak, K. *et al.* Cancer-associated fibroblasts induce high mobility group box 1 and contribute to resistance to doxorubicin in breast cancer cells. *BMC Cancer* **14**, 1–12 (2014).

2.   Li, S. & Wei, Y. Association of HMGB1, BRCA1 and P2 expressionin ovarian cancer and chemotherapy sensitivity. *Oncol. Lett.* **15**, 9572–9576 (2018).

3.   Xiao, Y. *et al.* High mobility group box 1 promotes sorafenib resistance in HepG2 cells and in vivo. *BMC Cancer* **17**, 1–11 (2017).

4.   An, Y. *et al.* MiR-23b-3p regulates the chemoresistance of gastric cancer cells by targeting ATG12 and HMGB2. *Cell Death Dis.* **6**, 1–11 (2015).

5.   Wu, Z. B. *et al.* High-mobility group box 2 is associated with prognosis of glioblastoma by promoting cell viability, invasion, and chemotherapeutic resistance. *Neuro. Oncol.* **15**, 1264–1275 (2013).

6.   Kwon, J. H. *et al.* Overexpression of high-mobility group box 2 is associated with tumor aggressiveness and prognosis of hepatocellular carcinoma. *Clin. Cancer Res.* **16**, 5511–5521 (2010).

7.   Balani, P. *et al.* High mobility group box2 promoter-controlled suicide gene expression enables targeted glioblastoma treatment. *Mol. Ther.* **17**, 1003–1011 (2009).

8.   Dasgupta, S. *et al.* Novel gene C17orf37 in 17q12 amplicon promotes migration and invasion of prostate cancer cells. *Oncogene* **28**, 2860–2872 (2009).

9.   Leung, T. H. Y. *et al.* The interaction between C35 and Δnp73 promotes chemo-resistance in ovarian cancer cells. *Br. J. Cancer* **109**, 965–975 (2013).

10.   Kumar, S., Kushwaha, P. P. & Gupta, S. Emerging targets in cancer drug resistance. *Cancer Drug Resist.* **2**, 161–177 (2019).

11.   Kim, J. Y. *et al.* Down-regulation and aberrant cytoplasmic expression of GLTSCR2 in prostatic adenocarcinomas. *Cancer Lett.* **340**, 134–140 (2013).

12.   Merritt, M. A. *et al.* Expression profiling identifies genes involved in neoplastic transformation of serous ovarian cancer. *BMC Cancer* **9**, 1–13 (2009).

13.   Uchi, R. *et al.* PICT1 regulates TP53 via RPL11 and is involved in gastric cancer progression. *Br. J. Cancer* **109**, 2199–2206 (2013).

14.   Kim, J. Y., Park, J. H. & Lee, S. GLTSCR2 contributes to the death resistance and invasiveness of hypoxia-selected cancer cells. *FEBS Lett.* **586**, 3435–3440 (2012).

15.   Chen, H. *et al.* PICT-1 triggers a pro-death autophagy through inhibiting rRNA transcription and AKT/mTOR/p70S6K signaling pathway. *Oncotarget* **7**, 78747–78763 (2016).

16.   Cámara-Quílez, M. *et al.* Differential characteristics of HMGB2 versus HMGB1 and their perspectives in ovary and prostate cancer. *Curr. Med. Chem.* **26**, 1–17 (2019).

17.   Kampan, N. C., Madondo, M. T., McNally, O. M., Quinn, M. & Plebanski, M. Paclitaxel and its evolving role in the management of ovarian cancer. *Biomed*

Res. Int. **2015**, 1–21 (2015).

18. Ceja, M. E., Christensen, A. M. & Sonal Patel, Y. Dosing Considerations in Pediatric Oncology. *Oncol. Supply. USPHARMACIST.* **38**, 8–11 (2013).

19. Hinderliter, P. & Saghir, S. A. Pharmacokinetics. *Encycl. Toxicol. Third Ed.* **3**, 849–855 (2014).

20. IQB Editorial Team. CARBOPLATIN IN VADEMECUM. *Centro colaborador de La Administración Nacional de Medicamentos, alimentos y Tecnología Médica (ANMAT); Argentina* https://www.iqb.es/cbasicas/farma/farma04/c020.htm (2013) Date of Access: 13-03-2020.

21. HOSPIRA INVICTA S.A. Ficha tecnica paclitaxel hospira 6 mg/ml concentrado para solución para perfusión EFG. *Agencia Española de Medicamentos y Productos Sanitarios* https://cima.aemps.es/cima/dochtml/ft/66311/FT_66311.html (2019) Date of Access: 13-03-2020.

22. Genentech USA Inc. Avastin® (bevacizumab) Dosage & Dosing in Approved Cancer Types. https://www.avastin.com/hcp/dosing.html (2020).

23. Bennouna, J. *et al.* Continuation of bevacizumab after first progression in metastatic colorectal cancer (ML18147): A randomised phase 3 trial. *Lancet Oncol.* **14**, 29–37 (2013).

24. Medscape. Lynparza (olaparib) dosing, indications, interactions, adverse effects, and more. *DRUG & DISEASES* https://reference.medscape.com/drug/lynparza-olaparib-999934 (2020) Date of Access: 13-03-2020.

25. Barata, P. C. *et al.* Phase I/II study evaluating the safety and clinical efficacy of temsirolimus and bevacizumab in patients with chemotherapy refractory metastatic castration-resistant prostate cancer. *Invest. New Drugs* **37**, 331–337 (2019).

26. Gross, M. E. *et al.* Safety and Efficacy of Docetaxel, Bevacizumab, and Everolimus for Castration-resistant Prostate Cancer (CRPC). *Clin. Genitourin. Cancer* **16**, e11–e21 (2018).

27. Fujiwara, M. *et al.* Efficacy and Safety of Carboplatin Plus Paclitaxel as the First-, Second-, and Third-line Chemotherapy in Men With Castration-resistant Prostate Cancer. *Clin. Genitourin. Cancer* **17**, e923–e929 (2019).

28. Zhao, H. F., Zhang, Z. C., Shi, B. K. & Jiang, X. Z. DANCR sponges MIR-135a to regulate Paclitaxel sensitivity in prostate cancer. *Eur. Rev. Med. Pharmacol. Sci.* **23**, 6849–6857 (2019).

29. Bocci, G., Di Paolo, A. & Danesi, R. The pharmacological bases of the antiangiogenic activity of paclitaxel. *Angiogenesis* **16**, 481–492 (2013).

30. Kpetemey, M. *et al.* MIEN1 drives breast tumor cell migration by regulating cytoskeletal-focal adhesion dynamics. *Oncotarget* **7**, 54913–54924 (2016).

31. Zhao, H., Zhang, X., Wang, H. & Zhang, M. Migration and invasion enhancer 1 (MIEN1) is overexpressed in breast cancer and is a potential new therapeutic molecular target. *Genet. Mol. Res.* **1**, 1–9 (2017).

32. Kim, J. Y. *et al.* Involvement of GLTSCR2 in the DNA Damage Response. *Am. J. Pathol.* **179**, 1257–1264 (2011).

33. Roisin E. O'Cearbhaill, M. Using PARP Inhibitors in Advanced Ovarian Cancer

Running head: PARP Inhibitors in Ovarian Cancer. *Physiol. Behav.* **176**, 139–148 (2017).

34. Sachdev, E., Tabatabai, R., Roy, V., Rimel, B. J. & Mita, M. M. PARP Inhibition in Cancer: An Update on Clinical Development. *Target. Oncol.* **14**, 657–679 (2019).

35. Adashek, J. J., Jain, R. K. & Zhang, J. Clinical Development of PARP Inhibitors in Treating Metastatic Castration-Resistant Prostate Cancer. *Cells* **8**, 1–12 (2019).

36. Tajuddin, N., Kim, H. Y. & Collins, M. A. PARP inhibition prevents ethanol-induced neuroinflammatory signaling and neurodegeneration in rat adult-age brain slice cultures. *J. Pharmacol. Exp. Ther.* **365**, 117–126 (2018).

37. Chen, H. *et al.* PICT-1 is a key nucleolar sensor in DNA damage response signaling that regulates apoptosis through the RPL11-MDM2-p53 pathway. *Oncotarget* **7**, 83241–83257 (2016).

38. Ko, H. L. & Ren, E. C. Functional aspects of PARP1 in DNA repair and transcription. *Biomolecules* **2**, 524–548 (2012).

39. Li, Z. *et al.* Destabilization of linker histone H1.2 is essential for ATM activation and DNA damage repair. *Cell Res.* **28**, 756–770 (2018).

40. Kim, J. Y. *et al.* Involvement of GLTSCR2 in the DNA Damage Response. *Am. J. Pathol.* **179**, 1257–1264 (2011).

41. Mukherji, S. K. Bevacizumab (avastin). *Am. J. Neuroradiol.* **31**, 235–236 (2010).

42. Ellis, L. M. Mechanisms of Action of Bevacizumab as a Component of Therapy for Metastatic Colorectal Cancer. *Semin. Oncol.* **33**, S1–S7 (2006).

43. Li, D., Wei, Y., Wang, D., Gao, H. & Liu, K. MicroRNA-26b suppresses the metastasis of non-small cell lung cancer by targeting MIEN1 via NF-κB/MMP-9/VEGF pathways. *Biochem. Biophys. Res. Commun.* **472**, 465–470 (2016).

44. Gough, D. R. & Cotter, T. G. Hydrogen peroxide: A Jekyll and Hyde signalling molecule. *Cell Death Dis.* **2**, 1–8 (2011).

45. Zeng, W. *et al.* Proteomic Strategy for Identification of Proteins Responding to Cisplatin-Damaged DNA. *Anal. Chem.* **91**, 6035–6042 (2019).

46. Syed, N. *et al.* Silencing of high-mobility group box 2 (HMGB2) modulates cisplatin and 5-fluorouracil sensitivity in head and neck squamous cell carcinoma. *Proteomics* **15**, 383–393 (2015).

47. Wang, Y. *et al.* Association of HMGB1 and HMGB2 genetic polymorphisms with lung cancer chemotherapy response. *Clin. Exp. Pharmacol. Physiol.* **41**, 408–415 (2014).

48. Wixted, W. E. *et al.* A model to identify novel targets involved in oxidative stress-induced apoptosis in human lung epithelial cells by RNA interference. *Toxicol. Vitr.* **24**, 310–318 (2010).

49. Kohlstaedt, L. A., King, D. S. & Cole, R. D. Native State of High Mobility Group Chromosomal Proteins 1 and 2 Is Rapidly Lost by Oxidation of Sulfhydryl Groups During Storage. *Biochemistry* **25**, 4562–4565 (1986).

50. Schwarzenbach, H. & Gahan, P. B. Resistance to cis- and carboplatin initiated by epigenetic changes in ovarian cancer patients. *Cancer Drug Resist.* **2**, 271–

296 (2019).

51.   Zhang, R. *et al.* Interference with HMGB1 increases the sensitivity to chemotherapy drugs by inhibiting HMGB1-mediated cell autophagy and inducing cell apoptosis. *Tumor Biol.* **36**, 8585–8592 (2015).

52.   Kim, I. W., Kim, J. H. & Oh, J. M. Screening of Drug Repositioning Candidates for Castration Resistant Prostate Cancer. *Front. Oncol.* **9**, 1–11 (2019).

53.   Kaighn, M. E., Narayan, K. S., Ohnuki, Y., Lechner, J. F. & Jones, L. W. Establishment and characterization of a human prostatic carcinoma cell line (PC-3). *Invest. Urol.* **17**, 16–23 (1979).

54.   Liu, Q. *et al.* Basic helix-loop-helix transcription factor DEC2 functions as an anti-apoptotic factor during paclitaxel-induced apoptosis in human prostate cancer cells. *Int. J. Mol. Med.* **38**, 1727–1733 (2016).

55.   Shu, W. Downregulation of high mobility group protein box-1 resensitizes ovarian cancer cells to carboplatin. *Oncol. Lett.* **16**, 4586–4592 (2018).

56.   Kukolj, E. *et al.* PARP inhibition causes premature loss of cohesion in cancer cells. *Oncotarget* **8**, 103931–103951 (2017).

57.   Zhao, Z. *et al.* Autophagy Inhibition Promotes Bevacizumab-induced Apoptosis and Proliferation Inhibition in Colorectal Cancer Cells. *J. Cancer* **9**, 3407–3416 (2018).

58.   Bernardini, M. *et al.* High-resolution mapping of genomic imbalance and identification of gene expression profiles associated with differential chemotherapy response in serous epithelial ovarian cancer. *Neoplasia* **7**, 603–613 (2005).

59.   Varma, R. R. *et al.* Gene expression profiling of a clonal isolate of oxaliplatin-resistant ovarian carcinoma cell line A2780/C10. *Oncol. Rep.* **14**, 925–932 (2005).

60.   Takeda, M. *et al.* The Establishment of Two Paclitaxel-Resistant Prostate Cancer Cell Lines and the Mechanisms of Paclitaxel Resistance withT wo Cell Lines. *Prostate* **67**, 955–967 (2007).

61.   Liu, H. *et al.* H19 promote calcium oxalate nephrocalcinosis-induced renal tubular epithelial cell injury via a ceRNA pathway. *EBioMedicine* **50**, 366–378 (2019).

62.   Kushwaha, P. P., Gupta, S., Singh, A. K. & Kumar, S. Emerging Role of Migration and Invasion Enhancer 1 (MIEN1) in Cancer Progression and Metastasis. *Front. Oncol.* **9**, 1–13 (2019).

63.   Chang, K. S. *et al.* Migration and Invasion Enhancer 1 Is an NF-kB-Inducing Gene Enhancing the Cell Proliferation and Invasion Ability of Human Prostate Carcinoma Cells In Vitro and In Vivo. *Cancers (Basel).* **11**, 1–17 (2019).

64.   Rajendiran, S. *et al.* microRNA-940 suppresses prostate cancer migration and invasion by regulating MIEN1. *Mol. Cancer* **13**, 1–15 (2014).

65.   Rajendiran, S., Gibbs, L. D., Treuren, T. Van & Klinkebiel, D. L. MIEN1 is tightly regulated by SINE Alu methylation in its promoter. **7**, (2016).

66.   Hsu, C., Shen, T., Chang, C., Chang, Y. & Huang, L. Solution Structure of the Oncogenic MIEN1 Protein Reveals a Thioredoxin-Like Fold with a Redox-Active Motif. *PLoS One* **7**, 1–10 (2012).

67.   Kang, Y. *et al.* Role of Focal Adhesion Kinase in Regulating YB – 1 – Mediated Paclitaxel Resistance in Ovarian Cancer. **105**, 1485–1495 (2013).

68.   Kpetemey, M., Chaudhary, P., Van Treuren, T. & Vishwanatha, J. K. MIEN1 drives breast tumor cell migration by regulating cytoskeletal-focal adhesion dynamics. *Oncotarget* **7**, 54913–54924 (2016).

69.   Kpetemey, M. *et al.* MIEN1, a novel interactor of Annexin A2 , promotes tumor cell migration by enhancing AnxA2 cell surface expression. *Mol. Cancer* **14**, 1–13 (2015).

70.   Wang, Y. *et al.* Annexin A2 could enhance multidrug resistance by regulating NF- κ B signaling pathway in pediatric neuroblastoma. *J. Exp. Clin. cancer Res.* **36**, 1–16 (2017).

71.   Chen, L. *et al.* Identification of cofilin-1 as a novel mediator for the metastatic potentials and chemoresistance of the prostate cancer cells. *Eur. J. Pharmacol.* **880**, 1–11 (2020).

72.   Annunziata, C. M. & Kohn, E. C. Novel Facts About FAK : New Connections to Drug Resistance ? **105**, (2013).

73.   Ikuzono, T. O. J. *et al.* Delta Np73 expression in thyroid neoplasms originating from follicular cells. *Anat. Pathol.* **38**, 205–209 (2006).

74.   Sloan, K. E., Bohnsack, M. T. & Watkins, N. J. The 5S RNP couples p53 homeostasis to ribosome biogenesis and nucleolar stress. *Cell Rep.* **5**, 237–247 (2013).

75.   Chen, H. *et al.* PICT-1 is a key nucleolar sensor in DNA damage response signaling that regulates apoptosis through the RPL11-MDM2-p53 pathway. *Oncotarget* **7**, 83241–83257 (2016).

76.   Kim, J. Y. *et al.* Down-regulation and aberrant cytoplasmic expression of GLTSCR2 in prostatic adenocarcinomas. *Cancer Lett.* **340**, 134–140 (2013).

77.   Kim, Y. J. *et al.* Suppression of putative tumour suppressor gene GLTSCR2 expression in human glioblastomas. *J. Pathol.* **216**, 218–224 (2008).

78.   Okahara, F. *et al.* Critical role of PICT-1, a tumor suppressor candidate, in phosphatidylinositol 3,4,5-trisphosphate signals and tumorigenic transformation. *Mol. Biol. Cell* **17**, 4888–4895 (2006).

79.   Sasaki, M. *et al.* Regulation of the MDM2-P53 pathway and tumor growth by PICT1 via nucleolar RPL11. *Nat. Med.* **17**, 944–951 (2011).

80.   Brandão, P. *et al.* Targeting the MDM2-p53 protein-protein interaction with prenylchalcones: Synthesis of a small library and evaluation of potential antitumor activity. *Eur. J. Med. Chem.* **156**, 711–721 (2018).

81.   Fonseca, J. *et al.* Prenylated chalcone 2 acts as an antimitotic agent and enhances the chemosensitivity of tumor cells to paclitaxel. *Molecules* **21**, 1–14 (2016).

82.   Leão, M. *et al.* Enhanced cytotoxicity of prenylated chalcone against tumour cells via disruption of the p53-MDM2 interaction. *Life Sci.* **142**, 60–65 (2015).

83.   Barreiro-Alonso, A. *et al.* High Mobility Group B Proteins, Their Partners, and Other Redox Sensors in Ovarian and Prostate Cancer. *Oxid. Med. Cell. Longev.* **2016**, 1–17 (2016).

84. Knox, R. J., Friedlos, F., Lydall, D. A. & Roberts, J. J. Mechanism of cytotoxicity of anticancer platinum drugs: evidence that cis-diamminedichloroplatinum(II) and cis-diammine-(1,1-cyclobutanedicarboxylato)platinum(II) differ only in the kinetics of their interaction with DNA. *Cancer Res.* **46**, 1972–1979 (1986).

85. Brabec, V. & Kasparkova, J. Modifications of DNA by platinum complexes Relation to resistance of tumors to platinum antitumor drugs. **8**, 131–146 (2005).

86. Goulooze, S. C., Cohen, A. F. & Rissmann, R. Olaparib. *Br. J. Clin. Pharmacol.* **81**, 171–173 (2016).

87. Ferrara, N., Hillan, K. J. & Novotny, W. Bevacizumab (Avastin), a humanized anti-VEGF monoclonal antibody for cancer therapy. *Biochem. Biophys. Res. Commun.* **333**, 328–335 (2005).

88. Lopes, N. M., Adams, E. G., Pitts, T. W. & Bhuyan, B. K. Cell kill kinetics and cell cycle effects of taxol on human and hamster ovarian cell lines. *Cancer Chemother. Pharmacol.* **32**, 235–242 (1993).

89. Corn, P. G. *et al.* Cabazitaxel plus carboplatin for the treatment of men with metastatic castration-resistant prostate cancers : a randomised , open-label , phase 1 – 2 trial. *Lancet Oncol.* **20**, 1432–1443 (2019).

90. Furukawa, K. & Mattson, M. P. Taxol stabilizes [Ca 2÷]i and protects hippocampal neurons against excitotoxicity. *Brain Res.* **689**, 141–146 (1995).

91. Burke, William J.; Raghu , Girija; Strong, R. TAXOL PROTECTS AGAINST CALCIUM-MEDIATED DEATH OF DIFFERENTIATED RAT PHEOCHROMOCYTOMA CELLS. *Pharmacol. Lett.* **55**, 313–319 (1994).

92. Kidd, J. F. *et al.* Paclitaxel Affects Cytosolic Calcium Signals by Opening the Mitochondrial Permeability Transition Pore. **277**, 6504–6510 (2002).

93. Pan, Z., Avila, A. & Gollahon, L. Paclitaxel induces apoptosis in breast cancer cells through different calcium-regulating mechanisms depending on external calcium conditions. *Int. J. Mol. Sci.* **15**, 2672–2694 (2014).

94. Yang, M. & Wei, H. Anesthetic neurotoxicity: Apoptosis and autophagic cell death mediated by calcium dysregulation. *Neurotoxicol Teratol.* **60**, 59–62 (2017).

95. He, S. J. *et al.* The dual role and therapeutic potential of high-mobility group box 1 in cancer. *Oncotarget* **8**, 64534–64550 (2017).

96. Kong, Q. *et al.* SIRT6-PARP1 is involved in HMGB1 polyADP-ribosylation and acetylation and promotes chemotherapy-induced autophagy in leukemia. *Cancer Biol. Ther.* **21**, 320–331 (2020).

97. Chai, Y. *et al.* High-mobility group protein B1 silencing promotes susceptibility of retinoblastoma cells to chemotherapeutic drugs through downregulating nuclear factor-kappaB. *Int. J. Mol. Med.* **41**, 1651–1658 (2018).

98. Wang, Y., Wang, L. & Gong, Z. Regulation of Acetylation in High Mobility Group Protein B1 Cytosol Translocation. *DNA Cell Biol.* **38**, 491–499 (2019).

99. Wei, S. *et al.* SIRT1-mediated HMGB1 deacetylation suppresses sepsis-associated acute kidney injury. *Am. J. Physiol. Physiol.* **316**, F20–F31 (2018).

100. Ye, T.-J., Lu, Y.-L., Yan, X.-F., Hu, X.-D. & Wang, X.-L. High mobility group box-1 release from H2 O2 -injured hepatocytes due to sirt1 functional inhibition. **25**, 5434–5450 (2019).

101. Cantó, C., Sauve, A. A. & Bai, P. Crosstalk between poly(ADP-ribose) polymerase and sirtuin enzymes. *Mol Asp. Med* **34**, 1–62 (2014).

102. Huang, D., Yang, C., Wang, Y., Liao, Y. & Huang, K. PARP-1 suppresses adiponectin expression through poly (ADP-ribosyl) ation of PPAR g in cardiac fibroblasts. *Cardiovasc. Res.* **81**, 98–107 (2009).

103. Yuan, Z. *et al.* PPARgamma inhibits HMGB1 expression through upregulation of miR-142-3p in vitro and in vivo. *Cell. Signal.* **28**, 158–164 (2016).

104. Kang, R., Zhang, Q., Zeh 3rd, H. J., Lotze, M. T. & Tang, D. HMGB1 in cancer: good, bad, or both? *Clin. Cancer Res.* **19**, 4046–4057 (2013).

105. Mahfouz, N. *et al.* Gastrointestinal cancer cells treatment with bevacizumab activates a VEGF autoregulatory mechanism involving telomerase catalytic subunit hTERT via PI3K-AKT, HIF-1α and VEGF receptors. *PLoS One* **12**, 1–20 (2017).

106. Zhao, D., Jia, P. & Wang, W. VEGF-mediated suppression of cell proliferation and invasion by miR-410 in osteosarcoma. *Mol cell Biochem* **400**, 87–95 (2014).

107. Kučírek, M., Bagherpoor, A. J., Jaroš, J., Hampl, A. & Štros, M. HMGB2 is a negative regulator of telomerase activity in human embryonic stem and progenitor cells. *FASEB J.* **33**, 14307–14324 (2019).

108. Lai, Y. *et al.* PARP1-siRNA suppresses human prostate cancer cell growth and progression. *Oncol. Rep.* **39**, 1901–1909 (2018).

109. Wang, C., Jette, N., Moussienko, D., Bebb, D. G. & Lees-Miller, S. P. ATM-Deficient Colorectal Cancer Cells Are Sensitive to the PARP Inhibitor Olaparib. *Transl. Oncol.* **10**, 190–196 (2017).

110. Mak, J. P. Y., Ma, H. T. & Poon, R. Y. C. Synergism between ATM and PARP1 inhibition involves DNA damage and abrogating the G2 DNA damage checkpoint. *Mol. Cancer Ther.* **19**, 123–134 (2020).

111. Riches, L. C. *et al.* Pharmacology of the ATM inhibitor AZD0156: Potentiation of irradiation and olaparib responses preclinically. *Mol. Cancer Ther.* **19**, 13–25 (2020).

112. Hoey, C., Ray, J., Ylanko, J., Andrews, D. W. & Boutros, P. C. miRNA-106a and prostate cancer radioresistance : a novel role for LITAF in ATM regulation. **12**, 1324–1341 (2018).

113. Kim, J. Y., Cho, Y. E., Park, J. H. & Lee, S. Expression of GLTSCR2/Pict-1 in squamous cell carcinomas of the skin. *Arch. Dermatol. Res.* **305**, 797–804 (2013).

114. Sayeon, C. *et al.* Binding and regulation of HIF-1alpha by a subunit of the proteasome complex, PSMA7. *FEBS Lett.* **498**, 62–66 (2001).

115. Swanson, P. C. Fine structure and activity of discrete RAG-HMG complexes on V(D)J recombination signals. *Mol. Cell. Biol.* **22**, 1340–1351 (2002).

116. Okumura, K., Zhao, M., DePinho, R. A., Furnari, F. B. & Cavenee, W. K. PTEN: A novel anti-oncogenic function independent of phosphatase activity. *Cell Cycle* **4**, 540–542 (2005).

117. Pusterla, T., de Marchis, F., Palumbo, R. & Bianchi, M. E. High mobility group B2 is secreted by myeloid cells and has mitogenic and chemoattractant activities similar to high mobility group B1. *Autoimmunity* **42**, 308–310 (2009).

118. Zhao, C. B. *et al.* Co-expression of RAGE and HMGB1 is associated with cancer progression and poor patient outcome of prostate cancer. *Am. J. Cancer Res.* **4**, 369–377 (2014).

119. Lei, C. *et al.* HMGB1 may act via RAGE to promote angiogenesis in the later phase after intracerebral hemorrhage. *Neuroscience* **295**, 39–47 (2015).

Chapter 4.

Identification of HMGB1/2 and related molecules in small extracellular vesicles from non-tumoural PNT-2 and cancerous PC-3 prostate cells and effects of TMZ and the hybrid compound 1D

Introduction

Prostate cancer is the most frequent adenocarcinoma in european men. The current biomarkers, as PSA, do not have enough specificity to allow an early diagnose of this disease, leading to invasive biopsies to confirm the pathology or a late detection and poor prognosis. In order to solve this problem, research has been focused on the discovery of new biomarkers that could be isolated from body fluids without performing aggressive procedures. In this context, the emerging identification of exosomes as novel extracellular vesicles (EVs) directly correlated with prostate cancer progression opens a new field of study in the searching of biomarkers and liquid biopsy[1,2]. Exosomes are small extracellular vesicles with a characteristic diameter size between 40-200 nm, which can mediate distant cell to cell interactions. Intercellular communication is critical in order to maintain homeostasis in a multicellular organism in response to external alterations. This makes exosomes an important tool that allows this communication to be specific and coordinated[3]. The generation of the exosomes take place by the formation of multivesicular bodies (MVBs) from mature endosomes, that finally release these vesicles to the extracellular medium through the fusion of endosomal and plasmatic membranes[4]. Exosomes mostly differ from the other types of extracellular vesicles by size and composition. Although several membrane proteins have been described to be specific exosome markers[5], such as CD63, CD9, CD81, or CD82, in fact none of them are exclusive for this type of vesicles. The luminal and membrane proteins in the exosome varies from one cellular type to another and, in cancerous cells, their content define their role in the promotion or inhibition of tumoral processes[6].

Tumour-derived exosomes (TDEs) have been described to be crucial in cancer dissemination due to the distant transfer of its cargo, containing miRNAs, mRNAs, DNA, proteins and lipids that enhance tumour progression in the receptor cells, while evading the immune response[3,5,7]. Thus, exosome cargo provides information about the current state of the cell that release them.

PCa studies have demonstrated the involvement of oncogenic proteins overexpressed in this type of cancer, such as Kirsten Rat Sarcome viral oncogene (KRAS)-associated binding (RAB) proteins, in the regulation of exosome trafficking. This trafficking process is meticulously modulated by post-transcriptional modifications and RNA specific motifs. Exosomes isolated from PCa patients presented high amount of specific PCa biomarkers associated to advanced stages of

this disease, e.g. endothelial growth factor receptor (EGFR), and miRNAs that promote metastasis and enhance tumour development[8]. These results confirmed the potential role of exosomes as a non-invasive novel source of biomarkers and as therapeutic targets. Specific miRNAs have been already associated with prognosis and diagnosis of PCa, such as miR-20a, miR-1, miR-21, miR-106b, miR-125b, miR-221 and miR-222[9]. More recently, the overexpression of a novel oncogenic miRNA, miR-155, has also been associated to prostate cancer[10,11]. Oppositely, there are miRNAs which develop tumour suppressor functions by silencing oncogenes, such as miR-146a and miR-124. In hormone-refractory prostate cancer (HRPC), the levels of miR-146a are strongly diminished, while its upregulation resulted in the arrest of the disease expansion[12,13]. In the same way, miR-124 overexpression has anti-tumour effects by silencing STAT3[14]. Although miR-155 and miR-146a interact with HMGB1 and HMGB2 in melanoma cancer cells[15], to the best of our knowledge, this interaction has not been still reported in prostate cancer cells. The tumour suppressor function of miR-124 in prostate cells[14] has been described to be mediated by silencing the Androgen receptor (AR)[16–18], which forms an activation loop with HMGB1[19–22] (Figure 1).
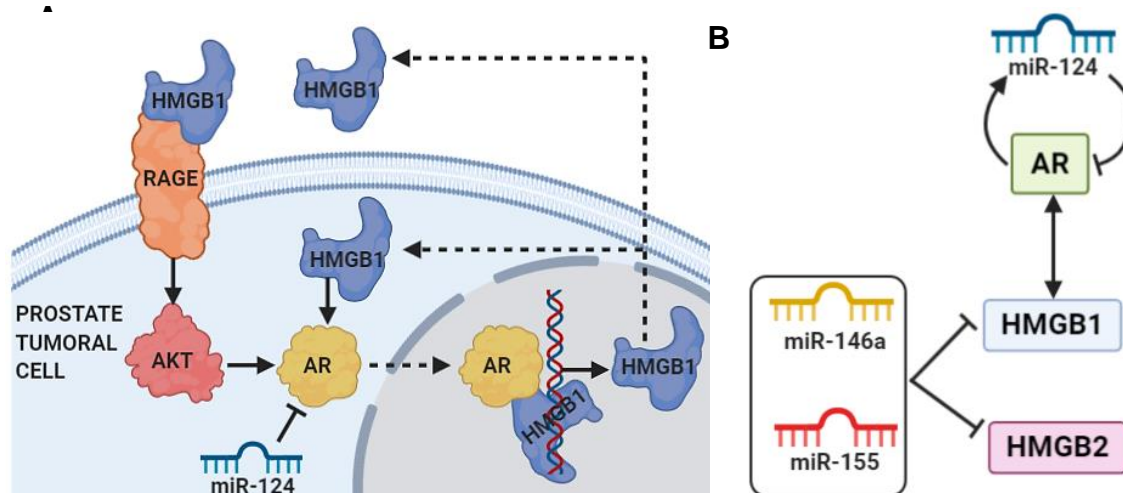
Figure 1. (A) Role of HMGB1 in the Androgen Receptor (AR) regulation pathway in a prostate tumoral cell[22,23]. **(B) Scheme of miRNAs miR-146a, miR-155 and miR-124 targeting HMGB1 and HMGB2**[15] **or AR. (** ➔ **):activation. (** ⊣ **): inhibition. (** ⤑ **): translocation.** Created with BioRender.com.

The important role of exosomes in cancer spreading, entails the important increase of chemotherapy agents capable to modulate exosome sorting to the medium. TMZ is a

conventional compound used in glioma treatment and composed by a triazene alkylating agent that converts into the functional metabolite 3-methyl-(triazen-1-yl) imidazole-4-carboxamide (MTIC), through a base catalyzed nucleophilic attack by water, when it reaches the central nervous system (CNS). TMZ is characterized for altering exosome sorting[24], being lipophilic and having a size small enough to cross the blood-brain barrier (BBB)[25]. Clinical studies have denoted the low anti-tumoural effect of TMZ agent in prostate cancer[26], as well as an improvement of its outcome when combined with PARP inhibitors in metastatic castration-resistant prostate cancer (mCRPC)[27,28]. In the improvement of TMZ in order to upgrade its effect emerges the 1D agent[29]. 1D is a novel triazene-hybrid compound reported by Dora Brites laboratory with higher anti-tumoural effect than TMZ in glioblastoma multiforme (GBM) cells[29]. 1D's structure is based on TMZ's and the anti-convulsive drug Valproic acid (VPA), also used as adjuvant in glioma treatment[29]. The hydrolytic ring opening of TMZ under alkaline conditions (or physiological pH) results in a monomethyltriazene intermediate which spontaneous de-composition releases the highly reactive methyldiazonium cation with ability for DNA alkylation[25,30] and EVs shuttling modulation[24]. On the other hand, 1D undergoes a similar activating process but with half-life values much higher ($t_{1/2}$>40 h) than those for TMZ ($t_{1/2}$=2 h), and a lower potential to alkylate DNA[29]. Therefore, considering the reported role of our proteins of study, HMGB1 and HMGB2, in the resistance to DNA altering chemotherapy agents such as cisplatin[31,32] we were interested to know how TMZ and 1D treatment change cargo content of the EVs sorted by prostate cells, and whether these EVs could spread proteins and miRNAs implicated in resistance mechanisms to therapy. In order to further analyse PCa exosomes, we perform a first approach using tumour and non-tumour cellular models, PC-3 and PNT-2 cell lines respectively, that already had reported differential EVs uptake kinetics in previous studies[33,34]. In the present work, these two cell lines were used for isolation of EVs in non-treated conditions and after incubation with these two compounds, TMZ or 1D. Evaluation of several proteins and miRNAs in their cargos was then performed. Concretely, HMGB1 and HMGB2, as well as the proteins NOP53 and MIEN1, which had been characterized as their binding partners in Y2H interactome (Chapter 1). In addition, miRNAs associated with the regulation of HMGB2 expression, miR-124, miR-146a and miR-155, were included in our analysis.

1. Materials and Methods

1.1. Cell cultures

PC-3 is an androgen-independent prostate cancer cell line derived from a bone metastasis[35] and it was obtained from American Type Culture Collection (ATCC). PNT-2 cell line (CVCL_2164, Normal prostate epithelium immortalized with SV40) was kindly provided by Professor Inés Díaz-Laviada Marturet (University of Alcala de Henares, ES, EU). Both human prostate cell lines, were regularly validated by DNA typing, and grown in RPMI-1640 (Gibco™, Thermo Fisher Scientific Inc., Waltham, MA, USA), supplemented with 1% exosome-depleted fetal bovine serum and 1% penicillin-streptomycin (Thermo Fisher Scientific Inc., Waltham, MA, USA). Cells were cultured at 37ºC and 5% CO_2 in a humidified incubator.

1.2. Cell viability assay

In order to assess the optimum concentration of 1D compound to treat the cells and compare its effect in cell viability with TMZ (Sigma-Aldrich, St. Louis, MO, USA), PC-3 and PNT-2 cell lines were treated with a range of concentrations of 1D or TMZ (1, 5, 10, 25, and 50 µM), during 24, 48 and 72 h. 1D is not commercially available and was kindly provided by Professor Dora Brites (Neuron-Glia Biology in health and disease, iMed.Lisboa, University of Lisbon, Lisbon, PT, EU). The vehicle of administration, DMSO (Sigma-Aldrich, St. Louis, MO, USA), was added to the cells in the same quantity used when adding the drugs as a negative control. Cell viability was determined by evaluating [3-(4,5-dimethylthiazol-2-yl)- 5-(3-carboxymethoxyphenyl)-2-(4-sulfophenyl)-2H-tetrazolium] (MTS) reduction in the presence of phenazine methosulfate (PMS), which forms a colored formazan product that is released to the culture medium. A combined MTS/PMS solution (1:20, with stock solution at 2 mg/mL and at 0.92 mg/mL, respectively) was freshly prepared and after the respective cell treatments, supernatants were removed and cells incubated for 45 min, at 37°C, in a dilution of 1:10 of MTS/PMS in culture medium. At the end of incubation, the absorbance of the medium was read at 490 nm using an ELISA plate reader PR 2100 (Bio-Rad Laboratories, Hercules, CA, USA). Results were expressed as percentage of survival *versus* the negative control treated with DMSO, considering this last one as 100% viability for each treatment.

1.3. Cell treatments

The same number of cells (250.000) were cultured in each well of a 6-well plate, prior to treatment with 5 µM of TMZ or 1D in 2 mL of RPMI-1640 (Gibco™, Thermo Fisher Scientific Inc., Waltham, MA, USA) medium per well during 48h. After incubation with the different compounds, supernatant was collected in order to analyze its content in EVs and free miRNAs. A total of 12 mL (equivalent to a 6-well plates) and 36 mL (equivalent to three 6-well plates) of medium was collected for miRNA or protein analysis respectively for each treatment condition.

1.4. Isolation and characterization of exosomes

The isolation of extracellular vesicles (EVs) was performed starting from 20 mL of extracellular media of the respective cell cultures. After centrifugation at 1000 x g, for 10 min, to remove dead cells and debris, the supernatant was centrifuged at 16000 x g for 60 min, to separate micro-vesicles (size ~1000 nm). The recovered supernatant was passed through a 0.2 µm filter to remove suspended particles and further centrifuged in the UltraL-XP100 centrifuge (Beckman Coulter Inc., CA, USA) at 100000 x g for 120 min. The recovered pellet fraction (containing EVs, size~100 nm) was re-suspended in PBS (Gibco™, Thermo Fisher Scientific Inc., Waltham, MA, USA) and centrifuged again at 100000 x g for 120 min. The new pellet, containing EVs, was re-suspended in different buffers depending on its final purpose: i) PBS for Nano-sight analysis and Transmission Electron Microscopy (TEM) characterization; ii) Qiazol lysis buffer (QIAGEN, Hilden, DE, EU)[36] for RNA extraction; iii) "Cell Lysis Buffer" (provided in the kit from Cell Signaling, Beverly, MA, USA) plus 1 mM phenyl-methyl-sulfonyl fluoride (PMSF, Sigma-Aldrich, St. Louis, MO, USA) for protein extraction. The profiling of isolated EVs from PNT-2 and PC-3 re-suspended in PBS was carried out by Nanoparticle Tracking Analysis (NTA), version 3.4, using Nanosight equipment (NS300, Malvern Panalytical, Malvern, UK, EU). Each sample was measured five times in order to assess the averages of EVs concentrations and sizes respectively. TEM technique was performed using the Jeol JEM 1400 Transmission Electron Microscope (Peabody, MA, USA).

1.5. Total RNA extraction, reverse transcription and Quantitative-PCR

miRNA expression levels were determined by real time-quantitative PCR (RT-qPCR) according with previous studies performed by Brites *et al.*[37]. Total RNA was extracted from PNT-2 or PC-3 cells, extracellular vesicles and culture media using TRIzol® (miRNeasy mini-kit from QIAGEN, Hilden, DE, EU) reagent according to the manufacturer instructions. Extracted RNA was quantified using Nanodrop® ND-100 Spectrophotometer (NanoDrop Technologies Inc., Wilmington, DE, USA) measuring at 230 nm.

Table 1. Oligonucleotides	
miRNA	Target sequence (5'-3')
hsa-miR-124-3p	UAAGGCACGCGGUGAAUGCC
hsa-miR-146a-5p	UGAGAACUGAAUUCCAUGGGUU
mmu-miR-155-5p	UUAAUGCUAAUUGUGAUAGGGGU
hsa *Homo sapiens*; mmu; *Mus musculus* Small nuclear RNA U6 was used as a reference gene (endogenous control); UniSp6, RNA spike-in control (exogenous control), was used to monitor PCR efficiency.	

Regarding miRNA expression, cDNA was synthetized using miRCURY LNA™ Universal RT miRNA PCR Kit (339340, QIAGEN Sciences, MD, USA) and 20 ng total RNA according to the following protocol: Retro-transcription reaction during 10 min at 25ºC, annealing reaction during 15 min at 50ºC followed by heat-inactivation of the reverse transcriptase for 5 min at 85ºC. For RT-qPCR, Power SYBR Green Master Mix (4367659, Applied Biosystems™ , Thermo Fisher Scientific, MA, USA) was used with predesigned (339340, Exiqon, QIAGEN Sciences, MD, USA) primers (Table 1) to target specific miRNA sequences (miR-124, miR-155 and miR-146a). U6 and RNU1A1 were used as reference genes, and synthetic RNA template spike-in (UniSp6) as a positive control to ensure the quality of the reaction and subsequent evaluations. RT-qPCR was performed on a Applied Biosystems™ QuantStudio™ 7 Flex RealTime PCR System (Thermo Fisher Scientific Inc., Waltham, MA, USA) using 384 well plates and applying these parameters: Polymerase activation for 2 min at 50ºC, followed by denaturation of double-stranded cDNA for 2 min 95ºC and 50 amplification cycles composed by denaturation at of double-stranded for 5 sec at 95ºC followed by annealing and elongation reaction for 30 sec at 62ºC. Each sample was performed in triplicate. The expression fold change vs. respective controls was determined by the $2^{-\Delta\Delta CT}$ method[38].

1.6. Western blot Assay

After performing EVs isolation through ultracentrifugation, the final pellet was resuspended in 50 µl of "Cell Lysis Buffer" (provided in the kit from Cell Signaling, Beverly, MA, USA) plus 1 mM phenyl-methyl-sulfonyl fluoride (PMSF, Sigma-Aldrich Inc., St. Louis, MO, USA). Briefly, total EVs extracts were lysed for 5 minutes on ice with shaking. The lysate was then centrifuged at 19000 x g for 10 min at 4 °C, and the supernatants were collected and stored at -80°C. In order to concentrate the samples, the Rotational Vacuum Concentrator RVC 2-33 CDplus (CHRIST, Martin Christ Gefriertrocknungsanlagen GmbH, DE, EU) was used, combining centrifugal force, and vacuum, at 4°C temperature for solvent removal and sample concentration. The concentrated eluate was stored at -80°C. Then, equal amounts of protein were subject to a 10% SDS-PAGE gel and transferred to a PVDF membrane. After blocking for 1 hour at room temperature with 5% (w/v) non-fat milk diluted in PBST, PBS (NZYTech Lda., Lisbon, PT, EU) containing 0.1% of Tween 20 (P1379, Sigma-Aldrich Inc., St. Louis, MO, USA), membranes were incubated with primary antibodies of HMGB1 (1:1000, ab18256, Abcam, Cambridge, UK), HMGB2 (1:1000, ab67282, Abcam, Cambridge, UK, EU), PICT-1 (1:500, sc-517088, Santa Cruz Biotechnology, CA, USA), MIEN1 (1:200, XTP4, 40-400, Invitrogen, Thermo Fisher Scientific Inc., Waltham, MA, USA), CD63 (1:1000, sc-5275, Santa Cruz Biotechnology, CA, USA) or FLOTILLIN-1 (1:1000, sc-74566, Santa Cruz Biotechnology, CA, USA) diluted in blocking solution overnight at 4°C, followed by G-protein HRP-linked (1:5000, 18-161, Millipore, Merck KGaA, Darmstadt, DE, EU) diluted in blocking solution for 1 hour at room temperature. Chemiluminescence-detection was performed by using Pierce ECL Western Blotting Substrate (A00042, Sigma-Aldrich, St. Louis, MO, USA) and bands were visualized in the ChemiDoc XRS System (Bio-Rad Laboratories, Hercules, CA, USA. The relative intensities of protein bands were analysed using the ImageLab analysis software (Bio-Rad Laboratories, Hercules, CA, USA).

1.7. Statistical analysis

Results were expressed as mean ± SEM. Comparisons between two different groups were performed using one-tailed Student's t-test. Analysis was performed in PRISM 7.0 software (GraphPad Software) and $p < 0.05$ was considered statistically significant.

2. Results

Results described in this chapter were majorly obtained in collaboration with the Dora Brites laboratory. Professor Dora Brites is the head of the group "Neuron-Glia Biology in health and disease" at iMed-Lisboa, University of Lisbon (Lisbon, PT, EU). I carried this work during a pre-doctoral international three months stay financed by EMBO. This group studies the effects of temozolomide (TMZ) and new compounds like 1D in the treatment of gliomas.

2.1. Viability assay

Taking into consideration previous studies testing TMZ in prostate cancer cells[27], the effects of TMZ and 1D were tested in PC-3 and PNT-2 cells to evaluate their sensitivity to these compounds. Since both drugs were dissolved in DMSO, a parallel control of cell viability with DMSO was carried out for each condition.
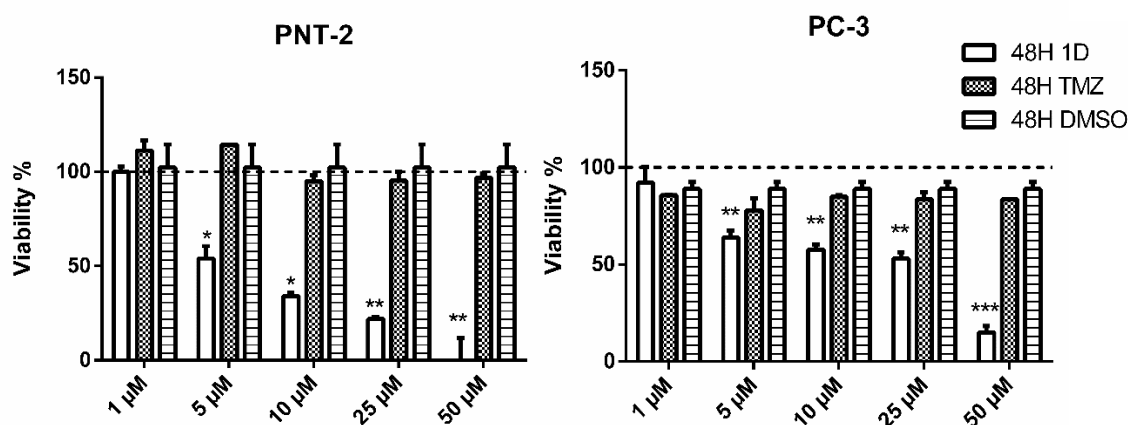
Figure 2. MTS assay in PC-3 and PNT-2 cell lines using different concentrations of Temozolomide (TMZ) and TMZ-Valproic hybrid compound, 1D. *** ($p < 0.001$). ** ($p < 0.01$). * ($p < 0.05$). Dashed lines represent 100% viability in controls without treatment nor DMSO.

According these results, PC-3 cells are more vulnerable to 1D than to TMZ treatment. The concentration of 1D, TMZ and DMSO selected for the following experiments was 5 µM for being the lower concentration at which significant effects on cell viability were observed (Figure 2).

2.2. Characterization micro-vesicles isolated from PC-3 and PNT-2 culture

2.2.1. Profiling of EVs derived from PC-3 and PNT-2 through TEM and NTA Analysis

Isolation of EVs from prostate cell lines was carried out in order to test the hypothesis of finding as cargos specific proteins related to PCa in our prior experiments: HMGB1, HMGB2, MIEN1 and NOP53 or miRNAs related to their regulation. The detection of these proteins or miRNAs in EVs might be valuable as potential new biomarkers for cancer diagnoses, prognosis and also for prediction of chemotherapy resistance. Previous studies have tried to solve the prostate cancer cells low sensitivity to TMZ by the addition of adjuvants like ABT-888[27]. The mechanism of resistance to TMZ or 1D had not been previously investigated in prostate cancerous cells. However, recent work with TMZ in glioblastoma revealed that activation of the p53 pathway, to which HMGB proteins[39–41], MIEN1[42,43] and NOP53[44] had been associated, had significant influence in the reversion of TMZ chemoresistance[45]. Besides, other study in glioblastoma, based on subcellular proteomics and bioinformatical analysis, identified dysregulated PI3K-AKT pathway as related with TMZ chemoresistance[46]. This result was also interesting to us because several proteins identified in the HMGB-PCa interactome are associated to the PI3K-AKT pathway as described in Chapter 1[47]. The EVs characterization by Nano-sight (Figure 4B) verified the micro-vesicle size expected (40-200 nm) and allowed the quantification of isolated particles. Interestingly in the assayed conditions, PNT-2 cell line produces a higher concentration of micro-vesicles than PC-3 (Figure 4A)**.** The isolation of EVs and the characteristic exosome cup shape was confirmed through TEM (Figure 3). Although exosomes are undoubtedly found in these samples, the absence of other kind of vesicles in our isolates cannot be assured with the used methodology. For this reason, it is more accurate to refer to these samples as EVs.

2.2.2 Effects of Temozolomide (TMZ) and 1D treatment in the biogenesis of exosomes by PC-3 and PNT-2

Previous studies in the laboratory of Professor Dora Brites characterized the motor neuron-microglia cross-talk through exosomes observing the presence of HMGB1 inside this type of EVs, as well as the inflamma-miRs: miR-124, miR-146a, and miR-155[48-49]. Besides, a different work from the same group analysed 1D compound chemotherapeutic advantages versus TMZ in glioblastoma cells[25,29]. Basing on Professor Dora Brites previous research and the evidence of TMZ role in glioblastoma exosome shuttling[24], we proceed to test the effect of TMZ and 1D compounds in the EVs produced by the two selected prostate cell lines. We analyzed exosome differences in shape, size and production rate between PC-3 and PNT-2 cell lines after incubating these cells with TMZ or 1D. Results obtained by TEM (Figure 3) revealed that the characteristic cup-shape that distinguish exosomes[49] from other EVs was not affected by these treatments.
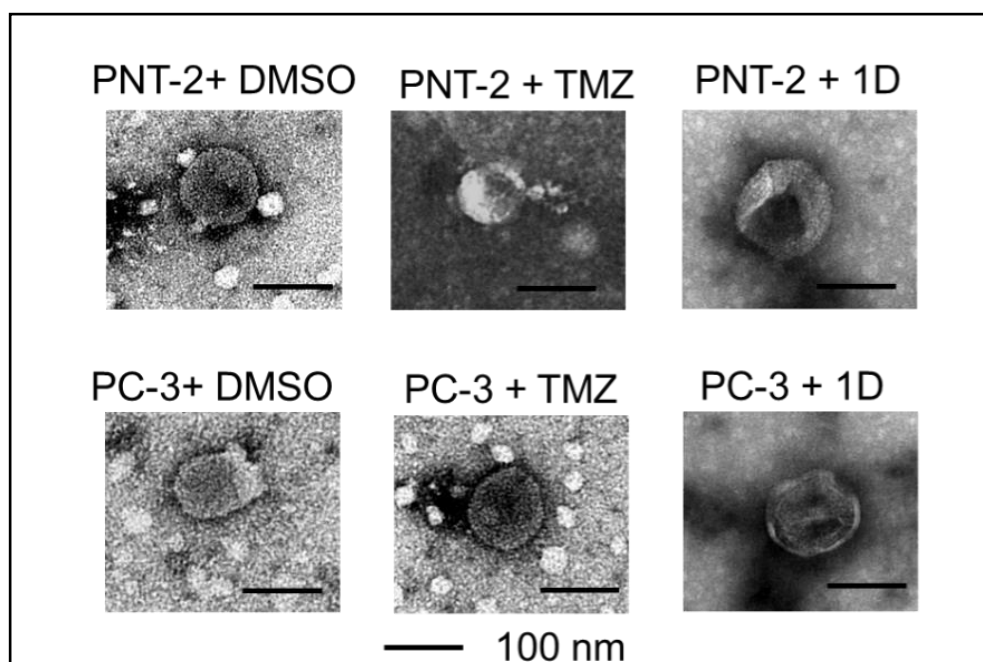
**Figure 3. Transmission Electron Microscopy (TEM) image of exosomes isolated from prostate non tumoral (PNT-2) and tumoral (PC-3) cell lines in different conditions:** DMSO control, treatment with 1D, and treatment with Temozolomide (TMZ).

Results obtained using NTA technology show that the treatment with 1D increases the number of EVs released by PC-3 in comparison with the DMSO vehicle-treated cells (control).
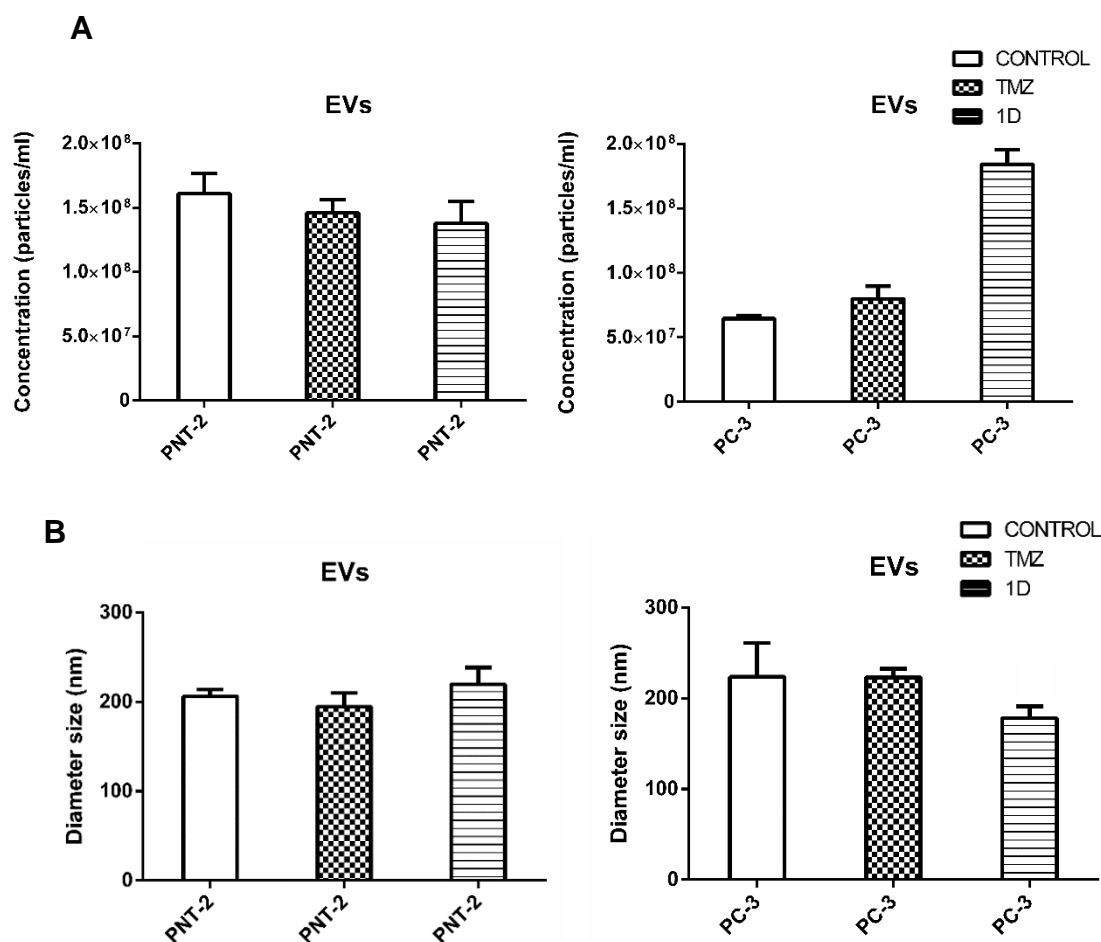
Figure 4. *Nano-sight* **data of (A) particles/ml and (B) diameter size (nm) from the EVs produced by PC-3 and PNT-2** in control conditions (DMSO), treatment with Temozolomide (TMZ), and treatment with 1D. The same number of cells were plated in each well of a 6 well-plate (250.000). *** ($p < 0.001$). ** ($p<0.01$). * ($p<0.05$).

Besides, oppositely to our initial observation that PNT-2 generates more EVs than PC-3 (Figure 4), the treatment with 1D reversed this effect and PC-3 produced more EVs than PNT-2 (Figure 4A). We also compared the diameter size of the extracellular vesicles obtained with or without treatment with TMZ and 1D (Figure 4B) and we observed a decrease in the size of PC-3 derived EVs when comparing with control conditions (Figure 4B and Figure 5). Figure 5 shows the graphs generated by NTA representing the Averaged Finite track length adjustment (FTLA) Concentration / Size for the EVs produced by the two cell lines in the different conditions. In this representation, a different profile can be noticed between the EVs produced by PNT-2 and PC-3 (Figure 5A and 5B). It is interesting to remark that the treatment with 1D compound seems to alter PC-3 EVs sorting leading to a PNT-2 similar profile (Figure 5C).
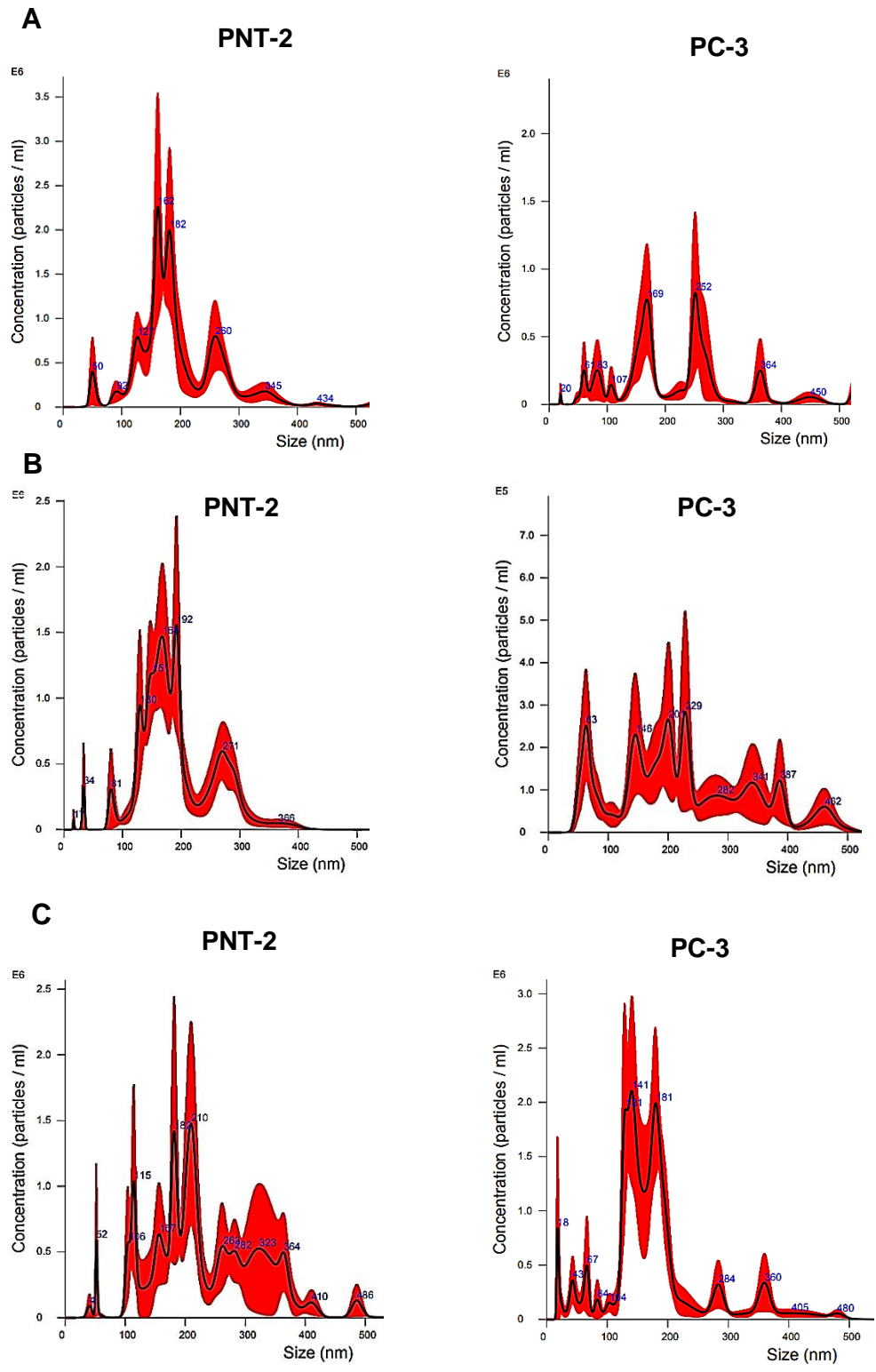
Figure 5. Averaged FTLA Concentration / Size for the EVs produced by (A) Control, (B) TMZ treatment and (C) 1D treatment.

2.3. Comparative analysis of miR-146a, miR-155 *and* miR-124 *levels in PC-3 and PNT-2 cell lines*

The content of specific miRNAs in exosomes is a useful tool for diagnostic purposes in cancer[8,9,50–52]. We were interested in analysing three specific miRNAs in EVs derived from prostate cell lines and that had been previously related both to PCa and HMGB proteins[11,15,22,53,54] because they target mRNA from HMGB1/2 (miR-146a, miR-155) or AR (miR-124)[16,22] as summarized in Figure 1. We first compared the expression of these miRNAs in the tumour PC-3 cells, extracellular media (secretome) and produced EVs to those obtained from non-tumour PNT-2 cells (Figure 6). The expression of miR-146a was very low and no significant differences could be observed between the two cell lines (data not shown). The expression of miR-155 was significantly lower in PC-3 than in PNT-2 when analysing cells, secretome or EVs. The expression of miR-124 in cells and secretome from PC-3 was also lower than in PNT-2. However, analyzing EVs, miR-124 expression in the tumoral cell line PC-3 was 5 times higher than in EVs derived from PNT-2 (Figure 6).
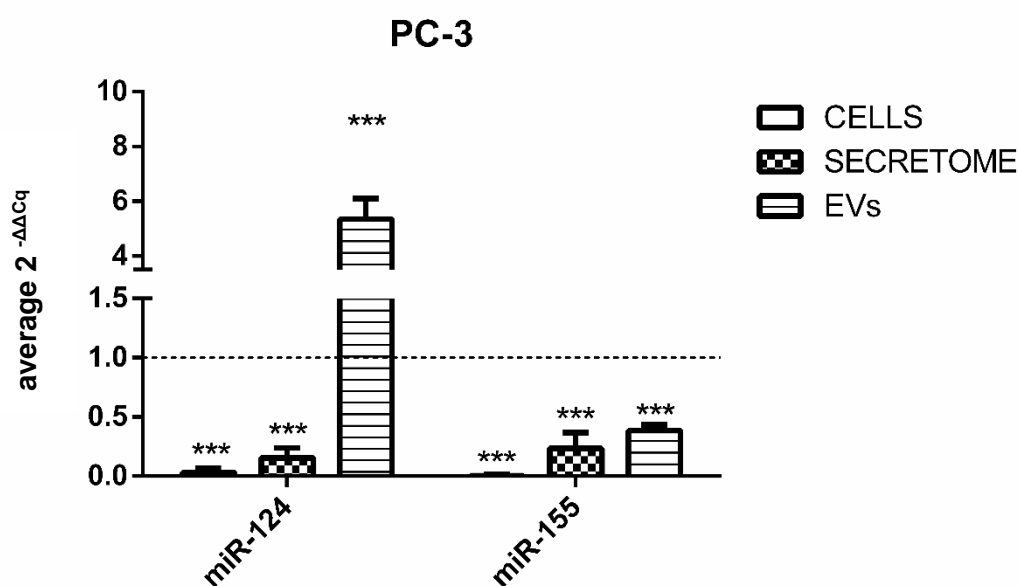
Figure 6. Relative expression of miRNAs in PC-3 cells, secretome and derived EVs incubated with DMSO *versus* PNT-2 cells. Discontinue line marks equivalent expression level to PNT-2. *** (p< 0.001). ** (p<0.01). * (p<0.05).

2.4. Effects of TMZ and 1D treatments on miR-155 *and* miR-124 *levels in PC-3 and PNT-2 cell lines*

In order to evaluate the effects of TMZ or 1D treatments in the EVs miRNA cargo, we also measured relative miRNA levels through RT-qPCR after incubating the cells 48 hours with 5 µM TMZ or 5 µM 1D. The concentration of compound was selected choosing the minimal amount of drug causing and impact in cell viability (Figure 2). The graphs in Figure 7 represent the relative expression of the selected miRNAs in reference to levels obtained in control DMSO-vehicle treated cells.
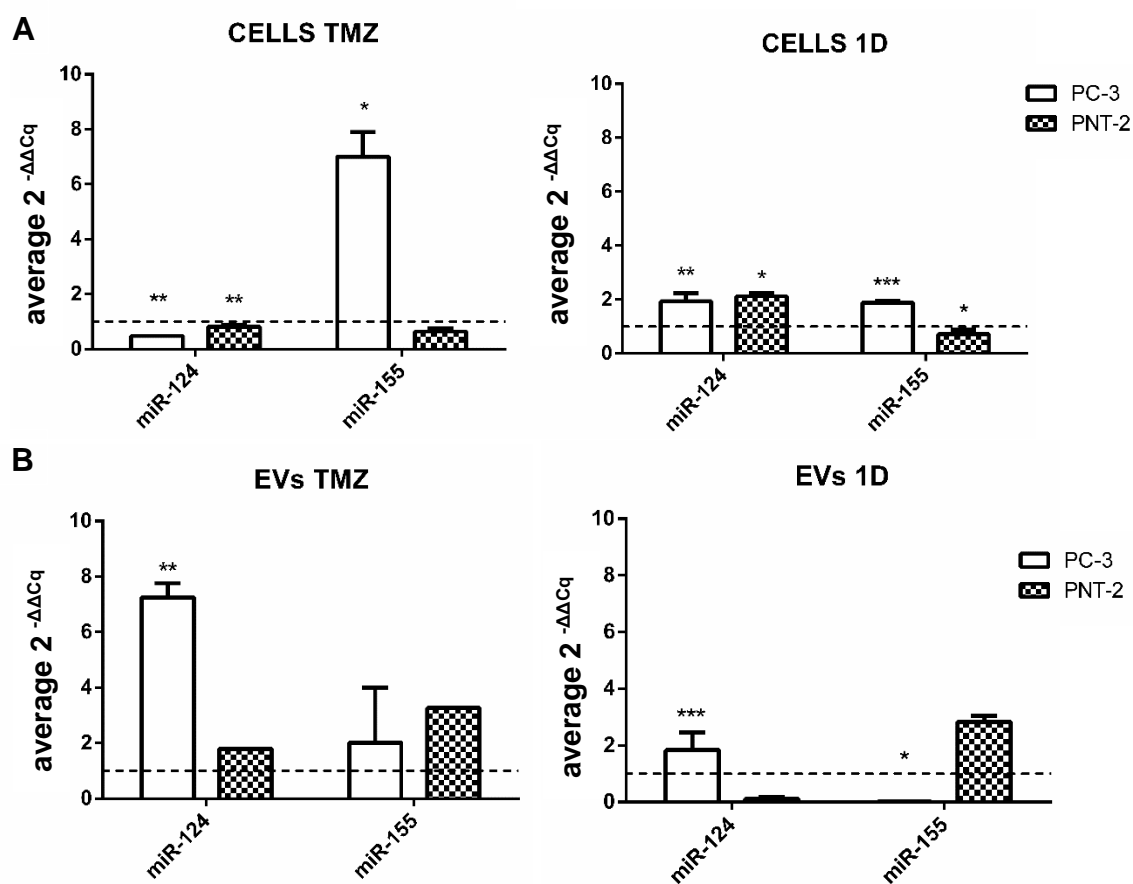
Figure 7. Relative quantity of miRNAs in cells and in EVs produced by the tumoral, PC-3, and non-tumoral, PNT-2, cell lines treated with Temozolomide (TMZ) or 1D, against the non-treated control. Discontinue line marks equivalent expression level to DMSO control. *** (p< 0.001). ** (p<0.01). * (p<0.05).

We first analyzed the effect of TMZ and 1D on both cell lines. We observed in PNT-2 only 1D triggered miR-124 upregulation with a fold increase of 2.13 but with low statistical significance (p<0.05). The effects were more notorious in PC-3: under TMZ treatment miR-124 expression underwent a fold decreased of 2.08 with a significance of p<0.01, while provoking an increase with a change fold of 7 and a statistical

significance of p<0.05 in miR-155 expression. Nevertheless, 1D increased both miRNAs (miR-124 and -155). The expression of miR-124 increased with a fold change of 1.94 and a statistical significance of p<0.01, while miR-155 expression was also up-regulated with a fold change of 1.88 and a significance value of p<0.001.

Analysing the efect of these compounds in EVs miRNA content (Figure 7B), a significant increase in miR-124 expression was observed in EVs derived from PC-3 cells after being treated with TMZ or 1D, while miR-155 levels were significantly downregulated in EVs derived from PC-3 cells treated with 1D. Comparing Figure 7A with Figure 7B it is possible to see that in most cases an increase in cellular expression is accompanied by a decrease in EVs expression and viceversa. Previous studies have reported this negative correlation between EVs and donor cell cytoplasm miRNA content, denoting an active RNA incorporation into the EVs[55].

2.5. Detection of HMGB1*,* HMGB2*,* NOP53 *and* MIEN1 *proteins inside PNT-2 and PC-3 EVs*

In order to confirm the presence of HMGB1, HMGB2, NOP53 and MIEN1 proteins inside the micro-vesicles isolated, Dot blot and Western blot assays were performed.

2.5.1. Dot blot assay

The Dot blot assay verified the presence of HMGB1, HMGB2, NOP53 and MIEN1 inside the EVs, while the presence of the exosome markers FLOTILLIN-1 and CD63[56] were included as a positive control of EVs isolation (Figure 8).
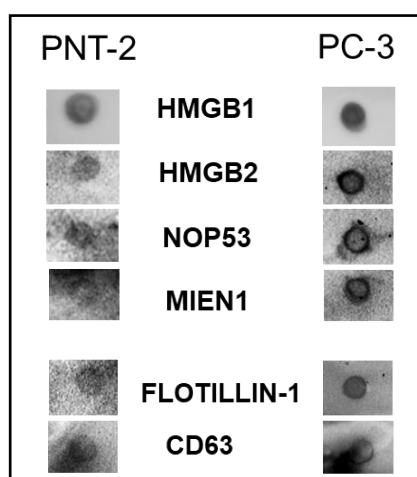
Figure 8. Dot blot from EVs lysate derived from PNT-2 and PC-3 cell lines. The EVs lysate derived from the different cell lines was added to a PDVF membrane. The antibodies used were against HMGB1, HMGB2, NOP53, MIEN1, and FLOTILLIN-1.

2.5.2. Western blot assay

Although HMGB1, HMGB2, MIEN1 and NOP53 were all identified in EVs isolated from PNT-2 and PC-3 cells in the dot blot assay, not all of them could be confirmed in all the conditions through western blot. In a first attempt to evaluate protein expression in EVs after treatments with TMZ and 1D, we isolated proteins from the samples at the same concentration at which they were measured in the NTA. The same quantity of EVs protein lysate was loaded in the 10% SDS-PAGE, and the antibodies against FLOTILLIN-1 and our candidate protein with higher relevance reported in prostate cancer, HMGB1[22,57], were used (Figure 9) in order to detect these proteins inside the EVs.
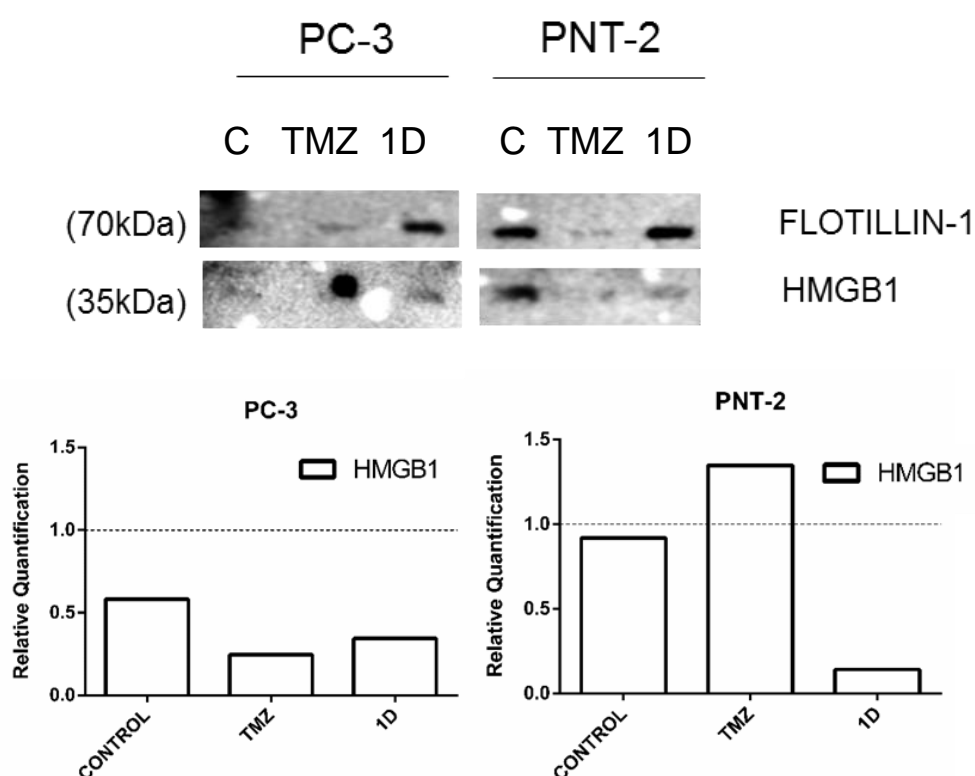
Figure 9. Western Blot and band relative quantification from EVs lysate produced by PC-3 and PNT-2 in conditions of non-treatment (Control DMSO, C), treatment with Temozolomide (TMZ) and treatment with the hybrid compound 1D. Discontinue line marks equivalent expression level to FLOTILLIN-1.

The FLOTILLIN-1 protein levels were not constant in the different conditions, suggesting a different EV concentration in each lysate. In order to analyse differences in EV cargo sorting, the western blot bands were quantified and HMGB1's bands were normalized against FLOTILLIN-1's. HMGB1 protein levels diminished in PC-3 EV lysate after treatment with TMZ oppositely to its upregulation under the same

conditions in PNT-2 EV lysate. Nevertheless, 1D treatment decreased HMGB1 EVs content in both cell lines (Figure 9).
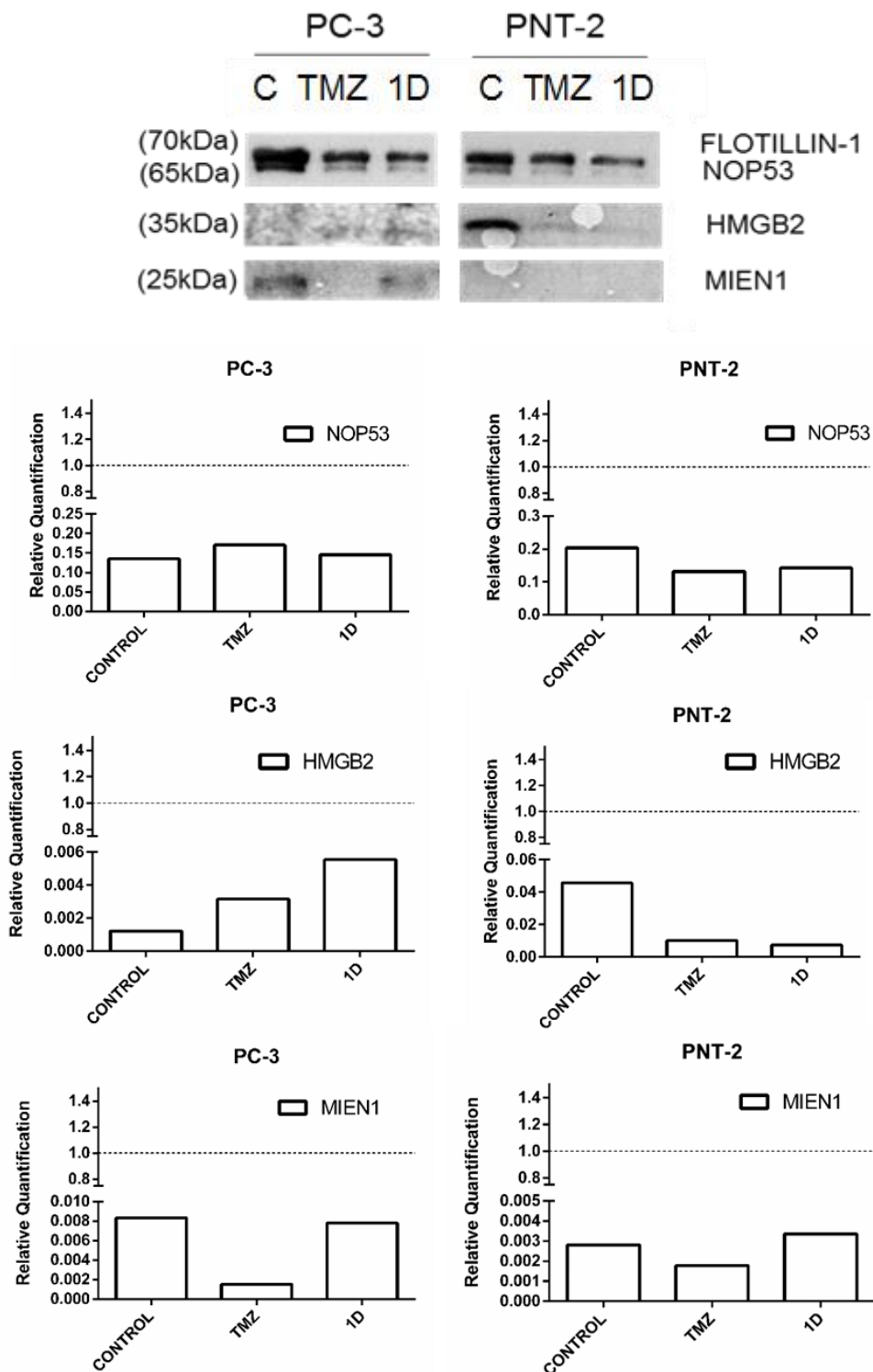
Figure 10. Western Blot and band relative quantification from concentrated EVs lysate produced by PC-3 and PNT-2 in conditions of non-treatment (Control DMSO, C), treatment with Temozolomide (TMZ) and treatment with the hybrid compound 1D. Discontinue line marks equivalent expression level to FLOTILLIN-1.

Samples were then concentrated with a speed vacuum centrifuge and quantified by western blot in order to identify HMGB2, NOP53 and MIEN1 in the EV lysates. NOP53 was identified in both PC-3 and PNT-2 derived EVs, MIEN1 only in PC-3 EVs, and HMGB2 (Figure 10) was scarcely detected in PC-3 derived EVs. The incubation of cells with 5µM TMZ or 1D diminished the intensities of the bands, when detected (Figures 9 and 10).

3. Discussion

Recent progress in EVs research have reported different types of EVs within the same size range (40-200 nm) but with high diversity concerning EVs biogenesis, cargo sorting, release pathways, targeting mechanisms, and vesicle processing[58]. The treatment of glioblastoma cells with TMZ have been described to affect biological processes that are involved in EVs active miRNAs incorporation, and the packaging of proteins related with cellular adhesion[24,58]. Although the effect of TMZ in prostate cancer has been previously studied[26–28] the effect of 1D had not been previously explored in this type of cancer, neither the possible effect of TMZ or 1D on the production and content of EVs derived from cancerous and non-cancerous prostate cell lines. We first analyzed the chemotherapeutic advantages that 1D treatment provides in comparison with the well described TMZ in PNT-2 and PC-3 cells. As shown in Figure 2, a significant cytotoxic effect was detected at 5 µM 1D while the concentrations of TMZ necessary to produce similar effects and cause variations in vesicle sorting[58] in these cells are much higher (40-200µM). This is a valuable result since opens the opportunity to explore 1D as a new drug useful in the chemotherapy of prostate cancer, once their effect and safety could be confirmed in animal models and clinical trials.

The "cell competition cycle" postulates that exosomes produced by cancerous and noncancerous cells compete in the liberation of miRNAs with antagonistic effects[59]. Following this mechanism, cancer cells would release pro-tumoural miRNAs through exosomes to the microenvironment in order to create an oncogenic niche, while normal cells would compete sorting anti-tumoural miRNAs inside their exosomes to restore the healthy phenotype[59]. In this work we have also analyzed the presence of miRNAs (miR-124, miR-146a and miR-155) in PNT-2 and PC-3 cells, culture media (secretome) and EVs derived from these cells. No significant changes were found for miR-146a (data not shown). The miRNA miR-124 has been well characterized as tumour suppressor[14,54], being considered as a potential treatment agent[60] whose

inactivation by methylation has been contemplated as a promising biomarker of cancer aggressiveness[18,61]. Therefore, according to the results obtained through RT-qPCR in our study (Figure 7), the downregulation of miR-124 observed in PC-3 cells and PC-3 derived secretome, in reference to those observed in PNT-2, matches the expectable phenotype; when comparing a cancerous *versus* a non-cancerous model we could predict, as confirmed, downregulation of cancer suppressor mechanisms in PC-3 cells[14]. Simultaneously, the increased levels of miR-124 inside the EVs produced by PC-3, in comparison with those produced by PNT-2 cells, denote an active incorporation of this miRNA as EVs cargo by the tumoural prostate cell line that has not been reported before. It has been described that RNA levels incorporated to EV usually differs from their donor cell cytoplasm[55,62] as a consequence of the active packaging. The exact mechanism through which the mentioned active packaging takes place remains to be elucidated but recent studies discussed different pathways that involve the mediation of RNA binding proteins such as sumoylated hnRNPA1 to recognize GAGAG specific sequences in the 3′ extreme of miRNA and promotes its sorting into EVs[55]. Whether this increase of miR-124 in EVs cargo is a mechanism to maintain low cellular levels and whether delivery of the cargo to other cells could produce cellular signaling and subsequent alteration in normal cells remains to be elucidated. On the other hand, the miRNA miR-155 has been described as pro-oncogenic and is involved in prostate cancer development[9,11,51], but unexpectedly, we observed downregulation of miR-155 in PC-3 cells, PC-3 derived secretome and EVs released by PC-3 when comparing with equivalent samples obtained from PNT-2 (Figure 7). Perhaps this divergence could be explained because some miRNAs have dual functions[58]. For instance, miR-940, is a pro-oncogenic miRNA[7] secreted by PC-3 exosomes, but it performs antitumoral functions in bone[34,63] and colorectal tissues[64].

Regarding to the alterations in miRNA EVs cargo caused by TMZ and 1D treatment, both increment the content of the anti-oncogenic miR-124 in PC-3 cells, while only 1D diminishes the content of the pro-oncogenic miR-155 in PC-3 cells. In this sense, treatment of PCa with 1D would be advantageous over TMZ treatment, but more experiments would be needed in order to clarify if 1D indeed restores healthy secretory phenotype in addition to induce tumour cell death.

It has been shown in chapter 1 that HMGB1, HMGB2, MIEN1 and NOP53 are dysregulated in prostate cancer and therefore we were also interested in knowing whether the corresponding encoded proteins are incorporated in PNT-2 and PC-3 derived EVs. Dot blot approach suggested the presence of all four proteins inside the EVs derived from PC-3 and PNT-2 cells (Figure 8), however HMGB2 was poorly

detected in PC-3 and MIEN1 was not detected in PNT-2 by western blot. Comparing with the data showed in Figure 7, the scarce amount of HMGB1/2 detected in EVs derived from PC-3 coincides with miR-124 overexpression. It is possible to speculate that downregulation of AR by miR-124[17,18] affects the signaling routes downstream AR in prostate cancer, including HMGB1 expression.

Once several candidate proteins have been identified inside the EVs, the question about if they were incorporated into the EVs in an active or passive manner remains to be answered. The presence of a plasmatic membrane protein such as MIEN1 inside EVs could be explained by passive incorporation, as well as the detection of the nuclear and nucleolar proteins HMGB1, HMGB2 and NOP53 inside the EVs could be also a consequence of a passive packaging due to their well described translocation from nucleus to cytoplasm under stressed conditions or cancer[65–68]. Indeed, NOP53 has been reported to be highly expressed in the cytoplasm of prostate adenocarcinoma cells[69]. Nevertheless, the active sorting of these proteins into the EVs is also a possibility to be considered and analyzed in the future since EVs derived from tumoural cells have been described to actively incorporate oncogenic factors[59] or RNA binding proteins along with miRNAs[55]. Our candidate proteins match this description due to their abilities to interact with RNA molecules[55], as in the case of HMGB1 and HMGB2[70]; modulate cell cycle, like NOP53, by p53 inhibition; or promote cell invasion and proliferation like MIEN1[71]. Besides, it has been reported that MIEN1 expression in PC-3 is downregulated by the overexpressed miR-940[63], and for this reason, it is not expectable to detect high levels of MIEN1 passively incorporated into de EVs when its intracellular levels are so low. On the contrary, in these circumstances, the detection of significant levels of MIEN1 into PC-3 derived EVs could imply an active incorporation of MIEN1 into them.

Regarding to the treatment effect on the EVs protein cargo it is observed that both treatments contribute to diminish protein levels, with the exception of HMGB1 in EV lysate from PNT-2 incubated with TMZ. It is interesting to compare the upregulation of miR-124 in PC-3 derived EVs under TMZ treatment with MIEN1 protein downregulation in the same conditions (Figure 10). An explanation of this observation could be that MIEN1 resulted indirectly downregulated by miR-124, because miR-124 suppresses cell motility in prostate cell lines by directly targeting the cytoskeletal protein TALIN1[54], involved in focal adhesion formation and downregulation of (FAK)/AKT pathway[72], and besides it has been also reported a direct interaction of MIEN1 with AKT[71] and FAK[73,74]. Furthermore, HMGB1 is other indirect target of miR-124[18,20,22,75] and it shows a similar pattern to MIEN1, decreasing its expression in EV

lysate from PC-3 under TMZ treatment, when miR-124 detected expression levels through RT-qPCR were higher (Figure 7B). Interestingly, HMGB2 protein levels were barely detected through western blot in EV lysate from PC-3, while its protein level in the PNT-2 control was significant, showing an important decrease under incubation with both treatments, while NOP53 seemed to maintain the same protein levels in all the different conditions (Figure 10). Also interesting, NOP53 mediates PTEN phosphorylation inactivating the AKT pathway[76,77] upstream of miR-124 targets, therefore the possible consequences of miR-124 dysregulation would not be reflected on NOP53 expression. On the other hand, a possible explanation for NOP53 slight downregulation in EV lysate from PNT-2 under TMZ or 1D treatments could be its important role in DNA damage response[78] being recruited outside the nucleolus and their proteins levels downregulated as a consequence of DNA modifications, such as the alkylation provoked by TMZ and 1D[25]. We can conclude that treatment with 1D is more effective than TMZ in causing PC-3 cell death. EVs derived from prostate cell lines PC-3 and PNT-2 carry HMGB1, HMGB2, MIEN1, NOP53 proteins and regulatory miRNAs related to them. Treatment with TMZ or 1D affects the size and concentration of EVs produced by prostate cell lines and also to their content in the selected biomolecules.

References

1.   Deep, G. *et al.* Exosomes secreted by prostate cancer cells under hypoxia promote matrix metalloproteinases activity at pre-metastatic niches. *Mol. Carcinog.* **59**, 323–332 (2020).

2.   Wang, J. *et al.* Exosomal microRNAs as liquid biopsy biomarkers in prostate cancer. *Crit. Rev. Oncol. Hematol.* **145**, 1–44 (2020).

3.   Mashouri, L. *et al.* Exosomes: Composition, biogenesis, and mechanisms in cancer metastasis and drug resistance. *Mol. Cancer* **18**, 1–14 (2019).

4.   Gurunathan, S., Kang, M., Jeyaraj, M., Qasim, M. & Kim, J. Review of the Isolation, Characterization, Biological Function, and Multifarious Therapeutic Approaches of Exosomes. *Cells* **8**, 1–36 (2019).

5.   Saber, S. H. *et al.* Exosomes are the Driving Force in Preparing the Soil for the Metastatic Seeds: Lessons from the Prostate Cancer. *Cells* **9**, 1–26 (2020).

6.   Jiang, K., Dong, C. & Wang, L. The critical role of exosomes in tumor biology. *J. Cell. Biochem.* **120**, 1–13 (2018).

7.   Feng, W., Dean, D. C., Hornicek, F. J., Shi, H. & Duan, Z. Exosomes promote pre-metastatic niche formation in ovarian cancer. *Mol. Cancer* **18**, 1–11 (2019).

8.   Sánchez, C. A. *et al.* Exosomes from bulk and stem cells from human prostate cancer have a differential microRNA content that contributes cooperatively over local and pre-metastatic niche. *Oncotarget* **7**, 3993–4008 (2016).

9.   Luu, H. N. *et al.* miRNAs associated with prostate cancer risk and progression. *BMC Urol.* **17**, 1–18 (2017).

10.   Kopcalic, K., Petrovic, N., Stanojkovic, T. P. & Stankovic, V. Association between miR-21 / 146a / 155 level changes and acute genitourinary radiotoxicity in prostate cancer patients : A pilot study. *Pathol. - Res. Pract.* **215**, 626–631 (2019).

11.   Cai, Z.-K. *et al.* microRNA-155 promotes the proliferation of prostate cancer cells by targeting annexin 7. *Mol. Med. Rep.* **11**, 533–538 (2015).

12.   Lin, S., Chiang, A., Chang, D. & Ying, S. Loss of mir-146a function in hormone-refractory prostate cancer. *RNA* **14**, 417–424 (2008).

13. Huang, Y. *et al.* Upregulation of miR-146a by YY1 depletion correlates with delayed progression of prostate cancer. *Int. J. Oncol.* **50**, 421–431 (2017).

14. Wu, Z. *et al.* Up-regulation of miR-124 inhibits invasion and proliferation of prostate cancer cells through mediating JAK-STAT3 signaling pathway. *Eur. Rev. Med. Pharmacol. Sci.* **21**, 2338–2345 (2017).

15. Shotorbani, S. S. *et al.* Association of Toll-like Receptors and High-mobility Group Proteins with MicroRNAs in Melanoma. **10**, 1–5 (2017).

16. Shi, X. *et al.* miR-124 and Androgen Receptor Signaling Inhibitors Repress Prostate Cancer Growth by Downregulating Androgen Receptor Splice. *Cancer Res.* **75**, 5309–5318 (2015).

17. Fernandes, R. C., Fernandes, R. C., Hickey, T. E., Tilley, W. D. & Selth, L. A. Interplay between the androgen receptor signaling axis and microRNAs in prostate cancer. *Endocr. Relat. Cancer* **26**, R237–R257 (2019).

18. Chu, M., Chang, Y., Guo, Y., Wang, N. & Cui, J. Regulation and Methylation of Tumor Suppressor MiR-124 by Androgen Receptor in Prostate Cancer Cells. *PLoS One* **1**, 1–11 (2015).

19. Verrijdt, G., Haelens, A., Schoenmakers, E., Rombauts, W. & Claessens, F. Comparative analysis of the influence of the high-mobility group box 1 protein on DNA binding and transcriptional activation by the androgen, glucocorticoid, progesterone and mineralocorticoid receptors. *Biochem. Soc.* **103**, 97–103 (2002).

20. Takayama, K. & Inoue, S. Transcriptional network of androgen receptor in prostate cancer progression. *Iternational J. Urol.* **20**, 756–768 (2013).

21. Boonyaratanakornkit, V. *et al.* High-mobility group chromatin proteins 1 and 2 functionally interact with steroid hormone receptors to enhance their DNA binding in vitro and transcriptional activity in mammalian cells. *Mol. Cell. Biol.* **18**, 4471–4487 (1998).

22. Gnanasekar, M. *et al.* HMGB1: A Promising Therapeutic Target for Prostate Cancer. *Prostate Cancer* **2013**, 1–8 (2013).

23. Srinivasan, M. *et al.* HMGB1 in hormone-related cancer: a potential therapeutic target. *Horm. Cancer* **5**, 127–139 (2014).

24. André-Grégoire, G., Bidère, N. & Gavard, J. Temozolomide affects Extracellular

Vesicles Released by Glioblastoma Cells. *Biochimie* **155**, 11–15 (2018).

25.   Pinheiro, R. *et al.* Targeting Gliomas: Can a New Alkylating Hybrid Compound Make a Difference? *ACS Chem. Neurosci.* **8**, 50–59 (2017).

26.   Van Brussel, J. P. *et al.* A phase II study of temozolomide in hormone-refractory prostate cancer. *Cancer Chemother. Pharmacol.* **45**, 509–512 (2000).

27.   Hussain, M. *et al.* Targeting DNA repair with combination veliparib (ABT-888) and temozolomide in patients with metastatic castration-resistant prostate cancer Maha. *Invest. New Drugs* **32**, 904–912 (2015).

28.   Palma, J. P. *et al.* ABT-888 confers broad in vivo activity in combination with temozolomide in diverse tumors. *Clin. Cancer Res.* **15**, 7277–7290 (2009).

29.   Braga, C. *et al.* Targeting gliomas with triazene-based hybrids: Structure-activity relationship, mechanistic study and stability. *Eur. J. Med. Chem.* **172**, 16–25 (2019).

30.   Moody, C. L. & Wheelhouse, R. T. The medicinal chemistry of imidazotetrazine prodrugs. *Pharmaceuticals* **7**, 797–838 (2014).

31.   Syed, N. *et al.* Silencing of high-mobility group box 2 (HMGB2) modulates cisplatin and 5-fluorouracil sensitivity in head and neck squamous cell carcinoma. *Proteomics* **15**, 383–393 (2015).

32.   Shu, W. Downregulation of high mobility group protein box-1 resensitizes ovarian cancer cells to carboplatin. *Oncol. Lett.* **16**, 4586–4592 (2018).

33.   Lázaro-Ibáñez, E. *et al.* Metastatic state of parent cells influences the uptake and functionality of prostate cancer cell-derived extracellular vesicles. *J. Extracell. Vesicles* **6**, 1–12 (2017).

34.   Duan, Y. *et al.* PC-3-Derived Exosomes Inhibit Osteoclast Differentiation by Downregulating miR-214 and Blocking NF-B Signaling Pathway. *Biomed Res. Int.* **2019**, 1–8 (2019).

35.   Kaighn, M. E., Narayan, K. S., Ohnuki, Y., Lechner, J. F. & Jones, L. W. Establishment and characterization of a human prostatic carcinoma cell line (PC-3). *Invest. Urol.* **17**, 16–23 (1979).

36.   QIAGEN.   QIAzol   Lysis   Reagent   . https://www.qiagen.com/us/products/discovery-and-translational-research/lab-

essentials/buffers-reagents/qiazol-lysis-reagent/?clear=true#orderinginformation (2020).

37. Caldeira, C. *et al.* Key aging-associated alterations in primary microglia response to beta-amyloid stimulation. *Front. Aging Neurosci.* **9**, 1–23 (2017).

38. Livak, K. J. & Schmittgen, T. D. Analysis of relative gene expression data using real-time quantitative PCR and the 2(-Delta Delta C(T)) Method. *Methods* **25**, 402–408 (2001).

39. Luo, P. *et al.* HMGB1 represses the anti-cancer activity of sunitinib by governing TP53 autophagic degradation via its nucleus-to-cytoplasm transport. *Autophagy* **14**, 2155–2170 (2018).

40. Wu, Z. B. *et al.* High-mobility group box 2 is associated with prognosis of glioblastoma by promoting cell viability, invasion, and chemotherapeutic resistance. *Neuro. Oncol.* **15**, 1264–1275 (2013).

41. Kim, H. K. *et al.* Transcriptional repression of high-mobility group box 2 by p21 in radiation-induced senescence. *Mol. Cells* **41**, 362–372 (2018).

42. Leung, T. H. Y. *et al.* The interaction between C35 and Δnp73 promotes chemo-resistance in ovarian cancer cells. *Br. J. Cancer* **109**, 965–975 (2013).

43. Ikuzono, T. O. J. *et al.* Delta Np73 expression in thyroid neoplasms originating from follicular cells. *Anat. Pathol.* **38**, 205–209 (2006).

44. Sasaki, M. *et al.* Regulation of the MDM2-P53 pathway and tumor growth by PICT1 via nucleolar RPL11. *Nat. Med.* **17**, 944–951 (2011).

45. Forte, I. M. *et al.* Targeted therapy based on p53 reactivation reduces both glioblastoma cell growth and resistance to temozolomide. *Int. J. Oncol.* **54**, 2189–2199 (2019).

46. Yi, G. Z. *et al.* Identification of Key Candidate Proteins and Pathways Associated with Temozolomide Resistance in Glioblastoma Based on Subcellular Proteomics and Bioinformatical Analysis. *Biomed Res. Int.* **2018**, 1–12 (2018).

47. Barreiro-Alonso, A. *et al.* Characterization of HMGB1/2 Interactome in Prostate Cancer by Yeast Two Hybrid Approach: Potential Pathobiological Implications. *Cancers (Basel).* **11**, 1–21 (2019).

48. Pinto, S., Cunha, C., Barbosa, M., Vaz, A. R. & Brites, D. Exosomes from NSC-

34 cells transfected with hSOD1-G93A are enriched in mir-124 and drive alterations in microglia phenotype. *Front. Neurosci.* **11**, 1–21 (2017).

49. Jung, M. K. & Mun, J. Y. Sample Preparation and Imaging of Exosomes by Transmission Electron Microscopy. *J. Vis. Exp.* **131**, 1–5 (2018).

50. Malla, B., Zaugg, K., Vassella, E., Aebersold, D. M. & Dal Pra, A. Exosomes and Exosomal MicroRNAs in Prostate Cancer Radiation Therapy. *Int. J. Radiat. Oncol. Biol. Phys.* **98**, 982–995 (2017).

51. Filella, X. & Foj, L. miRNAs as novel biomarkers in the management of prostate cancer. *Clin. Chem. Lab. Med.* **55**, 715–736 (2017).

52. Bhagirath, D., Dahiya, R., Majid, S., Tabatabai, Z. L. & Saini, S. Sequencing Small Non-coding RNA from Formalin-fixed Tissues and Serum-derived Exosomes from Castration-resistant Prostate Cancer Patients. *J. Vis. Exp.* **153**, 1–9 (2019).

53. Liu, K. *et al.* MIR34A regulates autophagy and apoptosis by targeting HMGB1 in the retinoblastoma cell. *Autophagy* **10**, 442–452 (2014).

54. Zhang, W. *et al.* MiR-124 suppresses cell motility and adhesion by targeting talin 1 in prostate cancer cells. *Cancer Cell Int.* **15**, 1–9 (2015).

55. Anand, S., Samuel, M., Kumar, S. & Mathivanan, S. Ticket to a bubble ride: Cargo sorting into exosomes and extracellular vesicles. *Biochim. Biophys. Acta - Proteins Proteomics* **1867**, 1–10 (2019).

56. Deng, F. & Miller, J. A review on protein markers of exosome from different bio-resources and the antibodies used for characterization. *J. Histotechnol.* **42**, 226–239 (2019).

57. Zhao, C. B. *et al.* Co-expression of RAGE and HMGB1 is associated with cancer progression and poor patient outcome of prostate cancer. *Am. J. Cancer Res.* **4**, 369–377 (2014).

58. Panzarini, E. *et al.* Molecular Characterization of Temozolomide-Treated and Non Temozolomide-Treated Glioblastoma Cells Released Extracellular Vesicles and Their Role in the Macrophage Response. *Int. J. Mol. Sci.* **21**, 1–18 (2020).

59. Kosaka, N. *et al.* Competitive interactions of cancer cells and normal cells via secretory microRNAs. *J. Biol. Chem.* **287**, 1397–1405 (2012).

60. Lang, F. M. *et al.* Mesenchymal stem cells as natural biofactories for exosomes carrying miR-124a in the treatment of gliomas. *Neuro. Oncol.* **20**, 380–390 (2018).

61. Oltra, S. S. *et al.* Methylation deregulation of miRNA promoters identifies miR124-2 as a survival biomarker in Breast Cancer in very young women. *Sci. Rep.* **8**, 1–12 (2018).

62. Baglio, S. R. *et al.* Human bone marrow- and adipose- mesenchymal stem cells secrete exosomes enriched in distinctive miRNA and tRNA species. *Stem Cell Res. Ther.* **6**, 1–20 (2015).

63. Rajendiran, S. *et al.* microRNA-940 suppresses prostate cancer migration and invasion by regulating MIEN1. *Mol. Cancer* **13**, 1–15 (2014).

64. Wang, Y. *et al.* MicroRNA-940 restricts the expression of metastasis-associated gene MACC1 and enhances the antitumor effect of Anlotinib on colorectal cancer. *Onco. Targets. Ther.* **12**, 2809–2822 (2019).

65. Defense, H. *et al.* Cytoplasmic Translocation of Nucleolar Protein NOP53 Promotes Viral Replication by Suppressing. *Viruses* **10**, 1–16 (2018).

66. Ellerman, J. E. *et al.* Masquerader: high mobility group box-1 and cancer. *Clin. Cancer Res.* **13**, 2836–2848 (2007).

67. Tang, D. *et al.* Endogenous HMGB1 regulates autophagy. *J. Cell Biol.* **190**, 881–892 (2010).

68. Fan, Z., Beresford, P. J., Zhang, D. & Lieberman, J. HMG2 interacts with the nucleosome assembly protein SET and is a target of the cytotoxic T-lymphocyte protease granzyme A. *Mol. Cell. Biol.* **22**, 2810–2820 (2002).

69. Kim, J. Y. *et al.* Down-regulation and aberrant cytoplasmic expression of GLTSCR2 in prostatic adenocarcinomas. *Cancer Lett.* **340**, 134–140 (2013).

70. Yanai, H. *et al.* HMGB proteins function as universal sentinels for nucleic-acid-mediated innate immune responses. *Nature* **462**, 99–103 (2009).

71. Dasgupta, S. *et al.* Novel gene C17orf37 in 17q12 amplicon promotes migration and invasion of prostate cancer cells. *Oncogene* **28**, 2860–2872 (2009).

72. Jin, H. *et al.* miR-124 Inhibits Lung Tumorigenesis Induced by K-ras Mutation and NNK. *Mol. Ther. Nucleic Acid* **9**, 145–154 (2017).

73. Kpetemey, M. *et al.* MIEN1 drives breast tumor cell migration by regulating cytoskeletal-focal adhesion dynamics. *Oncotarget* **7**, 54913–54924 (2016).

74. Kushwaha, P. P., Gupta, S., Singh, A. K. & Kumar, S. Emerging Role of Migration and Invasion Enhancer 1 (MIEN1) in Cancer Progression and Metastasis. *Front. Oncol.* **9**, 1–13 (2019).

75. Elangovan, I. *et al.* Targeting receptor for advanced glycation end products (RAGE) expression induces apoptosis and inhibits prostate tumor growth. *Biochem. Biophys. Res. Commun.* **417**, 1133–1138 (2012).

76. Okahara, F. *et al.* Critical role of PICT-1, a tumor suppressor candidate, in phosphatidylinositol 3,4,5-trisphosphate signals and tumorigenic transformation. *Mol. Biol. Cell* **17**, 4888–4895 (2006).

77. Okumura, K., Zhao, M., DePinho, R. A., Furnari, F. B. & Cavenee, W. K. PTEN: A novel anti-oncogenic function independent of phosphatase activity. *Cell Cycle* **4**, 540–542 (2005).

78. Chen, H. *et al.* PICT-1 is a key nucleolar sensor in DNA damage response signaling that regulates apoptosis through the RPL11-MDM2-p53 pathway. *Oncotarget* **7**, 83241–83257 (2016).

Concluding Remarks

Regarding objective 1, to analyze the interactome of HMGB1 and HMGB2 in prostate cancer (PCa) adenocarcinoma, the following conclusions can be drawn:

1.1. A pool of 18 proteins that interact with HMGB1 and 7 that interact with HMGB2 have been identified using the Yeast Two Hybrid System (Y2H) in libraries prepared from a adenocarcinoma primary tumour. The interaction of HMGB2 with MIEN1 and NOP53 has been validated by co-Immunoprecipition using the DU-145 cancer cell line. The function of the identified proteins is directly related to cancer hallmarks and their dysregulation associated with a worse prognosis. Our results therefore show that in PCa there is a correlation between HMGB1 and HMGB2 functions and those of their binding partners detected in this study.

1.2. Silencing of HMGB1 and HMGB2 by siRNA in the PC-3 cancer cell line reveals that HMGB proteins control mRNA levels of several of the targets identified in PCa Y2H approaches, being HMGB1 effects negative and HMGB2 effects positive over common targets such as DLAT, FLNA, MNAT1, MT2A, SNAPIN, UBE2E3 and UHBF2. This result argues in favour of a complex regulatory control of HMGB-interactome in PCa.

Regarding objective 2, to analyse the interactome of HMGB1 and HMGB2 in Epithelial Ovarian Cancer (EOC), the following conclusions can be drawn:

2.1. A pool of 5 proteins that interact with HMGB1 and 6 that interact with HMGB2 have been identified using the Yeast Two Hybrid System (Y2H) in libraries prepared from a tumour diagnosed as primary transitional cell carcinoma (TCC) of the ovary. The interaction of HMGB2 with MIEN1 and NOP53 has been validated by co-immunoprecipitation using the SKOV-3 and PEO-1 cancer cell lines. Identified proteins have been previously associated to ovarian cancer and/or to the Epithelial to Mesenchymal Transition (EMT). Bioinformatic's analysis of public data bases shows that HMGB1, HMGB2, as well as most of their detected interacting partners (91%) are expressed at higher levels in ovarian adenocarcinoma than in normal ovarian tissue, showing a positive functional correlation to EOC.

2.2. Confocal assays performed in PEO-1 cells overexpressing HMGB2 and NOP53 confirm that HMGB2 and NOP53 have bona-fide index of cellular co-localization that is observed in specific areas of nuclei and cytoplasm, confirming the physical interaction of these proteins when both are highly expressed.

Concluding Remarks

2.3. HMGB2 siRNA silencing causes mainly overexpression, whereas HMGB1 silencing has the opposite effect upon mRNA levels of selected proteins among the reported EOC interactome.

2.4. In a second approach, the HMGB2 interactome was also obtained by immunoprecipitation coupled with mass spectrometry (IP-MS) using SKOV-3 cells,and reporting 23 previously unknown HMGB2 interactants. Although identified HMGB2 partners differ in the Y2H and IP-MS results, as expected from differences attributable to cell origin, some resemblance in the function of the proteins detected in each approach can be found. Noticeably, proteins related with RNA binding and proteins related with HMGB2 cytoplasmic functions.

Regarding objective 3, to analyze expression changes of HMGB1, HMGB2 a MIEN1 and NOP53, in response to various chemotherapeutic drugs in EOC and PCa, the following conclusions can be drawn:

3.1. In cancerous ovarian SKOV-3 cells HMGB1, HMGB2, and MIEN1 are downregulated after treatment with paclitaxel, carboplatin or a combination of both and silencing of HMGB1 or HMGB2 increase cell viability of treated cells. Bevacizumab produces a significant downregulation in HMGB2 and NOP53 expression levels. Oppositely, olaparib has no effects in their mRNA levels.

3.2. In cancerous prostatic PC-3 cells, paclitaxel treatment does not affect the expression of these targets. Bevacizumab causes downregulation of HMGB2 and NOP53. Olaparib diminishes MIEN1 and NOP53 expression.

Regarding objective 4, to analyze the presence of HMGB1, HMGB2, MIEN1 and NOP53 and related miRNAs in exosomes derived from prostate PNT2 and PC-3 cell lines and the effects of Temozolomide (TMZ) and its derivative 1D, the following conclusions can be drawn:

4.1. Treatment with 1D is more effective than TMZ in causing PC-3 cell death.

4.2. In general selected proteins (HMGB1, HMGB2, MIEN1, NOP53) and regulatory miRNAs related to them (miR-124, miR-146a and miR-155) are detected in extracellular vesicles produced from prostate cell lines PC-3 and PNT-2. However

HMGB2 was poorly detected in PC-3 and MIEN1 was not detected in PNT-2 by Western blot. Levels of miR-146a were also very low in both cell lines.

4.3. Treatment with TMZ or 1D affects the size and concentration of EVs produced by prostate cell lines and also to their cargos. Both treatments contribute to diminish the levels of the selected proteins, with the exception of HMGB1 in EV lysate from PNT-2 incubated with TMZ. TMZ and 1D increment the content of the anti-oncogenic miR-124 in PC-3 cells, while only 1D diminishes the content of the pro-oncogenic miR-155 in PC-3 cells.

Appendix

Resumen

Introducción

La familia de proteínas HMGB (*High Mobility Group Box*) se definen como proteínas cromosómicas debido a que desempeñan funciones importantes en la modificación de la cromatina y la unión al ADN. Sin embargo, las proteínas HMGB también participan en otras funciones citoplasmáticas que promueven la autofagia y previenen la apoptosis[1], además de funciones extracelulares relacionadas con las respuestas inmunes, inflamatoria[2] o antimicrobiana[3]. Sus funciones extracelulares dependen de su estado redox, lo que determina su interacción con diferentes receptores celulares en células inmunológicas y no inmunológicas[4]. Se han caracterizado cuatro proteínas HMGB humanas, siendo HMGB1 y HMGB2 las más abundantes y ubicuas[5]. HMGB1 y HMGB2 tienen la capacidad de unirse a regiones del ADN que presentan conformaciones aberrantes (especificidad de estructura) e inducen modificaciones estructurales que promueven la unión de factores de transcripción y/o yuxtaposición de secuencias reguladoras distantes[6].

HMGB1 y HMGB2 tienen alta homología de secuencia (>80%)[5] y están evolutivamente conservadas en vertebrados. Ambas tienen 2 dominios HMG similares que interaccionan con el ADN, y una cola C-terminal larga compuesta por 30 residuos de Glu/Asp en HMGB1 y 22 en HMGB2 que modula la afinidad de unión al ADN y media otras interacciones intermoleculares[7,8]. Estudios previos han relacionado la sobreexpresión de HMGB1 en humanos con el cáncer de ovario[8,9] (CaO), mientras que la expresión de la proteína HMGB2 sufre un incremento en cáncer de próstata (CaP)[10] y en algunos tumores de CaO altamente invasivos[11]. Además, ambas proteínas han sido caracterizadas por su implicación en la resistencia a fármacos utilizados en quimioterapia[12,13]. Varios estudios ya han demostrado la desregulación transcripcional de los genes HMGB1 y HMGB2 en respuesta a agentes quimioterapéuticos en diferentes tipos de procesos tumorales[14–16] incluyendo CaP[17,18] y CaO[11,19,20.]. El silenciamiento de HMGB1 y HMGB2 ha revelado la influencia de ambas proteínas en la proliferación[21–26], invasión[25,27,28] y metástasis[29–31] de células tumorales. Aunque aún no se ha descrito la existencia de una regulación post-transcripcional de HMGB1 y HMGB2 modulada por miARN en CaO y CaP, la interacción bien documentada de algunos miARN, como el miR-124, con ARNms codificantes de proteínas que tienen una interacción con HMGB1 y HMGB2, podría tener una repercusión indirecta sobre su expresión en estos cánceres[32,33].

Sin embargo, a pesar de todos los avances conseguidos en la terapia, la dificultad para obtener un diagnóstico temprano y las resistencias emergentes a los tratamientos ponen de manifiesto la necesidad de búsqueda de nuevas dianas terapéuticas y biomarcadores

aplicables a estos tipos de cáncer. Entre los mecanismos presentes en las células tumorales para evadir la respuesta inmune, resistir el efecto de la quimioterapia y modular la expresión de proteínas en otras células, se encuentra la liberación de vesículas extracelulares (VEs), como exosomas, así como la alteración del contenido transportado en estas VEs, favoreciendo la diseminación de proteínas pro-oncogénicas y miARNs que tienen como diana proteínas anti-tumorales[34]. Aunque hasta la fecha no se han identificado proteínas HMGB dentro de exosomas derivados de CaP o de CaO, se ha detectado la presencia de HMGB1 en exosomas producidos por otros tipos de cánceres como carcinoma hepatocelular, cáncer gástrico, cáncer colorrectal[35], cáncer de cuello uterino[36] o la enfermedad de Alzheimer (EA)[37].

1. Objetivos

Las proteínas HMGB han sido relacionadas con procesos cancerosos entre los que se encuentran el CaP y CaO. Los interactomas asociados a una enfermedad en particular son herramientas valiosas para comprender sus mecanismos moleculares y para redefinir patrones de diagnóstico con biomarcadores específicos[38]. El objetivo general planteado en esta tesis es conocer el interactoma de las proteínas HMGB1 y HMGB2 en células aisladas de tumores de próstata y ovario, a fin de indentificar posibles dianas para el diagnóstico o la terapia y analizar su papel en la respuesta a tratamientos convencionales utilizados en quimioterapia. Para ello nos plantemos los siguientes objetivos

1) Analizar el interactoma de HMGB1 y HMGB2 a partir de células tumorales de próstata obtenidas de un adenocarcinoma primario.
2) Estudiar el interactoma de HMGB1 y HMGB2 a partir de células tumorales de cáncer de ovario obtenidas de biopsia.
3) Evaluar las variaciones de expresión de HMGB1, HMGB2 y dos proteínas seleccionadas del interactoma, MIEN1 y NOP53, en respuesta a diversos tratamientos utilizados en quimioterapia utilizando para ello células tumorales y no tumorales de próstata (PC-3 y PNT-2) y ovario (SKOV-3 y IOSE-80) en cultivo.
4) Analizar la presencia de HMGB1, HMGB2, MIEN1, NOP53 y miARNs relacionados en exosomas derivados líneas celulares de próstata tumorales y no tumorales de células de próstata en cultivo.

2. Metodología

Para analizar el interactoma de las proteínas HMGB1 y HMGB2 se utilizaron aproximaciones experimentales basadas en el doble híbrido. A partir de librerías ADNc preparadas a partir de muestras tumores de ovario y próstata aislados de pacientes, se determinaron nuevas interacciones no descritas previamente mediante el ensayo de Doble Híbrido de Levaduras (*Yeast Two Hybrid System*, Y2H). Su papel en el desarrollo de procesos tumorales y sus funciones concretas fueron contrastadas mediante meta-análisis bioinformático, recopilando información sobre sus niveles de expresión y su asociación a parámetros clínicos de supervivencia en estos tipos de cáncer.

Para validar las interacciones físicas de HMGB1 y HMGB2 observadas por primera vez en este trabajo, se llevaron a cabo ensayos de co-Inmunoprecipitación y localización celular mediante microscopía confocal.

La desregulación en respuesta a fármacos antitumorales convencionales de la expresión de HMGB1, HMGB2 y las interacciones seleccionadas en células tumorales de ovario y próstata, se evaluaron mediante RT-qPCR. Las células SKOV-3, IOSE-80, PC-3 y PNT-2 fueron expuestas a concentraciones de fármacos seleccionadas de acuerdo con estudios previos[39–42]. Se utilizó paclitaxel a 25 µM[39]; carboplatino a 25 µg / mL[40]; olaparib a 2 µM[41]; y bevacizumab a 100 µg / mL[42] durante 48 horas.

Además, se silenciaron mediante siRNA tanto el ARN mensajero de HMGB1 y HMGB2, como el de las proteínas MIEN1 y NOP53, seleccionadas en el ensayo de doble híbrido. El silenciamiento se validó mediante RT-qPCR y *Western blot*, antes de estudiar sus efectos sobre la eficiencia de los fármacos para producir muerte celular mediante el ensayo CCK-8 de viabilidad celular.

Por último, para evaluar la presencia de las proteínas HMGB1, HMGB2, MIEN1 y NOP53 en exosomas derivadas de células tumorales y no tumorales próstata, se llevaron a cabo ultracentrifugaciones seriadas para el aislamiento de las VEs. Su caracterización se llevó a cabo usando diversas técnicas como *Nano Tracking Assay* (NTA), *Transmission Electron Microscopy* (TEM), y *Western blot* para la detección de marcadores proteicos de membrana de exosomas. Tras lisar los exosomas se procedió a estudiar variaciones en su contenido en proteínas utilizando la técnica de *Western blot*, y en miARNs mediante RT-qPCR.

3. Resultados

3.1. Interactomas Y2H de HMGB1 y HMGB2 a partir de un tumor primario adenocarcinoma de CaP humano

El ensayo de doble híbrido de levaduras permitió la identificación de las siguientes proteínas: MAP1B[43,44], NOP53[45–48], RSF1[49–52], SRSF3[53–57],C1QBP[58–62], cFOS[63,64], DLAT[65], FLNA[66,67], GOLM1[68–72], HOXA10[73,74], PSMA7[75,76], PTPN2[77], RASAL2[78–80], SPIN1[81], TGM3[82], UBE2E3[83], Vigilin[84], WNK4[85], COMMD1[86,87], MAPKAPK5[88,89], MNAT1[90], MT2A [91], YY1[92,93], MIEN1[94,95]. Las interacciones de las proteínas identificadas con HMGB1 o HMGB2 no habían sido descritas previamente en BioGRID, String u otras bases de datos públicas de interacciones moleculares. Sin embargo, la capacidad oncogénica de varias proteínas identificadas en nuestro interactoma ya se había identificado en CaP u otros modelos cancerosos mediante una amplia gama de enfoques experimentales. Se pudo confirmar las interacciones de HMGB2 con MIEN1 y NOP53 mediante un ensayo de co-Inmunoprecipitación utilizando la línea celular de próstata tumoral DU-145.

Se analizó la frecuencia de mutaciones y alteraciones en el número de copias (CNA) en los genes HMGB1 y HMGB2, así como en aquellos genes que codifican proteínas del interactoma identificado y que se encuentran recopiladas en bases de datos referidas a CaP. El análisis demostró que las mutaciones y las CNA que afectan a estas proteínas están presentes con mayor frecuencia en cánceres con mayor malignidad y peor pronóstico, como el cáncer neuroendocrino de próstata y el CaP resistente a la castración hormonal. Existe una correlación entre los niveles de expresión de estos genes y periodos de supervivencia libres de enfermedad, con valores p muy significativos en la prueba de Logrank.

Por otra parte, el silenciamiento de HMGB1 y HMGB2 en la línea celular PC-3, llevado a cabo en colaboración con Martín Salamini[96], demostró que el silenciamiento de HMGB1 provoca la sobreexpresión de la mayoría de las proteínas identificadas en el interactoma Y2H de CaP, mientras que silenciar HMGB2 tuvo el efecto opuesto.

3.2. Interactomas HMGB1 y HMGB2 Y2H en tejido tumoral de ovario

En la librería génica preparada a partir de tejido tumoral de ovario, se identificaron 5 genes que codifican las proteínas: C1QA[97], DAG1[98], RPL29[99], RSF1[100–103], y TGM2[104] que interactúan con HMGB1. Mientras que utilizando HMGB2 se identificaron 6 genes que codifican para las proteínas COMMD1[105,106], MIEN1[107], PCBP1[108], TBC1D25[109], ZFR[110] y

ZNF428. Cabe destacar que las proteínas encontradas en este estudio se habían asociado previamente al CaO y/o a la Transición Epitelio–Mesenquima (EMT), típica de las células epiteliales en procesos de diferenciación maligna, aunque no habían sido relacionadas anteriormente a interacciones con proteínas HMGB.

Accediendo a los datos de Expression Atlas[111] del Instituto Europeo de Bioinformática (https://www.ebi.ac.uk) , a 39 muestras del Proyecto GTEx[112], y a datos públicos extraídos de Pan-Cancer Analysis of Whole Genomes (PCAWG) correspondientes a 110 tumores de adenocarcinomas de ovario, se confirmó una desregulación en los niveles de expresión génica de HMGB1, HMGB2 y sus interactuantes[113]. Se observó que se expresan más en adenocarcinoma de ovario que en tejido ovárico normal, siguiendo un patrón de co-regulación con HMGB1 y HMGB2 que es frecuente entre los genes que codifican proteínas que interactúan[114].

La interacción física de HMGB2 con MIEN1 y NOP53 se validó mediante co-inmunoprecipitación partiendo de un lisado de la línea celular SKOV-3. Seguidamente, la interacción HMGB2-NOP53 se confirmó con éxito a través de localización celular realizada en la línea celular PEO-1 con microscopía confocal. El análisis mediante RT-qPCR, del efecto del silenciamiento de HMGB1 y HMGB2 en PEO-1 y SKOV-3 sobre la expresión de los genes de gran parte de las proteínas detectadas en el Y2H, puso de manifiesto una función principalmente represora por parte de HMGB2, contraria al efecto activador de HMGB1.

Para analizar el interactoma de HMGB2 desde otro enfoque, se llevaron a cabo un total de tres ensayos de inmunoprecipitación acoplada con espectrometría de masas (IP-MS) utilizando células SKOV-3, encontrando un total de 23 proteínas no previamente identificadas. Las interacciones encontradas no fueron coincidentes con los resultados de Y2H, pero en ambas aproximaciones se detectaron principalmente proteínas relacionadas con la unión a ARN y con funciones citoplásmicas de HMGB2.

3.3. Efecto de los fármacos anti-tumorales sobre la expresión de los genes HMGB1, HMGB2, MIEN1 y NOP53 en CaO y CaP

Evaluamos el efecto de cuatro compuestos, utilizados en la terapia del CaO y CaP, sobre la expresión de los genes HMGB1, HMGB2, MIEN1 y NOP53 en células SKOV-3, IOSE-80, PC-3 y PNT-2 en cultivo. Las células fueron expuestas a concentraciones de fármaco seleccionadas de acuerdo con estudios previos[39–42]. Se utilizó paclitaxel a 25 μM[39];

carboplatino a 25 µg / mL[40]; olaparib a 2 µM[41]; y bevacizumab a 100 µg / mL[42] durante 48 horas. Cada compuesto seleccionado tiene un mecanismo de acción diferente.

En ovario, se observaron efectos significativos con más frecuencia en células cancerosas que en células no cancerosas. Para los tratamientos con carboplatino o paclitaxel, que se utilizan generalmente en la terapia de primera línea de CaO, los resultados indican que provocan una regulación negativa de los genes que están sobre-expresados en las células tumorales de ovario (HMGB1, HMGB2 y MIEN1). El silenciamiento de HMGB1 o HMGB2 disminuyó la viabilidad de las células SKOV-3 después del tratamiento con carboplatino. Sin embargo, el silenciamiento de HMGB1 aumentó la viabilidad celular después del tratamiento con paclitaxel. La viabilidad celular después del tratamiento con olaparib disminuyó con el silenciamiento de HMGB2. Finalmente, el silenciamiento de NOP53 aumentó la viabilidad celular después del tratamiento con bevacizumab.

Por otro lado, en las líneas celulares de próstata tumoral, PC-3, y no tumoral, PNT-2, observamos una sobreexpresión de HMGB2 bajo tratamiento con olaparib en PNT-2, mientras que en la línea celular tumoral, PC-3, sus niveles de expresión se mantuvieron estables. Además, este fármaco pareció tener efectos similares sobre la expresión de HMGB1, NOP53 y MIEN1, disminuyendo sus niveles de expresión en PC-3 y sólo y en menor grado el nivel de NOP53 en PNT-2.

3.4. Caracterización de VEs producidas por PC-3 y PNT-2 a través de TEM y NTA, y análisis de los efectos de los tratamientos TMZ y 1D sobre su contenido en miARN y proteína.

Teniendo en cuenta estudios previos que evaluaban el efecto de TMZ en células de CaP[115], se analizaron los efectos de TMZ y 1D en células PC-3 y PNT-2 para estudiar diferencias de sensibilidad a estos compuestos. Tanto PC-3 como PNT-2 resultaron ser más vulnerables al tratamiento con 1D que al tratamiento con TMZ.

La concentración de 1D, y TMZ seleccionada para los siguientes experimentos fue de 5 µM por ser la concentración más baja a la que se observaron efectos significativos sobre la viabilidad celular. Se analizaron las diferencias de las VEs producidas, en cuanto a morfología, tamaño y concentración entre las líneas celulares PC-3 y PNT-2 después de incubar estas células con TMZ o 1D. Los resultados obtenidos mediante TEM confirmaron la forma de copa característica que diferencia a los exosomas[116] de otras VEs, la cual no se vio afectada por ninguno de los tratamientos aplicados. Los resultados obtenidos

mediante NTA muestran que el tratamiento con 1D aumenta el número de VEs liberadas por PC-3 en comparación con las células tratadas con vehículo DMSO (control).

Tras el lisado de las VEs, se procedió al análisis de su contenido. La expresión de miR-155 fue significativamente menor en PC-3 que en PNT-2 al analizar células, secretomas o VEs. La expresión de miR-124 en células y secretoma de PC-3 también fue menor que en PNT-2. Sin embargo, al analizar las VEs, la expresión de miR-124 en la línea celular tumoral PC-3 fue 5 veces mayor que en las VEs, derivadas de PNT-2.

Seguidamente, se verificó mediante *Dot blot* la presencia de HMGB1, HMGB2, NOP53 y MIEN1 dentro de las VEs, así como los marcadores de exosomas FLOTILLIN1 y CD63[117]. Los niveles de proteína HMGB1 disminuyeron en el lisado de VEs derivadas de PC-3 tras ser incubadas con TMZ, de manera opuesta, se observó su incremento en las mismas condiciones en el lisado de VEs producidas por PNT-2. El tratamiento 1D disminuyó el contenido de HMGB1 en las VEs de ambas líneas celulares. NOP53 se identificó en las VEs derivadas de PC-3 y PNT-2. MIEN1 solo en las VEs liberadas por PC-3, y escasos niveles de HMGB2 se detectaron en VEs derivadas de PC-3. La incubación de células con TMZ o 1D 5µM disminuyó la intensidad de las bandas de western blot en todos los casos en los que se detectó proteína.

4. Conclusiones

En cuanto al objetivo 1, analizar el interactoma de HMGB1 y HMGB2 en el adenocarcinoma de CaP, se pueden extraer las siguientes conclusiones:

1.1. Se ha identificado un conjunto de 18 proteínas que interactúan con HMGB1 y 7 que interactúan con HMGB2 utilizando la técnica Y2H y partiendo de genotecas preparadas a partir de tumor primario de adenocarcinoma de próstata. La interacción de HMGB2 con MIEN1 y NOP53 ha sido validada por co-inmunoprecipitación utilizando la línea celular de cáncer DU-145. La función de las proteínas identificadas está directamente relacionada con las alteraciones asociadas a cáncer, y su desregulación asociada a un peor pronóstico. Por tanto, nuestros resultados muestran que en CaP existe una correlación entre las funciones de HMGB1 y HMGB2 y las de las proteínas detectadas en este estudio.

1.2. El silenciamiento de HMGB1 y HMGB2 por siARN en la línea celular de cáncer PC-3 revela que las proteínas HMGB controlan los niveles de ARNm de genes que codifican para las proteínas detectadas en el interactoma, siendo los efectos de HMGB1 negativos y los efectos de HMGB2 positivos sobre DLAT, FLNA, MNAT1, MT2A, SNAPIN, UBE2E3

y UHBF2. Este resultado argumenta a favor de un control complejo de la regulación del interactoma de HMGB en el CaP.

Respecto al objetivo 2, analizar el interactoma de HMGB1 y HMGB2 en el CaO epitelial (EOC), se pueden extraer las siguientes conclusiones:

2.1. Se ha identificado un conjunto de 5 proteínas que interactúan con HMGB1 y 6 que interactúan con HMGB2 utilizando el Y2H en genotecas preparadas a partir de un tumor de ovario diagnosticado como carcinoma primario de células de transición (TCC). La interacción de HMGB2 con MIEN1 y NOP53 ha sido validada por co-inmunoprecipitación, utilizando las líneas celulares cancerosas de ovario, SKOV-3 y PEO-1. Las proteínas identificadas se habían asociado previamente al CaO y/o a la transición epitelio mesenquima (EMT). El análisis bioinformático muestra que HMGB1, HMGB2, así como la mayoría de las proteínas que interaccionan con ellas (91%) se expresan en niveles más altos en el adenocarcinoma de ovario que en el tejido ovárico normal, lo que muestra una correlación funcional positiva con EOC.

2.2. Los ensayos de microscopía confocal realizados en células PEO-1 que sobre-expresan HMGB2 y NOP53 confirman que HMGB2 y NOP53 co-localizan en áreas específicas de núcleos y citoplasma, lo que confirma la interacción física de estas proteínas cuando ambas están altamente expresadas.

2.3. El silenciamiento de HMGB2 causa principalmente sobreexpresión, mientras que el silenciamiento de HMGB1 tiene el efecto opuesto sobre los niveles de ARNm de proteínas seleccionadas del interactoma EOC detectado.

2.4. En una segunda aproximación, el interactoma HMGB2 también se obtuvo por inmunoprecipitación acoplada con espectrometría de masas (IP-MS) utilizando células SKOV-3, e identificando 23 nuevas interacciones de HMGB2. Aunque las interacciones identificadas para HMGB2 difieren con los resultados de Y2H, lo que era predecible debido a que las muestras proceden de orígenes diferentes, las proteínas detectadas en cada caso comparten semejanzas funcionales, identificándose principalmente proteínas relacionadas con la unión del ARN y proteínas relacionadas con las funciones citoplásmicas de HMGB2.

En cuanto al objetivo 3: analizar los cambios de expresión de HMGB1, HMGB2, MIEN1 y NOP53, en respuesta a diversos fármacos utilizados en quimioterapia para EOC y CaP, se pueden extraer las siguientes conclusiones:

3.1. En las células cancerosas de ovario SKOV-3, HMGB1, HMGB2 y MIEN1 se regulan negativamente después del tratamiento con paclitaxel, carboplatino o una combinación de ambos y el silenciamiento de HMGB1 o HMGB2 aumenta la viabilidad celular de las células tratadas. Bevacizumab produce una regulación negativa significativa en los niveles de expresión de HMGB2 y NOP53. Por el contrario, olaparib no tiene efectos en los niveles de ARNm.

3.2. En las células cancerosas prostáticas PC-3, el tratamiento con paclitaxel no afecta a la expresión de HMGB1, HMGB2, MIEN1 y NOP53. Bevacizumab provoca una regulación negativa de HMGB2 y NOP53 mientras que olaparib disminuye la expresión de MIEN1 y NOP53.

Respecto al objetivo 4, analizar la presencia de HMGB1, HMGB2, MIEN1 y NOP53 y miARN relacionados en exosomas derivados de líneas celulares de próstata PNT-2 y PC-3 y los efectos de la Temozolomida (TMZ) y su derivado 1D, se pueden extraer las siguientes conclusiones:

4.1 El tratamiento con 1D es más eficaz que TMZ para provocar la muerte de las células PC-3.

4.2 En general, las proteínas seleccionadas (HMGB1, HMGB2, MIEN1, NOP53) y los miARN reguladores relacionados con ellas (miR124, miR146a y miR155) se detectaron mediante *Dot blot* en vesículas extracelulares producidas a partir de las líneas celulares de próstata PC-3 y PNT-2. Sin embargo, utilizando *Western blot*, HMGB2 se detectó a niveles bajos en PC-3 y MIEN1 no se detectó en PNT-2. Los niveles de miR146a también fueron muy bajos en ambas líneas celulares.

4.3 El tratamiento con TMZ o 1D afecta al tamaño y la concentración de VEs producidas por las líneas celulares de la próstata y también a sus contenidos. Ambos tratamientos contribuyen a disminuir los niveles de las proteínas seleccionadas, a excepción de HMGB1 en el lisado de EVs de PNT-2 incubado con TMZ. TMZ y 1D incrementan el contenido del miR-124 anti-oncogénico en las células PC-3, mientras que solo 1D disminuye el contenido del miR-155 pro-oncogénico en las células PC-3.

Referencias

1.   Tang, D. *et al.* Endogenous HMGB1 regulates autophagy. *J. Cell Biol.* **190**, 881–892 (2010).

2.   Tang, L. M., Lu, Z. Q. & Yao, Y. M. The extracellular role of high mobility group box-1 protein in regulation of immune response. *Sheng Li Ke Xue Jin Zhan* **42**, 188–194 (2011).

3.   Kuchler, R., Schroeder, B. O., Jaeger, S. U., Stange, E. F. & Wehkamp, J. Antimicrobial activity of high-mobility-group box 2: a new function to a well-known protein. *Antimicrob. Agents Chemother.* **57**, 4782–4793 (2013).

4.   Tang, D., Kang, R., Zeh 3rd, H. J. & Lotze, M. T. High-mobility group box 1, oxidative stress, and disease. *Antioxid. Redox Signal.* **14**, 1315–1335 (2011).

5.   Barreiro-Alonso, A. *et al.* High Mobility Group B Proteins, Their Partners, and Other Redox Sensors in Ovarian and Prostate Cancer. *Oxid. Med. Cell. Longev.* **2016**, 1–17 (2016).

6.   Paull, T. T., Haykinson, M. J. & Johnson, R. C. The nonspecific DNA-binding and -bending proteins HMG1 and HMG2 promote the assembly of complex nucleoprotein structures. *Genes Dev.* **7**, 1521–1534 (1993).

7.   Lee, K. B. & Thomas, J. O. The effect of the acidic tail on the DNA-binding properties of the HMG1,2 class of proteins: Insights from tail switching and tail removal. *J. Mol. Biol.* **304**, 135–149 (2000).

8.   Bukowska, B., Rogalska, A. & Marczak, A. New potential chemotherapy for ovarian cancer - Combined therapy with WP 631 and epothilone B. *Life Sci.* **151**, 86–92 (2016).

9.   Paek, J., Lee, M., Nam, E. J., Kim, S. W. & Kim, Y. T. Clinical impact of high mobility group box 1 protein in epithelial ovarian cancer. *Arch. Gynecol. Obstet.* **293**, 645–650 (2016).

10.   Rhodes, D. R. *et al.* Large-scale meta-analysis of cancer microarray data identifies common transcriptional profiles of neoplastic transformation and progression. *Proc. Natl. Acad. Sci. U. S. A.* **101**, 9309–9314 (2004).

11.   Ouellet, V. *et al.* SET complex in serous epithelial ovarian cancer. *Int. J. cancer* **119**, 2119–2126 (2006).

12. Bernardini, M. *et al.* High-resolution mapping of genomic imbalance and identification of gene expression profiles associated with differential chemotherapy response in serous epithelial ovarian cancer. *Neoplasia* **7**, 603–613 (2005).

13. Varma, R. R. *et al.* Gene expression profiling of a clonal isolate of oxaliplatin-resistant ovarian carcinoma cell line A2780/C10. *Oncol. Rep.* **14**, 925–932 (2005).

14. Machado, L. R. *et al.* High mobility group protein B1 is a predictor of poor survival in ovarian cancer. *Oncotarget* **8**, 101215–101223 (2017).

15. Wu, Z. B. *et al.* High-mobility group box 2 is associated with prognosis of glioblastoma by promoting cell viability, invasion, and chemotherapeutic resistance. *Neuro. Oncol.* **15**, 1264–1275 (2013).

16. Wang, Y. *et al.* Association of HMGB1 and HMGB2 genetic polymorphisms with lung cancer chemotherapy response. *Clin. Exp. Pharmacol. Physiol.* **41**, 408–415 (2014).

17. Gnanasekar, M. *et al.* HMGB1: A Promising Therapeutic Target for Prostate Cancer. *Prostate Cancer* **2013**, 1–8 (2013).

18. Cai, X. *et al.* Expression of HMGB2 indicates worse survival of patients and is required for the maintenance of Warburg effect in pancreatic cancer. *Acta Biochim. Biophys. Sin. (Shanghai).* **49**, 119–127 (2017).

19. Jiang, C. *et al.* Association between the HMGB1/TLR4 signaling pathway and the clinicopathological features of ovarian cancer. *Mol. Med. Rep.* **18**, 3093–3098 (2018).

20. Li, H., Zhang, H. & Wang, Y. Centromere protein U facilitates metastasis of ovarian cancer cells by targeting high mobility group box 2 expression. **8**, 835–851 (2018).

21. Tohme, S. *et al.* Hypoxia mediates mitochondrial biogenesis in hepatocellular carcinoma to promote tumor growth through HMGB1 and TLR9 interaction. *Hepatology* **66**, 182–197 (2017).

22. Gu, J., Xu, R., Li, Y., Zhang, J. & Wang, S. MicroRNA-218 modulates activities of glioma cells by targeting HMGB1. *Am. J. Transl. Res.* **8**, 3780–3790 (2016).

23. Wang, Z. *et al.* HMGB1 knockdown effectively inhibits the progression of rectal cancer by suppressing HMGB1 expression and promoting apoptosis of rectal cancer cells. *Mol. Med. Rep.* **14**, 1026–1032 (2016).

24. Li, Z. *et al.* Silencing HMGB1 expression by lentivirus-mediated small interfering

RNA (siRNA) inhibits the proliferation and invasion of colorectal cancer LoVo cells in vitro and in vivo. *Zhonghua Zhong Liu Za Zhi* **37**, 664–670 (2015).

25. Liu, X. & Wu, J. Mechanism of inhibitory effects of silencing high mobility group box-1 on invasion and migration of endometrial carcinoma of uterus. *Zhong nan da xue xue bao.Yi xue ban [Journal Cent. South Univ. Sci.* **41**, 251–257 (2016).

26. Gnanasekar, M., Thirugnanam, S. & Ramaswamy, K. Short hairpin RNA (shRNA) constructs targeting high mobility group box-1 (HMGB1) expression leads to inhibition of prostate cancer cell survival and apoptosis. *Int. J. Oncol.* **34**, 425–431 (2009).

27. Song, B. *et al.* Effect of HMGB1 silencing on cell proliferation, invasion and apoptosis of MGC-803 gastric cancer cells. *Cell Biochem. Funct.* **30**, 11–17 (2012).

28. Cui, G., Cai, F., Ding, Z. & Gao, L. HMGB2 promotes the malignancy of human gastric Cancer and indicates poor survival outcome. *Hum. Pathol.* **84**, 133–141 (2018).

29. Li, Y. *et al.* HMGB1 attenuates TGF-beta-induced epithelial-mesenchymal transition of FaDu hypopharyngeal carcinoma cells through regulation of RAGE expression. *Mol. Cell. Biochem.* **431**, 1–10 (2017).

30. Xu, Y. F. *et al.* High-mobility group box 1 expression and lymph node metastasis in intrahepatic cholangiocarcinoma. *World J. Gastroenterol.* **21**, 3256–3265 (2015).

31. Liu, P. L. *et al.* High-mobility group box 1-mediated matrix metalloproteinase-9 expression in non-small cell lung cancer contributes to tumor cell invasiveness. *Am. J. Respir. Cell Mol. Biol.* **43**, 530–538 (2010).

32. Filella, X. & Foj, L. miRNAs as novel biomarkers in the management of prostate cancer. *Clin. Chem. Lab. Med.* **55**, 715–736 (2017).

33. Luu, H. N. *et al.* miRNAs associated with prostate cancer risk and progression. *BMC Urol.* **17**, 1–18 (2017).

34. Mashouri, L. *et al.* Exosomes: Composition, biogenesis, and mechanisms in cancer metastasis and drug resistance. *Mol. Cancer* **18**, 1–14 (2019).

35. Huang, C. Y. *et al.* HMGB1 promotes ERK-mediated mitochondrial Drp1 phosphorylation for chemoresistance through RAGE in colorectal cancer. *Cell Death Dis.* **9**, (2018).

36. Jin, Y. *et al.* ALA-PDT promotes HPV-positive cervical cancer cells apoptosis and

DCs maturation via miR-34a regulated HMGB1 exosomes secretion. *Photodiagnosis Photodyn. Ther.* **24**, 27–35 (2018).

37. Fernandes, A. *et al.* Secretome from SH-SY5Y APPSwe cells trigger time-dependent CHME3 microglia activation phenotypes, ultimately leading to miR-21 exosome shuttling. *Biochimie* **155**, 67–82 (2018).

38. Das, J., Gayvert, K. M., Bunea, F., Wegkamp, M. H. & Yu, H. ENCAPP: elastic-net-based prognosis prediction and biomarker discovery for human cancers. *BMC Genomics* **16**, 263–269 (2015).

39. Liu, Q. *et al.* Basic helix-loop-helix transcription factor DEC2 functions as an anti-apoptotic factor during paclitaxel-induced apoptosis in human prostate cancer cells. *Int. J. Mol. Med.* **38**, 1727–1733 (2016).

40. Shu, W. Downregulation of high mobility group protein box-1 resensitizes ovarian cancer cells to carboplatin. *Oncol. Lett.* **16**, 4586–4592 (2018).

41. Kukolj, E. *et al.* PARP inhibition causes premature loss of cohesion in cancer cells. *Oncotarget* **8**, 103931–103951 (2017).

42. Zhao, Z. *et al.* Autophagy Inhibition Promotes Bevacizumab-induced Apoptosis and Proliferation Inhibition in Colorectal Cancer Cells. *J. Cancer* **9**, 3407–3416 (2018).

43. Gylfe, A. E. *et al.* Identification of candidate oncogenes in human colorectal cancers with microsatellite instability. *Gastroenterology* **145**, 540–3.e22 (2013).

44. Harrison, B. *et al.* DAPK-1 binding to a linear peptide motif in MAP1B stimulates autophagy and membrane blebbing. *J. Biol. Chem.* **283**, 9999–10014 (2008).

45. Kim, J. Y., An, Y. M. & Park, J. H. Role of GLTSCR2 in the regulation of telomerase activity and chromosome stability. *Mol. Med. Rep.* **14**, 1697–1703 (2016).

46. Moon, A. *et al.* Downregulation of GLTSCR2 expression is correlated with breast cancer progression. *Pathol. Res. Pract.* **209**, 700–704 (2013).

47. Lee, S. *et al.* Nucleolar protein GLTSCR2 stabilizes p53 in response to ribosomal stresses. *Cell Death Differ.* **19**, 1613–1622 (2012).

48. Yoshimoto, M., Tokuda, A., Nishiwaki, K., Sengoku, K. & Yaginuma, Y. Abnormal Expression of PICT-1 and Its Codon 389 Polymorphism Is a Risk Factor for Human Endometrial Cancer. *Oncology* **95**, 43–51 (2018).

49. Sheu, J. J. *et al.* Rsf-1, a chromatin remodeling protein, induces DNA damage and

promotes genomic instability. *J. Biol. Chem.* **285**, 38260–38269 (2010).

50.   Liu, Y., Li, G., Liu, C., Tang, Y. & Zhang, S. RSF1 regulates the proliferation and paclitaxel resistance via modulating NF-kappaB signaling pathway in nasopharyngeal carcinoma. *J. Cancer* **8**, 354–362 (2017).

51.   Li, H. *et al.* Rsf-1 overexpression in human prostate cancer, implication as a prognostic marker. *Tumour Biol.* **35**, 5771–5776 (2014).

52.   Zhang, X. *et al.* Overexpression of Rsf-1 correlates with poor survival and promotes invasion in non-small cell lung cancer. *Virchows Arch.* **470**, 553–560 (2017).

53.   He, X. & Zhang, P. Serine/arginine-rich splicing factor 3 (SRSF3) regulates homologous recombination-mediated DNA repair. *Mol. Cancer* **14**, 151–158 (2015).

54.   Zhou, L., Guo, J. & Jia, R. Oncogene SRSF3 suppresses autophagy via inhibiting BECN1 expression. *Biochem. Biophys. Res. Commun.* **509**, 966–972 (2019).

55.   Kim, J. *et al.* Splicing factor SRSF3 represses the translation of programmed cell death 4 mRNA by associating with the 5'-UTR region. *Cell Death Differ.* **21**, 481–490 (2014).

56.   Kim, H. R. *et al.* SRSF3-regulated miR-132/212 controls cell migration and invasion by targeting YAP1. *Exp. Cell Res.* **358**, 161–170 (2017).

57.   He, X. *et al.* Knockdown of splicing factor SRp20 causes apoptosis in ovarian cancer cells and its expression is associated with malignancy of epithelial ovarian cancer. *Oncogene* **30**, 356–365 (2011).

58.   Scully, O. J. *et al.* Complement component 1, q subcomponent binding protein is a marker for proliferation in breast cancer. *Exp. Biol. Med. (Maywood).* **240**, 846–853 (2015).

59.   Huang, Y. *et al.* Upregulation of miR-146a by YY1 depletion correlates with delayed progression of prostate cancer. *Int. J. Oncol.* **50**, 421–431 (2017).

60.   Amamoto, R. *et al.* Mitochondrial p32/C1QBP is highly expressed in prostate cancer and is associated with shorter prostate-specific antigen relapse time after radical prostatectomy. *Cancer Sci.* **102**, 639–647 (2011).

61.   Zhang, X. *et al.* Interactome analysis reveals that C1QBP (complement component 1, q subcomponent binding protein) is associated with cancer cell chemotaxis and metastasis. *Mol. Cell. Proteomics* **12**, 3199–3209 (2013).

62. Chen, R. *et al.* Identification of a novel mitochondrial interacting protein of C1QBP using subcellular fractionation coupled with CoIP-MS. *Anal. Bioanal. Chem.* **408**, 1557–1564 (2016).

63. Long, Y. *et al.* MicroRNA-101 inhibits the proliferation and invasion of bladder cancer cells via targeting c-FOS. *Mol. Med. Rep.* **14**, 2651–2656 (2016).

64. Lu, C. *et al.* cFos is critical for MCF-7 breast cancer cell growth. *Oncogene* **24**, 6516–6524 (2005).

65. Goh, W. Q., Ow, G. S., Kuznetsov, V. A., Chong, S. & Lim, Y. P. DLAT subunit of the pyruvate dehydrogenase complex is upregulated in gastric cancer-implications in cancer therapy. *Am. J. Transl. Res.* **7**, 1140–1151 (2015).

66. Salimi, R. *et al.* Blocking the Cleavage of Filamin A by Calpain Inhibitor Decreases Tumor Cell Growth. *Anticancer Res.* **38**, 2079–2085 (2018).

67. Vitali, E. *et al.* FLNA is implicated in pulmonary neuroendocrine tumors aggressiveness and progression. *Oncotarget* **8**, 77330–77340 (2017).

68. Gai, X. *et al.* mTOR/miR-145-regulated exosomal GOLM1 promotes hepatocellular carcinoma through augmented GSK-3beta/MMPs. *J. Genet. Genomics* **46**, 235–245 (2019).

69. Zhang, R. *et al.* Golgi Membrane Protein 1 (GOLM1) Promotes Growth and Metastasis of Breast Cancer Cells via Regulating Matrix Metalloproteinase-13 (MMP13). *Med. Sci. Monit.* **25**, 847–855 (2019).

70. Yang, L., Luo, P., Song, Q. & Fei, X. DNMT1/miR-200a/GOLM1 signaling pathway regulates lung adenocarcinoma cells proliferation. *Biomed. Pharmacother.* **99**, 839–847 (2018).

71. Yan, G. *et al.* GOLM1 promotes prostate cancer progression through activating PI3K-AKT-mTOR signaling. *Prostate* **78**, 166–177 (2018).

72. Zhou, M., Chen, X., Wu, J., He, X. & Ren, R. microRNA-143 regulates cell migration and invasion by targeting GOLM1 in cervical cancer. *Oncol. Lett.* **16**, 6393–6400 (2018).

73. Li, B. *et al.* HOXA10 is overexpressed in human ovarian clear cell adenocarcinoma and correlates with poor survival. *Int. J. Gynecol. Cancer* **19**, 1347–1352 (2009).

74. Tang, W. *et al.* miR-135a functions as a tumor suppressor in epithelial ovarian cancer and regulates HOXA10 expression. *Cell. Signal.* **26**, 1420–1426 (2014).

75. Ren, C. C. *et al.* Effects of shRNA-mediated silencing of PSMA7 on cell proliferation and vascular endothelial growth factor expression via the ubiquitin-proteasome pathway in cervical cancer. *J. Cell. Physiol.* **234**, 5851–5862 (2019).

76. Yang, L. *et al.* PSMA7 directly interacts with NOD1 and regulates its function. *Cell. Physiol. Biochem.* **31**, 952–959 (2013).

77. Morales, L. D. *et al.* The role of T-cell protein tyrosine phosphatase in epithelial carcinogenesis. *Mol. Carcinog.* **58**, 1640–1647 (2019).

78. Fang, J. F., Zhao, H. P., Wang, Z. F. & Zheng, S. S. Upregulation of RASAL2 promotes proliferation and metastasis, and is targeted by miR-203 in hepatocellular carcinoma. *Mol. Med. Rep.* **15**, 2720–2726 (2017).

79. Pan, Y. *et al.* RASAL2 promotes tumor progression through LATS2/YAP1 axis of hippo signaling pathway in colorectal cancer. *Mol. Cancer* **17**, 102–106 (2018).

80. Li, N. & Li, S. RASAL2 promotes lung cancer metastasis through epithelial-mesenchymal transition. *Biochem. Biophys. Res. Commun.* **455**, 358–362 (2014).

81. Li, Y., Ma, X., Wang, Y. & Li, G. miR-489 inhibits proliferation, cell cycle progression and induces apoptosis of glioma cells via targeting SPIN1-mediated PI3K/AKT pathway. *Biomed. Pharmacother.* **93**, 435–443 (2017).

82. Li, W., Zhang, Z., Zhao, W. & Han, N. Transglutaminase 3 protein modulates human esophageal cancer cell growth by targeting the NF-kappaB signaling pathway. *Oncol. Rep.* **36**, 1723–1730 (2016).

83. Plafker, K. S., Farjo, K. M., Wiechmann, A. F. & Plafker, S. M. The human ubiquitin conjugating enzyme, UBE2E3, is required for proliferation of retinal pigment epithelial cells. *Invest. Ophthalmol. Vis. Sci.* **49**, 5611–5618 (2008).

84. Yang, W. L. *et al.* Vigilin is overexpressed in hepatocellular carcinoma and is required for HCC cell proliferation and tumor growth. *Oncol. Rep.* **31**, 2328–2334 (2014).

85. Moniz, S. & Jordan, P. Emerging roles for WNK kinases in cancer. *Cell. Mol. Life Sci.* **67**, 1265–1276 (2010).

86. Mu, P., Akashi, T., Lu, F., Kishida, S. & Kadomatsu, K. A novel nuclear complex of DRR1, F-actin and COMMD1 involved in NF-kappaB degradation and cell growth suppression in neuroblastoma. *Oncogene* **36**, 5745–5756 (2017).

87. van de Sluis, B. *et al.* COMMD1 disrupts HIF-1alpha/beta dimerization and inhibits

human tumor cell invasion. *J. Clin. Invest.* **120**, 2119–2130 (2010).

88. Dwyer, S. F. & Gelman, I. H. Cross-Phosphorylation and Interaction between Src/FAK and MAPKAP5/PRAK in Early Focal Adhesions Controls Cell Motility. *J. cancer Biol. Res.* **2**, (2014).

89. Zhou, J. *et al.* MK5 is degraded in response to doxorubicin and negatively regulates doxorubicin-induced apoptosis in hepatocellular carcinoma cells. *Biochem. Biophys. Res. Commun.* **427**, 581–586 (2012).

90. Zhou, S. *et al.* MNAT1 is overexpressed in colorectal cancer and mediates p53 ubiquitin-degradation to promote colorectal cancer malignance. *J. Exp. Clin. Cancer Res.* **37**, 283–284 (2018).

91. Marikar, F. M., Jin, G., Sheng, W., Ma, D. & Hua, Z. Metallothionein 2A an interactive protein linking phosphorylated FADD to NF-kappaB pathway leads to colorectal cancer formation. *Chinese Clin. Oncol.* **5**, 76 (2016).

92. Bonavida, B. Linking Autophagy and the Dysregulated NFkappaB/ SNAIL/YY1/RKIP/PTEN Loop in Cancer: Therapeutic Implications. *Crit. Rev. Oncog.* **23**, 307–320 (2018).

93. Galloway, N. R., Ball, K. F., Stiff, T. & Wall, N. R. Yin Yang 1 (YY1): Regulation of Survivin and Its Role In Invasion and Metastasis. *Crit. Rev. Oncog.* **22**, 23–36 (2017).

94. Kpetemey, M., Chaudhary, P., Van Treuren, T. & Vishwanatha, J. K. MIEN1 drives breast tumor cell migration by regulating cytoskeletal-focal adhesion dynamics. *Oncotarget* **7**, 54913–54924 (2016).

95. Rajendiran, S. *et al.* microRNA-940 suppresses prostate cancer migration and invasion by regulating MIEN1. *Mol. Cancer* **13**, 1–15 (2014).

96. Barreiro-Alonso*, A. *et al.* Characterization of HMGB1/2 Interactome in Prostate Cancer by Yeast Two Hybrid Approach: Potential Pathobiological Implications. *Cancers (Basel).* **11**, 1–21 (2019).

97. Kim, S., Hagemann, A. & DeMichele, A. Immuno-modulatory gene polymorphisms and outcome in breast and ovarian cancer. *Immunol. Invest.* **38**, 324–340 (2009).

98. Pathak, H. B. *et al.* A Synthetic Lethality Screen Using a Focused siRNA Library to Identify Sensitizers to Dasatinib Therapy for the Treatment of Epithelial Ovarian Cancer. *PLoS One* **10**, 1–19 (2015).

99.   Jones, D. T. *et al.* Endogenous ribosomal protein L29 (RPL29): a newly identified regulator of angiogenesis in mice. *Dis. Model. Mech.* **6**, 115–124 (2013).

100. Yang, Y. I., Ahn, J. H., Lee, K. T., Shih, I. & Choi, J. H. RSF1 is a positive regulator of NF-kappaB-induced gene expression required for ovarian cancer chemoresistance. *Cancer Res.* **74**, 2258–2269 (2014).

101. Sheu, J. J. *et al.* Rsf-1, a chromatin remodelling protein, interacts with cyclin E1 and promotes tumour development. *J. Pathol.* **229**, 559–568 (2013).

102. Maeda, D. *et al.* Rsf-1 (HBXAP) expression is associated with advanced stage and lymph node metastasis in ovarian clear cell carcinoma. *Int. J. Gynecol. Pathol.* **30**, 30–35 (2011).

103. Choi, J. H. *et al.* Functional analysis of 11q13.5 amplicon identifies Rsf-1 (HBXAP) as a gene involved in paclitaxel resistance in ovarian cancer. *Cancer Res.* **69**, 1407–1415 (2009).

104. He, W., Sun, Z. & Liu, Z. Silencing of TGM2 reverses epithelial to mesenchymal transition and modulates the chemosensitivity of breast cancer to docetaxel. *Exp. Ther. Med.* **10**, 1413–1418 (2015).

105. Maine, G. N., Mao, X., Komarck, C. M. & Burstein, E. COMMD1 promotes the ubiquitination of NF-kappaB subunits through a cullin-containing ubiquitin ligase. *EMBO J.* **26**, 436–447 (2007).

106. Fedoseienko, A. *et al.* Nuclear COMMD1 Is Associated with Cisplatin Sensitivity in Ovarian Cancer. *PLoS One* **11**, 1–21 (2016).

107. Ren, H., Qi, Y., Yin, X. & Gao, J. miR-136 targets MIEN1 and involves the metastasis of colon cancer by suppressing epithelial-to-mesenchymal transition. *Onco. Targets. Ther.* **11**, 67–74 (2017).

108. Zhang, H. Y. & Dou, K. F. PCBP1 is an important mediator of TGF-beta-induced epithelial to mesenchymal transition in gall bladder cancer cell line GBC-SD. *Mol. Biol. Rep.* **41**, 5519–5524 (2014).

109. Guo, S. *et al.* TBC1D25 Regulates Cardiac Remodeling Through TAK1 Signaling Pathway. *Int. J. Biol. Sci.* **16**, 1335–1348 (2020).

110. Zhang, H., Zhang, C. F. & Chen, R. Zinc finger RNA-binding protein promotes non-small-cell carcinoma growth and tumor metastasis by targeting the Notch signaling pathway. *Am. J. Cancer Res.* **7**, 1804–1819 (2017).

111. Papatheodorou, I. *et al.* Expression Atlas: gene and protein expression across multiple studies and organisms. *Nucleic Acids Res.* **46**, D246–D251 (2018).

112. Consortium, Gte. The Genotype-Tissue Expression (GTEx) project. *Nat. Genet.* **45**, 580–585 (2013).

113. Barreiro-Alonso, A. Interactome of lxr1, HMGB1 and HMGB2 proteins in relation to their cellular function. *PhD Thesis* (2018).

114. Wang, J., Peng, X., Peng, W. & Wu, F. X. Dynamic protein interaction network construction and applications. *Proteomics* **14**, 338–352 (2014).

115. Hussain, M. *et al.* Targeting DNA repair with combination veliparib (ABT-888) and temozolomide in patients with metastatic castration-resistant prostate cancer Maha. *Invest. New Drugs* **32**, 904–912 (2015).

116. Jung, M. K. & Mun, J. Y. Sample Preparation and Imaging of Exosomes by Transmission Electron Microscopy. *J. Vis. Exp.* **131**, 1–5 (2018).

117. Deng, F. & Miller, J. A review on protein markers of exosome from different bio-resources and the antibodies used for characterization. *J. Histotechnol.* **42**, 226–239 (2019).